High-precision micro-machining of glass for mass-personalization

Lucas Abia Hof

A Thesis

In the Department

of

Mechanical, Industrial and Aerospace Engineering

Presented in Partial Fulfillment of the Requirements

For the Degree of

Doctor of Philosophy (Mechanical Engineering) at

Concordia University

Montreal, Québec, Canada

June 2018

CONCORDIA UNIVERSITY
School of Graduate Studies

This is to certify that the thesis prepared

By: Lucas Abia Hof

Entitled: High-precision micro-machining of glass for mass-personalization

and submitted in partial fulfillment of the requirements for the degree of

Doctor of Philosophy (Mechanical Engineering)

complies with the regulations of the University and meets the accepted standards with respect to originality and quality.

Signed by the final examining committee:

_____ Chair
Dr. K. Schmitt

_____ External Examiner
Dr. P. Koshy

_____ External to Program
Dr. M. Nokken

_____ Examiner
Dr. C. Moreau

_____ Examiner
Dr. R. Sedaghati

_____ Thesis Supervisor
Dr. R. Wüthrich

Approved by: _____
                    Dr. A. Dolatabadi, Graduate Program Director

August 14, 2018 _____
                    Dr. A. Asif, Dean
                    Faculty of Engineering and Computer Science

Abstract

High-precision micro-machining of glass for mass-personalization

Lucas Abia Hof, Ph.D.

Concordia University, 2018

With the fourth industrial revolution manufacturing industry faces new challenges. Small batches of personalized parts, where the geometry changes per part, must be produced in an economically viable manner. In such cases of mass personalization new manufacturing technologies are required which can keep manufacturing overhead related to change of part geometries low. These processes need to address the issues of extensive calibration and tooling costs, must be able to handle complex parts and reduce production steps. According to recent studies hybrid technologies, including electrochemical technologies, are promising to address these manufacturing challenges.

At the same time, glass has fascinated and attracted much interest from both the academic and industrial world, mainly because it is optically and radio frequency transparent, chemically inert, environmentally friendly and it has excellent mechanical and thermal properties, allowing tailoring of new and dedicated applications. However, glass is a hard to machine material, due to its

hardness and brittleness. Machining smooth, high-aspect ratio structures is still challenging due to long machining times, high machining costs and poor surface quality. Hybrid methods like Spark Assisted Chemical Engraving (SACE) perform well to address these issues.

Nevertheless, SACE cannot be deployed for high-precision glass mass-personalization by industry and academia, due to 1) lack of process models for glass cutting and milling, relating SACE input parameters to a desired output, 2) extensive calibration needed for tool-workpiece alignment and tool run-out elimination, 3) part specific tooling required for proper clamping of the glass workpiece to attain high precision.

In this study, SACE technology was progressively developed from a mass-fabrication technology towards a process for mass-personalization of high-precision glass parts by addressing these issues. Key was the development of 1) an (empirically validated) model for SACE cutting and milling process operations allowing direct relation of the machining input to the desired machining outcome, enabling a dramatical increase of automation across the manufacturing process workflow from desired design to establishing of machinable code containing all necessary manufacturing execution information, 2) in-situ fabrication of the needed tooling and 3) the use of low-cost rapid prototyping, eliminating high indirect machining costs and long lead times.

To show the viability of this approach two novel applications in the microtechnology field were proposed and developed using glass as substrate material and SACE technology for rapid prototyping: a) fabrication of glass imprint templates for microfabricating devices by hot embossing and b) manufacturing of glass dies for micro-forming of metal micro parts.

Acknowledgements

Traveller, there is no path – The path is made by walking. - Antonio Machado

Before starting this exciting journey of experimenting, observing, analyzing, modeling, validating, machining, coffee/beer drinking, lunching, networking, failing, waiting, discovering, discussing, developing, debugging, inventing, writing, publishing, presenting and much more, I could have never imagined to even have started it all. Having gained ten years of industrial, teaching and entrepreneurial experience in The Netherlands after finishing successfully my master's degree in mechanical engineering (werktuigbouwkunde) it was the one year of research experience at the Bleuler lab - Ecole Polytechnique Fédérale de Lausanne - that made me decide to pursue an academic career. Ten years and one email later, I was welcomed in the multidisciplinary research group of my supervisor Dr. Rolf Wüthrich.

Rolf, I would like to express my deepest and warmest appreciation of your never-ending support and friendship during this PhD research adventure. Without your support, academic freedom and responsibilities you have given me, I would have never been the researcher I am now. Merci énormément et vous m'avez appris tout les outils necessaire pour poursuivre ma carrière dans la recherche! I am looking forward to continue working together on future research projects.

I am grateful to Dr. Moreau, Dr. Dolatabadi, Dr. Sharifi and Dr. Ben Ettouil for the support and permission to use their microscopy facilities. Many thanks to D. Juras, R. Oliver, G. Huard and the EDML team for their technical support and use of their facilities. I am thankful to the ISO team and the MIAE administrative staff for the support on all non-research related, administrative issues.

Dedication

Dedicated to my loving wife, Gertie,

my son, Émile and daughter, Annabelle

…zonder jullie liefde, vrolijkheid en aanmoedigingen zou deze dissertatie nooit tot stand gekomen zijn…

Dedicated to my loving parents

Contribution of authors [1]

Chapter 2 Micro-Hole Drilling on Glass Substrates—A Review

Lucas A. Hof [1] and Jana Abou Ziki [2]

[1] *Department of Mechanical & Industrial Engineering, Concordia University, Montreal, QC H3G 1M8, Canada*
[2] *Bharti School of Engineering, Laurentian University, Sudbury, ON P3E 2C6, Canada*

L.A.H. conceived the review article, constructed the graphs, wrote the paper and oversaw the article structure. J.A.Z. contributed in writing the paper and overseeing the article structure.

Chapter 6 Glass imprint templates by spark assisted chemical engraving for microfabrication by hot embossing

Lucas A. Hof[1], Shane Guo[2], Minseok Seo[2], Rolf Wüthrich[1,3], Jesse Greener[2,4]

[1] *Department of Mechanical & Industrial Engineering, Concordia University, Montreal, QC H3G 1M8, Canada*
[2] *FlowJEM Inc., 80 St. George Street, Toronto, ON M5S 3H6, Canada*
[3] *Posalux SA, 18, Fritz Oppliger, CH-2504 Biel/Bienne, Switzerland*
[4] *Département de Chimie, Université Laval, Québec, QC G1V 0A6, Canada*

L.A.H. initiated the project with J.G., designed and prepared CAD files, fabricated the glass moulds and characterized them and contributed in writing the paper; X.G. prepared CAD files and conduced embossing, moulding and characterization of polymer and glass parts; M.S. conduced fabrication by embossing and some characterization of embossed polymer parts; R.W. oversaw the project regarding

---

[1] Note that only co-authored work is mentioned in this section.

glass mould fabrication by SACE technology; J.G. conceived of and oversaw the project and contributed in writing the paper.

Chapter 6 Towards high precision manufacturing of glass tools by Spark Assisted Chemical Engraving (SACE) for micro forming techniques

Lucas A. Hof[1], Lukas Heinrich[2], Rolf Wüthrich[1,3]

[1] Department of Mechanical & Industrial Engineering, Concordia University, Montreal, QC H3G 1M8, Canada
[2] BIAS - Bremer Institut für angewandte Strahltechnik GmbH, Klagenfurter Straße 5, D - 28359 Bremen, Germany
[3] Posalux S.A., 18, F. Oppliger, PO Box 6075, CH-2500 Biel/Bienne 6, Switzerland

L.A.H initiated the project, wrote the article, designed and performed the glass micromachining experiments and characterized them. L.H. performed the metal micro-forming experiments and characterization. R.W. oversaw the project.

Table of Contents

List of Figures

List of Tables

List of Abbreviations

AC	Adaptive Control
AJM	Abrasive Jet Micromachining
AM	Additive Manufacturing
ASJM	Abrasive Slurry Jet Machining
AWJM	Abrasive Water Jet Machining
CAD	Computer-aided Design
CAM	Computer-aided Manufacturing
CCD	Charge-coupled Device
CIRP	College International Pour la Recherche en Productique
CNC	Computer Numerical Control
COP	Cycloolifin Polymer
CPS	Cyber-physical Systems
CUSM	Chemical-assisted Ultrasonic Machining
DC	Direct Current
DI	Deionized
DMLS	Direct Metal Laser Sintering
DPSS	Diode-pumped Solid State
DRIE	Deep Reactive Ion Etching
EBM	Electron Beam Melting
ECDM	Electrochemical Discharge Machining
EDM	Electrical Discharge Machining

EP	Electrochemical Polishing
EPD	Electrophoretic Deposition
EPDG	Electrophoretic Deposition Grinding
ER	Electrorheological
FDM	Fused Deposition Modeling
FEDM	Focused Electrical Discharge Method
FFMS	Focused Flexible Manufacturing Systems
FMS	Flexible Manufacturing Systems
HAZ	Heat-affected Zone
HF	Hydrofluoric Acid
IoT	Internet-of-Things
JIT	Just-in-Time
KOH	Potassium Hydroxide
LALP	Liquid-assisted Laser Processing
LASER	Light Amplification by Stimulated Emission of Radiation
LCD	Liquid-crystal Display
LIPMM	Laser-induced Plasma Micromachining
LOC	Lab-on-a-chip
LSL	Lower Specification Limit
MEL	Mechanical Engineer Laboratory
MEMS	Micro-Electro-Mechanical-Systems
MOEMS	Micro-Optical-Electro-Mechanical-Systems
MRR	Material Removal Rate
NaOH	Sodium Hydroxide
NC	Numerical Control
Nd:YAG	Neodymium-doped Yttrium Aluminum Garnet
PC	Polycarbonate
PDE	Partial Differential Equation
PDMS	Polydimethylsiloxane
PID	Proportional-Integral-Derivative
PIN	Personal Identification Number

PMMA	Polymethyl Methacrylate
PP	Polypropylene
PS	Polystyrene
RF	Radio Frequency
RFID	Radio-frequency Identification
RMS	Root Mean Square
SACE	Spark Assisted Chemical Engraving
SACP	Spark Assisted Chemical Polishing
SDI	Surface Distance Index
SEM	Scanning Electron Microscopy
TEM	Transmission Electron Microscopy
TGV	Through-Glass-Via
TPS	Toyota Production System
TQC	Total Quality Control
USB	Universal Serial Bus
USL	Upper Specification Limit
USM	Ultrasonic Machining
USP	Ultra-short Pulse
UV	Ultraviolet
WE	Working Electrode
WEDG	Wire Electrical Discharge Grinding
μTAS	Micro Total Analysis Systems
3D	Three Dimensional
4D	Four Dimensional

List of symbols

$\bar{h}_r$	Normalized Heat Propagation Rate
$\bar{t}_0$	Normalized Time needed to reach the machining temperature
h_r	Heat Propagation Rate
$\bar{I}$	Mean Current
$\bar{T}$	Normalized Temperature
$\bar{t}$	Normalized Time
$\bar{e}$	Normalized Ring Thickness
t_h	Time to heat a distance p
t_F	Time of tool moving over its own size
$t_{machining}$	Machining Time
$\bar{x}$	Process Mean
$\bar{z}$	Normalized Length
A	Surface Area
a	Thermal Diffusity
b	Tool Radius
C	Concentration
c	Specific Heat Capacity
C_p	Process Capability
C_{pk}	Process Capability (considering that process mean may not be centered)
d	Depth
D_0	Initial Blank Diameter

D_p	Punch Diameter
d_s	Total Path Length (roughness parameter)
d_{sl}	Distance Straight Line (roughness parameter)
D_z	Die Diameter
E	Potential
e	Ring Thickness
E_{max}	Electric Field
F	Feed-rate
$F_{machining}$	Machining Force
F_p	Polishing Feed-rate
F_r	Rough Cut Feed-rate
$F_{trapping}$	Particle Trapping Force
h	Height
I	Current
I^{crit}	Critical Current
k	Stiffness
L	Length
n	Number of Steps / Cycles or Normal to the Plane
p	Depth of Cut
P	Number-of-Passes
p_e	Embossing Pressure
P_o	Heat Source Power
P_E	Mean Heat power
$\dot{q}$	Heat Flux
r	Radius
R_a	Arithmetic Mean Average Roughness
r_i	Inner Radius
r_o	Outer Radius
r_p	Punch Radius
R_z	Average Maximum Peak-to-Valley Roughness
r_z	Die Radius

s_0	Sheet Thickness
S_a	Arithmetic Mean Surface Roughness
S_z	Average Maximum Peak-to-Valley Surface Roughness
T	Temperature
t	Time
t_0	Time needed to reach the machining temperature
t_d	Dehydration Time
T_d	De-embossing Temperature
T_e	Embossing Temperature
t_e	Temperature Stabilization Time at the Embossing Temperature
T_g	Glass Transition Temperature
t_{high}	Time of High Level Pulse
t_{low}	Time of Low Level Pulse
T_M	Machining Temperature
T_m	Melting Point
$T_{melting}$	Melting Temperature
T_o	Ambient Temperature (at infinity)
T_{tool}	Tool Temperature
$t_{trapping}$	Particle Trapping Time
$T_{vaporisation}$	Vaporization Temperature
U	Voltage
$U_{applied}$	Applied Voltage
U_{avg}	Average Input Voltage
U^{crit}	Critical Voltage
U_{high}	High Level Pulsed Voltage
U_{low}	Low Level Pulsed Voltage
U_{pulse}	Pulsed Voltage
w	Weight
w	Width
x	Coordinate PDE Toolbox (equivalent of z coordinate)
X	Stage Direction along cartesian x-axis

y	Coordinate PDE Toolbox (equivalent of r coordinate)
Y	Stage Direction along cartesian y-axis
z	Cylindrical Coordinate (Axial Length)
Z	Stage Direction along cartesian z-axis
β	Drawing Ratio
δ	Deformation
Δx	Polishing Gap
ε_0	Permittivity of Vacuum
ε_r	Relative Dielectric Constant
ζ	Zetapotential
η	Viscosity
λ	Thermal Conductivity
ρ	Density
σ	Standard Deviation
ω	Tool-rotation
ω_p	Polishing Tool-rotation
ω_r	Rough Cut Tool-rotation
κ	Normalized Heat Power
θ	Cylindrical Coordinate (Angle)
τ	Characteristic Time

Chapter 1

Introduction

1.1. Manufacturing

The presented research study evolves around the following emerging engineering question: *how can we mass-manufacture batch-size-1, i.e. mass-personalized, high-precision products (made of hard-to-machine materials) economically on-demand?*

To put it differently: what kind of manufacturing processes are needed to meet the demand of mass-personalized high-precision products (of hard-to-machine materials) at economical cost? In the framework of this study we focus on the specific case of manufacturing high-precision devices flexibly made of hard-to-machine materials such as glass. As this material is challenging to machine, the results of this study can be used as reference for other materials afterwards.

Before addressing the research question, we first need to analyze each key element of it and understand how they relate to each other, which will be done progressively throughout this chapter.

Let us start with defining 'manufacturing' as denoted by the Oxford English Dictionary [1]:

Manufacture, *v.*

Compare Middle French, French manufacturer (c1576; 1538 as participial adjective), post-classical Latin manifacturare (a1567 in a document from Genoa), Italian manifatturare (Florio, 1598).

1. *trans.* **a.** To make (a product, goods, etc.) from, of, or out of raw material; to produce (goods) by physical labour, machinery, etc., now esp. on a large scale.

2. a. *trans.* To make up or bring (raw material, ingredients, etc.) into a form suitable for use; to work up as or convert into a specified product.

This conversion into complete functional products per design specification is achieved by using a wide array of processes that apply energy to produce controlled changes in the configuration properties of materials. The nature of this energy can be mechanical, thermal, electrical, chemical or a combination of these components (referred to as hybrid technologies). Contrary of the past, modern manufacturing requires involvement of different engineering disciplines, ranging from design and materials engineering to mechanical, electrical and computer networking engineering to fulfill the constant need for smaller lot size manufacturing, more diversity, better quality and lower cost [2-4]. Coined in Germany in 2011, Industry 4.0 [5] appeared as answer to address these challenges.

The response of manufacturing industry across history on needs from the markets and the evolution of (precision) manufacturing in general is detailed in section 1.2 of the introduction.

Section 1.3 gives a more comprehensive overview of Industry 4.0 and Smart Manufacturing initiatives and its requirements for industrial implementation.

General criteria for precision manufacturing providing guidelines for precision machine design and setting requirements for new high-precision fabrication processes to be designed are outlined in section 1.4. In addition, it aims to relate the needs from precision manufacturing perspective to the new 'Industry 4.0' fabrication approaches for mass-personalized products.

Section 1.5 compromises a brief review on glass as building element and conducted research work on customized high-precision glass parts with different techniques.

The final sections 1.6 and 1.7 of the introduction present respectively the scope and structure of this thesis.

1.2.   Manufacturing historical background

Manufacturing industry has been a key element in the prosperity of regions and countries around the world for long time [6]. Actually, the development of mass manufacturing ranks among the most important contributions to human living conditions ever – of the same magnitude as agriculture and modern medicine [7]. Across manufacturing history, a common theme is the

evolution of manufacturing from an art to a science [8, 9]. This shift from art to science parallels to changes in both knowledge about and process control of the physical technology [7].

Historically, manufacturing processes date back to some 4000 BC where hammering of metals for jewelry or simple tools were practiced [10]. Progressively, over the first five or six millenia, more sophisticated tools were used often part of distinct unit processes (individual manufacturing steps) such as the casting process or tube rolling as part of deformation-based processes. According to Boothroyd [11] the progress in development of these manufacturing methods originates from improvement of the following elements necessary in any unit process: 1) source of energy or relative motion, 2) means to secure the work, 3) means to secure and orient the tool, 4) control of the source of energy and means above [9]. Examples of crucial historical advancements of technologies for improved manufacturing ability are the introduction of machine tools such as the turning lead screw carrying the tool in a lathe developed by Maudslay around 1800 [7, 9] which improved drastically the controllability of the manufacturing process and eventually resulted in the first manufacturing system based on interchangeable parts and the invention of the horizontal-boring machine by Wilkinson [11] enabling James Watt [12] to overcome the difficulties of boring a steamtight cylinder casting in order to produce a successful steam engine [13, 14].

More importantly, these developments were the onset of the first industrial revolution [14], in the late nineteenth century, enabling mechanization of manufacturing processes to produce goods on much larger scale at higher quality. Moreover, the persistent growing technology push and the constant increasing demand for new and better products at economical cost were among the driving forces of the successive second and third industrial revolutions, each one enabled by new inventions (resp. electricity leading to mass-fabrication and computers resulting in automation of production processes) and introducing new engineering domains (resp. electrical engineering and computer engineering) [15]. A more refined and differentiated overview of the past industrial revolutions is described by Jaikumar [7] stating that there have been six revolutionary transformations in manufacturing, each involving a shift in hard technology, the nature of human work, and the nature of process control. Incrementally the control of the manufacturing processes improved permitting simultaneous increase in both force and precision.

Introduction of the Japanese system by Toyota [16] (also referred to as the 'Toyota Production System (TPS)' [17]) is another milestone that significantly improved the quality and efficiency of manufacturing mass-fabricated goods. This system consists essentially of two types of procedures

and techniques, productivity and quality. Its most important principles are *just-in-time* (JIT) and *total quality control* (TQC), where productivity is improved through avoidance of waste in its broadest sense and low stock of materials and products used [16]. Derived from these principles, the terminology *lean manufacturing* [18] was introduced early nineties, which transformed significantly the way of manufacturing.

The increased technical complexity of manufactured products and the consumer demand for high quality at affordable cost are the main driving forces behind the search of ever more demanding levels of manufacturing accuracy capability and ever smaller feature creation [9, 19, 20]. These drivers include demands from defence, automotive and aerospace industries, microelectronics, telecoms, medical technologies and science programs [20] and the need for high-precision manufacturing emerged (Figure 1.1 A).

Classic measures of engineering relative size-scales and of progress in precision manufacturing over time are given by respectively McKneown [19] and Taniguchi [21] (Figure 1.1 B). According to their definitions precision machining defines processes having a precision of around one micron, whereas ultra-precision machining is defined by technologies obtaining precision in the order of one nanometer. Taniguchi emphasized the need of machine systems for processing together with appropriate measurement and control techniques for production technologies required for nanotechnology [20, 21]. This recognition of the fundamental need for measurement can be traced back to Lord Kelvin [22] and the maxim attributed to Galileo stating that 'to measure is to know'.
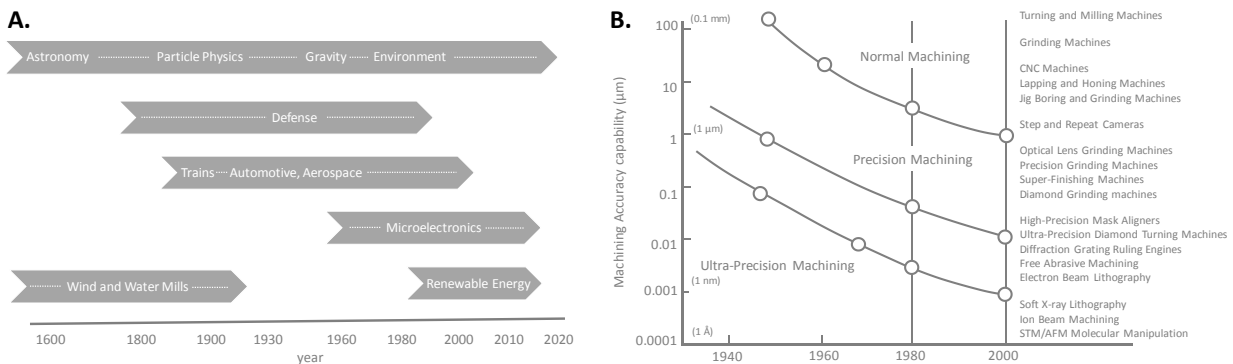
Figure 1.1. A. Drivers of achievable accuracy capability in precision machining (adapted from [20]). **B.** An interpretation of the Taniguchi curves [20, 21], depicting the general improvement of machine accuracy capability with time during much of the twentieth century.

Throughout the presented thesis work we will focus on precision machining (creating features with precision ~1 μm) with some applications in the field of nanotechnology (ultra-precision).

As precision manufacturing is basically the process of acting on a workpiece it can be closely related to precision machining or material removal, i.e. creation of the artifact on the part. Parallel to the progress in manufacturing ability across history can be viewed the development of machines over time. Shirley and Jaikumar [23] refer to a classification of seventeen levels over time of mechanization of 'machines' related to their power and control sources [9]. At the last level they envisioned machines able to make decisions 'for themselves' based on sensor inputs and 'intelligence' containing an objective function and means for optimization. This evolution of machines over time is presented by Moriwaki [24, 25] as depicted in Figure 1.2. It can be noted that this 'intelligent machine', proposed already in 1994 [24], is nowadays in use in state-of-the-art factories based on techniques such as machine learning, artificial intelligence and precise automatized system communication (see section 1.3 Mass personalization - Industry 4.0).
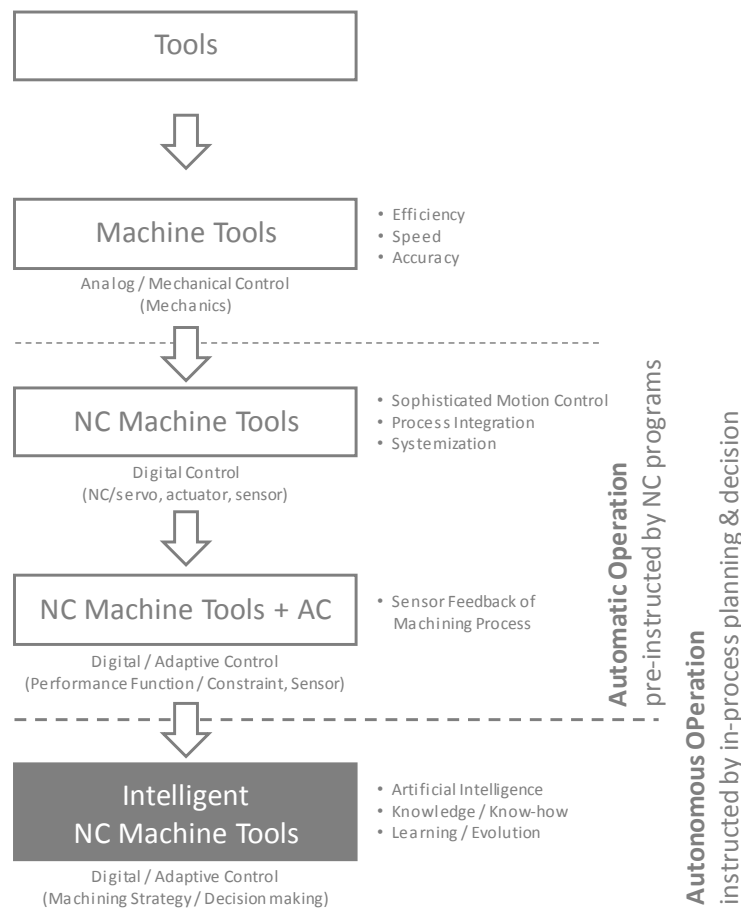
Figure 1.2. History of machine tool development. Adapted from Moriwaki [24, 25].

Other visions on manufacturing and machine tools dating back to decades ago were described by Jaikumar, Csiszár and Shirley [7, 23] wondering if "*the Computer Integrated Manufacturing / Flexible Manufacturing System epoch, is still the last word, or we can distinguish a new epoch, one based on computer networking? How should we think about process control extending across entire supply chains?*", which is exactly the case in the Industry 4.0 philosophy as we will see in the next session. Dornfeld and Lee [2, 26] mentioned in their work on precision manufacturing in 2008 the concept and advantages of the 'digital factory' using a digitalized 'manufacturing pipeline' to built on competent process models and extensive data bases to increase precision and reduce cycle times. They stressed out as well the importance of the environmental impact of the production and use of products and proposed a methodology for sustainable design and manufacturing by establishing a sustainable budget including all sources and their possible impact on the environmental performance of a machine.

1.3. Mass-personalization – Industry 4.0

Having past three industrial revolutions over the past centuries, current manufacturing is at the dawn of a new revolution: the fourth industrial revolution [27] (Figure 1.3).
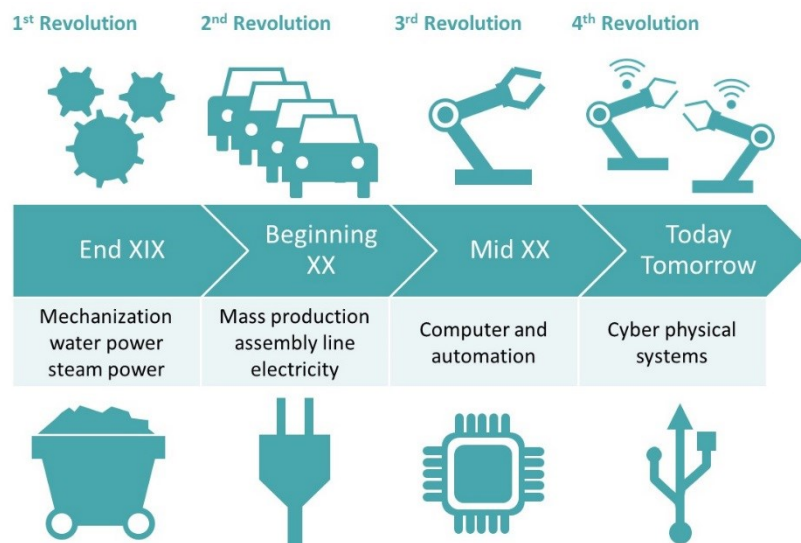
Figure 1.3. Chronology of the past three industrial revolutions
and the emerging fourth industrial revolution.

Increasing global competition [28] and complex market dynamics due to unpredictable forecasts and short innovation and product cycles [29, 30] are causing a paradigm shift towards

more flexibility to respond quickly and efficiently to constant changing customer needs, increasing product variety and new technologies. An increasingly high degree of individualization is demanded by the market [31] resulting in a first step in the need of mass-customized products [32-34]. In fact, this is a first step towards the even more demanding and challenging concept of mass-personalization which is discussed in more depth later in this section. Mass-customization is the assembly of individual parts to custom products such as done today in several industries (e.g. automotive or consumer electronics industry since the late 80's [32]). Flexible manufacturing systems are required to economical produce such small batch sizes as this is incompatible with established manufacturing systems designed to produce large quantities of identical parts.

Manufacturing flexibility to achieve mass-customization, as a strategic perspective, introduced with a developed framework by Gerwin [35] almost thirty years ago, has been discussed in engineering and management literature for several decades [28]**.** Flexible manufacturing systems (FMS) were developed, usually consisting of computer numeric control (CNC) machine tools, fed by industrial robots, which are connected by automated material handling and storage systems controlled by an integrated computer system [36]. It was recognized that differentiation and identification of the different parts, agile operating instruction configuration and fast exchange of the machining setup were key requirements for these FMS. Manufacturing flexibility ranges from product and mix flexibility to volume, and delivery flexibility [37], defining respectively the capability of a manufacturing system to fabricate a variety of components with the same equipment (machine), the ability to change the range of products within a defined period, the capacity to change the level of output and the ability to change planned or expected delivery dates. The new manufacturing paradigm demands integration and flexibility of these four classified types to a high level, setting firm requirements to manufacturing processes to be used. It is important to note that the manufacturing process itself is often the main limiting factor in FMS to reach the desired level of flexibility in a timely manner as shown by a recent study [36].

Due to complexity of managing operations in an FMS and its high investment costs, focused flexible manufacturing systems (FFMS) [31] are introduced by machine tool builders to serve manufacturing companies that don`t need the full FMS. This alternative (FFMS) represents a relatively new concept, based on system configuration to meet exactly the companies` flexibility requirements without any unnecessary, expensive, features.

It is highlighted by a recent product flexibility assessment study [30] that *adaptable interfaces* between the product and resources, such as setting and gripping interfaces or tooling interfaces, are key actors for building cost-effective and flexible production lines. Part specific interfaces may require more setup time and higher setup costs. An example of adaptive gripping interfaces for the automotive industry is presented in this study [30] as a first attempt to contribute in solving this tooling issue.

All these ongoing efforts by academia and industry on developing flexible manufacturing systems contribute to address the challenges for mass-customization. In these cases, the shape of the sub-parts is essentially always the same and the final product is built out of individual modules.

However, manufacturing industry will progressively have to deal with situations where shapes of parts change as well. The customer will not only choose from existing options (modules) but actively be involved in the full product design to manufacturing cycle (e.g. co-design [38]). This next step beyond mass-customization is referred to as mass-personalization [39], demanding an even higher level of flexibility of manufacturing systems.

Industry 4.0 [5], coined in 2011 in Germany, is one of the key initiatives aiming to address these challenges for producing increasingly individualized goods economically [40-42]. It is based on introduction of the Internet-of-things (IoT) into manufacturing industries leading to vertically and horizontally integrated production systems across the entire supply chain [43] creating smart factories [44] (Figure 1.4).
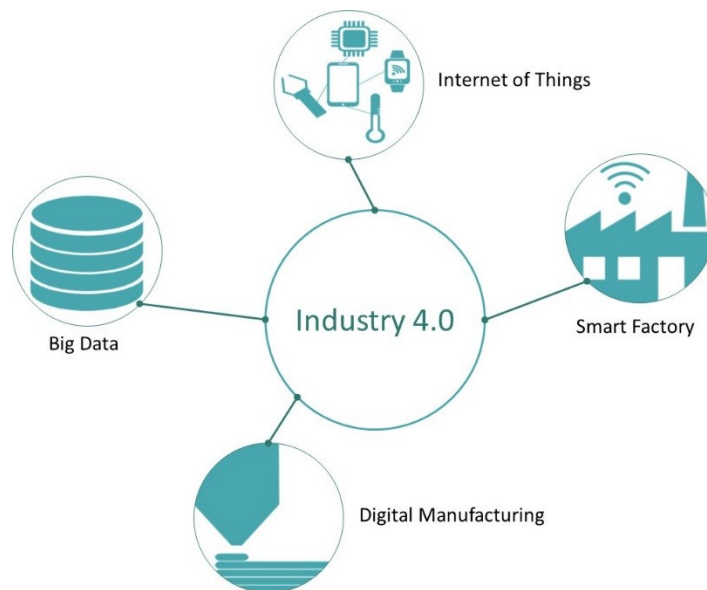
Figure 1.4. Schematic of Industry 4.0 with its key components.

Similar initiatives emerged in other industrial nations such as Japan and Korea and North-American countries where the term `Smart Manufacturing` was introduced. Main objective is the development of smart factories consisting of cyber-physical systems (CPS), which are physical entities (machines, vehicles, workpieces) equipped with advanced technologies such as radio-frequency identification (RFID) sensors, microprocessors, telematics or complete embedded systems to let the physical and virtual world grow together (digital twins [45]) enabling considerable flexibility in the design and operation of machines or entire plants. As these initiatives might have practically similar implications on the manufacturing industry, its origin is different. While the Smart Manufacturing concept, coined in the United States, can be described as 'a data intensive application of information technology at the shop floor level and above to enable intelligent, efficient, and responsive operations' [46], Industry 4.0 covers a paradigm shift from automated to intelligent manufacturing with the main objective of producing highly personalized (individualized) products at low batch size (most extreme case: batch-size 1) economically. The focus on human ingenuity is an important aspect differentiating these two initiatives from many others [43], i.e. humans are not simply replaced by artificial intelligence and automation, but their capabilities are enhanced by smart design of customized solutions for a specific area. This implies as well the use of collaborative robots (cobots [47]) interacting directly with human workers.

It is pointed out by recent case studies that *new manufacturing processes* needing *low fixed cost* and *short setup time*, such as additive manufacturing (AM) [48], are required to address the manufacturing challenges for these highly personalized products [30]. In fact, highly *flexible* and *agile* fabrication methods are needed. It is generally thought that agile manufacturing needs to be adopted where demand is volatile (as the case for personalized products) and lean manufacturing adopted where there is a stable demand (in the case of mass-fabricated goods) [18]. These new manufacturing technologies need to keep manufacturing overhead related to change of part shapes low by eliminating the drivers of manufacturing costs related to specific part design. In summary (see Figure 1.5) they have to be able to address the issues of tooling costs (avoid any part specific tooling [30]), able to handle complex parts and to reduce production steps (as in each new step parts will have to be transferred from one manufacturing system to another resulting in new overhead and error introduction due for example to alignment or tooling) and must abandon long calibration runs (in-process automated calibration strategies are recommended).

Figure 1.5. Drivers of manufacturing costs related to part design

Additive manufacturing (AM), initially developed for rapid prototyping, appears to be one of such new technologies and is cited in literature as the solution to mass personalization for diverse applications [49, 50]. Tooling costs are small as the machine builds the needed tooling during manufacturing and very complex shapes can be produced. General Electric (GE) [51] recently demonstrated that AM can produce assembled parts in one step reducing subsequent assembly steps (GE produces injector nozzles by AM which before had to be made out of over 20 subparts). As such, AM appears as one of the corner stones of Industry 4.0. However, besides presenting its own challenges, AM will likely not be the sole manufacturing technology on which industry will rely. Current limitations of AM processes are the limited variety of available feedstock materials, limited resolution for metal AM parts (features are build with a focused laser or electron beam, with spot sizes around 100 µm, from metal powder with typical particle sizes around 25 µm to 75 µm limiting lateral feature sizes to around 250 µm) and the difficulty of printing high quality parts with non-traditional materials such as glass and ceramics.

Other technologies able to work together with or independently from AM (e.g. for materials that cannot be printed well such as glass) will be needed. Academia and industry just started to develop such technologies [52]. For example, for mass customization of curvilinear panels (a novel approach of tooling was developed) [53] or office scissors (a combination of AM and injection molding was integrated into a smart factory) [54]. An example of material not well suited for AM but where mass personalization starts to become reality is fabric. The European project FASHION-ABLE aims to develop strategies for it [55].

However, the main efforts in academia remain in AM and surprisingly little research is conducted on alternate technologies. According to a recent case study made by the Universities of Michigan and Cincinnati for the World Economic Forum, hybrid technologies, in particular including electrochemical technologies, would have a great potential towards this aim [56].

Industrial efforts on development of such hybrid manufacturing approaches are mainly focused on the integration of metal AM processes and conventional CNC milling for enhanced efficiency of part repair and obtaining better surface finish by milling the surface of the part during the AM fabrication cycles [57]. Furthermore, the smart factory (or digital factory) concept is gaining increasingly interest by manufacturing companies and an emerging effort on digitalization for increased process control and flexibility is observed nowadays. A recent example in the field of AM is the integrated process-flow modular industrial AM system by Additive Industries [58] automatizing part handling, heat treatment and storage of metallic additively manufactured parts.

Besides AM process and CNC machining techniques, laser machining is commonly identified as flexible process for manufacturing personalized products in the Industry 4.0 paradigm. For example, laser technology is the core manufacturing process in the recently realized smart factory of Trumpf [59] - machine tool and laser systems manufacturer – where a high degree of digitalization and communication across the full supply chain and processes is implemented.

These few currently available technologies for use as Industry 4.0 manufacturing processes are summarized in Figure 1.6 together with their main features on achievable structures, surface finish, range of materials to be used, and workpiece handling.

Laser machining
- Mainly cutting operations
- Restricted to 2D machining
- Wide range of materials that can be processed

CNC machining
- Requires specific clamping
- 3D machining is challenging
- Wide range of materials that can be processed

3D printing
- Low surface quality (1 – 100 μm R_a)
- Poor geometrical accuracy
- Limited amount of materials available
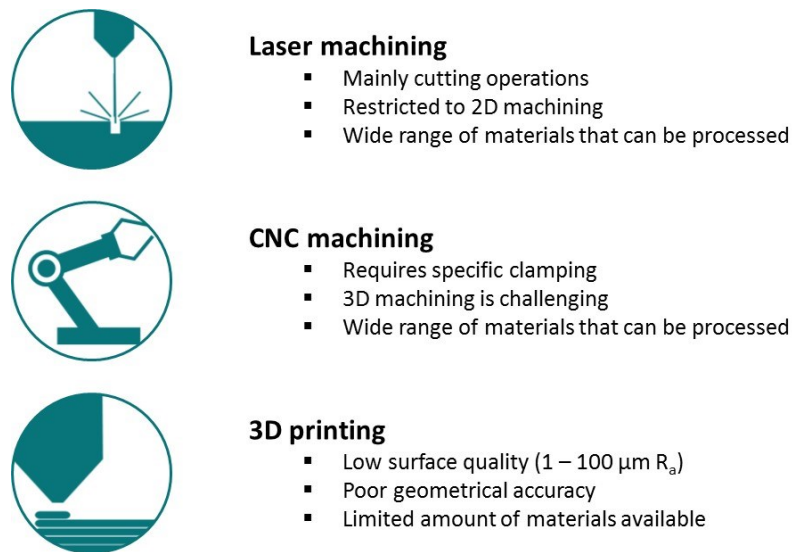
Figure 1.6. Available manufacturing technologies as Industry 4.0 compatible process

In this research we explore the possibilities of electrochemical technologies as suitable hybrid process for manufacturing of mass-personalized high-precision parts of challenging to machine materials (e.g. glass). In this study, an electrochemical discharge machining process, spark assisted

chemical engraving (SACE), is developed to an industrial level machine tool [60] and the process is further optimized as flexible manufacturing technology for realizing high-precision products on glass, which is detailed throughout this thesis.

Before proceeding to the subsequent section on precision manufacturing it is interesting to make a parallel with the emerging need for efficiently produced personalized high-precision products and the concept of *microfactories* introduced in 1990 by the Mechanical Engineer Laboratory (MEL) in Japan [61-63]. This concept represents an approach to design and manufacture which aims to minituarize production systems to match the size of the (micro-) parts they produce. Its objective is to address the issue of energy consumption by reducing occupied space of the factory, to reduce investment and operational costs and to reduce emissions and workload of the operators. Essentially, it provides a versatile system with dynamic reconfigurability, aiming at a light and agile automated manufacturing system optimized for fabrication of customized parts [4, 62]. In fact, this concept, introduced decades ago, can be regarded as the 'embryo' of Industry 4.0 for small components.

As this work focuses on personalized high-precision parts of glass, the definitions of precision together with its criteria and implications on manufacturing are discussed in section 1.4. Section 1.5 discusses the details of glass material for manufacturing and its relation to be used as material for mass-personalized parts.

1.4. Precision manufacturing

Critical elements of precision manufacturing are denoted by McKeown [19] as 1) elimination of fitting and promotion of assembly (automatic assembly), 2) improving interchangeability of manufactured components, 3) improving quality control through higher machining accuracy capabilities, hence reducing scrap, rework and conventional inspection, 4) achieving longer wear and fatigue life of components, 5) achieving greater 'miniaturization and packing densities, 6) achieving further advances in science and technology [9]. These elements address the primary objective of the role of precision manufacturing – to reduce uncertainty at the interfaces between processes and products.

Precision manufacturing processes rely, primarily, on mechanical devices and structures as the basis of their operation. Several major sub-systems which directly contribute to its performance

can be identified in a typical precision machine [64]: 1) the mechanical structure, 2) the spindle and drive system, 3) the tooling and fixture system, 4) the control and sensor system and 5) the measurement and inspection system. In order to fulfill the requirements as set above (minimizing machining errors) the *position loop*, defined as the relative position between the workpiece and the tool, the *stiffness loop*, which includes the tool, tool-holder, positioner stages, collet/chuck, fixtures, and internal vibrations and which defines deformations introduced by compliance, and the *thermal dynamic loop*, which is similar to the stiffness loop with the difference that temperature and heat flux are transmitted in the loop, needs to be properly designed to reduce errors caused by these loops. In general, high static and dynamic stiffness of the machine structure are desired to reduce errors. Error sources are identified with respect to part and machine contributions to systematic and random/dynamic errors [7, 21, 23].

Systematic errors can be compensated by applying an appropriate off-set, while random errors are extremely challenging to be compensated as they vary highly non-linearly over the used process parameters. Upon producing large batch-size precision products, systematic errors can be easily eliminated after some trial runs, however this is not an effective strategy for batch-size 1 production (mass-personalization) as it will dramatically increase setup times before processing the final part. This demands the use of machines and processes with high accuracy (i.e. low bias) and high precision (i.e. repeatability), which will be discussed later in more depth.

Another key aspect for successfully manufacture a high-precision part (i.e. maintaining tolerances and surface finish) is the integration of the requirements of each process step with the limitations of precision [65]. High level of integration, between the tasks of design, process planning and manufacturing [66], with subsequent digitalization in the design to fabrication cycle of (precision) mechanical components is one of the pillars of Industry 4.0 [40, 41]. For mass-produced identical parts, this process flow can be highly optimized over product runs. However, this is a high challenge for batch-size 1 production, where the design of the product changes for each production cycle. A possible solution could be the implementation of to be developed machine learning algorithms fed by real-time process and production data, which needs further research and is beyond the scope of the presented work.

From Nakazawa [67] it becomes clear that a proper designed *precision* machine is required to perform well with respect to the following elements: 1) Dimensional precision; 2) Angular precision; 3) Form precision; 4) Surface roughness; 5) Kinematic precision; 6) Surface layer

alterations. In the scope of the presented study it is important to note that these are both elements required to be *designed in* to the machine (i.e. in to the manufacturing process) and also be *measured* to evaluate the machine performance [64, 68]. This asks for machines specifically designed for high-precision purposes, rather than trying to transform conventional machining approaches (less precise) into high-precision processes.

Because realized characteristics of components produced by a manufacturing process are not perfectly identical to the target specification their behaviour is commonly described by frequency distributions [7, 68] (Figure 1.7).
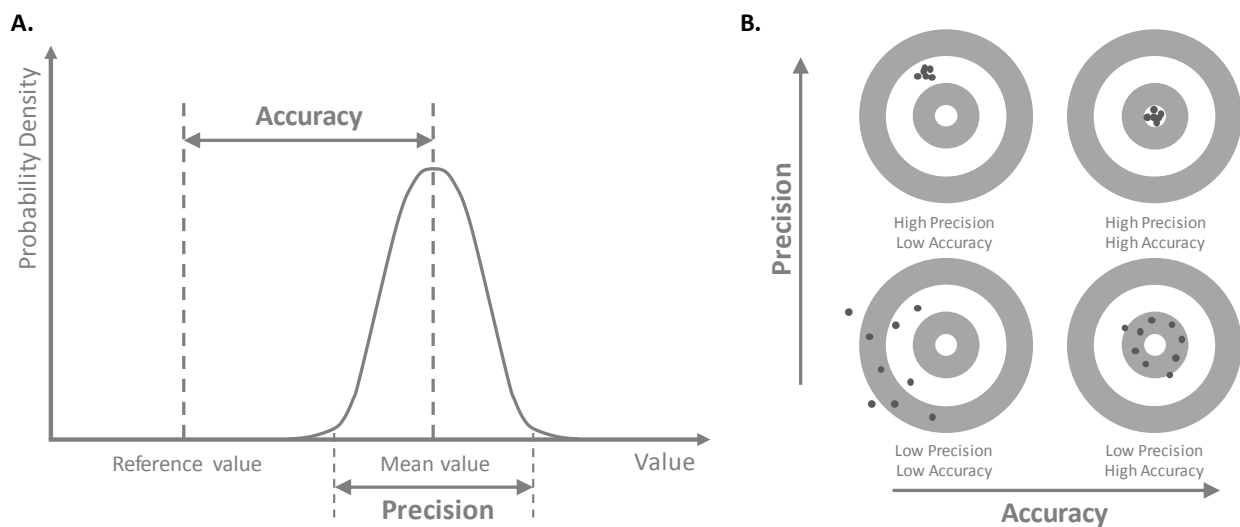
Figure 1.7. A. Distribution of dimensions of a part machined to a specific *'mean value'*, illustrating *accuracy* and *precision*. **B.** Bulls eye representation of precision versus accuracy.

It is important to distinguish *accuracy* from *precision* or *repeatability* of a manufacturing process, where the reciprocal of precision is *variance* and defines to what degree the process can attain the desired performance. Accuracy can be defined as the difference between the achieved mean and the desired dimension. Process precision measures the ability of a machine to execute identical performances and the ability of people and procedures to direct this machine [7, 64, 68], which is measured by the dispersion around the process mean. A measure for process performance to reliably manufacture a product or component that is generally used is the process capability *Cp* described by [65]:

$$C_p = \frac{USL - LSL}{6\sigma} \tag{1.1}$$

where σ is the standard deviation, USL is the upper specification limit and LSL is the lower specification limit. The higher this C_p value, the better the manufacturing technology performs. Usually, a C_p value of 1.33 or higher is considered adequate. A process can be out of the specification, even when the recommended C_p value is met, if it is biased (bias defined as the difference of the nominal and mean dimension of the actual targeted dimension distribution), i.e. the process is off-centre from the nominal [69]. In this case, a more appropriate measure to use is C_{pk} defined as [65]:

$$C_{pk} = \frac{min\left[\left(\frac{USL - \bar{x}}{\sigma}\right) - \left(\frac{LSL - \bar{x}}{\sigma}\right)\right]}{3} \tag{1.2}$$

where $\bar{x}$ is the process mean. Process C_{pk} values ≥ 1.00 are acceptable for a suitable process. It becomes clear that the latter measure (C_{pk}) is of better use for defining relevant manufacturing technologies for mass-personalization, since both high precision (repeatability) and high accuracy (low bias) is crucial here. In processes for producing large quantities of the same product, only stability (measuring the shift of bias over time) and precision are key as inaccuracies can be compensated by adjusting components of the machine (offsets).

Parallels can be observed of the transition from current manufacturing to mass-personalization for precision manufacturing, with the transition around 1800 from the English to the American system of manufacturing (respectively focused on accuracy against interchangeability, consequently repeatability/precision) [7, 13, 14]. This works well for large batch sizes, but less good for low batch sizes as it is costly (i.e. time consuming) to find out the bias (offset) of the manufacturing system. On the contrary, a system with high accuracy doesn't need to be adjusted, so it can readily be used for manufacturing unique components.

However, in a constantly changing manufacturing environment, which is the case for mass-personalization of high-precision products where continuously new parts are being introduced with tight tolerances, error avoidance alone is not likely to prevent all defects [7]. Sources of mechanical and thermal disturbance need to be located, their magnitudes be determined, and their mechanisms be identified, requiring detailed examination of the machine tools. In this case, enhanced knowledge and analytical skills are becoming the dominant driver in manufacturing competence needed by industry to create new products and processes [7].

For precision manufacturing, one must make sure to be sufficiently precise in all the process steps required for the manufacturing of a certain feature [66], consequently it is evident that diminishing the number of process steps will facilitate the realization of a certain feature with precision. Manufacturing processes for both mass-fabricated and mas-personalized high-precision products benefit from this reduction, although for mass-personalized products, this requirement becomes key to choose a suitable manufacturing technology.

The relation of critical requirements from precision machining point of view for manufacturing processes able to fabricate high-precision personalized products and its comparison to conventional mass-fabrication of identical products are summarized in Table 1.1.

Table 1.1. Critical requirements for precision manufacturing.

Precision manufacturing requirements/characteristics	Mass-fabrication parts	Mass-personalization parts
Quality demands high accuracy i.e. small bias (difference between nominal and machined dimension) [7, 9]	Less important as a bias/offset can be corrected over a production run (i.e. calibration)	Highly important to prevent/minimize calibration (reducing time/costs), bias needs to be measured and adjusted every production cycle (not effective)
High level of interchangeability (for assembly) asks for high repeatability (precision) [7, 9]	Highly important since a lot of parts need to be produced within a specific tolerance	Important to reduce setup time and making the component within specification
Precision (dimensional, angular, from, kinematic) designed into the machine [64, 68]	Important as mass-fabrication processes are highly repetitive: process repeatability is key	Important to prevent mean deviation errors of machined features (increased process prediction)
High precision for all process steps (error of process is accumulation of individual process errors) [9, 19, 66]	Trial runs are needed to compensate errors introduced by accumulated process errors (i.e. calibration required)	Number of process steps need to be reduced to a minimum as each step introduces machining errors
Structural stiffness (static and dynamic) [9]	Important to reduce position errors over time	Important to reduce position errors over time
Levels of integration in the design to fabrication cycle (ability of software tools to influence & optimize process metrics) [40, 41]	Beneficial but not a crucial element (large volume product runs demands less setup changes)	Essential requirement as the overhead costs need to be reduced as much as possible

Evaluating carefully Table 1.1 reveals that the precision manufacturing requirements as established by literature [7, 9, 19, 40, 41, 64, 66, 68] are appropriate and valid for mass-fabrication assessment as commonly used. However, most requirements do not distinguish strongly between mass-fabrication and mass-personalization. Incremental differences can be remarked as presented in Table 1.1. However, to better assess a given technology on performance as manufacturing process for mass-personalization other criteria are needed. These were proposed and discussed in section 1.3 (Figure 1.5) and are summarized briefly in Table 1.2.

In chapter 2 (Table 2.2), micro-machining technologies are assessed against these criteria to evaluate their performances to be adopted as manufacturing processes for mass-personalization.

Table 1.2. Key drivers of manufacturing costs related to part design for mass-personalization manufacturing processes.

Part related manufacturing cost drivers hampering mass-personalization	Description
Calibration	Calibration runs increase dramatically the setup times for each different workpiece jeopardizing effective manufacturing process work flow as needed for mass-personalization
Tooling	Part specific tooling add significantly to machining overhead increasing drastically the cost per product
Complexity	As mass-personalization demands manufacturing of a wide variety of geometries, compatible processes need to be able to handle complex shapes.
Multiple processing steps	Each new manufacturing step demands transfer of parts from one manufacturing system to another resulting in new overhead and error introduction due for example to alignment or tooling

1.5. Glass precision manufacturing

Glass, existing for millions of years in its natural form, has fascinated and attracted much interest from both the academic and industrial world. For long, glass was considered a 'fourth state of matter' before the realization of its 'liquid-like' structure [70]. Glass appears on cooling down a liquid continuously until its viscosity becomes so high that it freezes to a glassy state. This

happens at some range of temperatures that depends on thermal history, letting glass be a mysterious material, since the way it is prepared may change its properties.

The application of glass science to the improvement of industrial tools occurred only in the past century, with a few exceptions. Glass has been employed in many forms to fabricate glazing and containers for centuries while it is now entering new applications that are appearing in micro and even nanotechnology like fibers, displays and Micro-Electro-Mechanical-Systems (MEMS) devices. Many qualities make glass attractive since it is transparent, chemically inert, environmentally friendly and because of its mechanical strength and thermal properties (e.g. its allowance for adapting its thermal expansion coefficients to those of other materials [71]). Glass can be electrically insulating, but it can also be a good ion conductor or even a semiconductor. The amorphous character of glasses implies that all its properties are isotropic and that the ability of micro-structuring is therefore independent on predefined directions of crystal lattices [71] eliminating limitations on achievable machined shapes, which is of high interest for personalized products.

In fact, no other materials being mass-produced have shown such qualities over so many centuries. Nowadays glass offers recycling opportunities and allows for tailoring new and dedicated applications. Moreover, glass is RF transparent, making it an excellent material for sensor and energy transmission devices. Another advantage of using glass in microfluidic MEMS devices [72-74] is its relatively high heat resistance, which makes these devices suitable for high temperature microfluidic systems [75] and sterilization by autoclaving.

Key in the new manufacturing paradigm *Industry 4.0* is the fabrication of personalized parts. Therefore, it seems promising to consider glass as fabrication material. Glass can be transformed into very complex, unique shapes on demand by for example glassblowing techniques as used since long time by industry for producing high precision glass products (e.g. SCP Science [76]). In this way, manufacturing of customized parts can be achieved. Nevertheless, glassblowing techniques are very labor intensive and difficult to control by high degree of automation. An interesting new paradigm for increased automation of glass blowing is presented for design and batch fabrication of isotropic 3-D spherical shell resonators by the Micro Systems Laboratory [77]. This approach uses pressure and surface tension driven plastic deformation (glassblowing) on a wafer scale as a mechanism for creating inherently smooth and symmetric 3-D resonant structures.

However, scaling down to the sub-millimeter and micron domain for glass features enabling personalized high-precision devices (e.g. MEMS) of glass, other versatile technologies are needed.

Recently, AM techniques to produce customized glass parts are extensively researched to contribute in addressing this issue. Lawrence Livermore National Laboratory created an ink from concentrated suspensions of silica particles with well controlled flow properties for printing at room temperature. A thermal heat treatment of the printed structures makes them denser and remove print lines to achieve optical quality [78]. A different approach is developed by the Institute of Microstructure Technology using a photocurable silica nanocomposite that is 3D printed by an adapted stereolithography 3D printer and converted to high-quality fused silica glass via heat treatment [79]. Nevertheless, these technologies are very premature and still need multiple process steps and (expensive) equipment with relatively long setup times which is undesired for economically fabrication of personalized high-precision parts as discussed in section 1.2 and section 1.3.

Conventional CNC micro-milling is an excellent cost-effective choice for rapid prototyping of micro-sized customized plastic devices. It outperforms, in many cases, other technologies such as embossing, stereolithography and injection molding [80] with regard of costs and ability for producing customized parts with precision. These excellent manufacturing characteristics are valid for easy-to-machine materials like plastics, but these are not valid for glass.

Unfortunately, glass is a hard to machine material, due to its hardness and brittleness. In particular, machining high-aspect ratio structures is still challenging due to long machining times, high machining costs and poor surface quality [81, 82]. High surface quality (smooth surface) is key to enhance the strength of glass products [71], as this depends on the number and length of flaws appearing on the glass surface (crack initiation sites). Micro-structured glass takes advantage of this characteristic, since the probability of flaws to occur is limited for small dimensions, hence they exhibit higher strength.

Hybrid electrochemical methods like Spark Assisted Chemical Engraving (SACE) [81, 83] (Figure 1.8) perform well to machine high aspect ratio and relatively smooth surface structures on glass. These assets of SACE technology combined with its relative high machining speeds compared to chemical methods and low-cost compared to femto-laser technologies make SACE suitable for rapid prototyping of micro-scale glass devices.

SACE process was first presented in the sixties of the last century in Japan and has remained an academic process for decades [81], mainly because of the lack of process control and repeatability. It is only recently that the technology was developed to industrial level by Posalux SA, Switzerland together with the Electrochemical Green Engineering Group, Concordia University, Canada. The work performed throughout this thesis study contributed to the latest phase of the SACE technology knowledge transfer (in particular by providing a predictive model for selecting cutting parameters, identifying optimal tool sizes, presenting an approach for time-efficient elimination of tool runout and misalignment, and demonstrating its use for applications needing glass-to-glass bonding).

In SACE process, a voltage is applied between tool and counter electrode dipped in an alkaline solution (Figure 1.8.A.). At sufficiently high voltages (critical voltage U^{crit} of around 30V), the bubbles evolving around the tool electrode coalesce into a gas film (Figure 1.8.B.). Discharges occur from the tool to the electrolyte through this gas film. Glass machining is possible due to thermally promoted etching (breaking of the Si-O-Si bond) [81, 221].
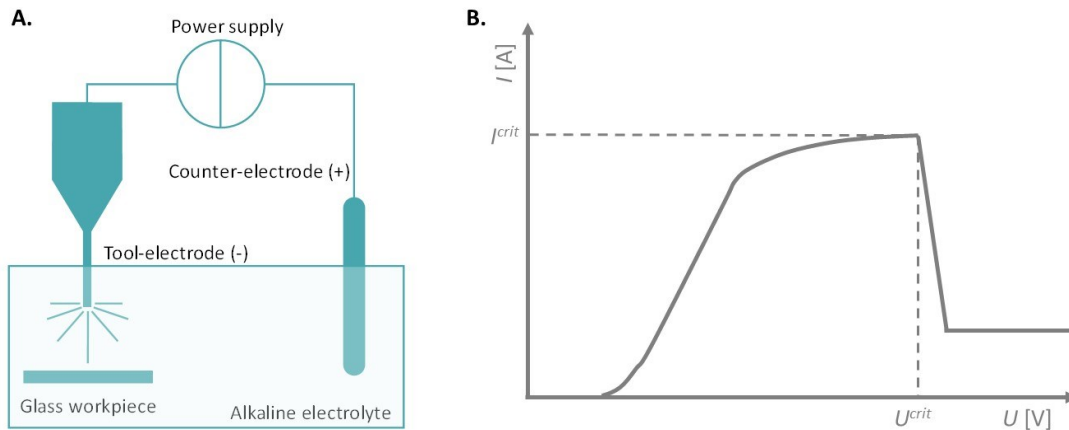
Figure 1.8. A. Principle of SACE machining: the workpiece (glass) is dipped in an alkaline electrolyte (typically sodium or potassium hydroxide) and **B.** a voltage above a critical voltage U^{crit} is applied between a tool- and counter-electrode. Sparking occurs around the tool and local thermally promoted etching of the workpiece takes place.

Material removal is accomplished in two steps [81]: 1) the workpiece is locally heated up by the electrochemical discharges (sparks). The water in the aqueous electrolyte is locally evaporated, which leaves only molten salt in the vicinity of the tool-electrode; 2) high temperature etching of the softened workpiece takes place. This process needs the presence of OH radicals. During this process, the hydrodynamics around the tool-electrode, which is highly influenced by the discharge

activity, the gas film, and the geometry of the machined shape, will affect the etching kinetics. The influence of the key parameters on MRR increase during SACE machining can be summarized as; increasing electrolyte concentration, increasing electrolyte temperature, increasing machining voltage, decreasing machining depth.

The temperature in the machining zone around the tool-electrode tip (controllable from ~200 to 600°C by using pulsed input voltage) is high enough to achieve high etch rates (few 100 μm/s in drilling) but low enough to avoid the formation of heat affected zones (HAZ) or micro-cracks [221]. This machining temperature is not a well-defined value, but depends on the used machining strategy, used electrolyte and tool material [81]. A forced electrolyte flow is needed to insure adequate flushing of the machining zone to avoid drop in material removal rate (MRR) and formation of HAZ. Local supply of fresh electrolyte around the tool is recommended. Typically used alkaline electrolytes are potassium hydroxide (KOH) and sodium hydroxide (NaOH), where KOH is less viscous than NaOH at a specific weight concentration and therefore often preferred for increased flushing performance. In addition, mixed solutions were studied to obtain a eutectic NaOH-KOH melt in the machining zone, which showed a slightly improved machining performance. Tungsten carbides are found to perform well as tool-electrode material. Its high stiffness compared to other metals such as stainless steel and copper limits tool-bending and -vibrations which is important for precision glass machining. Another key property is its significantly lower specific heat capacity compared to other standard metals, resulting in increased tool-electrode temperature and so a higher discharge activity.

Although the performance of SACE process depends on several parameters including the tool shape and motion, voltage, electrolyte, and machining gap, the machining voltage proved to have the most significant effect on the MRR [83, 181, 182].

As several models are established for SACE drilling operations relating machining voltage to MRR, no such model exists for SACE cutting and milling, whereas these last operations are required for most applications (glass micro devices). Chapter 3 presents the development of a practical model (empirically validated) relating the three main SACE machining input parameters:

- machining voltage;
- tool feedrate;
- depth of cut.

During SACE milling and cutting operations, flushing happens easily around the tool in the machining zone. In this case, machining is limited by heat propagation inside the workpiece. This, in contrary of cases when flushing does not happen easily (as in high-depth drilling) and machining is limited by availability of electrolyte in the machining zone and the difficulty in removing the machined material from it. It needs to be noted that the developed model (chapter 3) aims to provide a practical guide for proper SACE machining taking into account the three key machining input parameters and it is not trying to represent all exact physical phenomena of SACE process as most are still largely poorly described and explored.

Main requirement for fabrication of personalized parts (batch-size 1) in any material, here glass, is the use of versatile machining methods which are cost-effective and precise. One has to keep in mind that not only the machining technology itself must be versatile, but in fact the complete process from the drawing of the part until the fabrication of the finished product. If one considers for example conventional CNC- milling technology, one can right away see a problem: the tooling. Since high forces are exerted on the work-piece to be machined, the required tooling has to be adequately engineered with sufficient precision, stiffness and mechanical strength, making it an expensive approach for batch-size 1 production of parts.

Even worse are technologies requiring highly specialized tooling such as injection molding [82] or chemical processes needing masks (e.g. cleanroom technologies such as DRIE [84] or wet etching [85]). Such processes are excellent and unbeatable when it comes to mass production, but not suited for batch-size one production (e.g. mass-personalization).

Considering both the machining requirements for glass micro-machining and the necessity for low-cost tooling, SACE appears a promising candidate among the available micromachining and manufacturing approaches. The ability to make use of low-cost tooling is due to its low forces exerted on the work-piece to be machined (typical in the sub-Newton range) [60].

1.6. Scope of the thesis

The presented research work aims to contribute in developing new hybrid manufacturing technologies for high-precision mass-personalized parts meeting the demand of Industry 4.0. Hence, a novel approach for flexible micro-machining of glass devices by SACE technology was developed and the SACE process was optimized to industrial level (resulting in a patent of the

developed machine tool head with controllable stiffness [60]) to satisfy requirements for industrial high-precision manufacturing.

Research objective of this study is to answer the emerging engineering question:

How can we mass-manufacture batch-size-1, i.e. mass-personalized, high-precision products made of hard-to-machine materials such as glass economically on-demand?

Manufacturing technologies for mass-personalization need to keep manufacturing overhead related to change of part shapes low by eliminating the drivers of manufacturing costs related to specific part design. It is proposed and proven that they must have the capability to 1) address the issues of tooling costs (avoid any part specific tooling), 2) handle complex parts and 3) reduce production steps (as in each new step parts will have to be transferred from one manufacturing system to another resulting in new overhead and error introduction due for example to alignment or tooling) and 4) must abandon long calibration runs (in-process automated calibration strategies are needed).

Throughout this thesis, SACE technology is progressively developed from mass-fabrication technology towards a process for mass-personalization of high-precision glass parts by addressing the challenges of the four drivers of part related manufacturing costs.

The rationale behind the use of this material is that glass being a hard-to-machine material, methodologies developed in this study can potentially be expanded to machining of other materials for personalized product manufacturing requiring high-precision.

SACE technology is chosen as it seems to be a good candidate for machining process in the era of Industry 4.0 [86] because it has the potential of fulfilling some key requirements towards this new paradigm:

1. Precision and accuracy can be *built in* the manufacturing process (e.g. *in-situ* tool fabrication) to eliminate calibration and expensive tools and to reduce setup time;
2. Real time data acquisition can be performed easily as it has many sensors integrated in the process (tool-workpiece force, current signal, applied (pulsed)voltage, toolpath, tool rotation, variable axial stiffness [60]);
3. Implemented control loop to measure force on tool during process real-time to adjust tool-workpiece gap if needed to enhance machining performance;
4. Digital controlled machining process (CAD drawing processed in machinable code by CAM software).

In addition, novel high-precision applications for glass in the field of MEMS and microfluidics (hot embossing template fabrication) and micro-forming (die fabrication) are presented using this approach.

1.7. Thesis structure

This thesis is divided into seven chapters and supplementary data on feature characteristics for drilling micro-holes in glass (supporting chapter 2) is provided in the Appendix.

Progressively a hybrid electrochemical technology (SACE process) is proposed and developed for use as manufacturing method for mass-personalized high-precision parts of glass (devices and tools). Since glass is challenging to machine, the results of this study can be used as reference for development of mass-personalized manufacturing processes of other materials in future research work.

Chapter one introduces manufacturing and its paradigm shifts across history ultimately leading to the fourth industrial revolution and concurrently resulting in the emergence of the Industry 4.0 concept for manufacturing of mass-personalized (batch size 1) products. The increasing need for high-precision parts is discussed together with the interesting properties of glass as substrate material for small scale (< 1 mm) devices. Challenges and requirements for flexible high precision machining are detailed for glass as workpiece material.

Chapter two – *Micro-Hole Drilling on Glass Substrates—A Review* – comprises a detailed review on prevalent and non-traditional technologies, used by industry and academia, for a basic and frequently needed high-precision machining operation on glass substrates: micro-hole drilling. These technologies are assessed on critical characteristics for batch size 1 manufacturing such as flexibility of machining and achievability of machined structures (e.g. aspect ratio, surface finish). It is concluded that SACE technology is, among others, a promising candidate for flexible micro-drilling in glass and this technology has the potential to fulfill the requirements for high-precision manufacturing of mass-personalized parts of hard-to-machine materials such as glass.

Chapter three – *Glass micro-cutting by Spark Assisted Chemical Engraving (SACE)* – presents the derivation and development of a basic model, based on numerical solving the transient two-dimensional heat equation with the heat generated by the sparks around the tool-electrode taken as input in the model, for glass cutting and milling. The proposed model, which correlates the

machining input parameters to a desired outcome, was empirically verified and validated, allowing further optimization of industrial implementation of SACE technology as no predictive model for cutting existed before. This model contributes in addressing the requirement of a high level of integration in the design to fabrication cycle for precision product manufacturing, which is essential for mass-personalization fabrication processes to reduce the machining overhead (here: dramatic reduction of setup time by eliminating trial and error runs for process optimizing).

Chapter four – *Industry 4.0–Towards fabrication of mass-personalized parts on glass by Spark Assisted Chemical Engraving (SACE)* – introduces SACE technology as suitable manufacturing process for industry 4.0. This chapter entails the essence of the thesis research study by providing an overview of the process cycles by SACE technology for manufacturing of mass-personalized parts. The developed fabrication process addresses possible solutions to eliminate or reduce the key manufacturing cost drivers related to part design – 1) reduction of tooling costs, 2) elimination of time-consuming calibration procedures, 3) ability to fabricate complex structures with high precision, 4) reduction of process steps in the overall manufacturing cycle. Examples are given for complex machined structures on glass, which are flexible machined by SACE, for various fields of application.

Chapter five – *Rapid prototyping of packaged glass devices: eliminating a process step in the manufacturing workflow from micromachining to die singularizing* – details the study on using SACE technology as machining step in the fabrication of packaged glass devices (glass-to-glass bonded). It is shown by fabrication of a simple microfluidic Y-mixer that deploying SACE machining eliminates a post-processing step after machining of the desired structure on a glass substrate for subsequent glass-to-glass bonding. This method provides a solution to reduce one of the manufacturing cost drivers – reduction of manufacturing process steps. Quality of the achieved glass-to-glass bonding is assessed both qualitatively and quantitatively by the razorblade insertion test, acoustic imaging (Sonoscan®), electron microscopy (SEM) and leakage testing by microfluidic mixing at high pressure.

Chapter six includes several research studies on novel (non-traditional) high-precision applications using glass exploiting its excellent thermomechanical properties. SACE process is used as flexible manufacturing (i.e. rapid prototyping) technology for fabrication of consequently glass templates for microfabricated devices by hot embossing (section 6.1 – *Glass imprint templates by spark assisted chemical engraving for microfabrication by hot embossing*) and glass

dies for micro-forming of metal micro parts (section 6.2 – *Towards high precision manufacturing of glass tools by Spark Assisted Chemical Engraving (SACE) for micro forming techniques*). This part of the study gives detailed examples of fabricated tooling of glass providing interesting novel solutions to reduce indirectly the manufacturing cost drivers related to part design – 1) reduction of tooling costs and rapid prototyping of tooling, 2) reduction of calibration procedures by high-precision machining, 3) ability to create complex parts (e.g. 2.5D or 3D features on tooling), 4) reduction of process steps in tooling fabrication.

Chapter seven – *Conclusions, contributions and outlook* – summarizes the conclusions and contributions of the presented research work. An outlook is provided as well for future research.

Appendix - *Table A.1 - List of different drilling techniques with their main feature characteristics for drilling micro-holes in glass* – provides supporting values on technologies for micro-hole drilling on glass as presented in chapter two.

Chapter 2

Glass, being one of the oldest materials known to mankind, is among the most important high-performance materials used for scientific research, in industry and in society, mainly because of its unrivalled optical transparency, outstanding mechanical, chemical and thermal resistance as well as its thermal and electrical insulating properties [79, 87]. However, its hardness and brittleness are hindering machining, especially when aiming for high-precision applications such as recent emerged ultra-thin glass (< 100 μm) for tactile screens with digital fingerprint sensors to allow future secure use of smart phones as wallets with fingerprints as PIN, smartphone enclosures entirely made out of glass (e.g. iPhone8 [88]) and usage of glass as interposer layer of printed circuit boards (here, straight vertical micro-holes/vias are strongly preferred over tapered vias to minimize signal losses) [89, 90].

This chapter covers a detailed review on prevalent and on non-traditional technologies, used by industry and academia, for a basic and frequently needed high-precision machining operation on glass substrates: micro-hole drilling. As this work aims to study high-precision machining technologies, available drilling technologies such as water jet cutting with relative low resolutions (~ 250 μm [91]) were omitted in this review study.

The reviewed micro-technologies are assessed on critical characteristics for batch size-1 manufacturing such as flexibility of machining and achievability of machined structures (respectively feed-rate and surface finish against aspect ratio). It is concluded that SACE technology is a promising candidate for flexible micro-drilling in glass and this technology has the potential to fulfill the requirements for high-precision manufacturing of mass-personalized parts made of hard-to-machine materials such as glass.

However, SACE technology is so far never used for mass-personalization as machining overhead of this process is still very high jeopardizing its use for this batch size-1 production.

New approaches are needed to eliminate extensive setup calibration (e.g. for tool run-out reduction) and workpiece clamping devices commissioning to make this electrochemical discharge machining process suitable for batch size 1 production. Chapter 4 will present a novel strategy and realized setup to achieve this objective. A predictive model, for several machining operations, providing guidelines for a quick setup of SACE process parameters, reducing dramatically the time in several fabrication cycles, is presented in chapter 3.

Micro-Hole Drilling on Glass Substrates—A Review

Lucas A. Hof [1] and Jana Abou Ziki [2]

[1] *Department of Mechanical & Industrial Engineering, Concordia University, 1455 de Maisonneuve Blvd. West, Montreal, QC H3G 1M8, Canada*

[2] *Bharti School of Engineering, Laurentian University, Sudbury, ON P3E 2C6, Canada*

Abstract

Glass micromachining is currently becoming essential for the fabrication of micro-devices, including micro-optical-electro-mechanical-systems (MOEMS), miniaturized total analysis systems (μTAS) and microfluidic devices for biosensing. Moreover, glass is radio frequency (RF) transparent, making it an excellent material for sensor and energy transmission devices. Advancements are constantly being made in this field, yet machining smooth through-glass vias (TGVs) with high aspect ratio remains challenging due to poor glass machinability. As TGVs are required for several micro-devices, intensive research is being carried out on numerous glass

micromachining technologies. This paper reviews established and emerging technologies for glass micro-hole drilling, describing their principles of operation and characteristics, and their advantages and disadvantages. These technologies are sorted into four machining categories: mechanical, thermal, chemical, and hybrid machining (which combines several machining methods). Achieved features by these methods are summarized in a table and presented in two graphs. We believe that this paper will be a valuable resource for researchers working in the field of glass micromachining as it provides a comprehensive review of the different glass micromachining technologies. It will be a useful guide for advancing these techniques and establishing new hybrid ones, especially since this is the first broad review in this field.

Keywords: micro-drilling techniques; glass; micro-devices; micro-fluidics; MEMS

2.1. Introduction

Micromachining is one of the most important aspects among state-of-the-art manufacturing technologies. In the constantly emerging field of micro-electro-mechanical-systems (MEMS) and miniaturized total analysis systems (µTAS), silicon and glass are the primarily used materials.

Many applications need glass because of its unique properties [75, 84, 92-99]. The micro-optical-electro-mechanical-system (MOEMS) uses glass due to its optical properties, and radio frequency (RF)-MEMS applications take advantage of its good isolation properties [94, 95]. Dimensions of the structures to be machined vary from sub-micron to sub-mm and aspect ratios of 0.1 up to 10 or higher. In the packaging process, glass is common as a die for thermal compensation for two of the most commercialized MEMS devices—piezoresistive pressure sensors and accelerometers [94]—and glass can be used as a core material for interposer substrates for laminated semiconductors [95, 96]. Typical feature sizes of 50 µm with a depth of 100 µm are required. Glass in this case is chosen due to its good ability to bond to silicon, its similar coefficient of expansion compared to silicon, and its low electrical conductivity [84, 95, 96]. Bio-MEMS devices are fabricated on glass substrates due to its optical transparency, hydrophilicity, chemical stability and bio-compatibility [94]. The emerging field of Lab-on-a-chip devices for energy (e.g., oil and gas) applications demand high temperatures (subsurface temperatures increase at 30 °C·km^{-1}), high pressures (pressure increase at 10 MPa·km^{-1}) and volatile fluids, requiring the

mechanical strength and chemical properties of glass [75]. Other examples where micromachined glass is used due to its optical transparency and mechanical properties are optical data storage devices and spacers for cellphone cameras.

An important challenge is connecting the micro-components of a microfluidic device to the macro-environment of the world. This is often referred to as the macro-to-micro interface, interconnect, or world-to-chip interface. For commercial success of any microfluidic device, especially for high throughput applications where manual manipulation is not economical, the macro-to-micro interface must be developed [100, 101]. Machining of high-aspect ratio micro-holes in glass is the first requirement to manufacture these interconnects. Recently, drilling high density through glass vias (TGVs) became more important for the development of thin (~100 μm) glass interposers in new 2.5D and 3D chip package strategies, due to the demand for higher functionality in small consumer electronics [95, 96]. These, often metalized, TGVs (diameters: 10 to 50 μm, depths: up to 100 μm) are used to connect traces and pads on the top and bottom surfaces of the glass interposers [95, 96, 102, 103].

Nowadays, there is a wide variety of methods for glass machining of micro-holes which includes conventional mechanical drilling and non-conventional drilling methods. These methods can be categorized as: (1) mechanical, such as ultrasonic drilling, powder blasting or abrasive jet micromachining (AJM), abrasive slurry jet machining (ASJM) and abrasive water jet machining (AWJM); (2) thermal, such as laser machining; (3) chemical, including wet etching, deep reactive ion etching (DRIE) or plasma etching; and (4) hybrid technologies (which combine two or more methods of the aforementioned for better machining outcomes), such as spark-assisted chemical engraving (SACE), vibration-assisted micromachining, laser-induced plasma micromachining (LIPMM) and water-assisted micromachining. Each method has its advantages and limiting factors on the achievable machined features, including the range of hole diameters, aspect ratios, surface roughness, and machining speed, as well as its associated costs of investment and operation. While review papers exist about machining micro-holes on glass substrates, each review is specific to certain technologies, such as the quantitative comparison of various hole-drilling methods on glass using different laser-machining techniques [104] and review papers on hybrid processes [105-108] and tool-based micromachining processes [109].

A comprehensive overview of commonly used technologies for machining micro-holes on glass is presented and discussed in this work. Important characteristics of each technique, e.g.,

achievable aspect ratio, machining speed and machined dimensions, are listed in Table A.1 of the Appendix based on the academic and industrial literature. Final conclusions of the different technique capabilities (surface roughness, aspect ratio and machining speed) are presented in a graph, thereby delineating the best-suited machining technique for each application.

2.2. Common Glass Micro-Drilling Techniques

Glass is, by definition, a mixture of oxides, whereby their composition and concentration determine the main properties of the glass. Contrary to fused silica, which is formed of pure SiO_2, a wide range of other glasses contain different kinds of network modifiers, like boron in the widely used Borosilicate glass. As a result, there are a large number of glass types available on the global market, each with different characteristics and applications.

A glass microfabrication technology is chosen for a certain device depending on the glass type (as each type has a different micro-structure [94, 110]) and on the required device properties. The main common challenge for glass micromachining technologies, though, is to deal with the relatively large glass hardness and brittleness. Since conventional techniques such as mechanical drilling have their limitations, a wide range of different non-conventional techniques are used for glass micro-hole drilling. In this review, these methods are discussed by being grouped into mechanical, thermal, chemical, and hybrid drilling processes. Throughout the text, the surface roughness will be described by the arithmetical mean deviation, R_a.

2.2.1. Mechanical Methods

2.2.1.1. Mechanical Drilling

Mechanical drilling is the most conventional and relatively low-cost method to drill micro-holes in glass. Most often, peck drilling (depth of cut is sub-divided into small drilling cycles [111]) is applied to evacuate chips created inside the holes during drilling [112].

Reported aspect ratios vary from 0.33 to 3.96 with corresponding depths of respectively 130 µm to 4 mm. Typical drilling feed rates are around 5 µm/s [113], which can be increased up to 125 µm/s under special conditions [114].

Mechanical drilling is simple, cost effective and potentially suited for rapid prototyping as it is a mask-less process. However, it may easily result in cracks due to deformation of glass by the thrust force of the drill acting at the bottom surface of the workpiece [112-114]. Cracks are more pronounced at the exit of holes than their entrance. Exit cracks on glass plates are mainly cone cracks of relatively large diameter. It is reported in [114] that crack size (typically 50 μm) can be reduced to 15 μm by decreasing thrust forces (from typical values of 2.5 N reduced to 0.8 N), but drilling at low thrust forces makes the process long and impractical. Moreover, using sacrificial pads to support the glass sample to be machined reduces chipping and crack formation [112-114]. Changing the cutting conditions may also reduce cracks (down to 29 μm), as shown in [112], when drilling with 0.3 mm cemented carbide micro-drills at a spindle speed of 35,000 rpm and a feed rate of 3 mm/min. Diamond-abrasive drills result in large cone cracks (390 μm), hence radial and median cracks rarely occur [112]. Tool wear is typically much higher for cemented carbide tools compared to diamond tools (>40%). Another approach is to integrate force-feedback (typical forces are around 8 N) in the drilling setup to ensure an optimal feed rate (5–7 μm/s) with minimal chipping [113]. Chipping (typical 70 μm) can be reduced by more than 50% on optical-grade glass.

Research has shown that also exit cracks could be reduced (from 50 μm down to 10 μm) upon attaching a supporting backplate with liquids, including alcohol, water and oil [113, 114]. Although several methods to reduce cracks during mechanical drilling are reported [112-114], machined surfaces are normally rough. This limits the mechanical drilling applicability to precision micro-device fabrication. In addition, diameters of holes that can be machined are limited to 100 μm [114], and costly high-strength tooling is required to keep the samples in place during machining.

2.2.1.2. Powder Blasting

Powder blasting—also referred to as abrasive jet machining (AJM), impact abrasive machining or sand blasting—is a technique where a particle jet is directed towards a workpiece for mechanical material removal [98, 115-118, 119]. Fine abrasive particles (< 100 μm) are propelled by compressed air at the workpiece where material is mechanically removed due to small chipping. Alumina (Al_2O_3) particles are commonly used as abrasives [117, 119]. To localize material removal, an elastic, particle-resistant foil is placed as mask material. For applications requiring bonding the workpiece to another sample, this mask is added around the hole during

blasting to protect the surface from damages caused by the backscattered particles which may jeopardize the bonding process [118]. When using specially designed photoresists as a mask, precise structures (tolerance < 25 μm) can be machined, like in photolithography, in any sort of glass. Adjustment of the angle between nozzle and sample and using multiple nozzles are some options to control and/or decrease the dependence of width and depth of machined features with this technique. Resist-foil masks are typically removed in 10% KOH solution at room temperature followed by ultrasonic cleaning to ensure particle removal from inside the etched structures [119].

Powder blasting is a fast drilling process on brittle materials with no resulting burrs, surface micro-cracks, or heat-affected zone (HAZ) around the machined holes. However, the resulting machined surface is rough (R_a is several microns). This technique is cost effective for relatively large batch sizes as it operates outside a cleanroom environment [119] and can, as it is mask-based, machine holes in parallel. However, this process is not very suitable for rapid prototyping of structures in glass.

Feature sizes down to 30 μm can generally be obtained with aspect ratios up to 2.5. Drilling speeds vary from 0.1 μm/s to 32 μm/s. According to the physics of powder blasting, a taper angle (~15° [93]) is produced for through holes resulting in a narrow hole exit compared to its entrance. This limits the aspect ratio to a maximum of 2.5 [117, 118], which can be improved if blasting is performed from both sides of the workpiece; however, this requires precise alignment of the workpiece. Masks and small abrasive particles (< 30 μm [117]) are needed for blasting, making the lower limit of the hole diameter around 50 μm. Actual research shows that the mask material affects the hole size. The utilization of higher-resistant mask material, like electroplated copper, can reduce feature sizes from 75 μm down to 50 μm [117]. Moreover, working with smaller ablation particles (~9 μm) further enhances the aspect ratio. During the machining process, particles stick usually to the workpiece surface which leads to difficulties in further fabrication steps like bonding substrates. Post-processing of the powder-blasted workpiece by, for example, wet etching, is a possible solution. Although powder blasting is not clean, it is particularly interesting to different companies (e.g. early recognized by Philips) as it can machine thousands of through holes simultaneously at high accuracy which makes it a well-established technology in micro-manufacturing.

Techniques similar to abrasive jet machining have been reported [120-122]. These methods include abrasive slurry jet micromachining (ASJM) and abrasive water jet micromachining

(AWJM) which make use of abrasive slurries or water to machine blind and through holes in glass. Reported values for machined diameters vary from 390 μm to 2 mm with aspect ratios of respectively 0.9 and 1.5 machined at corresponding feed rates of 4.4 μm/s and 0.6 μm/s.

These techniques are discussed below:

(A)   Abrasive slurry jet micromachining (ASJM)

In ASJM, a slurry with abrasive particles (typically 1 wt % 10 μm Al_2O_3 particles [122]) is pumped through a small orifice (~180 μm) and the derived jet is directed to the workpiece causing material removal. ASJM operates normally at pressures of 1 MPa to 14 MPa [121]. Although this technique does not require mask materials, research investigations show the possibility to reduce frosted areas around the holes when using sacrificial polymeric or glass surfaces [122].

Features of this technology are its machining flexibility, absence of HAZ around the holes and the non-pronounced tool wear. However, the resulting holes have frosted areas at the entrance and the inner walls are not flat. Additional process steps can be applied to overcome frosted areas such as using different slurry additives, e.g., polyethylene oxide (PEO) [122].

(B)   Abrasive water jet micromachining (AWJM)

Although the machining mechanism in AWJM shows many similarities with the ASJM technology, the main difference is the high-pressure operation of AWJM (up to 345 MPa [122]) compared to low-pressure ASJM (typically around 1 to 14 MPa, although up to 70 MPa is reported [121]). Similar to ASJM, tool wear is not measurable and no HAZ are present. However, chipping occurs at the exit of the through holes, which is most likely due to the high operating pressure [122].

2.2.1.3. Ultrasonic Drilling

This abrasive process comprises a vibrated tool, a slurry supply unit, and a movable machine body to which the workpiece is mounted. During ultrasonic machining (USM), the tool (called sonotrode) oscillates at high ultrasonic frequencies, usually 20 to 40 kHz with an oscillating amplitude of several microns, and hammers abrasive particles (e.g., boron carbide (B4C) grits with a size of 5 μm) into the hard-brittle workpiece [123]. This causes indentation, micro-cracks and finally material removal. When reducing tool diameter, abrasive grain size and vibration amplitude to the micro-scale, this technology is referred to as micro ultrasonic-assisted lapping [124]. For

this technique, several innovative strategies are applied to the machine, such as helical tool rotation (50 rpm), on-machine tool preparation by electrical discharge machining (EDM) to avoid alignment issues, workpiece vibration, and force feedback control loops [124-128]. Micro-ultrasonic-assisted lapping can produce very small diameter holes (down to 10 μm) with straight sidewalls [124, 129] and high aspect ratios (up to 10). The tool wear is high, however, making redressing operations necessary for every 25 to 50 machined holes to avoid feature degradation. USM requires rather large capital investment and operates at relatively low feed rates. Moreover, the machined surface presents sometimes chipping and cracks in the subsurface. Average surface roughness is typically >10 μm, while it can be improved down to 1 μm R_a when using micro-pins for grinding operation [130, 131].

Minimum hole diameters obtained by ultrasonic machining are typically around 150 μm with aspect ratio 4 and drilled at feed rate 0.15 μm/s; however, the lowest USM diameter on glass is reported as 10 μm [130]. Here, EDM-machined cemented tungsten carbide micro pins were deployed. As well, feed rates of 16.67 μm/s can be achieved when using diamond core drills and machining relatively large holes (~950 μm).

2.2.2. Thermal Methods

2.2.2.1. Laser Machining

Material removal by thermal shock or ablation can be achieved by laser-based processes. This may be used to drill micro-holes in glass. Transferring photon energy of the laser light to glass is challenging, however, as the last is transparent to a wide range of wavelengths [132, 133], which requires generation of high peak intensities to trigger a nonlinear absorption effect. Carbon dioxide (CO_2) lasers are among the most frequently used lasers for industrial applications over long periods, since its equipment is relatively simple and requires low capital investment [134]. At present, different laser processes resulting in innovative hybrid technologies, are being developed by many research groups and industries like Femtoprint [135] and Fraunhofer ILT [136]. These two use ultra-short pulse (USP) laser as a preprocessing 'flexible masking method' and wet etching as a second step to obtain the desired structure. (The laser-treated areas have enhanced etch rates (20 to 50 times higher than untreated surfaces) and therefore etching is favored in these areas (i.e., acting like a mask to define the structure geometry)).

Despite all extensive research and development, laser systems still suffer from HAZ, ranging from sub-micron (USP-laser) dimensions to tens of microns (CO_2-laser), and bulges around the rims of the machined holes (typical height: 15 µm) caused by recast (debris). This causes difficulty to bond the glass substrate after machining. Hole diameters, machined with liquid-assisted femtosecond lasers down to 5 µm, with aspect ratios as high as 70, have been reported [137]. There is no upper limit in achievable hole sizes and a typical roughness value, R_a, is around 1 µm. Machining speed per hole differs from 30 µm/s [137] up to 2000 µm/s [102] depending on laser type and desired quality.

Novel strategies like PDMS masking [138] and using ultra-short pulse lasers (femtosecond pulses) [137, 139-146], already succeeded in reducing the unwanted side effects of laser machining. Bulge heights around the hole entrances can be reduced by factor 13 to 1.2 µm using 150 µm-thick PDMS masks and a 10 to 15 W CO_2 laser [138]. Furthermore, preheating the workpiece proved to reduce thermal stresses by reducing the temperature gradient [138, 140, 143, 147]. Improved aspect ratios of micro-holes can be achieved using two laser beams on opposite glass surfaces [134, 148].

Another option besides CO_2 lasers and ultra-short pulse lasers is the nanosecond-pulse, Q-switched diode-pumped solid state (DPSS) laser, which is a good trade-off in terms of technological complexity, costs and quality [134, 149]. Pulse energies around 200 µJ and 100 kHz repetition rates were reported for machining 5 mm holes in Gorilla glass® [150] with DPSS lasers.

In general, laser systems are flexible. Most do not need masking layers as they are direct-write technologies, but they are still expensive. The high throughput of laser machining of glass makes it a good option for the MEMS industry, wherein large amounts of holes have to be produced. The most popular laser-drilling types are summarized in the following:

(A)   Carbon dioxide (CO_2) laser

The CO_2 laser technique is a serial thermal laser process which removes material through ablation by relatively long pulses. This causes a thermal impact on the glass and generates mechanical stress, which leads to crack formation during cooling. Many solutions are investigated to reduce this phenomenon, like local preheating of the workpiece, heating of the entire workpiece during drilling and thermal post-treatment of the drilled substrate using an oven [102, 114, 140, 151]. In fact, smooth surfaces ($R_a \sim$ several microns) are possible to achieve due to the generated

heat [152]. Hole diameters on glass down to 25 μm with aspect ratio 4 and machined at 20,000 μm/s per hole are claimed [153]. Although the reliability of CO_2 laser drilling of glass is low, its fast drilling speed and low equipment costs make it a good option for industry. Some examples of CO_2-laser-machined micro-holes in 500 μm-thick glass (Schott D263Teco, SCHOTT AG, Mainz, Germany) are illustrated in [152]. These holes have relatively high aspect ratio and high conicity.

(B)   Excimer laser

The excimer lasers are gas-type lasers that offer access to the ultraviolet (UV) or deep UV region with short pulse rates and durations (respectively 1 to 100 Hz and 5 to 50 ns). This results in high pulse intensity and high resolution, making excimer lasers suitable for machining glass materials where high precision and good surface quality are required. While CO_2 and solid-state Nd:YAG lasers are generally employed in direct writing (serial mode) during machining, excimer lasers are normally used for projection printing (parallel mode), which has higher throughput [97]. Some typical excimer-laser-drilled micro-holes machined at 500 Hz repetition rate and energy levels 4 to 5 J/cm^2 show bulges around the rims on the hole entrance (bulge heights around 10 μm) [148]. However, when using lower laser fluence, reduced cracks and material break-off results. Drilling from both sides can also eliminate these problems while enlarging the diameter at the rear side of the workpiece, which lowers the taper angle [148, 154]. Reported hole diameters range from 30 μm to 200 μm [148] with aspect ratios of 2.2 [142] up to 16.7 [154].

(C)   Liquid-assisted laser processing (LALP)

Liquid-assisted laser processing (LALP) was developed to reduce the formation of bulges on the rims of machined holes and residual stress reduction [151]. Machining is done while the substrate is immersed in water to reduce the temperature gradient, bulges and HAZ region. Chung et al. [151] deployed a 6 W CO_2 laser and they quantified as well the reduction in efficient laser power in LALP machining, e.g., at four passes and constant initial laser power (6 W), the machined depth decreased by 100 μm upon 0.5 mm water depth. The residual stress is reduced by 136 MPa when the sample is immersed in 1 mm water and a 100 μm hole is machined.

The bulges are mainly caused from re-solidification of evaporated debris. LALP reduces the bulge height by the stronger natural convection in water, due to the laser heating, which carries the debris away [140, 151].

This technology is attractive for improved CO_2 laser machining, saving the costs of moving to technologically complex and expensive methods (e.g., USP laser). Machined holes of 280 μm are reported with aspect ratio ~2 μm at a speed of 11,400 μm/s.

(D)   Polydimethylsiloxane (PDMS) protection mask

Upon, protecting the glass workpiece with a polydimethylsiloxane (PDMS) layer, the temperature gradient in laser machining is reduced. This decreases HAZ formation and can result in crack-free machining of Pyrex glass [138]. The PDMS protection layer also eliminates common defects and diminishes the bulge height around the hole entrance by a factor of 13 compared to the process in air (without PDMS cover layer) to 1.2 μm. Moreover, the feature sizes that can be machined are reduced by 10%. CO_2 laser machining in combination with 150 μm-thick PDMS masks are used by Chung et al. [138] reporting hole diameters of 120 μm with aspect ratio 4.

(E)   Ultra-short pulse (pico/femtosecond) laser

Ultra-short laser pulses do not produce a large HAZ due to the smaller amount of heat penetration into the glass sample [141, 142]. These lasers can induce strong absorption even in materials that are transparent to the laser wavelength. This method can produce smooth holes with small diameters (7 to 10 μm) and depths of 30 μm in fused silica, without forming micro-cracks or surface welling [141]. However, this high quality can only be obtained at reduced process speed (~30 μm/s [137]). For example, excimer lasers with nanosecond pulse width are still much faster (typically 10 times faster) [142, 148]. As for the equipment costs, they are relatively high compared to other laser techniques such as CO_2 lasers.

(F)   Laser-induced plasma

To machine small-sized shallow features with very smooth surface finish (R_a = 50 nm), laser-induced plasma can be used. The key to this method is the production of charged particles by targeting the focused laser beam on a metal surface [139].

Spherical crater-like blind holes with a typical diameter of 15 μm and a depth of 4.5 μm are formed. This technique cannot machine high aspect ratio through holes.

(G)   UV laser with absorbent powder

To machine high aspect ratio micro-holes with reduced micro-cracks, research is conducted

with a nanosecond pulsed laser and absorbent powder. This powder is deposited on the glass surface and on the bottom of the machined holes. The deposition is repeated during machining. Although fewer cracks are formed in this case, several micro-cracks are present, as witnessed by the non-transparency of the hole [147]. Aspect ratios of 12 and higher and hole diameters of 200 μm at 100 μm/s are achieved by Kono et al. [147].

2.2.2.2. Focused Electrical Discharge Method

Recently, a through-glass via (TGV) formation method by electrical discharging was introduced: focused electrical discharge method [95, 96]. This technology, where the targeted glass is kept in a space between two axial aligned electrodes, consists mainly of two steps. First, the electrical discharging is focused and controlled to generate heat, which decreases the glass viscosity locally. Second, dielectric breakdown and internal high pressure occurs due to Joule heating. This results in the ejection of glass. This process can produce small diameter holes (down to 20 μm [95]) precisely in thin glass workpieces (100 μm to 500 μm) during a relatively short time (200 ms to 500 ms). Aspect ratios of 5 up to 7.6 and machining speeds of 200 to 500 μm/s are achieved by Takahashi et al. [95]. Annealing is needed in order to remove the residual stresses. High aspect ratio and smooth-machined surfaces are obtained. Fabricating ultra-thin glass interposers in laminated semiconductors is the main targeted application of this method [96].

2.2.3. Chemical Methods

2.2.3.1. Wet Etching

Glass machining by wet etching is due to dissolving glass by immersing the workpiece in an etchant, most commonly hydrofluoric acid (HF). Mask material, which must be etchant resistant, is used to define the pattern to be removed [85, 92, 155]. When applying intermediate masks, multiple levels can be machined using this process. Due to the amorphous nature of glass, the process is isotropic, resulting in rounded sidewalls and undercutting and low aspect ratio machining (<1). Pinholes and notching defects on the edges of etched structures are other limitations of this process. These defects are mainly due to the residual stress in the mask, the compressive or tensile stress, the stress gradients (for multilayer mask), and the hydrophobicity of the masking surface [85]. Partial improvements can be achieved when optimizing the mask

material, i.e., enhancing etchant resistance, and annealing of the workpiece. Although this results in higher etch rates, it causes higher surface roughness. Small, highly detailed features (hole diameters greater than 1 μm [156]) with smooth surfaces (30 nm to 60 nm R_a [115]) and aspect ratio <1 can be created with wet etching by using accurate lithography-fabricated masks. Roughness and etching rate are strongly influenced by the glass composition. The presence of some oxides (such as CaO, MgO, Al_2O_3) in the glass composition give insoluble products in HF solution [157]. A large number of holes can be machined at the same time, as the technique is a batch process. Typical etching speeds vary from 0.07 μm/s to 0.24 μm/s. No micro-cracks and no HAZ are formed around the features [85, 94]. Wet etching with highly concentrated HF (around 50%) is, however, hazardous to the environment and humans as it uses an acid etchant—even low concentrations (>2%) are already seriously toxic.

Recently, a novel wet-etching technology, electrochemical local acidification of fluoride-containing solution, was introduced [158]. The central idea is to produce the highly toxic hydrofluoric acid (HF) locally near a tool electrode where this causes local etching of the glass substrate around the tool tip. Using this method, holes can be machined at a slightly higher speed (0.45 μm/s) than standard HF etching, and no masks are required [158]. Systematic study will be necessary to optimize this technology for specific applications.

2.2.3.2. Deep Reactive Ion Etching (DRIE)

Deep reactive ion etching (DRIE), or deep plasma etching, relies on sulfur hexafluoride [159, 160], perfluorocyclobutane [161] or trifluoromethane [162] gases as the main etch precursors (dissociated into radicals and ions) for both chemical and physical etching, as in plasma etching. Although the gas chemistry is geared more towards silicon etching, glass can be processed as well [93]. In glass, the fluorine radicals carry away the silicate, and carbon difluoride radicals carry away the oxygen as volatile compounds. To direct the ions and create the desired features, metal masks can be used such as nickel with a gold-chromium seed layer. Other studies investigated the use of silicon wafers, a-silicon, and SU-8 as mask material [159, 161, 163, 164]. DRIE can compete with other glass deep-etching technologies in terms of aspect ratio, wall verticality, feature depth and throughput. Very small, accurate features (diameters down to 1 μm) with smooth surfaces (R_a = 2 nm [165]) and high aspect ratio (up to 40 [165]) can be achieved in this highly anisotropic process.

The major disadvantages of DRIE are the amount of process steps needed (e.g., different masks), and the extremely low etch rate (around 0.009 μm/s), although the number of holes that can be produced simultaneously is greater than 200,000 [84]. Moreover, the process is limited by the relatively low heat transfer of glass (typical thermal conductivity of glass is 100 times lower than silicon) making it challenging to achieve deep-etching and high etch rates.

2.2.4. Hybrid Methods

In order to overcome the limitations encountered while using the above-listed technologies, researchers worked on combining different machining processes, leading to what is called hybrid machining. Many definitions were proposed for hybrid machining, the most common being that hybrid machining is a method by which two or more machining processes are applied independently or simultaneously on a single machine. Recently, hybrid machining was defined by the College International Pour la Recherche en Productique (CIRP) as a process that uses simultaneous and controlled interaction of several machining mechanisms, tools and energy sources to enhance the machining performance [108]. Based on this definition, Chavoshi et al. [105] classified hybrid micromachining processes into two groups: assisted and combined hybrid micromachining processes.

In assisted hybrid micromachining, the major machining process is applied while input from other types of energy is added [166, 167]. In combined hybrid micromachining, all the combined micromachining processes simultaneously contribute to the material removal and machining properties. In this category, research is focused on electrochemical processes for machining nonconductive materials while improving the material removal rate and the machined surface quality and reducing the machining time.

The major assisted hybrid glass micromachining techniques and combined hybrid micromachining processes are discussed below.

2.2.4.1. Assisted Hybrid Micromachining Techniques

(A)   Vibration-assisted micromachining

In this process, mainly tool vibration (also sometimes workpiece or machining fluid vibrations) is added to the main machining process. This has been applied to several processes

including micro-milling and micro-electrochemical discharge machining (ECDM) [105]. For appropriate combinations of cutting velocity, and vibration amplitude and frequency, the tool periodically loses contact with the chip, resulting in reducing the machining forces and enhancing the tool life and surface finish [107]. Furthermore, higher depth of cut, smoother surfaces, and near-zero burr are achieved compared to conventional machining [168-170]. On the other hand, this technique may result in surface cracks due to the hammering of the tool [166].

(B)   Laser-assisted micro-cutting/milling

This technique enhances machining of especially hard brittle materials as the laser beam softens the materials to be machined. It is used to machine ceramics and glass where the local softening of the material during the process enables geometrically defined cutting edge, uniform surfaces and reduced surface roughness [108]. For further improvement of surface quality and machining accuracy, these processes can be combined with other ones.

(C)   Laser-induced plasma micromachining (LIPMM)

In this method, plasma is induced in a liquid at the focal point of the laser beam which allows micromachining of shiny materials and transparent materials with high reflectivity like glass [171]. The shape of the plasma can be optically or magnetically manipulated to obtain specific micro-patterns while reducing machining time.

(D)   Water-assisted micromachining

Machining by laser produces debris which reduces the machined surface quality. To remove this debris while machining, water is added on top of the substrate, resulting in a better machined surface (less taper and heat affected zones) and in an accelerated ablation rate (twice as fast as the case of laser machining in air) [105]. With this technique, high aspect ratio holes could be ablated in silicon, LCD glass and alumina by water-assisted femtosecond and CO_2 laser pulse ablation. However, due to the rapid solidification of the molten material, rough surfaces result [172].

(E)   Chemical-assisted micromachining

In this technique, methanol is added on the substrate surface that is to be machined with laser. Methanol has better wettability and lower boiling temperature than water which enhances cooling

and cleaning of ablated particles produced during laser machining. The result is cleaner and smoother surfaces [105].

(F)   Chemical-assisted ultrasonic machining (CUSM)

In order to improve the efficiency of ultrasonic machining of glass, hydrofluoric (HF) acid is added to the abrasive slurry but in low concentrations, normally less than 5% HF solution [173]. This leads to increasing the material removal rate for micro-drilling by up to 40% and enhancing the surface quality as HF acid weakens the Si bonds. However, the hole gets enlarged.

(G)   Electrorheological (ER) fluid-assisted ultrasonic machining

In micro-ultrasonic machining of hard and brittle materials like glass, chipping and low machining accuracy are generally the result. To reduce these problems, electrorheological (ER) fluid-assisted ultrasonic machining is used. In this method, ER fluid is mixed with the abrasive particles and added into the machining zone. This fluid has dielectric particles where increased electric field intensity results in increasing viscosity.

As a voltage is applied between the cathode located on the workpiece surface and the vibrating micro-tool which is the anode, machining results. The resulting electric field in the machining zone in the vicinity of the tool tip increases the ER fluid viscosity and thus traps the abrasive particles (in the ER fluid) beside the tool tip. This results in enhanced machining accuracy and efficiency [174-176].

(H)   Electrical discharge machining (EDM) with an assisted electrode

Another machining method for glass, which can be used for micro-hole drilling, is micro-electrical discharge machining (EDM) with an assisted electrode [177, 178]. The EDM process is based on ablation of material through melting and evaporation, by electrical discharges. These discharges take place upon applying a voltage between the tool electrode and the electrical conductive workpiece, which are separated by a dielectric medium. To achieve machinability of non-conductive materials such as glass with micro EDM, the process has to be initially started by a conductive starting layer on top of the workpiece [177, 178]. While machining the starting layer, the dielectric (typically a hydrocarbon oil) is cracked, providing conductive carbon that settles onto the glass surface, generating a new conductive layer that enables the next discharges to take place. This sequence of removing the layer including the underlying targeted material and creating new

thin conductive layers can be repeated by controlling the process environment. Non-conductive ceramics could be machined with aspect ratios >5 as reported by Schubert et al. [177]. This process can be used both for serial prototyping using a single tool and it can be used for batch-based manufacturing when using multi-tool heads to produce many holes at the same time. However, preprocessing is needed for deposition of the conductive starting layer, and sophisticated process control is required for stable operation.

(I)   Hot embossing

Micro-structuring of glass can also be done by forming processes such as hot embossing which is based on viscous flow of glass at high temperatures. This technology makes use of a micro-patterned mould and a heated glass workpiece and it is mostly used for large batch size fabrication of optical lenses [179]. Almost any possible shape that can be patterned on the metal mould can be transferred to the glass workpiece. A critical parameter is the process temperature. If the temperature is high, this will reduce the glass viscosity, resulting in adherence of the glass to the mould surface. However, if the process is carried out at lower temperatures, glass would have relatively higher viscosity, and will require higher mechanical forces to pattern it. To overcome these issues, the mould surface or glass substrate can be coated to prevent the glass from sticking to the mould [179]. This technology is most suited for large batch size production of features in glass, due to the need of mould fabrication and the setup required for this process, e.g., sophisticated heat control.

2.2.4.2. Combined Hybrid Micromachining Processes

Micro-electrochemical discharge machining (ECDM) or spark-assisted chemical engraving (SACE).

In this process, used to machine non-conductive materials, a voltage is applied between the tool-electrode (positioned above the substrate) and counter electrode which are both dipped in an alkaline solution. At voltages higher than the critical voltage (around 30 V), bubbles around the tool coalesce into a gas film and discharges are generated through it. Glass machining is possible due to thermally promoted etching and bombardment of discharges [99, 180]. Although the performance of this process depends on several parameters including the tool shape and motion, voltage, electrolyte, and machining gap, the machining voltage proved to have a more significant effect on the material removal rate [181, 182].

SACE allows manufacturing of small and large holes (up to 2000 μm in diameter) and can produce high aspect ratios (>10), while achieving relatively transparent and smooth machined surfaces (R_a = 0.13 μm) on glass [180, 183-185]. Compared to laser processes, HAZ are less apparent in SACE, due to the reduced machining temperature (typically ~500 °C compared to ~2000 °C for laser). Also, compared to ultrasonic drilling, wet- and dry-etching of the machining speed per hole is high. However, the surface roughness is higher than that in most conventional wet and dry etch techniques.

Significant research work has been carried out to reduce HAZ and surface roughness by machining at the lowest possible temperature though reducing the critical voltage [186, 187], or using pulsed voltage [183, 188, 189]. Further improvement was achieved by post-processing of machined holes with electrophoretic deposition grinding (EPDG) which results in reduced HAZ, smooth surface and excellent taper angles (as low as 0.2 degrees) [180], while increasing the machining time (by 5 times).

A major problem encountered with SACE is the limited flushing of the machined material at high machined depths which reduces both the machining speed and quality. Several methods were proposed to allow more localized flushing of the machining zone, including:

- Adjusting the tool shape: different tool shapes including tools with side insulation, flat sidewalls, and spherical ends proved to reduce the taper and overcut [190], enhance machining accuracy [191-193], and reduce the hole entrance diameter by up to 65% and the machining time by up to 83% for a 500 mm deep hole [194].
- Tool rotation: results in smooth sidewalls (R_a down to 0.13 μm [183]) and reduced taper [184].
- Tool, electrolyte or workpiece vibrations: low frequency vibrations (0–30 Hz) of a cylindrical 400 μm tool increase the material removal rate (MRR) by factor of two [195] where square waveform showed better improved compared to sinusoidal tool vibration [196, 197]. Electrolyte ultrasonic vibration (1.7 MHz) shows improvements in machining depth (320 μm to 550 μm), and reduction in taper and overcut when applying ultrasonic vibrations to the electrolyte [198].
- Pulsed voltage: results in better machining and surface finish [199].

- Inducing a local magnetic field: locally stirs the electrolyte which enhances the surface quality and machining depth while reducing machining time (by around 57.4%) and the overcut (by 23.8%) and at low electrolyte concentration [200].
- Using force feedback control algorithms for drilling: algorithms applied to control the tool motion during drilling are promising for improving the machining quality and speed [81, 201-203].

2.3. Discussion

According to [92, 100, 101], high aspect ratio (>5) and low surface roughness (<1 μm), i.e., smooth surface morphology, of drilled micro-holes are the main requirements to achieve novel glass micro-devices, such as those in MEMS, MOEMS and bio-MEMS. Another important issue, especially for industry, is the machining speed, or more generally the cycle time, since this determines the process throughput and therefore its costs. Targeted hole diameters depend entirely on the application, varying from sub-micron (e.g., many MEMS applications) to sub-millimeter (e.g., smartphone cover glass). A comparison of these outcomes for all described technologies is shown in Figure 2.1, Figure 2.2, and Figure 2.3, constructed based on the values reported in Table A.1 (Appendix). Most of these values were given by the literature as discussed before; however, to have a sufficiently large sample number, more data was added in Table A.1 from additional literature [204-218]. Each area in the figures represents a different drilling technique. Figure 2.3 presents the minimum feature size of micro-holes to be machined on glass by the different technologies.
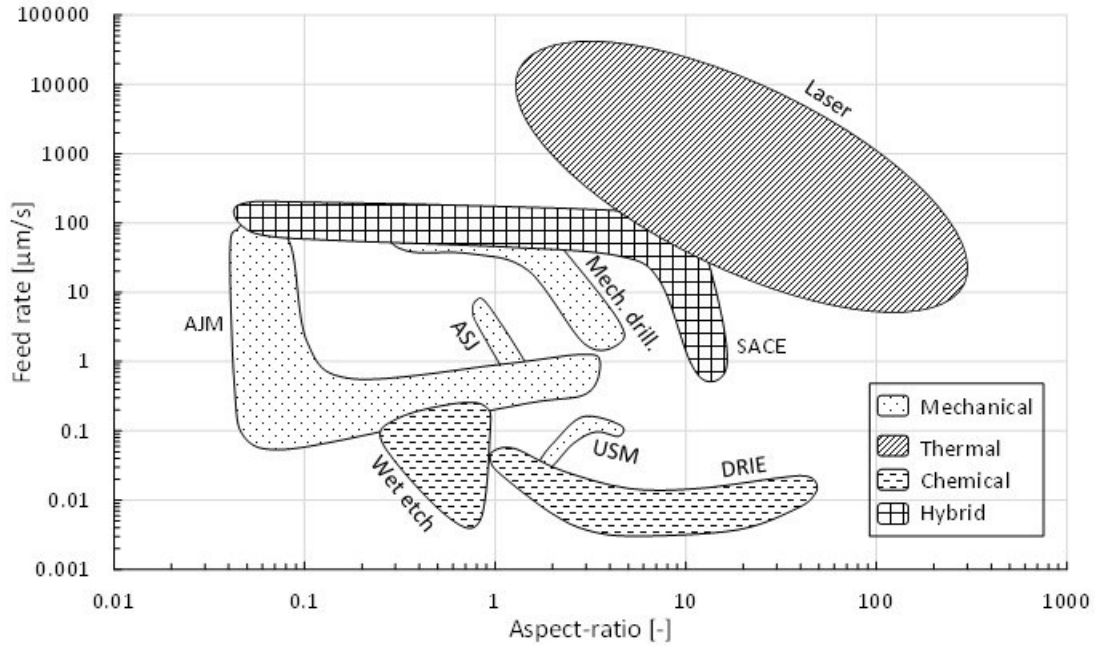
Figure 2.1. Feed rate (µm/s) vs. aspect ratio (µm/µm) for different glass drilling methods, grouped into four categories (mechanical, thermal, chemical and hybrid). Values in graph based on Table A.1.
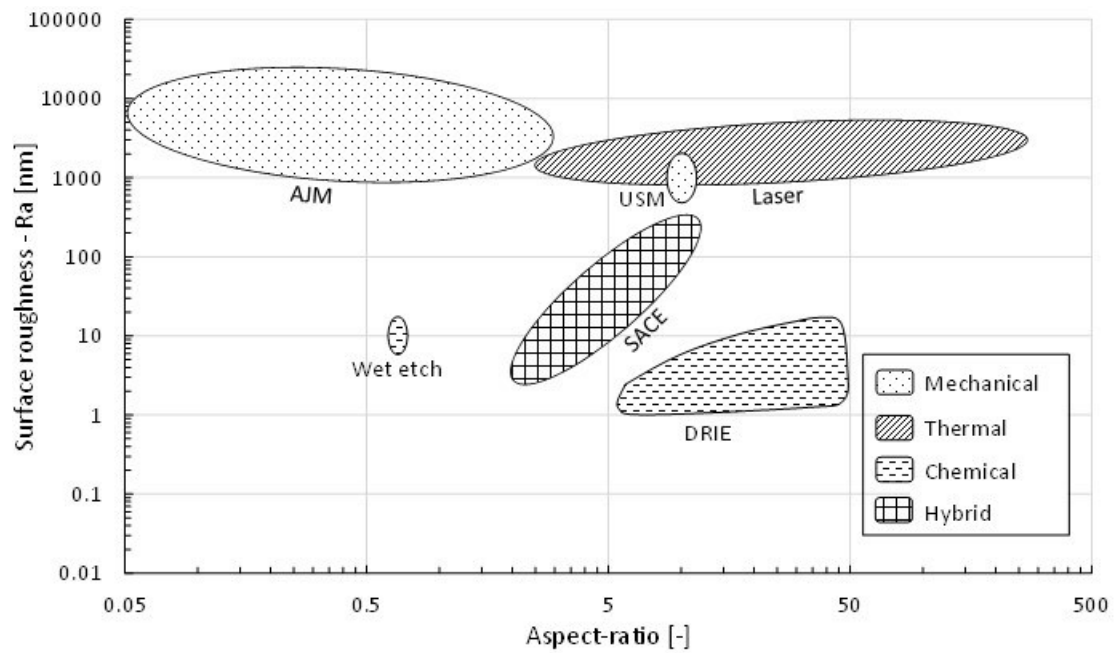
Figure 2.2. Surface roughness, R_a (nm) vs. aspect ratio (µm/µm) for different glass drilling methods, grouped into four categories (mechanical, thermal, chemical and hybrid). Values in graph based on Table A.1.
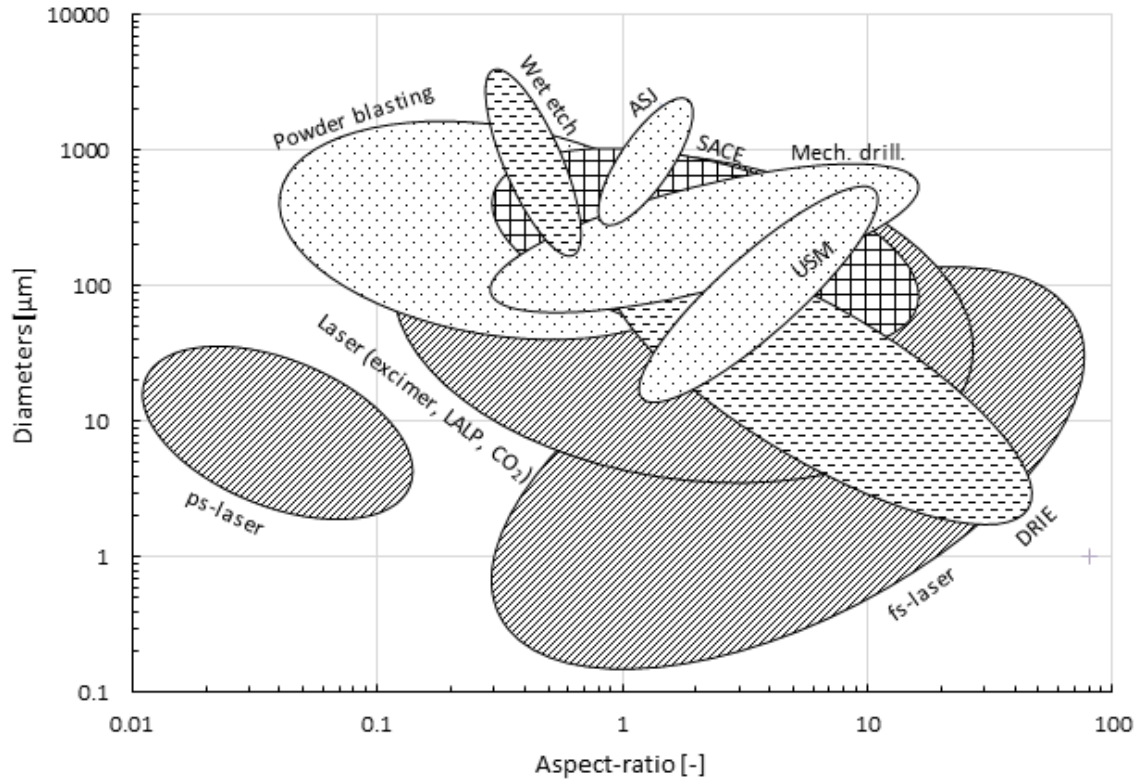
Figure 2.3. Machined diameters (µm) vs. aspect ratio (µm/µm) for different glass drilling methods, grouped into four categories (mechanical, thermal, chemical and hybrid). Values in graph based on Table A.1.

To produce high aspect ratio holes (up to 40) with low surface roughness ($R_a \sim 1$ µm), a chemical drilling technology like DRIE (Figure 2) can be used. DRIE has further the important ability to machine in parallel a large amount of holes (>200,000) with high accuracy. However, this batch process is slow (etching rates ~ 0.01 µm/s), complex (e.g., masks, operating conditions) and expensive. It has extremely low etch rate (per etched hole), uses sophisticated metal masks, and the equipment is rather expensive and complicated thus limiting its usage in industry. Furthermore, problems may occur when dry etching glasses containing lead or sodium (such as the most commercial standard soda-lime glasses) since this produces non-volatile halogen compounds as reaction products. Exclusively fused silica (formed mainly of silica) can be etched by this process, which restricts its use for a wide range of applications.

Thermal-based technologies, especially laser drilling, also produce high aspect ratio micro-holes (typical ~ 10–50) but with much higher speeds (up to 2000–20,000 µm/s) and less complexity compared to chemical machining (Figure 2.1). However, a good surface finish is not achievable in this case ($R_a > 500$ nm) and bulges form around the rims of the hole entrance for glass substrates, which prevent bonding. Similar to chemical processes, thermal processes are also expensive.

Regarding the ease of handling the machining process, mechanical drilling (Figure 2.1 and Figure 2.2) is in general the most favorable as it is well-established (e.g., powder blasting). Moreover, it is significantly cheaper than thermal and chemical processes. However, mechanical drilling cannot machine high aspect ratio micro-holes (typical ~ 4) and the resulting surfaces are rough

(chipping > 10 μm), requiring costly and time-intensive post-processes (polishing). As shown in Figure 2.1, Figure 2.2, and Figure 2.3, hybrid technologies like SACE provide a trade-off between acceptable machining speed and surface roughness with reasonably high aspect ratio (up to 11) and workable minimum dimensions for most glass applications.

While the above-mentioned comparison presents average ranges and values of hole specifications established in the four machining categories (mechanical, thermal, chemical and hybrid), in all manufacturing cases, specific requirements are needed and trade-offs are always necessary. Figure 2.1, Figure 2.2, and Figure 2.3 allow choosing the machining process based on trade-offs between the aspect ratio and machining quality and speed depending on the fabrication requirements.

For example, for an aspect ratio of 1, chemical (wet etching, ASJ) mechanical (powder blasting, mechanical drilling), thermal (laser drilling) and hybrid (SACE) machining can be used. Wet-etching (chemical) provides the best quality (10 nm R_a) but is the slowest (speed around 0.3 μm/s). A similar speed (0.25 μm/s) can be achieved with powder blasting (mechanical), but the surface roughness can increase from 2500 nm to 10,000 nm R_a. For fastest drilling, laser (thermal) can be used (speed can reach 20,000 μm/s) but quality is not the best (2000 nm R_a). For acceptable speed and quality, SACE drilling (hybrid) can be applied as speed reaches 120 μm/s, which is faster than chemical and mechanical techniques, and the resulting surface is smooth (<200 nm), which has lower roughness than achieved surface roughness by thermal and mechanical processes.

For a high aspect ratio of 10, DRIE etching (chemical) provides the best quality (4 nm R_a) but is very slow (0.01 μm/s speed). Laser machining (thermal) is the fastest (120 μm/s), but roughness is in average around 1000 nm. SACE (hybrid) provides a trade-off between good quality (200 nm R_a) and acceptable speed (reaches 10 μm/s in this case).

In summary, based on these comparisons, wet etching is relatively expensive due to the need of a cleanroom and multiple process steps (e.g., masking), although it is still a good option for mass production of low aspect ratio structures requiring high surface quality. Laser drilling is also

relatively expensive, due to the need of sophisticated setups and laser sources, but it is a good option for fast and flexible drilling requiring good surface quality. Mechanical drilling and hybrid technologies such as SACE/ECDM may be the most suitable for prototyping as they are the cheapest processes; unfortunately, they either do not result in good surface quality or are relatively slow.

We constructed Table 2.1 based on the information presented in this review. Table 2.1 summarizes the qualitative comparison of the different technologies based on the achievable aspect ratios, machining speed and surface roughness. Low aspect ratios are defined as below 10, low machining speeds refer to speeds below 100 μm/s and low surface roughness (high quality) refers to roughness lower than 100 nm ($R_a < 100$ nm).

Table 2.1. Features of the four main groups of drilling technologies for glass.

Process	Mechanical				Thermal		Chemical		Hybrid
	Mechanical Drilling	Powder Blasting	ASJ	USM	Laser Drilling	FEDM	Wet Etching	DRIE	SACE
Aspect Ratio [1]	−	−−	−−	−	++	−	−−	++	+
Machining Speed (Serial) [1]	+	−	−−	−−	++	+	−−	−−	+
Surface Roughness [2] (R_a)	−	−−		−	−	+	+	++	+
Minimum Dimensions (μm)	150	50	300	200 (10)	5	20	1	0.5	100
Rapid Prototyping (Serial Mode) [3]	++	−−	+	+	++	−	−−	−−	++
Mass Fabrication (Parallel Mode) [3]	−−	++	−	−	−	+	++	++	−−
Tooling Complexity/Costs [4]	−−	−−	−	−	++	+	−−	−−	++
Applicable to Wide Range of Glass Types [3]	++	++	++	++	+	−−	−	−−	++
Equipment Costs/Complexity [5]	++	+	+/−	−	−	−	−	−−	+

On a scale of 1 to 4, the above symbols indicate: (−−) Level 1; (−) Level 2; (+) Level 3; (++) Level 4. Level 1 and Level 4 are indicated for each column on the table. [1] low −−, high ++; [2] high −−, low ++; [3] non-applicable −−, applicable ++; [4] complex −−, simple ++; [5] expensive −−, cheap ++.

2.4. Conclusions

2.4.1. Evaluation of glass micro-hole drilling technologies

An overview of commonly used technologies for micro-hole drilling in glass is presented. The technologies are divided into four categories: mechanical, thermal, chemical and hybrid drilling technologies. Based on the review, graphs are constructed for aspect ratio versus machining speed and aspect ratio versus surface roughness to get a comprehensive comparison of the different technologies. Furthermore, a qualitative comparison of the main characteristics of the technologies is summarized in a table. This paper helps in identifying the glass micromachining technology that is currently most suitable for a certain application based on machining requirements.

Each of the drilling technologies has certain limitations. While thermal processes such as laser drilling are fast and flexible, they lack high surface quality. Chemical processes such as wet etching establish smooth surfaces; however, masks are required, resulting in more complexity, low flexibility and higher cost of the process. Mechanical methods such as conventional drilling are relatively slow and exhibit poor surface roughness. To overcome the burdens of certain technologies while taking advantage of the good process outcomes, research is ongoing on developing and implementing hybrid micro-technologies which combine two or more machining technologies to reach an outcome that satisfies most requirements for the desired micro-holes in glass.

2.4.2. Assessment on mass-personalization requirements

As we have now compared and evaluated the different glass micro-drilling technologies quantitatively (Figure 2.1, Figure 2.2, Figure 2.3, Table A.1) and qualitatively (Table 2.1), it is interesting to assess these technologies on the key requirements for mass-personalization. These requirements were proposed in Chapter 1 (Figure 1.5, Table 1.2) by identifying the main manufacturing cost drivers related to specific part design:

1) abandon lengthy calibration runs;

2) avoid any part specific tooling (reduce tooling costs and complexity);

3) be able to handle complex parts;

4) reduce production steps (each step increases overhead and introduces machining errors);

which is detailed in Table 2.2.

Table 2.2. Assessment of glass micro-drilling technologies to the four key part related manufacturing cost drivers to be eliminated for mass-personalization.

Glass drilling technology		Part related manufacturing cost drivers			
		Calibration [1]	Tooling [2]	Complexity [3]	Number of processing steps [4]
Mechanical	Mechanical drilling	--	--	+	-
	Powder blasting	--	--	-	--
	ASJ	--	--	-	--
	USM	--	-	+	-
Thermal	Laser drilling	+	+	-	+
	FEDM	+	+	--	-
Chemical	Wet etching	--	--	+	--
	DRIE	--	--	+	--
Hybrid	SACE	-	+	+	+

On a scale of 1 to 4, the above symbols indicate: (――) Level 1; (−) Level 2; (+) Level 3; (++) Level 4. Level 1 and Level 4 are indicated for each column on the table. [1] intricate/lengthy ――, simple/quick ++; [2] complex ――, simple ++; [3] no-capability ――, capability ++; [4] high ――, low ++.

Evaluating Table 2.2, it can be concluded that hybrid technologies such as SACE process or thermal processes such as laser drilling are promising candidates for flexible micro-drilling in glass and they have the most potential to fulfill the requirements for high-precision manufacturing of mass-personalized parts made of hard-to-machine materials such as glass. Considering the evaluation presented in Table 2.1 it is determined that SACE technology outperforms laser drilling on achievable surface roughness, its almost unlimited range of machinable glass types and its relatively simple setup and low investment cost compared to ultrashort (femtosecond) laser equipment. Therefore, it is chosen to further study this (hybrid) SACE technology on mass-personalization for high-precision glass parts.

However, SACE technology is so far never used for mass-personalization as machining overhead of this process is still very high. New approaches are needed to eliminate extensive setup calibration (e.g. for tool run-out reduction) and workpiece clamping devices commissioning to make this electrochemical discharge machining process suitable for batch size 1 production. Chapter 4 will present a novel strategy and realized setup to achieve this objective. A predictive model, for several machining operations, providing guidelines for a quick setup of SACE process parameters, reducing dramatically the time in several fabrication cycles, is presented in chapter 3.

Chapter 3

Glass cutting, and milling are essential machining operations, which are required for most glass parts to be machined. Contrary to micro-hole drilling on glass substrates, which is well researched by academia [83, 199] resulting in defined drilling strategies [195, 219] showing the need for force feedback-controlled tool-electrodes [203, 220], no models are available for glass cutting and milling, relating SACE process input parameters to MRR (feed-rate together with depth-of-cut per machining pass). Such a model is a key requirement for setting up efficiently (i.e. low setup time) manufacturing systems with a high degree of automation. Currently, it takes a significant number of time-consuming trial and error runs before the process parameters (machining voltage, feed-rate, depth-of-cut) for cutting and milling operation settings are found.

This chapter presents the derivation and development of a predictive model for glass cutting and milling by SACE process. It is based on solving numerically the transient two-dimensional heat equation with the heat generated by the sparks around the tool-electrode taken as input in the model. The proposed model, which correlates the machining input parameters to a desired outcome, was empirically verified and validated, allowing further optimization of industrial implementation of SACE technology as no predictive model for SACE glass cutting existed before. This model contributes in addressing the requirement of a high level of integration in the design to fabrication cycle for precision product manufacturing, which is essential for mass-personalization fabrication processes to reduce the machining overhead. A dramatic reduction of setup time by eliminating trial and error runs for process optimizing is realized by use of the developed model for glass cutting by SACE technology. Furthermore, a strategy is developed to reduce the surface roughness of cut by introducing Spark Assisted Chemical Polishing (SACP).

Glass micro-cutting and -milling by Spark Assisted Chemical Engraving

3.1. Introduction

3.1.1. Glass machining and applications

The application of glass science to the improvement of industrial tools occurred only in the past century, with a few exceptions. Glass has been employed in many forms to fabricate glazing and containers for centuries while it is now entering new applications that are appearing in micro and even nanotechnology like fibers, displays and Micro-Electro-Mechanical-System (MEMS) devices [70, 71]. Many qualities make glass attractive since it is transparent, chemically inert, environmentally friendly and its mechanical strength and thermal properties. In fact, no other materials being mass-produced have shown such qualities over so many centuries. Nowadays glass offers recycling opportunities and allows for tailoring new and dedicated applications. Moreover, glass is radio frequency (RF) transparent, making it an excellent material for sensor and energy transmission devices. Another advantage of using glass in microfluidic MEMS devices [72] is its relatively high heat resistance, which makes these devices suitable for high temperature microfluidic systems [75] and sterilization by autoclaving.

However, glass remains a difficult to machine material. Its brittleness, chemical resistance and relatively high thermal conductivity challenges available technologies. An interesting approach is the use of hybrid technologies such as Spark Assisted Chemical Engraving (SACE) [81] which is a thermochemical process (Figure 3.1).

In SACE process, a voltage is applied between tool- and counter-electrode dipped in an alkaline solution - typically Sodium Hydroxide (NaOH) or Potassium Hydroxide (KOH) (Figure 3.1). At high voltages (around 30 V), the bubbles evolving around the tool electrode coalesce into a gas film and discharges occur from the tool to the electrolyte through it. Glass machining becomes possible due to thermally promoted etching (breaking of the Si-O-Si bond) [81, 221].
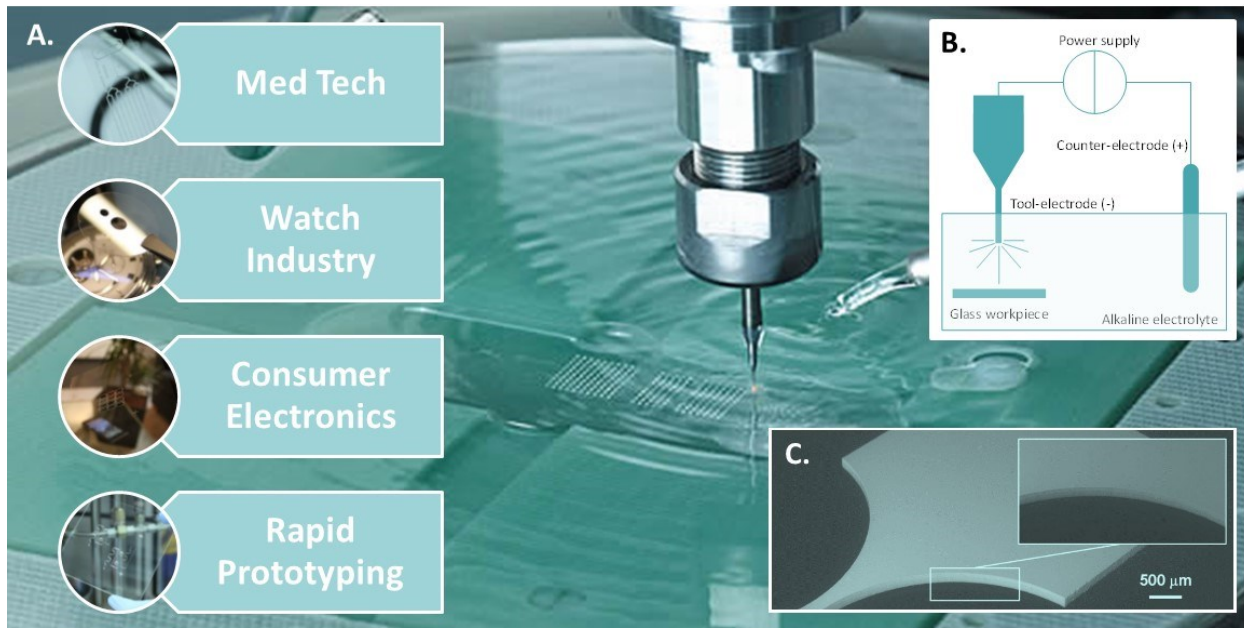
Figure 3.1. A. Overview of targeted applications/markets for SACE glass machining. **B.** SACE principles. C. SACE machined micro-hinge (scale bar = 500 μm - width of 'hinge' = 30 μm - thickness glass = 100 μm).

Developed since the sixties in last century in academia [222, 223], SACE found recently its entrance in the industrial world [224]. Micro-drilling was intensively characterised and developed. The introduction of pulsed voltage machining did make a further significant step forward in terms of quality of machining [192, 225]. High precision micro-holes with good quality can be obtained as shown in Figure 3.2.
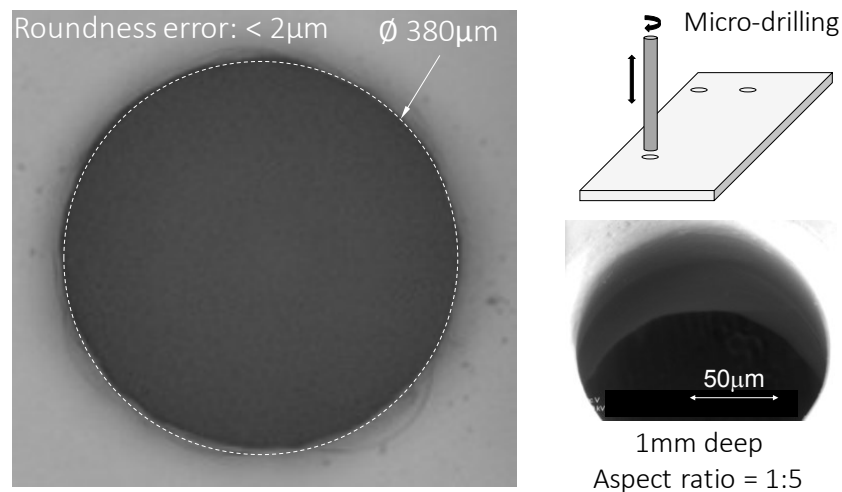
Figure 3.2. High quality micro-holes in glass machined by SACE technology. Roundness errors smaller than 2 μm can be achieved (machined on the Microfor SACE developed together with Posalux SA [224]).

SACE can however as well be used to micro-cut glass. This aspect was so far never discussed in the literature and no systematic data about its performance are available. Glass micro-milling by SACE process is reported in literature [199], but machining guidelines to choose input process parameters for a desired outcome are lacking, leading to time-consuming trial runs before machining can be performed. This limits its use as agile manufacturing process as needed for fabrication of mass-personalized products.

3.1.2. Requirements for high-precision glass machining of mass-personalized parts

High level of integration in the design to fabrication cycle, by digitalization, is required for efficient manufacturing of products (parts) in both large and small batch size production (see table 1.1). Particularly for batch size 1 production, e.g. mass-personalization, it is indispensable to have a time- and cost-efficient workflow from part design (model) to the manufacturing process. First step is generally generating the desired model in a Computer Aided Design (CAD) environment or another software. Subsequently, a specific machine code, most often G-code (based on ISO 6983) [226] or a more associative communication protocol such as STEP-NC (based on ISO 14649) [227], is created from the digital model for proceeding to the manufacturing step (e.g. define the toolpath for glass machining, which is fed into the machine). This translational digital coding step is a critical tool for batch size 1 manufacturing to enable agile handling of constantly changing part manufacturing requests. Such a tool allows quick loading of new part designs into the machine and automated conversion into important machine process instructions like toolpath definition, feed-rate, and other process related input parameters.

Fundamental knowledge of the machining process and the machine itself, based on both experience and predictive models, is essential to enable this step [228]. In the case of established conventional Computer Numerical Control (CNC) machining techniques, such as mechanical milling and turning, machine codes can relatively easily be derived as these processes are well-known and a wide range of models exists for these operations. For instance, surface roughness prediction models for CNC machining of polypropylene [229], predictive models for the cutting force in wood machining [230], and finite element models (FEM) to relate feed-rates and surface roughness for face milling of titanium alloys [231], advanced predictive models (based on artificial neural networks or fuzzy logic models) for machining parameter optimization for metal alloys [232-235], models for performance prediction in multi-axis machining [236], material removal

rate (MRR) predictive models for CNC turning of steel alloys [237] and predictive models for feed-rate control of milling machines [228] are well-established in literature.

However, as these mechanical methods are suitable for machining relatively soft materials such as wood [230] or polymer material [229] and standard engineering materials such as metals, it is challenging to machine glass, because of its hardness and brittleness, with high quality and precision (refer to chapter 1 and 2 for comparative studies on micro machining technologies).

Furthermore, the high forces exerted on machining tool and workpiece by these conventional high precision machining techniques [238, 239] demand rigid and sophisticated clamping (i.e. complex tooling), making these methods non-compatible as flexible machining processes required for batch size 1 fabrication [30] of glass components.

Intermittent contact technologies like ultrasonic machining [240] can be deployed for glass micro machining, nevertheless besides having its own process limitations, these approaches still need rigid and high precision clamping tools disfavouring its utility as mass-personalization fabrication technology.

Non-contact glass micro machining processes like wet etching [85] and DRIE etching [82, 160] eliminate the need of rigid clamping tools, but they require sophisticated and time-consuming masking techniques in clean-room environment and are limited to producing 2D structures, making them highly inappropriate for flexible machining of low batch sizes.

SACE technology, being a hybrid thermochemical process, provides high precision glass micro-drilling, micro-milling, micro-cutting and micro 3D machining operations in one setup. The implementation of a force-sensitive machining head enables the usage of the machining tool to be used as an accurate profilometer to measure machined features within the same setup to an accuracy of 1 μm, enabling continuous three-dimensional control of the machined features. These characteristics and its ability to execute different machining operations on the same setup makes SACE an interesting potential candidate for flexible, high precision glass machining meeting the demand of batch size 1 production (i.e. mass-personalization).

As of today, SACE process was never deployed for glass mass-personalization by industry and academia. In fact, we can identify three main issues of the current SACE method preventing its use for this highly flexible manufacturing approach:

1. Contrary to micro-hole drilling on glass substrates, which is well researched by academia [83, 199] resulting in defined drilling strategies [195, 219] showing the need

for force feedback-controlled tool-electrodes [203, 220], no models are available for glass cutting and milling, relating SACE process input parameters to MRR (feed-rate together with depth-of-cut per machining pass). Such a model is a key requirement for setting up efficiently (i.e. low setup time) manufacturing systems with a high degree of automation. Currently, it takes a significant number of trial and error runs before the process parameters (machining voltage, feed-rate, depth-of-cut) for appropriate cutting and milling operation settings are found;

2. Extensive calibration is needed for tool-workpiece alignment and tool run-out elimination to achieve the desired high-precision (~ 1 µm);

3. Part specific tooling is required for proper clamping of the glass workpiece (almost each production cycle demands changing dimensions in the case of mass-personalization) to attain high precision.

As issues 2 and 3 will be addressed by the subsequent chapter 4, this chapter aims to develop SACE cutting and milling strategies to overcome the issue of lacking fundamental knowledge and models to efficiently execute these machining operations (addressing issue 1). As a first step, basic parameters such as depth of cut and tool feed rate must be determined. In fact, key input parameters for operating SACE process are 1) machining voltage, 2) depth of cut, and 3) machining speed (feedrate). Objective of chapter 3 is to find a basic, valid model for SACE machining (milling, cutting) to avoid time-consuming trial runs before part machining. It needs to be stressed out that the aim of the model is not to describe precisely the process' physics, but the goal is to develop a practical model, which can be used to increase the SACE operating efficiency.

Systematic experiments are reported on micro-cutting glass by SACE and it is demonstrated how using available data from SACE micro-drilling maximal depth-of-cut and tool feed can be determined.

3.2. Theory

Material removal rate in SACE machining is limited, in case flushing of the machining zone happens easily, by heat propagation in the glass workpiece [81, 221]. In the case of micro-cutting and -milling, electrolyte can access freely to the machining zone by appropriate flushing, using side tubes for electrolyte supply in the machining cell (Figure 3.1). Further machined material is

removed readily from it through the cut. Consequently, as a first approximation, one can discuss the relation between the axial depth of cut p and horizontal feed rate F (see Figure 3.3 for a schematic) in terms of time needed for the heat to propagate inside the workpiece: one has to give enough time to the workpiece to heat up while one moves the tool.
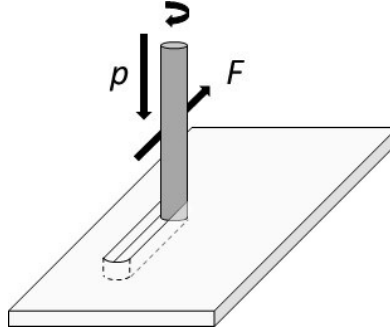
Figure 3.3. Schematic representation of micro-cutting by SACE process with a rotating tool-electrode (radius r) moving horizontally with feed-rate F at an axial depth of cut p.

Consider a tool of radius r. In the time interval

$$t_F = \frac{2r}{F} \tag{3.1}$$

the tool will move over its own size. If heat propagates at the rate h_r inside the workpiece, then the time t_h needed to heat a distance p is given by

$$t_h = \frac{p}{h_r} \tag{3.2}$$

If heat propagation is the rate limiting process, the tool is not allowed to move faster than the feed rate F at an axial depth of cut p such that (t_F and t_h must be of the same order of magnitude):

$$F \cdot p = 2r \cdot h_r \tag{3.3}$$

Equation (3.3) shows that, under the stated hypothesis that machining is only limited by heat propagation, the maximal value of the product $F{\cdot}p$ is, for a given tool and workpiece, a constant value. Note that, as the time t needed to cut a path of length L and depth d is given by

$$t = L \cdot d \frac{1}{F \cdot p} \tag{3.4}$$

and consequently, the time needed to perform a given cut is essentially constant for a given product $F{\cdot}p$ as chosen.

The heat propagation rate h_r is function of the geometry of the problem and the energy put into the system (i.e. energy produced by the spark activity around the tool electrode).

As a first step, the model developed in the frame of SACE drilling is attempted to be used [81]. The heat brought to the substrate by the electrochemical discharges is approximated by a heat source (cylindrical tool-electrode of radius b) of power P_o inside a homogenous material of density ρ, specific heat capacity c and thermal conductivity λ (Figure 3.4). At infinity, the temperature is assumed to be constant and equal to T_o. Further we assume that machining occurs when the temperature of the work piece reaches the machining temperature noted as T_M. For a more detailed discussion on the different machining mechanisms and physical meaning of this machining temperature the reader is referred to [81].

The heat power P_o can be estimated as a fraction of the mean heat power P_E of the electrochemical discharges as this will only be partially be transferred to the machined substrate. Here, P_E is a function of the machining voltage, water decomposition potential, mean current and inter-electrode resistance of the electrolyte [81].
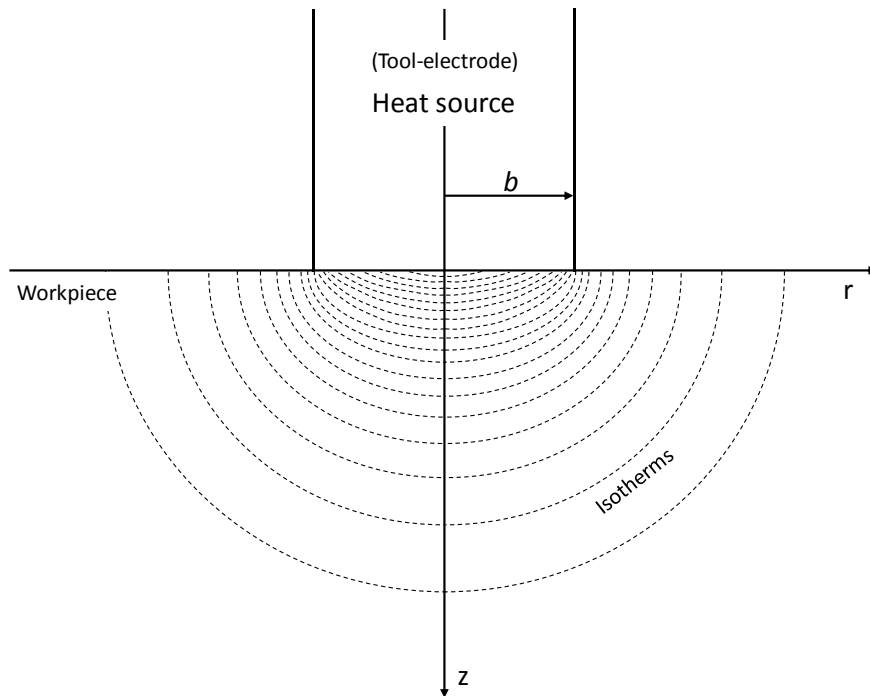
Figure 3.4. Model of the temperature distribution for SACE machining. A cylindrical homogeneous disc heat source with radius b provides the heat power needed to locally heat up the workpiece.

In the space outside the heat source, the temperature distribution T satisfies [241, 242]:

$$\frac{\rho c}{\lambda} \frac{\partial T}{\partial t} = \nabla^2 T.$$ (3.5)

It is convenient to use dimensionless variables, so the results of this study can be applied to any specific situation and geometry. Here, we use the same normalization as used in previous models in the case of SACE machining and define the normalised length $\bar{z} = z/b$ and the normalized time $\bar{t} = t/\tau$ with the characteristic time $\tau = b^2/4a$ [81]. Here, a is the thermal diffusity of the workpiece $a = \lambda/\rho c$. For the temperature we define [81]:

$$\bar{T} = \frac{T - T_o}{P_o/(\lambda \pi b)},$$ (3.6)

Using this normalization, equation (3.5) writes

$$4 \cdot \frac{\partial \bar{T}}{\partial \bar{t}} = \nabla^2 \bar{T}$$ (3.7)

In SACE theory, it is common to introduce the *normalized heat power – κ* [81]:

$$\kappa = \frac{P_o}{\lambda \pi b (T - T_M)}.$$ (3.8)

As will be seen below, this parameter is convenient for normalizing the heat power P_o of the heat source.

So far in the literature, Equation (3.5) was solved considering a disk heat source, which assumes that the heat is essentially uniformly distributed over the entire tool:

$$\lambda \frac{\partial T}{\partial z}(r, z = 0, t) = \begin{cases} 0 & r > b, \\ -\dfrac{P_o}{\pi b^2} & r \le b. \end{cases}$$ (3.9)

The aim in solving Equation (3.5), is to determine at which rate h_r the isotherm of the machining temperature T_M is propagating inside the workpiece. In order to do this, it is needed to compute

$$h_r = \frac{dz(t_o)}{dt}$$ (3.10)

where t_o is the time needed for the temperature at the workpiece surface to reach the machining temperature (i.e. $T(0,t_o)=T_M$) and $z(t)$ is the z-coordinate on the symmetry axis at which the isotherm T_M is located. In normalized form, $\bar{z}(t)$ is determined by solving

$$\bar{T}(\bar{z},\bar{t})=\frac{1}{\kappa}. \tag{3.11}$$

Solution of equation (3.5) with boundary condition (3.6) allows to compute the rate at which this isotherm propagates in the workpiece in the z direction [81]:

$$\bar{h}_r = \frac{d\bar{z}(\bar{t}_o)}{d\bar{t}} = \frac{1}{2\sqrt{\pi}}\frac{1-e^{-1/\bar{t}_o}}{\sqrt{\bar{t}_o}}. \tag{3.12}$$

A relevant case for SACE in the case of glass machining is when one considers low heat power ($\kappa \approx 1$, $\bar{t}_o \gg 1$) [81]. This relates to machining scenarios when voltages in the range of 20 V $< U$ < 50 V are applied. In this case one obtains for the heat propagation rate [81]:

$$\bar{h}_r \cong \frac{\kappa-1}{2\kappa}\left[1-\exp\left(-\frac{\pi(\kappa-1)^2}{\kappa^2}\right)\right], \tag{3.13}$$

If one assumes now that h_r is a typical order of magnitude for the heat propagation, one can estimate the product $F \cdot p$, using equation (3.3), as:

$$F\cdot p = 4a\cdot\frac{\kappa-1}{\kappa}\left[1-\exp\left(-\pi\left(\frac{\kappa-1}{\kappa}\right)^2\right)\right] \tag{3.14}$$

Consequently, under the hypothesis of a disc heat source, cutting time in SACE is independent of the tool radius. This is a very important result, not only from theoretical point of view, but from practical too. It shows that if the hypothesis to consider the heat source as a uniform disc source is acceptable, then cutting time becomes independent of the choice of the tool radius.

Relations between the dimensionless *normalized heat power* - κ and applied machining voltage U are empirically derived in section 5.2 of [81] in case of drilling with cylindrical tools:

$$\kappa = 0.018 \cdot U + 0.615 \tag{3.15}$$

Equation (3.14) and (3.15) allow to establish a direct relationship between the machining voltage U and the product $F \cdot p$ which can be used to define the material removal rate (MRR), for

glass machining by SACE technology ($a \sim 6 \cdot 10^{-7}$ m^2/s for Pyrex$^{®}$ glass [243]), when multiplying with the tool diameter ($2 \cdot b$).

Equation (3.14), holds for the case of small tools (tool radii < 100 μm as will be shown by the experimental results in the results and discussion section). However, for larger tools cutting happens at significantly smaller feed rates, respectively lower depth of cuts than the one predicted by equation (3.14). As a first attempt to enhance this simplified model, a more realistic heat source model is proposed using a ring heat source of radius b and ring thickness e (Figure 3.5):

$$\lambda \frac{\partial T}{\partial z}(r, z = 0, t) = \begin{cases} 0, & r > b \\ -\dfrac{P_0}{\pi[b^2 - (b-e)^2]}, & r \leq b \end{cases} \qquad (3.16)$$

Equation (3.16) allows to model the reduced efficiency of the center of the tool compared to the tool edge in terms of heat source. To solve equation (3.5) with boundary condition (3.16) a numerical model was implemented in the Matlab$^{®}$ PDE Toolbox [244].
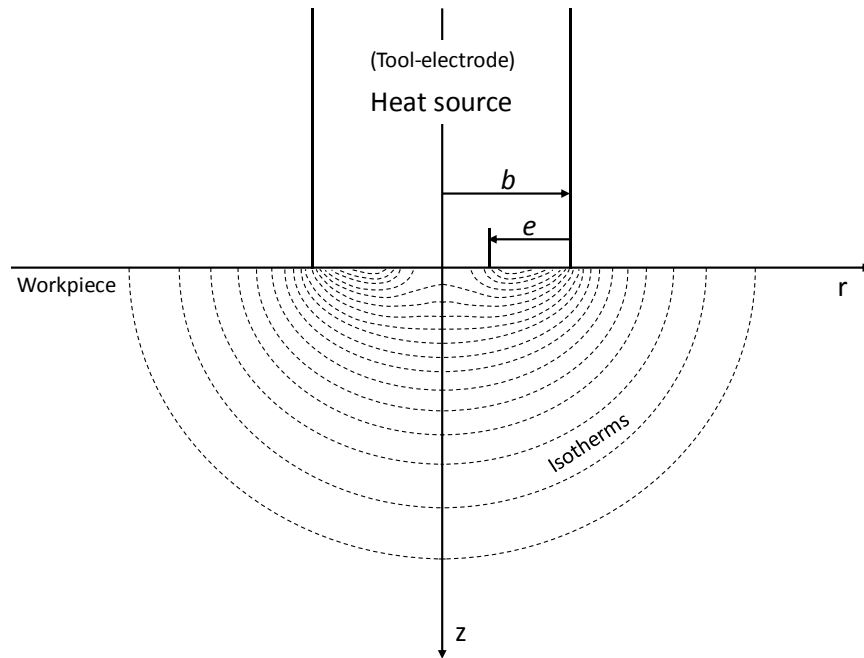
Figure 3.5. Model of the temperature distribution for SACE machining. A cylindrical homogeneous heat source (ring heat source for $0 < e < b$ and a disc heat source for $e = b$) provides the heat power needed to locally heat up the workpiece.

To facilitate general use of the model after calculations, the normalized heat equation (3.7) was used and equation (3.16) was written in normalized form. The boundary condition (3.16) in normalized form writes:

$$\frac{\partial \bar{T}}{\partial \bar{z}}(\bar{r}, \bar{z} = 0, \bar{t}) = \begin{cases} 0, & \bar{r} > 1 \\ \left[-\cfrac{1}{1 - \left(1 - \cfrac{e}{b}\right)^2} \right], & \bar{r} \leq 1 \end{cases} \tag{3.17}$$

Since model (3.5) is axisymmetric (Figure 3.5), it is convenient for the numerical analysis to write this equation in cylindrical coordinates [241, 242]. Noting that $\partial T / \partial \theta = 0$ and after multiplying by r equation (3.5) becomes:

$$r\rho c \frac{\partial T}{\partial t} - \frac{\partial}{\partial r}\left(\lambda r \frac{\partial T}{\partial r}\right) - \frac{\partial}{\partial z}\left(\lambda r \frac{\partial T}{\partial z}\right) = 0 \tag{3.18}$$

This equation is converted to the form supported by the PDE Toolbox [244] if r is defined as y and z is defined as x (Figure 3.6, left above). Rewriting equation (3.18) gives:

$$\rho c y \frac{\partial T}{\partial t} - \nabla \cdot (\lambda y \nabla T) = 0 \tag{3.19}$$

Equation (3.19) can be written in normalized form (equation (3.7) multiplied with $\bar{y}$):

$$4 \cdot \bar{y} \cdot \frac{\partial \bar{T}}{\partial \bar{t}} = \bar{y} \cdot \nabla^2 \bar{T} \tag{3.20}$$

Figure 3.6 presents the used cylindrical coordinate system in the PDE Toolbox and the solutions of the numerically solved equation (3.20) with boundary condition (3.17) for various values of normalized ring thickness $\bar{e} = e/b$ (ranging from $\bar{e} = 1.0$ to $\bar{e} = 0.6$). Boundary conditions of the second kind (Neumann [241]) are applied along the r axis as defined by equation (3.17) multiplied with y, and along the z axis as this is the centerline of the cylindrical tool-electrode (heat source). Boundary conditions of the first kind (Dirichlet [241], here $\bar{T} = 0$) are applied at the borders of the modeled workpiece, parallel to the $\bar{r}$ axis at $\bar{z} = 10$ and parallel to the $\bar{z}$ axis at $\bar{r} = 10$.

It can be noted from the simulation results that heat propagation in axial (z) direction is of the same order of magnitude (only slightly slower) as heat propagation in radial (r) direction for all

cases of $0 < \bar{e} \leq 1$. This justifies the use of axial heat propagation (dz/dt) in the modelization of the cutting operations.
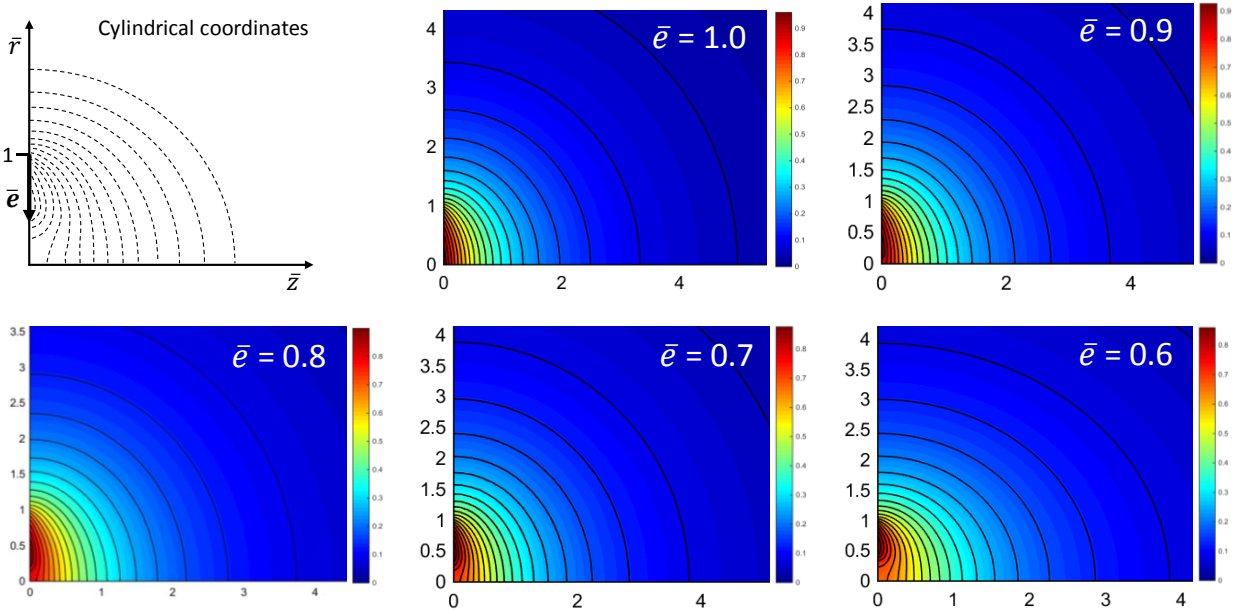
Figure 3.6. Solutions (isotherms $- 1/\kappa$) of the numerically solved (Matlab® PDE Toolbox) equation (3.20) with boundary condition (3.17) for various values of ring thickness $\bar{e} = 1.0$ down to $\bar{e} = 0.6$ at $\bar{t} = 2000$.

Employing condition (3.11), graphs were constructed for $\bar{z}$ versus $\bar{t}$ at different values of the normalized heat power κ (ranging incrementally from $\kappa = 1$ to $\kappa = 1.5$ as typical working range for SACE machining). Through differentiating the polynomial fits (varying from order 2 to 4) of these graphs around the time $\bar{t}_0$ (normalized time needed for the temperature at the workpiece surface to reach the machining temperature), the rate of normalized heat propagation $d\bar{z}(\bar{t}_0)/d\bar{t}$ could be derived, which is plotted for different ring thickness ($\bar{e} = 1.0$ to $\bar{e} = 0.6$) at different values for normalized heat power ($\kappa = 1.1$ to $\kappa = 1.5$) in Figure 3.7.
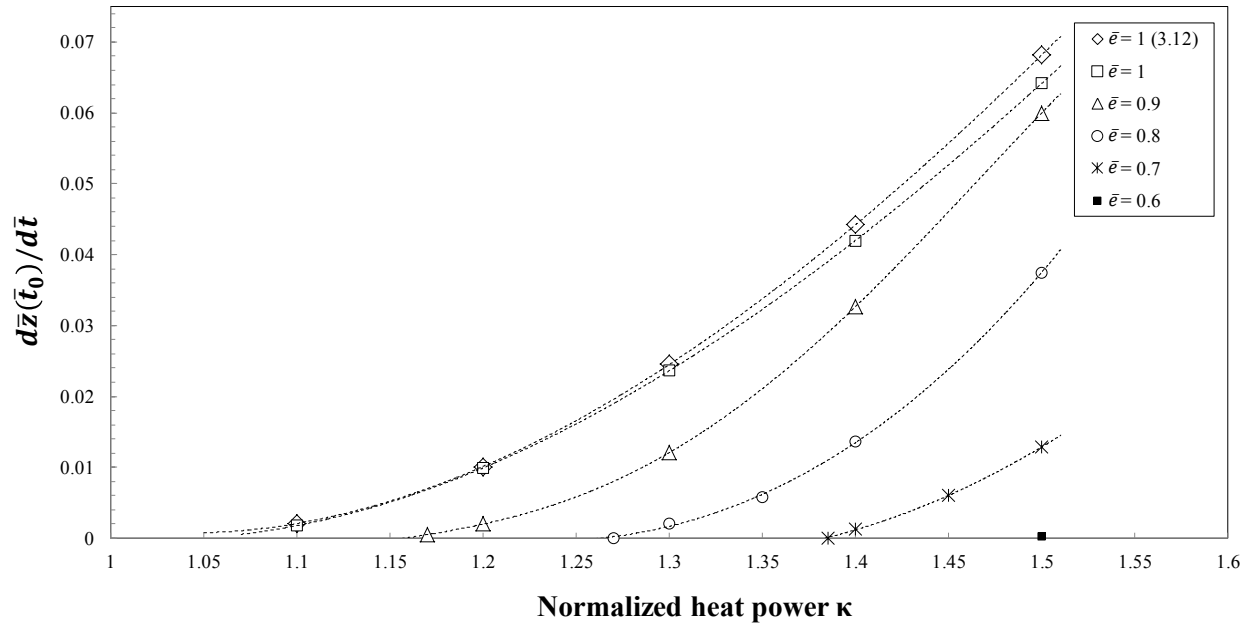
Figure 3.7. Rate of normalized heat propagation - $d\bar{z}(\bar{t}_0)/d\bar{t}$ versus normalized heat power κ for different values of ring thickness $\bar{e}$ = 1.0 down to $\bar{e}$ = 0.6.

3.3. Materials and Methods

Micro-cutting and -milling of Pyrex® glass (microscope slides, 25 mm x 75 mm, Corning) were performed on an in-house built laboratory setup (Figure 3.8.A.) and on a Posalux Microfor SACE machine (Figure 3.8.E.). The machine incorporates a force sensor in the machining head that allows online measurement of the axial force (down to 1 mN) exerted on the tool-electrode. Section 3.4 discusses in more depth why such force-sensitive machining tool-head is essential for efficient SACE machining. The developed industrial machining head, which is patented [60], is discussed in more detail in section 3.5.

Control of the developed industrial Microfor SACE machine is performed by G-code [226] and a LabVIEW [245] interface, processed by a Siemens IPC 477D Win AC RTX controller [246]. The machining head is mounted on precision (~1 µm) xyz-translational axes and consists of a spindle rotating in air bearings to deliver high degree of stiffness control. The machine enclosure is connected to a ventilation system with air filter reducing machine placement requirements and environmental issues. An electrolyte circulation system consisting of a pulse-damped rotary pump connected to tube outlets around the tool-electrode enables control of a uniform and smooth, bulk

and local, electrolyte flow in the working cell. This is important for SACE process repeatability as found empirically and confirmed by [247].

The developed home-built setup comprises a high-precision (~1 µm) Newport cartesian robot [248] (xy-stage – M-ILS150CC, z-stage – M-ILS50CC), where the working electrochemical cell was mounted on the xy-stage and the machining head on the z-stage. Rotation of the spindle, mounted in two ball-bearings on a flexible structure [249], was performed by a brushless DC motor (Maxon, EC 32 flat, 15 Watt) via a flexible round belt (SDP/SI, neoprene, 1/16" diameter). Axial displacement was real-time measured by an optical sensor (SFH9201, OSRAM Opto Semiconductors) and the axial force was measured and controlled using a voice coil actuator (LA-08-10-100, BEI Kimco Magnetics), which was used as well for fine axial displacement of the tool. Force feedback control (PID) implementation, xyz-stage motion, voice coil and spindle servo drives were controlled on a dSPACE and a Newport XPS controller [250]. Tool Command Language (Tcl) [251] was deployed as dynamic programming language for programming the motion and servo drive systems.

As electrolyte, 30 wt% Potassium Hydroxide (KOH) [252], prepared from de-ionized water, was used. Low viscous electrolyte is chosen to reduce the chance that flushing with fresh electrolyte at the machining zone becomes the limiting factor for machining (cutting, milling).

Cylindrical tool electrodes, made of tungsten carbide, 100 µm and 200 µm diameter with a bevel of 45° where used (machined by external grinding). Use of beveled tools were empirically found to perform better than flat tools, most probably due to improved electrolyte flushing in the machining zone. The spindle was rotated at 1000 rpm. Cuts were performed over an equivalent length of at least two minutes of micro-cutting, adapted at the operating cutting speed.

After cutting, images were acquired with an optical microscope (Keyence VHX 5000) and a Scanning Electron Microscope (SEM) (Hitachi S-3400N - variable pressure) to evaluate precisely the realized depth-of-cut and to evaluate the cut qualitatively.
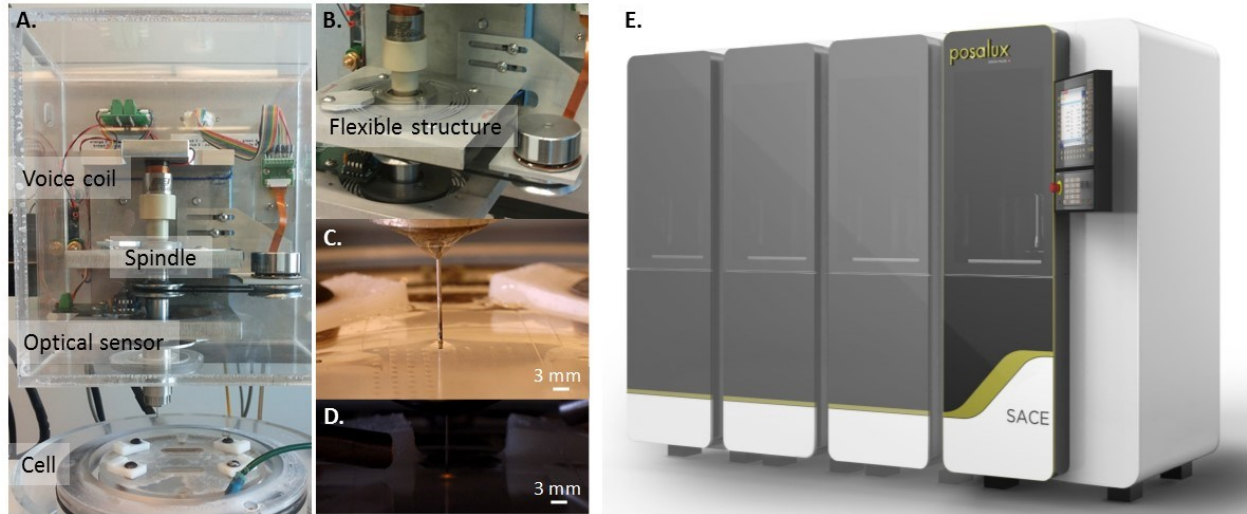
Figure 3.8. A. Developed laboratory setup for SACE machining with its key elements - electrolytic cell, spindle with tool-electrode integrated in a flexible structure (**B.**) with low axial stiffness and high lateral stiffness, optical sensor, and a voice coil actuator / force sensor. **C.** SACE drilling in operation. **D.** Observed sparking during glass drilling. **E.** Posalux FP1-SACE machine (modular system with four independent machining heads).

3.4. Results and Discussion

3.4.1. Model analysis and validation

The derived normalized model was validated by SACE cutting/milling experiments with small and large tool diameters were deployed (100 µm and 200 µm diameter tools). To determine experimentally the maximal depth-of-cut p at a given tool feed rate F a series of cuttings of 0.4 mm thick glass slides (Pyrex®) were performed. The cut was considered to be successful if

    a) The tool didn't break, and

    b) The measured depth of the cut was equal or higher than the imposed depth of cut during machining.

From a practical point of view, thanks to the force sensor inside the tool-electrode holder, it was possible to detect none successful cuts due to an increased force acting on the tool (a few mN). Pulsed voltage with 2.5ms pulse high (t_{high}) and 0.1ms pulse low time (t_{low}) was used. In such conditions the gas film shows high stability and very few bubbles are observed around the tool-electrode as found empirically (Figure 3.9), which was also confirmed by [247]. Deploying short pulse off times (0.1 ms) reduces dramatically the hydrodynamic region (bubble evolution). This

region doesn't contribute to glass machining (no heat generated by sparks) and should therefore be kept as short as possible for most effective process performance.

A. $U_{high} : U_{low} = 28\text{ V} : 14\text{ V}$ - $t_{on} : t_{off} = 2.5\text{ ms} : \textbf{1.5 ms}$

B. $U_{high} : U_{low} = 30\text{ V} : 15\text{ V}$ - $t_{on} : t_{off} = 2.5\text{ ms} : \textbf{0.1 ms}$
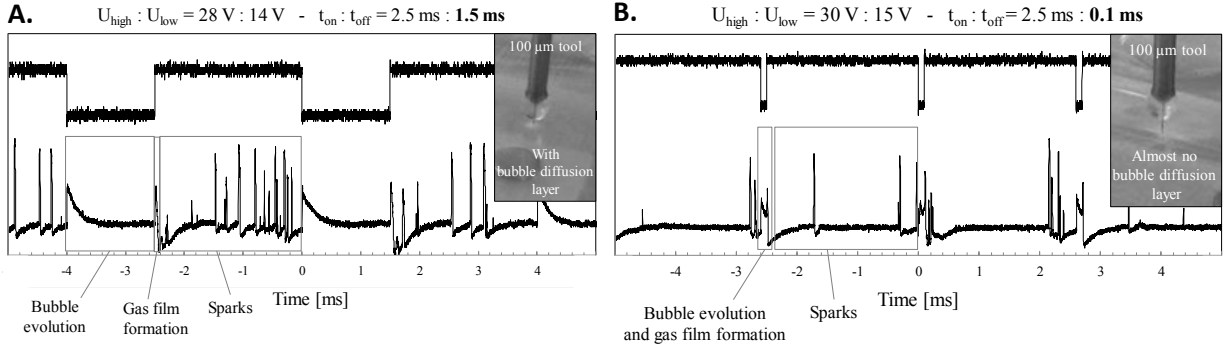
Figure 3.9. A. Typical voltage and current signals during SACE machining ($U_{applied} > U_{critical}$) upon applying pulsed voltage with relatively large pulse off time (1.5ms). Note the relative long bubble evolution region. **B.** Typical voltage and current signals upon applying pulsed voltage with short pulse off time (0.1 ms). Note the significantly reduced bubble evolution region.

Cutting experiments were performed at three pulsed machining voltages (high, intermediate and low) as denoted in Table 3.1.

The average input voltage U_{avg} was calculated according:

$$U_{avg} = \Delta U_{pulse} \cdot (t_{high} - t_{low}) / (t_{high} + t_{low}) + U_{lowlevel} \tag{3.21}$$

Table 3.1. SACE machining settings

	Pulsed Voltage Input			
	High Level	**Low Level**	**Period**	**Duty Cycle**
Low	30 V	17.5 V	2.6 ms	96.15 %
Intermediate	33 V	17.5 V	2.6 ms	96.15 %
High	35 V	17.5 V	2.6 ms	96.15 %

Using these machining voltages (Table 3.1 to calculate the average voltage (equation (3.21)) as input in equation (3.14) and equation (3.15) and taking for the thermal diffusity $a \sim 6 \cdot 10^{-7}$ m²/s for Pyrex® glass [243], we estimate the values for $F \cdot p$ as outlined in Table 3.2.

69

Table 3.2. Heat propagation in glass workpiece

Machining Voltage		F·p
High Level	Average	
30 V	29.0 V	1.0 mm^2/min
33 V	31.8 V	1.6 mm^2/min
35 V	33.7 V	2.2 mm^2/min

Figure 3.10 presents the empirical values for maximal depth of cut p versus tool feed-rate F for SACE glass cutting with two different tool diameters, respectively 100 μm (non-filled markers) and 200 μm (filled markers). The products $F\,p$ = constant (equation (3.3)) are plotted on this graph (dashed lines) such that it matches best the empirical values. It can be evidently observed that the values of these constants ($F\,p$) are accurately predicted by equation (3.14), where the tool was modeled as a disc heat source (heat is applied homogeneously over the entire tool diameter onto
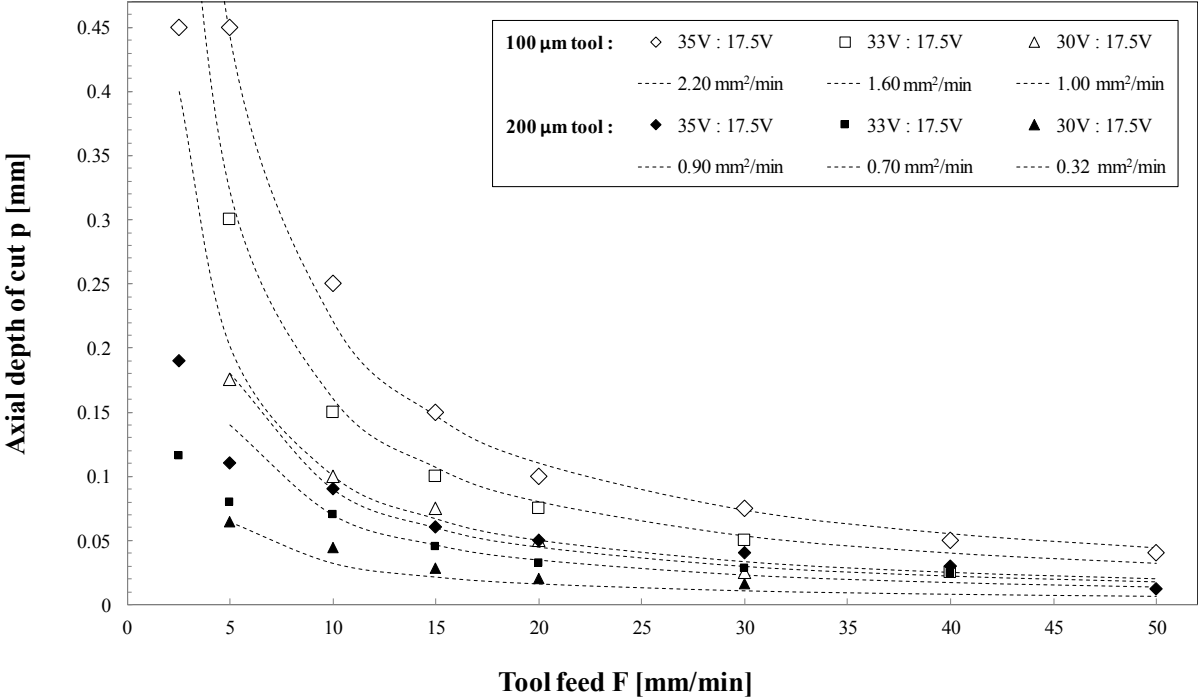
Figure 3.10. Empirical values for maximal depth-of-cut p [mm] versus tool feed-rate F [mm/min] – non-filled markers represent values for tungsten carbide 100 μm diameter tools – filled markers represents values for tungsten carbide 200 μm diameter tools. *Dashed lines*: Equation (3.3) - $F\,p$ = constant (upper three lines based on Table 3.2).

the workpiece), for 100 μm diameter tools (see Table 3.2). However, these constants are not correctly predicted by equation (3.14) for larger, 200 μm diameter tools.

Hence, the assumption that the tool can be modeled as disc heat source and is independent of tool size (as stated by equation (3.14)) is not valid for tool diameters > 100 μm. A more realistic heat source model is needed, therefore the ring heat source model (defining radius b and ring thickness e) as proposed and developed in the theory section (3.2) will be investigated.

To compute the value of the product $F\,p$ from this heat model with the ring heat source boundary condition (3.16) we use the following equation (making use of (3.3) and (3.10) in normalized form):

$$F \cdot p = 8a \cdot \bar{h}_r = 8a \cdot \frac{d\bar{z}(\bar{t}_0)}{d\bar{t}} \tag{3.22}$$

Graphs can now be constructed for $F \cdot p$, using equation (3.22), at different values of normalized heat power κ and using $a \sim 6 \cdot 10^{-7}$ m^2/s as thermal diffusity for Pyrex$^{\circledR}$ glass [243] (see Figure 3.11 and Figure 3.12).
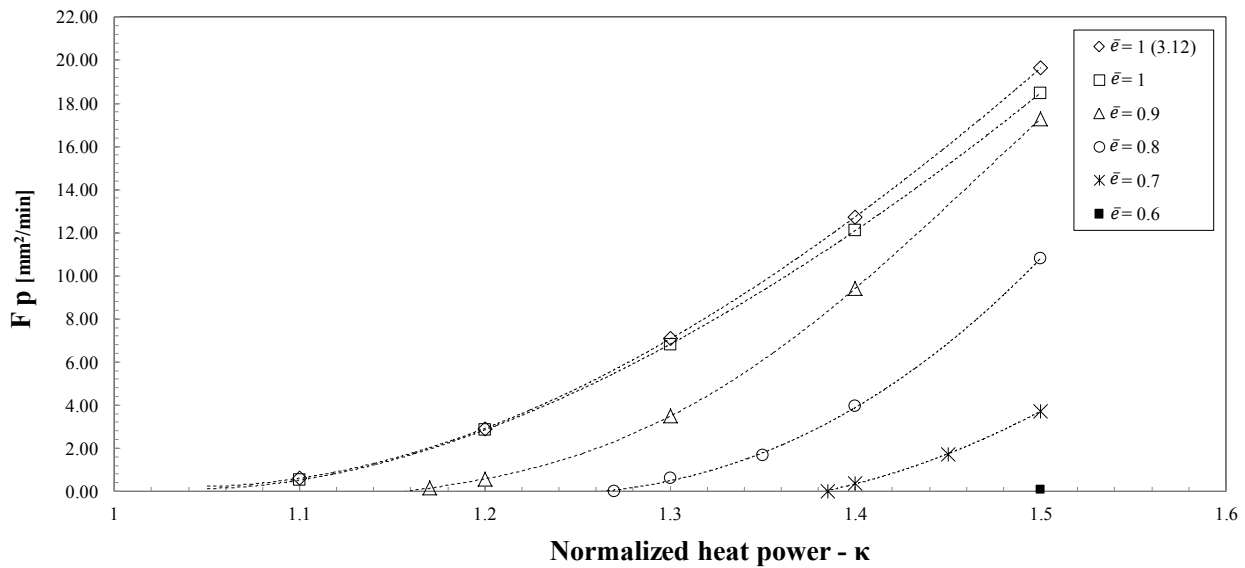
Figure 3.11. Product of tool feed and maximal cut of depth - $F \cdot p$ [mm^2/min] versus normalized heat power κ for different values of ring thickness $\bar{e} = 1.0$ down to $\bar{e} = 0.6$.
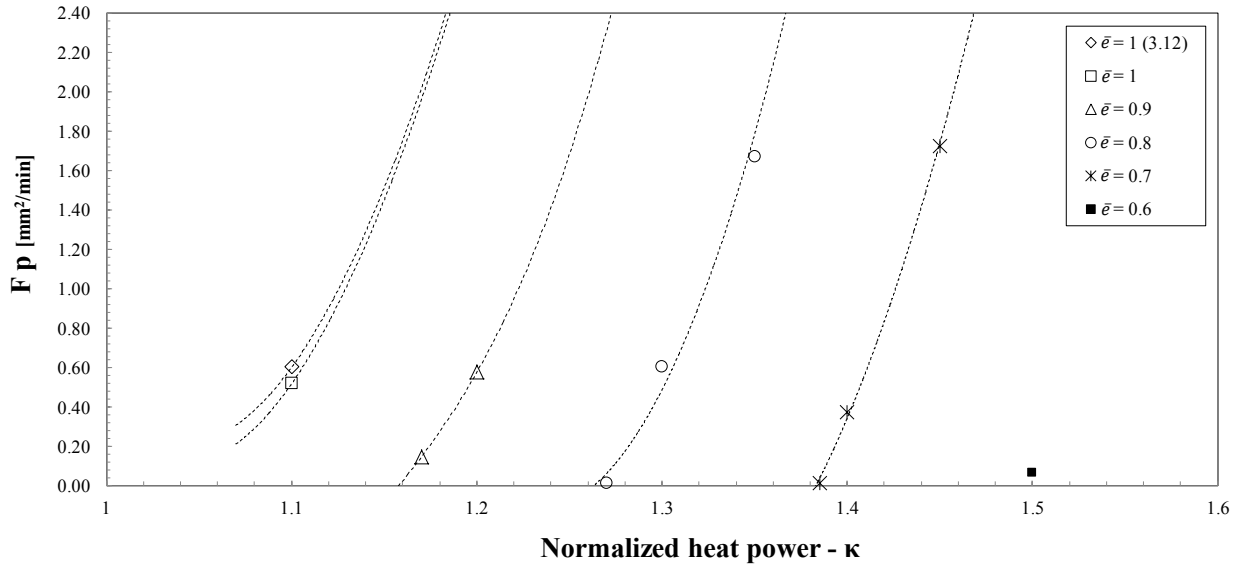
Figure 3.12. Zoom (lower values of the product $F\,p$) of product of tool feed and maximal cut of depth - $F \cdot p$ [mm^2/min] versus normalized heat power κ for different values of ring thickness $\bar{e} = 1.0$ down to $\bar{e} = 0.6$.

Numerical solutions were validated using the case of $\bar{e} = 1$ where the problem reduces to the situation of a disc heat source, which is analytically solved [81], presented by equation (3.12). Comparing the constructed graph of $F \cdot p$ versus κ when numerically solved with the graph when using the exact solution (3.12), it can be concluded that the error by the numerical analysis is lowest for small values of κ (error < 2.5 %).

The empirical results of micro cutting with 200 μm diameter tools (Figure 3.10) fit well with the constructed graph in Figure 3.12 for $\bar{e} = 0.9$. Consequently, this shows that for these larger tool diameters (200 μm) the heat source is less efficient at the center of the tool compared to the tool edge (as hypothesized by equation 3.16). This heat source efficiency decreases even further when using tools larger than 200 μm. Progressively higher normalized heat power κ is needed for increasing tool diameters for SACE process input to achieve similar performances compared to 100 μm diameter tools. This is represented by decreasing values of ring thickness e in the boundary condition (3.16). On the other hand, the heat source becomes not more efficient for tools smaller than 100 μm (disc heat source model ($\bar{e} = 1$) is valid for all tool diameters ≤ 100 μm).

Hence, for glass micro-cutting by SACE technology it is optimal to use tools of 100 μm diameter. Using larger tool diameters will rapidly decrease the heat source efficiency (as then $\bar{e} < 1$) and subsequently reduce dramatically the machining speed (by a factor ~ 5 upon using a tool diameter of 200 μm, see Figure 3.10). Using smaller tools than 100 μm diameter will not contribute

to increased efficiency as for tools with 100 μm we reach already $\bar{e} = 1.0$ and as shown by Equation (3.14) cutting time becomes independent of the tool diameter (i.e. can not become shorter by using smaller tools).

An important consequence from the practical point of view is that the usage of a force sensitive machining head is an essential requirement for SACE machining. Indeed, without such a head, tools of 100 μm could not be used without bending and/or breaking them. This confirms the relevance of prior studies investigating and developing force-feedback strategies for SACE [203, 220], which, together with the results of the presented study, has led to the development of a force sensitive machining head with controlled stiffness (low stiffness is preferred for high performance SACE process) together with our industrial partner Posalux SA [224]. The presented thesis work contributed in development of this patented machining head [60] for the industrial Microfor SACE machine, which is briefly discussed in section 3.5.

The findings of the developed model and analysis for glass micro-cutting and -milling can be used to investigate the possible routes for increasing MRR for SACE micro-cutting and -milling. Essentially three solutions can now be proposed to increase this removal rate:

a) Using small tool diameters to reach the optimal value of $\bar{e} = 1$. This is the case for tool-electrodes with diameter of 100 μm (representing a disc heat source) as for ring thickness $\bar{e} = 1.0$ the normalized heat propagation $\bar{h}_r$ through the glass workpiece is independent of the tool radius. Using lower diameters does not longer increase efficiency as for $\bar{e} = 1$, cutting time is independent of tool diameter;

b) Increase the normalized heat power κ. However, this results in poor machining quality (large roughness, indents > 50 μm). This can be partially addressed by applying the developed SACP technique, where a first (rough) cut is made at relatively high tool feed, subsequently followed by a low machining input voltage cut at lower tool feed (SACP will be discussed in section 3.6). Figure 3.7 together with relation (3.22) can be deployed to determine the tool feed and depth of cut for a given normalized heat power κ.

c) Solutions a) and b) are good strategies for fabrication of mass-personalized glass parts. An alternative to increase MRR of SACE process is the use of a multiple tool machining head as illustrated in Figure 3.13. This strategy to parallelize machining is not suitable as mass-personalized manufacturing method, but it works well for low to medium batch size production. When using the developed model, Figure 3.7 together with relation (3.22),

conservative tool feed and depth of cut can be chosen to prevent damage of the tools, leading to effective parallel SACE machining. It should be noted that the required tool rotation, for creating a more uniform machining zone around the tool, does not come here from a tool spindle, but the circular motion is applied on the two translational axes holding the tool. In fact, this implies that 'drilling' operations become 'cutting' operations, allowing use of the developed model to find the best process parameters.
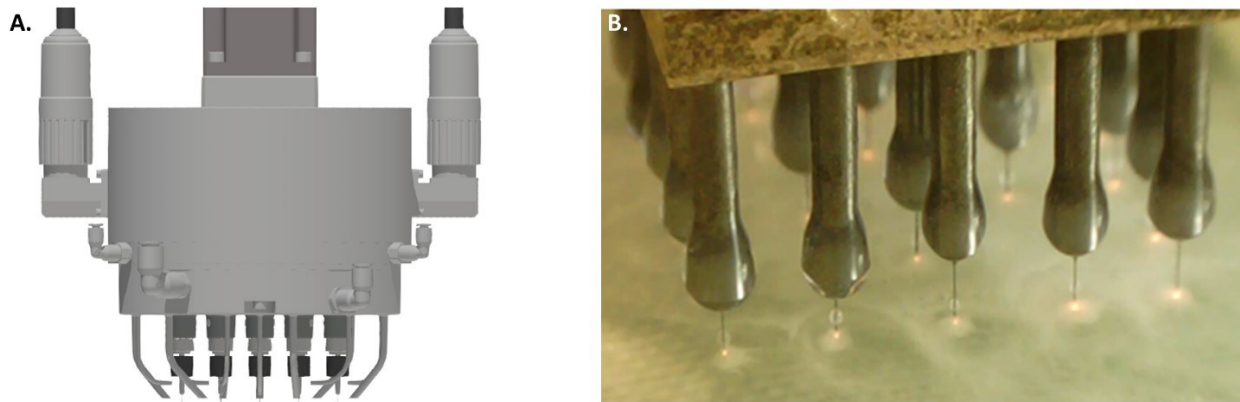
Figure 3.13. Schematics of the multi-tool machining head (25 tools) for parallel SACE machining, developed at Posalux SA [224]. **A.** 3D model of the developed multi-tool to be mounted on the machining head. **B.** SACE machining (here micro-hole drilling) using a prototype of the multi-tool machining head.

Another key result from this study is the showed significance of heat propagation through the glass workpiece as main limiting factor to determine the maximal machining speed in the case electrolyte flushing around the tool happens easily (as in micro-cutting and -milling operations). This confirms statements made in our previous studies on the machining temperature in SACE machining [221].

Efficient setup (i.e. low setup time) of manufacturing systems with a high degree of automation is crucial for batch size 1 compatible machining processes. Process models such as developed in this chapter for micro-cutting and -milling are key and a first step to achieve this requirement. As of today, it takes a significant number of trial and error runs before the process parameters (machining voltage, feed-rate, depth-of-cut) for appropriate cutting and milling operation settings are found resulting in time consuming machining setup. Using the here developed models enables direct (i.e. fast) transfer of the desired drawing to be machined into machinable code with the appropriate process parameters eliminating long test runs.

3.4.2. Glass micro-cutting experimental results

The quality of the cut is assessed by optical microscopy for the different machining voltages (low – intermediate – high voltage) and at varying feed rate and depth-of-cut (Figure 3.14) using 100 µm diameter tungsten carbide tools with a 45° bevel. Machining quality deploying 200 µm diameter tools leads to similar typical machining roughness results and this analysis is therefore omitted here.
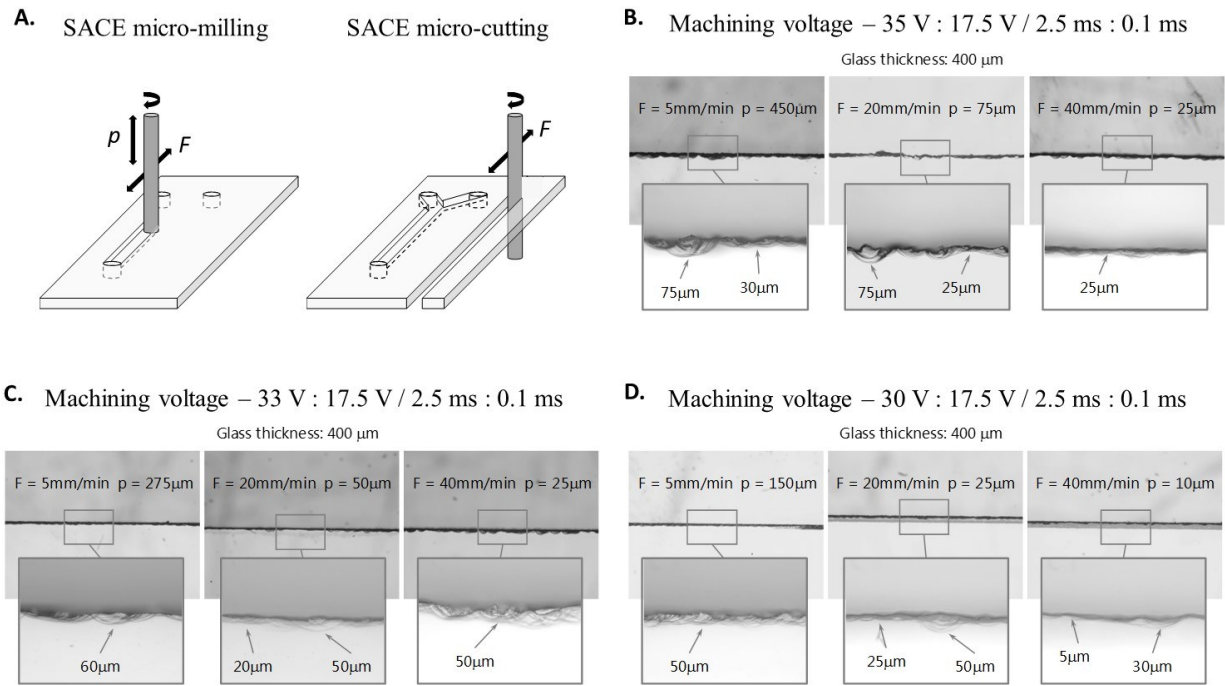
Figure 3.14. Microscopy (Keyence VHX 5000) analysis of cut quality, using 100 µm diameter tungsten carbide tools, at different machining voltage, feed-rate F and depth-of-cut p. **A.** Schematic of SACE micro-milling and -cutting. **B.** Cut surface at high pulsed voltage (35 V). **C.** Cut surface at intermediate pulsed voltage (33 V). **D.** Cut surface at low pulsed voltage (30 V).

It can be observed that quality of the glass cut generally increases when the machining voltage reduces (indents of ~ 75 µm – 60 µm – 50 µm for respectively 35 V – 33 V – 30 V at maximum cutting depth for each voltage and feed-rate F = 5 mm/min.)). Decreasing the depth of cut results generally also in higher machining quality. In the extremes, when machining at same feed-rate F = 40 mm/min - and low depth of cut, the machining quality is around the same for all applied machining voltages.

Reasonable quality of cut in glass by SACE technology can be obtained using the derived tool feed versus depth of cut relations (Figure 3.14). Further increase of the quality of cut surface can

be achieved deploying other strategies, such as 'SACE polishing' by approaching the surface with small lateral increments of the tool-electrode at very low voltage. This SACE polishing method was developed to achieve smooth cut surfaces (roughness < 1 µm), which is discussed in more detail in section 3.6.

3.5. Force-sensitive machining head with actively controlled stiffness

Following the glass micro-cutting experimental and modeling results (sections 3.2 and 3.4), efficient SACE machining is achieved deploying 100 µm diameter tools (larger tools, starting at 200 µm diameter, have decreased efficiency in terms of heat source and tools smaller than 100 µm diameter will not further improve machining efficiency, so are unnecessary complicated). In order to prevent bending and breaking of such small tools, the development of a force-sensitive machining head for SACE machining is an essential requirement. In addition, it is empirically found that low axial tool stiffness is preferred for high quality machining which can be controlled by such force-sensitive machining head. This guarantees that no mechanical contact (i.e. very low (~ 1 mN) to zero force) occurs between tool and workpiece during machining, and the tool is not mechanically pressed onto the glass workpiece.

This force-sensitive machining head with actively controlled stiffness was developed and patented [60] during this thesis research work together with industrial partner Posalux SA [224] resulting in an industrial grade SACE machining head system, which is briefly described in this section. For a more detailed description is referred to the patent WO 2017/064583 A1 (2017) [60].

The arrangement [60] results in a machining head with a controlled stiffness. The stiffness k is defined as the resistance offered by the machining head to deformation δ when a machining force $F_{machining}$ is applied

$$k = \frac{F_{machining}}{\delta} \tag{3.23}$$

where $F_{machining}$ is the machining force applied to the tool and δ is the deformation of the machining head, i.e., its variation of length between the distal extremity of the tool and a fixed point of the machine that is caused by $F_{machining}$.

The control module is programmed so as to adapt the stiffness k of the machining head during machining. In particular, the machining head according to the present invention has a low stiffness.

The low stiffness of the machine head is provided by a reactive motor that reacts rapidly to actuate the tool electrode, here a voice coil motor is implemented. The low stiffness allows high quality machining by minimizing the constraints on the tool and on the glass during machining.

Summarizing, the invention relates to a SACE machine for machining a glass workpiece, the machine comprising [60]:

- A support for fastening the workpiece during machining, said support being dipped into an electrolytic;

- A machining head operated by a feed motor for translating said machining head along a feed axis extending along said machining head;

- A tool electrode protruding from the machining head toward the support to dip at least partially into the electrolytic;

- Guiding means for guiding the translation of the machining head with respect to the support along said feed axis;

- A counter electrode dipped into the electrolytic;

- A sensor for measuring the axial machining force exerted on the tool electrode during machining;

- A control module arranged for progressively adapting the translation speed of the tool electrode depending on said machining force.

Figure 3.15 presents the three-dimensional model and the cross-section of the invented machining head and its components. The reference numbers used in Figure 3.15 are detailed below:

1. Machine	2. Headstock	3. Rotation element
4. Translational element	5. First translational motor	6. Second translational motor
7. Support	8. Rotation motor	9. Belt
10. Coupling element	11. Tool electrode	12. Tool portion
13. Motor portion	14. Tool holder	15. Tilting element
16. Tool guide	17. First air bearing	18. Ball bearing
19. Motor guide	20. Second air bearing	21. Voice coil
22. Sensor		
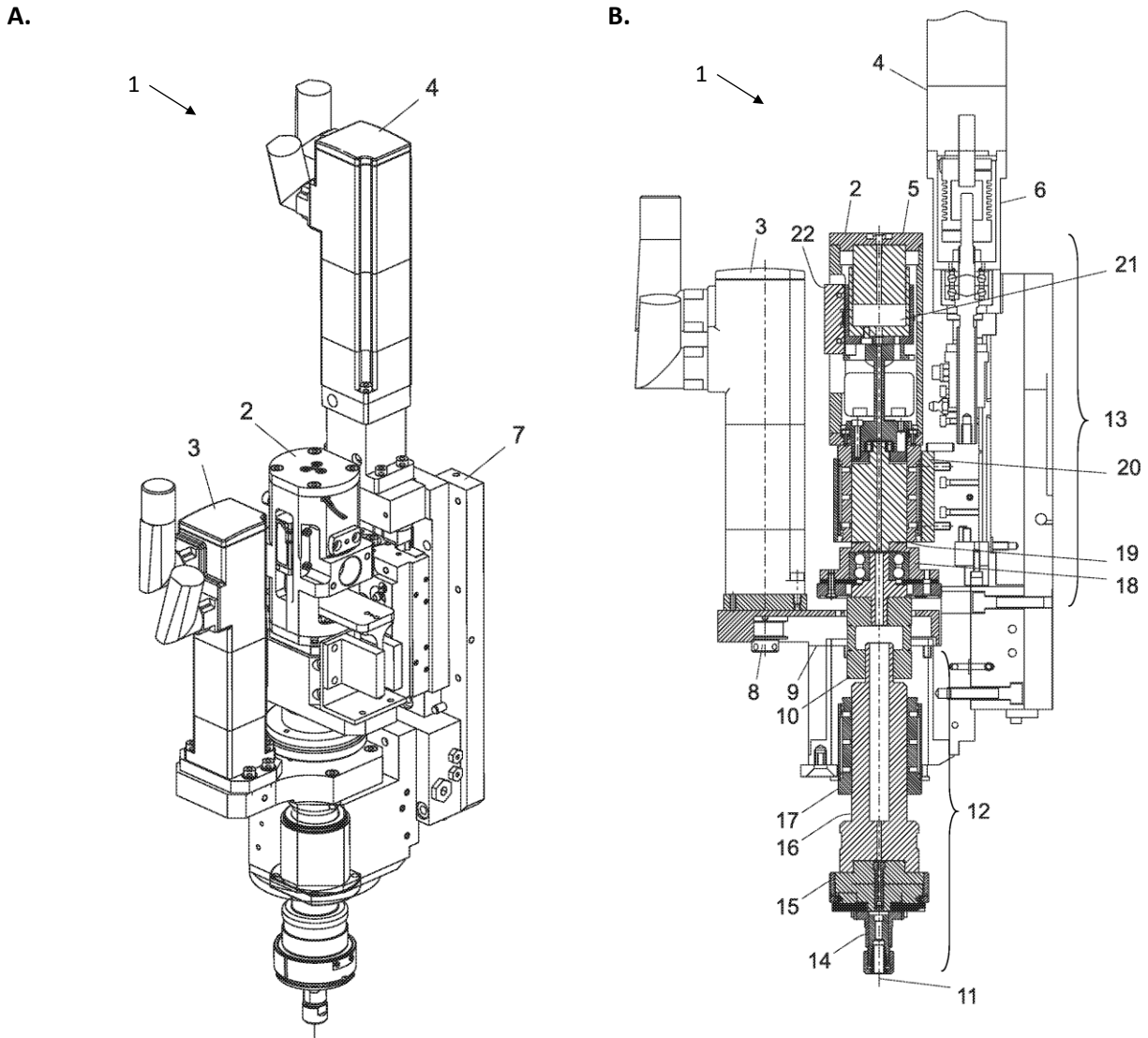
Figure 3.15. Developed force-sensitive machining head with actively controlled stiffness for the industrial SACE machine to achieve high quality glass machining of SACE process, detailed in patent WO 2017/064583 A1 (20 April 2017) [60]. **A.** Three-dimensional model of the machining head and its components. **B.** Cross section of the machining head and its components. Reference numbers used in this figure are detailed in the text below.

The developed industrial SACE machine offers high precision glass micro-drilling, micro-milling, micro-cutting and micro 3D machining operations (Figure 3.16) while leaving the glass surface intact to allow subsequent processing steps for device manufacturing. It will be shown further in this thesis that this is an essential requirement for efficient (i.e. flexibly) glass-to-glass bonding for device packaging, which is detailed in chapter 5 and crucial both for efficient glass-to-polymer templating as proposed and discussed in chapter 6 and for using glass as dies for metal micro-forming, which is also presented and discussed in chapter 6. The implementation of the

force-sensitive machining head with force-feedback algorithms allows detection and maintaining forces down to 1 mN. This enables the usage of the small machining tool (100 μm diameter tungsten carbide cylindrical tool) to be used as an accurate profilometer to measure machined features within the same setup to an accuracy of 1 μm, enabling continuous three-dimensional control of the machined features.
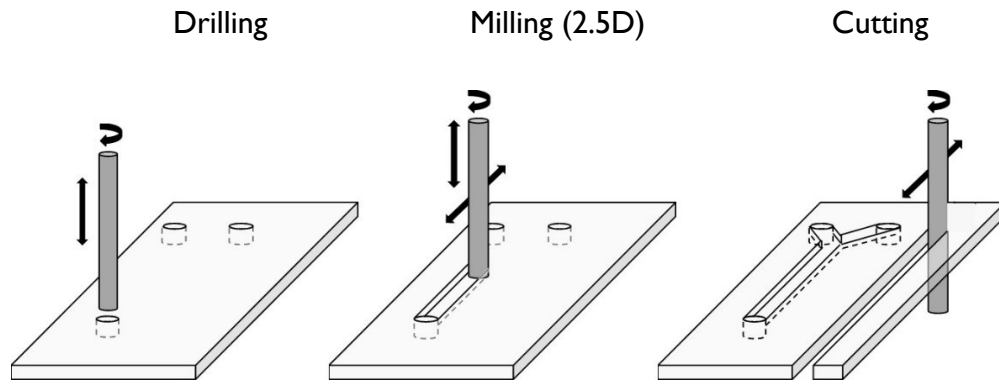
Figure 3.16. Versatile glass machining by SACE technology: drilling, milling and cutting by the same technology on the same setup.

3.6.   Spark Assisted Chemical Polishing (SACP)

Reasonable quality of cut in glass by SACE technology can be achieved using the derived tool feed versus depth of cut model presented in sections 3.3 and 3.4. It was shown that highest quality machining could be obtained at low depth of cut. For instance, for a specific feed-rate (e.g. $F = 40$ mm/min) and low depth of cut ($p = 10$ to 25 μm), the machining quality was similar for all applied machining voltages (30 V – 33 V – 35 V). In this case, cut surface roughness (R_z – peak-to-valley) of $R_z \sim 25$ to 50 μm could be obtained. In order to achieve higher quality of cut as required for high-precision glass applications a novel strategy - Spark Assisted Chemical Polishing (SACP) – was developed and is presented in this section.

In SACP, the surface to be machined is approached with small increments (typically few microns) of the tool-electrode at very low voltage, achieving surface qualities (size of indents) in the order of a few microns. The resulting smooth surfaces are required for many applications and will dramatically increase the mechanical resistance of the machined glass against fracture by reducing the number of potential fracture sites on a smooth glass surface compared to a rough one.

Experiments were carried out to investigate the effect of a dual pass machining process whereby critical processing parameters were changed between an initial rough cut and a second polishing step (process parameters established by use of the derived model, Figure 3.10, in sections 3.2 and 3.4). Parameters included applied potential to the tool-electrode U, feed-rate F, tool-rotation ω, and distance between the tool and wall Δx and the displacement of the tool between the two passes. Figure 3.17 shows a schematic of this dual step process.
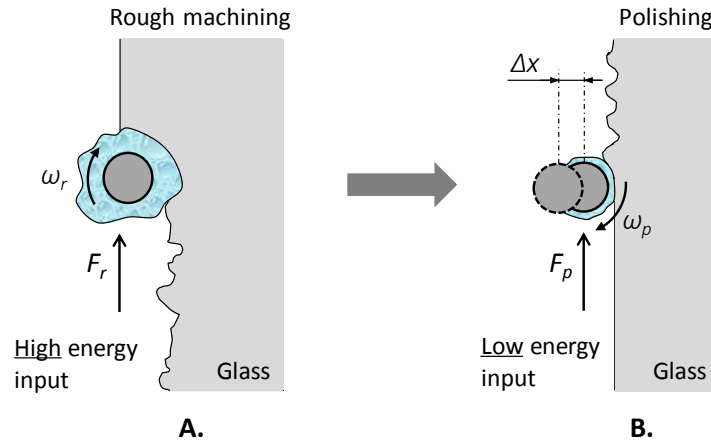
Figure 3.17. Polishing approach by SACE to reduce the roughness of machined features in glass. Schematic showing SACE machining for an initial rough cut (**A**.) with applied voltage ($U_{r,high}/U_{r,low}$), feed-rate (F_r) and tool rotation (ω_r). A subsequent polishing step (**B.**) entails displacement of the tool closer to the glass surface by distance Δx and processing parameters are changed for applied voltage ($U_{p,high}/U_{p,low}$), feedrate (F_p) and tool rotation (ω_p). The relationship between processing parameters is as follows: $U_{r,high} > U_{p,high}$, $U_{r,low} = U_{p,low}$, $F_r > F_p$ and $\omega_r \leq \omega_p$.

The idea behind SACE polishing is to use low applied voltages in order to reduce the effective machining (etching) zone around the tool and to avoid thermal stresses and, in combination with a higher tool rotational speed ω, to produce a more uniform machining zone around the tool-tip, resulting in a smoother electrolyte flow to the glass surface. As seen in Figure 3.17, the machining zone around the tool is significantly smaller, so the tool position is adjusted by a distance Δx closer to the surface. As the etching zone is less energetic, the etching rate is slower, and the feed rate of the instrument had to be reduced by about half (feed-rate and machining voltage for a specific depth of cut were easily found by applying the models established in section 3.2). Specific details of the relation between the SACE parameters are given in the Figure 3.17 caption.

Experiments were conducted with SACP method for varying pulsed polishing voltage amplitudes (high level), keeping the low level, period and duty cycle constant (respectively 17. V,

2.6 ms and 96.15 %) and for varying polishing gap Δx. The derived model (section 3.2) was used to relate a chosen tool feed-rate to a suitable depth of cut.

Glass milling (F_p = 5 mm/min) with pulsed polishing voltage with high levels, ranging from 22 V – 23 V – 24 V – 25 V – 26 V – 27 V – 29 V were carried out after a first rough cut (F_r = 15 mm/min, U_{high} = 38 V), revealing that good polishing results are obtained by using U_{high} = 23 V (see Table 3.3).

Table 3.3. SACP machining settings

SACP - Pulsed Voltage Input				
	High Level	**Low Level**	**Period**	**Duty Cycle**
First (rough) step	38 V	17.5 V	2.6 ms	96.15 %
Polishing step	23 V	17.5 V	2.6 ms	96.15 %

Deploying this polishing voltage and according to the described procedure in Figure 3.17, a series of channels was machined adding for each new channel a distance Δx to the polishing steps after rough machining. Results of this SACP experiment are presented in Figure 3.18. It can be clearly observed that the channel sides are best polished when using Δx = 20 µm with intermediate polishing steps of 2 µm increments. Polishing for larger Δx causes slight over etching of the glass surface and does not contribute anymore to reducing surface roughness.

Optical microscopic images for an overview of the glass polishing experiment is shown in Figure 3.19. The transition from rough machining ($R_z \sim$ 20 µm) via intermediate polishing to final polishing of glass (R_z < 1 µm) is clearly observed.

Scanning electron microscopy (SEM) images reveal smooth glass surfaces after SACP process in greater detail as shown in Figure 3.0 where a 300 µm thick glass slide was machined as micro-hinge example. Note that the part magnified in the insert is the part of the work-piece which was polished. The outer rectangular shape was not polished, and one can clearly observe the change in surface roughness. As well, the detailed SEM image illustrates tiny (< 5 µm) stream (or flow) lines caused by the electrolyte flow around the glass cut during machining.

It is interesting to evaluate as well the effect on machining time when using SACP process. The time to create a channel feature on a glass substrate can be estimated as:

$$t_{machining} = L\frac{P}{F_r} + 2nL\frac{P}{F_p}$$

(3.23)

where L is the length of the feature, P is the number of passes required to achieve the set depth, F_r is the rough-cut feed-rate and F_p is the polishing feed-rate. Since the polishing steps have to be done multiple – n – times (approaching the side wall in small increments of 2 μm) and they have to be done on each side of a channel feature, it is multiplied respectively by n and 2 in (3.23).
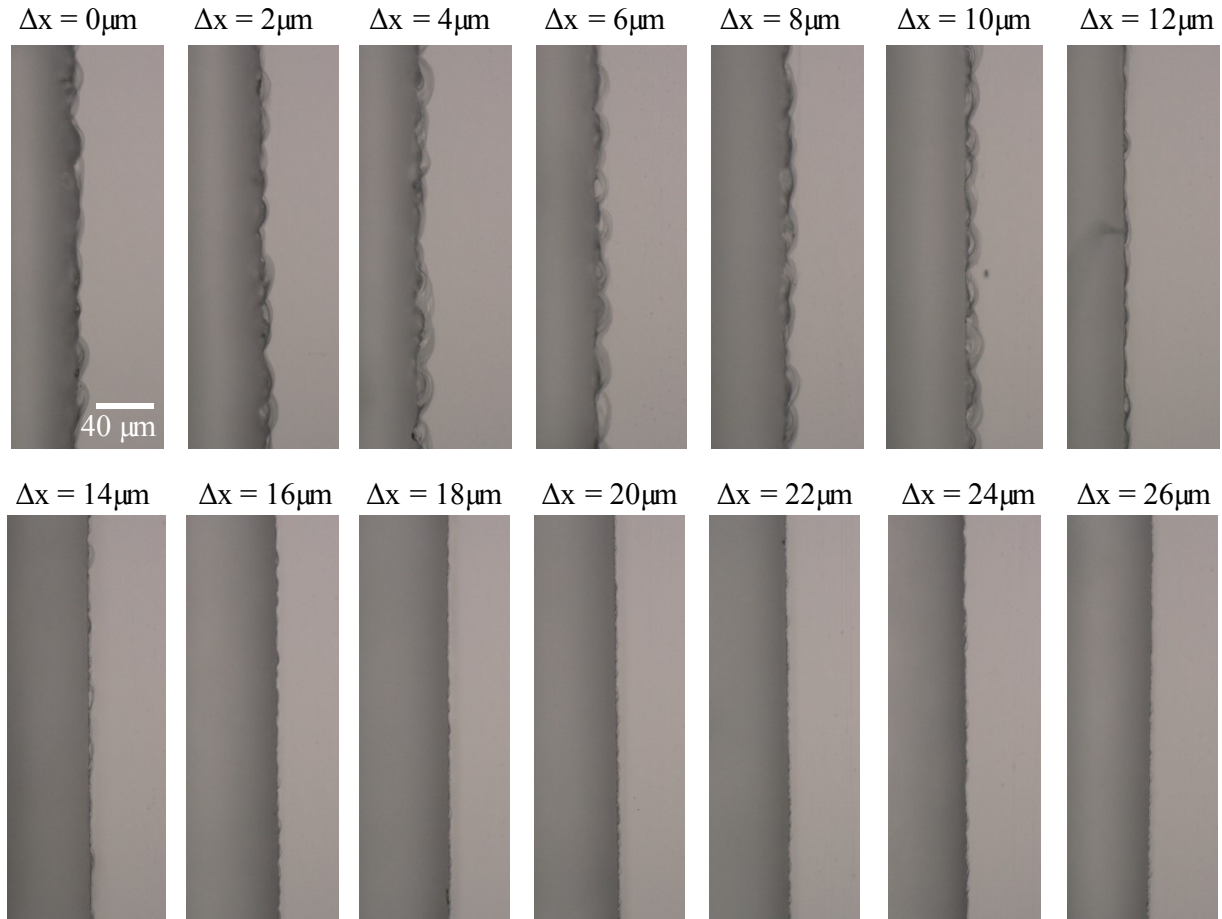
Figure 3.18. Experimental results of SACP process after rough SACE glass cutting (*first image*, machining conditions: U_{high} = 38 V, U_{low} = 17.5 V, F_r = 200 μm·s-1 and ω_r = 500 rpm) for increasing values of Δx. The polishing steps after rough cutting were performed at U_{high} = 23 V, U_{low} = 17.5 V, F_p = 80 μm·s-1 and ω_p = 1,000 rpm. Period and duty cycle between the U_{high} and U_{low} were the same for both rough cut and polishing steps, 2.6 ms and 96.15 %, respectively. Scale bar in the image is 40 μm.

This relation together with the previous developed cutting model (section 3.2) are valuable tools to quickly estimate the most time effective strategy for glass milling and cutting with high quality (low surface roughness). There are two different possible routes:

1. carry out the glass machining only at low machining voltage and low depth of cut (determined by the Fp model), resulting in reasonable qualities (Figure 3.) and requiring multiple passes depending on the feature depth to be achieved;

2. use SACP strategy after a first quick and rough cut (high values of normalized heat power κ imply high values of Fp) to obtain very smooth ($R_z < 1$ µm is possible) channel feature side walls.

Trade-offs should be made, and best strategy depend on the feature geometry (e.g. depth) and required surface roughness that must be achieved.

The capability to machine and polish the machined glass surface on the same machine, opens up new applications for SACE. For example, the mechanical strength of machined glass part is greatly enhanced as less flaws appear on the surface. As shown in Figure 3.0 it becomes possible to machine high precision, thin structures without damaging. Note as well the straightness of the machined surfaces where no taper angle can be observed.
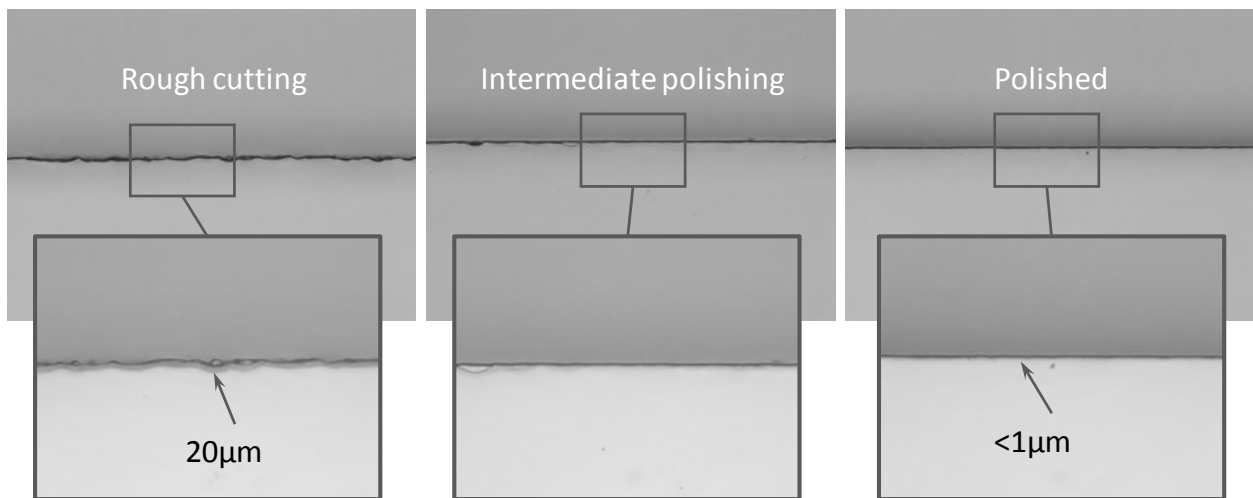
Figure 3.19. Microscopic images showing the transition from rough machining ($R_z \sim 20$ µm) via intermediate polishing to final polishing of glass ($R_z < 1$ µm) when deploying the developed SACP strategy.
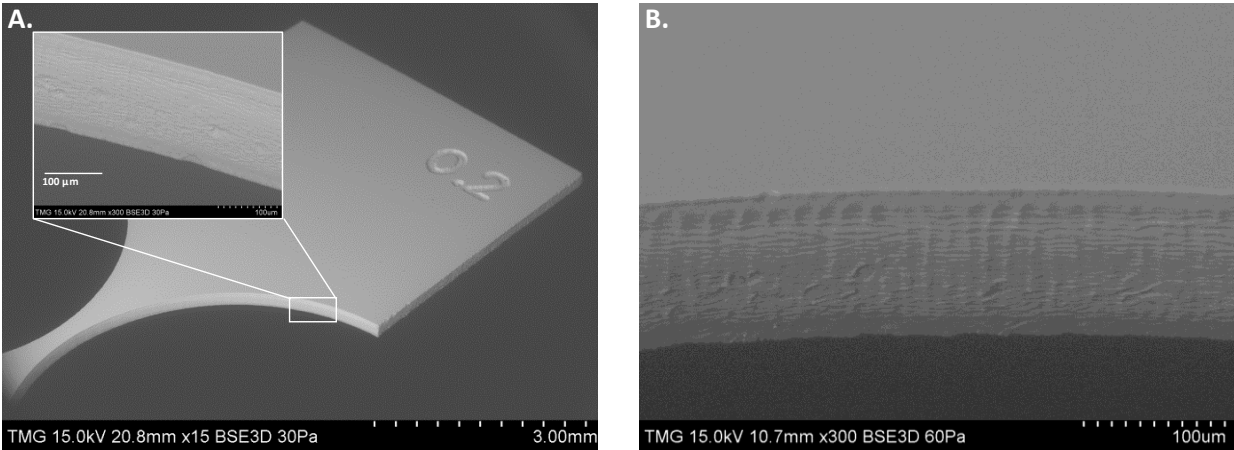
Figure 3.20. Scanning electron microscope (SEM) image of a SACE machined micro-hinge out of a 300 μm thick glass slide (**A.**Overview of machined hinge, **B.** Magnification of the polished curved cut). The curved cut (shown on inset and image **B.**) is polished by SACP after rough cutting following process parameters as presented in Table 3.3. Scalebar on the inset is 100 μm.

3.7. Conclusions

The developed model allows to predict the maximum depth of cut for a given tool feedrate, which eliminates time-consuming 'trial runs' before machining to determine the best cutting parameters, as no model relating these process parameters was available until now. Hence, this study significantly contributes to enabling use of SACE technology as an *Industry 4.0* compatible process, e.g. for fabrication of mass-personalized glass parts. The model for cutting and milling process operations allows direct relation of the machining input parameters (e.g. voltage, feed-rate) and the desired machining outcome (e.g. feature depth), enabling a higher degree of automation in the SACE process flow from client model to finished glass product in one setup/machine.

- Cutting (and milling) parameters for tungsten carbide cylindrical tools (with 45° bevel) with respectively 100 μm and 200 μm diameter were determined for SACE process;

- A model was presented relating the lateral tool feed-rate F to the maximum depth of cut p for a given machining voltage based on the assumption that machining is only limited by heat transfer in the workpiece and matches well the measured process data;

- The proposed model, which correlates the machining input parameters to a desired outcome, was empirically validated, allowing further optimization of industrial

implementation of SACE technology as no predictive model for SACE glass cutting existed before;

- This model contributes in addressing the requirement of a high level of integration in the design to fabrication cycle for precision product manufacturing, which is essential for mass-personalization fabrication processes to reduce the machining overhead. A dramatic reduction of setup time by eliminating trial and error runs for process optimizing is realized by use of the developed model for glass cutting by SACE technology;

- It is found, empirically and confirmed by a numerical transient heat model, that tools of 100 μm diameter are optimal for glass micro-cutting by SACE technology:
  - Using larger tool diameters will rapidly decrease the heat source efficiency and subsequently reduce dramatically the machining speed (by factor 5 using a 200 μm diameter tool);
  - Deploying smaller tools (< 100 μm) will not contribute to increased efficiency as for 100 μm diameter tools cutting time becomes independent of the tool diameter;

- It is shown that the usage of a force sensitive machining head is essential to prevent bending and/or breaking of such small (100 μm diameter) tools;

- The significance of heat propagation through the glass workpiece as main limiting factor to determine the maximal machining speed was confirmed

- The findings of the developed model and analysis for glass micro-cutting and -milling was used to investigate the possible routes for increasing MRR for SACE micro-cutting and -milling:
  - Using small tool diameters are most efficient. This is the case for 100 μm diameter tool-electrodes (representing a disc heat source), lower diameters do not longer increase efficiency as then cutting time is independent of tool diameter;
  - Increase the normalized heat power κ. However, this result in poor machining quality ($R_z > 50$ μm), applying the developed SACP technology can partially solve this roughness issue.
  - For small and medium batch sizes (lots > 1) a multi-tool head can be deployed as effective strategy.

- Cut quality was evaluated by optical and electronic micro-graphs for different machining voltages (high, medium and low voltage);

- An industrial grade force-sensitive SACE machining head (sensitivity ~ 1 mN) was developed (resulting in patent WO 2017/064583 A1 (2017) [60].

- A strategy was developed to reduce the surface roughness of cut (down to R_z ~ 1 μm) by introducing Spark Assisted Chemical Polishing (SACP).

It can be concluded that issue – *the lack of a model relating SACE process input parameters to MRR* – of the current SACE method preventing its use as manufacturing process for mass-personalization of high precision glass parts (section 3.1.2), is addressed by the contributions described in this chapter.

The proceeding chapter 4 aims to address the remaining two essential issues

- *need of extensive calibration (alignment and run-out reduction)*
- *need of part specific tooling*

of current SACE technology hampering its ability for mass-personalized manufacturing.

Chapter 4

SACE technology offers high-precision micro-machining of glass. As SACE technology was developed to industrial maturity [224], it is still not well-suited for fabrication of batch size 1 production of glass parts. Section 3.1.2 of chapter 3 discussed three main issues of current SACE technique hampering its use for such mass-personalization. Development of a model, based on heat propagation through the glass workpiece, relating input process parameters to desired machining results addressed the issue of lengthy trial runs before high machining quality could be achieved. This permits a drastically increase of automation across the manufacturing process workflow from desired (customer) design to establishing of machinable code containing all necessary manufacturing execution information (e.g. toolpath definition, machining voltage settings, feed-rate, depth of cut, machining time, achievable quality), which is key for suitable manufacturing processes for mass-personalization.

However, two main issues remain in current (academic and industrial) SACE process restricting its ability for batch size 1 production:

- Extensive calibration is needed for alignment between tool and workpiece and to reduce tool-electrode run-out (currently effected manually on the industrial machine);
- Part specific tooling is required for precise clamping of the workpiece to obtain the required high precision and allowing a consistent, smooth electrolyte flow across the glass workpiece.

This chapter introduces new strategies and developments, which can serve as solutions to overcome these issues. It aims to make SACE technology a suitable manufacturing process for

Industry 4.0. This chapter entails an essential part of the thesis research study by providing an overview of the process cycles by SACE technology for manufacturing of mass-personalized parts.

The developed fabrication process addresses possible solutions to eliminate or reduce the key manufacturing cost drivers related to part design – 1) reduction of tooling costs, 2) elimination of time-consuming calibration procedures, 3) ability to fabricate complex structures with high precision, 4) reduction of process steps in the overall manufacturing cycle. Examples are given for complex machined structures on glass, which are flexible machined by SACE, for various fields of application.

Note that technical details specifically on the developed *in-situ* fabrication method for tool-electrodes can be found in [253].

Industry 4.0 – Towards fabrication of mass-personalized parts on glass by Spark Assisted Chemical Engraving (SACE)

Lucas A. Hof and Rolf Wüthrich

Department of Mechanical & Industrial Engineering, Concordia University, 1455 de Maisonneuve Blvd. West, Montreal, QC H3G 1M8, Canada

Abstract

With the fourth industrial revolution manufacturing industry faces new challenges. Small batches of personalized parts must be produced in an economically viable manner. In this study,

we show the feasibility of an approach using Spark Assisted Chemical Engraving to achieve personalized parts of hard-to-machine materials like glass with a low-cost setup. Key is the use of low-cost rapid prototyping and in-situ fabrication of the needed tooling, eliminating high indirect costs and long lead times. This approach can be used for on-demand manufacturing of personalized high precision applications of glass such as smartphone covers, advanced medical devices or fiber optic telecommunications.

4.1. Introduction

Manufacturing industry faces a new trend: mass customization, a term introduced in academia in 1970 [34], but only recently the market pull driven by shorter life-time cycles, increased complexity and the demand for individualized products attracted industry to this concept. Mass customization [33] presents new challenges: economical production of small batch sizes is incompatible with established manufacturing systems designed to produce large quantities of identical parts. Recently a new paradigm appeared as answer and was termed in Germany in 2011 as Industry 4.0 [40, 254]. The key idea is a new type of manufacturing systems, smart factories, in which manufacturing entities communicate via the Internet of Things allowing higher flexibility, quicker adaption to new designs, technology options, and regulations and increased productivity [44, 255].

A first step towards mass customization is the assembly of individual parts to custom products such as done in several industries (e.g. automotive or consumer electronics industry [256]). In these cases, the shape of the sub-parts remains essentially the same and the final product is built out of individual modules. However, as the industry 4.0 paradigm will be implemented progressively across global companies, manufacturing industry must deal with situations where geometry of the sub-parts change as well. In this case the customer will not only choose from existing options but will be actively involved in the design. In such cases of mass personalization [39] new manufacturing technologies are required which can keep manufacturing overhead related to change of part geometries low. They need to address the issues of tooling costs (avoid part

specific tooling) able to handle complex parts and reduce production steps (eliminate overhead due for example to alignment or tool change).

Additive manufacturing (AM) appears to be one of such technologies and is cited in literature as a solution to mass personalization [49]. Tooling costs are small as the machine builds them during manufacturing and very complex shapes can be produced. As such, AM appears as one of the corner stones of Industry 4.0. However, besides presenting its own challenges, AM will likely not be the sole manufacturing technology on which industry will rely. Other technologies able to work together or independently from AM (e.g. for materials that cannot be printed well such as glass) will be needed. Academia and industry just started to develop such technologies [52-54].

Glass is entering new applications appearing in micro and nanotechnology like fibers, tactile screens and MEMS devices because of its transparency, chemically inertness, environmentally friendliness and its mechanical strength and thermal properties. In fact, no other materials being mass-produced have shown such qualities over so many centuries [70]. Further, glass is RF transparent, making it an excellent material for sensor and energy transmission devices. Another advantage of using glass in microfluidic devices [72] is its relatively high heat resistance, which makes these devices suitable for high temperature microfluidic systems [75] and sterilization by autoclaving.

Unfortunately, due to its hardness and brittleness, glass is hard to machine and needs expensive tooling such as molds, masks (e.g. in wet etching), or specialized fixtures in the case of mechanical machining and polishing. Further, machining high-aspect ratio structures is still challenging due to long machining times, high machining costs and poor surface quality [81, 83].

In this study, a novel approach for manufacturing of personalized parts in glass using Spark Assisted Chemical Engraving (SACE) is presented. This method allows on demand fabrication of high precision applications such as glass components for smart phones, advanced medical devices, green energy devices or fiber optic telecommunications.

4.2. Manufacturing principles and approach

4.2.1. SACE principles

In SACE process (Figure 4.1.A), a voltage is applied between tool- and counter-electrode dipped in an alkaline solution [81]. At high voltages (around 30 V), the bubbles evolving around the tool electrode coalesce into a gas film and discharges occur from the tool to the electrolyte through it. Glass machining becomes possible due to thermally promoted etching (breaking of the Si-O-Si bond) [221].

SACE has recently reached industrial maturity for mass-fabrication (Figure 4.1.B) [224]. Breakthrough was the implementation of a force-sensitive machining head allowing the use of ultra-thin machining tools (diameter down to 30 µm), applying force-feedback algorithms (detecting forces down to 1 mN) and usage of the head as profilometer to measure machined features within the same setup [60]. Nevertheless, it is not yet equipped for flexible manufacturing as required for mass-personalized products. Research and optimization is needed. For example, tooling (both electrode and sample holder/bath) and tool-substrate alignment are still cumbersome processes resulting in relatively long setup times.
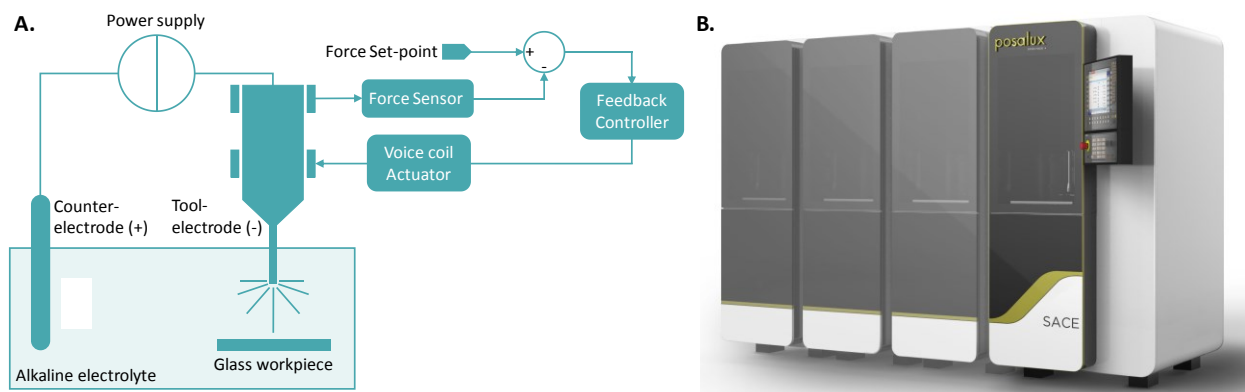
Figure 4.1. A. SACE process principle **B.** Developed industrial SACE machine [224].

4.2.2. Fabrication process cycle
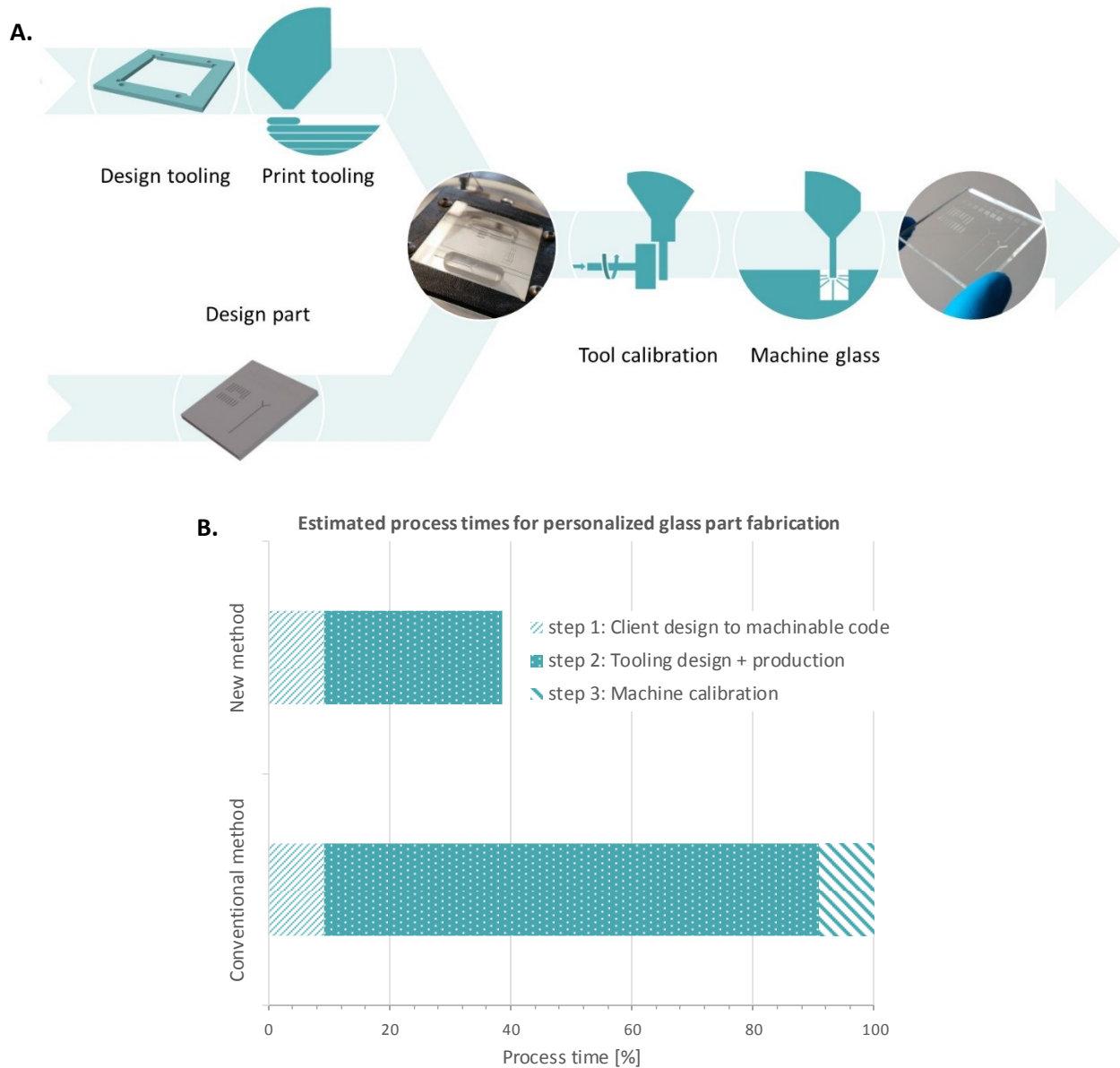
Figure 4.2. A. Process steps for fabrication of a client-specific workpiece in glass by SACE technology. **B.** Comparison of average process times for personalized glass parts fabricated by SACE using the conventional and new proposed method.

In the presented study, an integrated approach is developed for fabrication of personalized glass devices by SACE (Figure 4.2.A). The tooling, micro-sized cylindrical tool-electrodes and adequate sample holders, is manufactured on demand by flexible processes to meet requirements of low-cost personalization. One of the advantages to use SACE is the absence of high forces exerted on the tool and consequently the work-piece. Therefore, the tool-electrode can be

fabricated on the same setup as used for machining the workpiece and the sample holder can be manufactured by low-cost additive manufacturing, like Fused Deposition Modeling (FDM) [257]. The same digital design file is used for programming the machining trajectory and for designing a 3D model of the sample holder. As discussed in section 4.3.2, the proposed tool fabrication method, calibrates the tool-electrode as well, i.e. the tool is aligned relatively to the workpiece and run-out is reduced, eliminating the need of a costly high precision spindle or subsequent alignment after each tool change. This methodology allows significant reduction of setup times (about 60% compared to the conventional approach). Figure 4.2.B compares the process time of the involved steps until the machine is ready to start with a first machining (i.e. converting client design file to machine code, design and fabrication of the needed tooling and subsequent machine calibration allowing the usage of the produced and mounted tools). Note that in the presented numbers it is assumed that all facilities to produce the tooling are in-house. This is usually not the case for the conventional approach where tooling fabrication is often outsourced, adding significantly more time. With the proposed approach, considering the low investment costs for tooling fabrication, this can now be done on demand in-house.

4.3. Manufacturing process for custom glass parts

Contrary to conventional manufacturing processes, like numerical control milling and turning, SACE makes use of heat promoted chemical etching of hard-to-machine materials as glass. Therefore, the process is characterized by low forces and consequently the only focus for tooling is its precision. Required mechanical strength and stiffness is small compared to tooling for conventional mechanical methods.

4.3.1. Sample holder design and fabrication

FDM is used for on-demand sample holder fabrication from acrylonitrile butadiene styrene (resistant to the corrosive machining environment). The holder can be straightforwardly designed using the geometrical data from the targeted workpiece to be machined (Figure 4.2.A). Here, the holder was printed by an Ultimaker 2+ and the layer thickness was set to 80 μm.

4.3.2. In-situ tool fabrication method

Stainless steel tool-electrodes are demonstrated to be suitable for use in SACE technology [258]. For high precision fabrication of these tools and to eliminate misalignment of the tool bottom with respect to the substrate, an in-situ setup is developed on the same setup as used for micro-machining (Figure 4.3.A). The tool fabrication process, to reduce tool diameter and eliminate run-out, starts with mechanical grinding by a high-speed spindle (25,000 rpm) with an aluminum oxide abrasive wheel. The tool, mounted on the SACE machining head spindle, is rotated at low speed (500 rpm). Grinding takes place by moving the abrasive wheel slowly (10 μm/s) towards the tool until the desired tool diameter is reached. Thereafter (while spindle still rotates) the tool is moved upwards at 100 μm/s. Monitoring of the grinding process is done by an USB microscope. Tool bottom-substrate alignment is done by mechanical polishing on the same setup. Fine grit size abrasive paper (1200 grit) is mounted on the same position as the workpiece and moved laterally when pressing the tool on it [221], therefore eliminating misalignment of the tool bottom.

After grinding, the tool is subsequently electro-polished in an ethylene glycol + 0.9 molar sodium chloride solution at an anodic voltage of 20 V for a short time (40 s). Note that during the entire process the tool is never disassembled from the machining head avoiding alignment problems during the machining of the actual workpiece.

Typical results of a mechanically grinded tool-electrode, achieving tool diameters down to 60 μm, are outlined in Figure 4.3.B. The arithmetic average roughness R_a of the tool can be reduced to 70 nm by electro-polishing. This surface roughness reduction is important to obtain high resolution machined glass parts with good surface finish. Characteristic tool-electrode manufacturing time (including all steps) is ten minutes.
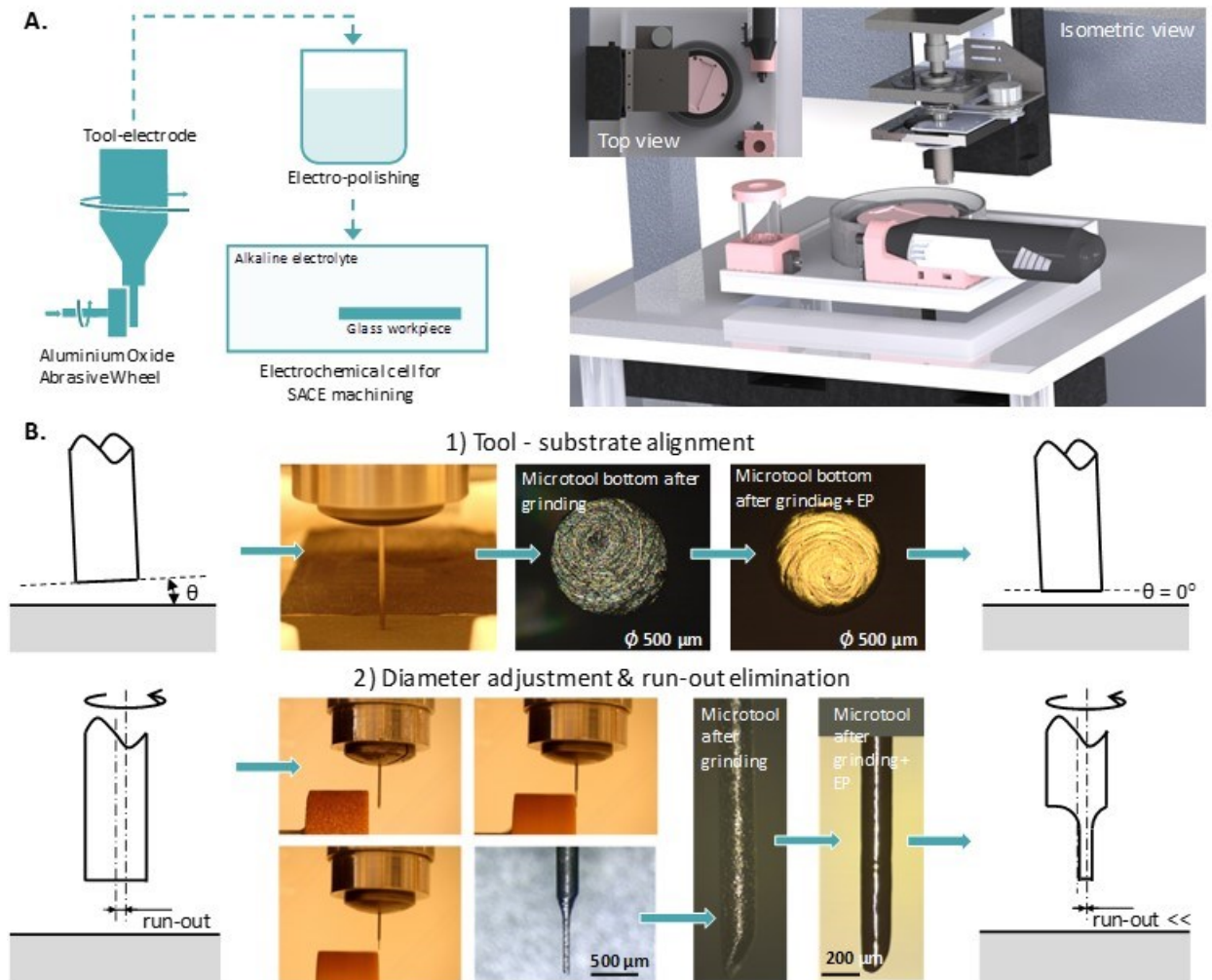
Figure 4.3. A. In situ microtool fabrication setup for glass micro-machining by SACE: tool fabrication starts with grinding followed by electro-polishing. **B.** 1) Misalignment correction of tool – substrate 2) Tool diameter reduction and run-out elimination.

4.3.3. Glass micro-machining examples

Integration of all process steps results in manufacturing of personalized glass products. SACE machining of different features in glass like holes, channels, microfluidic mixers, though-glass-vias, contour cutting and engraving of hardened smartphone cover glasses is achieved with high machining accuracy (typically with geometrical errors below 10 μm compared to the design of the customer). Results of this variety of glass applications, machined by SACE technology on demand, are presented in Figure 4.4.

The typical machining voltage applied across tool- and counter electrode was pulsed voltage between a high voltage (32 V) and a low voltage 17.5 V) with period = 2.6 ms, and duty cycle =

96.15 %. During machining, the tool was rotated at 500 rpm and a feedrate of 200 µm/s was used. As electrolyte, 20 wt.% KOH was used in most cases.
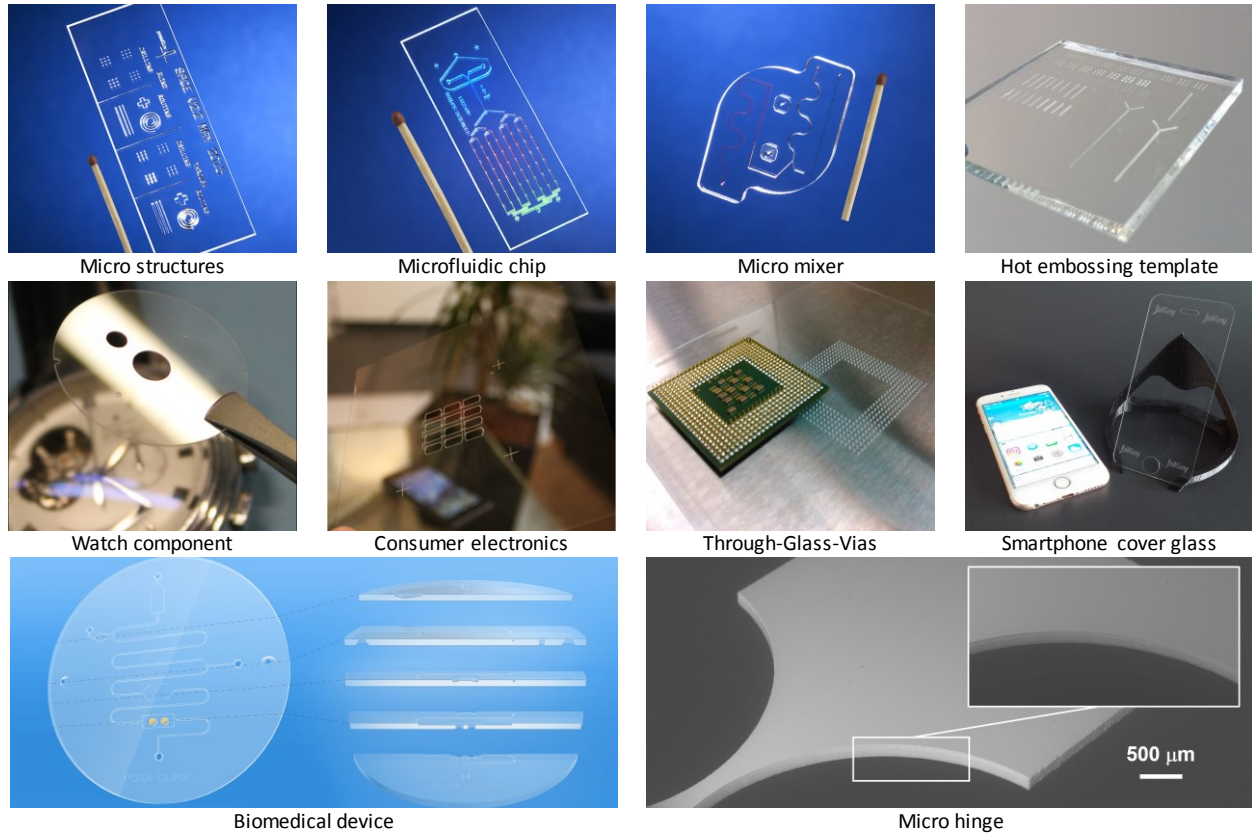
Figure 4.4. Examples of personalized micro-machining structures in glass by SACE process.

4.4. Conclusions

The results of this study show the feasibility of an approach using SACE to achieve personalized parts of hard-to-machine materials such as glass with a low-cost machining setup adding to novel manufacturing approaches fitting Industry 4.0. Key is the use of low-cost rapid prototyping technology and an in-situ fabrication method for the needed tooling, reducing costs and lead times compared to conventional SACE machining approaches. Traditional manufacturing techniques are typically optimized for one or few different operations, while hybrid technologies as SACE have a great potential to support manufacturing in the Industry 4.0 approach as they are flexible and can reduce the overhead associated with each specific manufacturing technique to allow mass personalization at reasonable cost. The presented manufacturing methodology is a

good example of process adaptation to satisfy changing requirements such as geometries or volume to achieve mass personalized goods.

Besides these assets, the proposed method has some other significant advantages compared to traditional glass machining technologies, such as wet etching or abrasive jet machining:

- The product design files can be used straight forward in the manufacturing process without the need of additional steps as e.g. layered masks in wet etching techniques;
- Almost no restrictions for the desired geometry to be machined e.g. no taper restrictions as in abrasive jet machining;
- 2.5 D structures in glass can easily be machined.

This approach can be used for fabrication of high precision applications made of glass such as smart phones, advanced medical devices like Lab-on-Chip, green energy devices and fiber optic telecommunications.

Chapter 5

Bonding, being the last and most critical step in most glass micro-device manufacturing (e.g. microfluidic chips) can be a main factor of failure of glass chip manufacturing. Especially, direct glass-to-glass bonding after micro-structuring features in glass remains a challenging task at batch size 1. Most often necessary intermediate steps between machining and bonding jeopardize one of the key requirements for batch size 1 manufacturing – *reduction of processing steps in the manufacturing workflow*. Large batch processes such as wet etching do not require extensive post-processing steps before proceeding to bonding, however these batch processes are not appropriate for batch size 1 production by its parallel nature and complexity (e.g. requiring use of cleanroom, masking and extensive alignment operations). On the other hand, flexible technologies (e.g. Laser, mechanical machining) need extensive post-processing steps before bonding can be performed. Hybrid technologies as SACE are interesting to explore on its performance as machining step before glass-to-glass bonding.

This chapter details the study on deploying SACE technology as machining step in the fabrication of packaged glass devices (glass-to-glass bonded). It is shown by fabrication of a simple microfluidic Y-mixer that using SACE machining eliminates a post-processing step after machining of the desired structure on a glass substrate for subsequent glass-to-glass bonding. This method provides a solution to reduce one of the manufacturing cost drivers – reduction of manufacturing process steps. Quality of the achieved glass-to-glass bonding is assessed both qualitatively and quantitatively by the razorblade insertion test, acoustic imaging (Sonoscan®), electron microscopy (SEM) and leakage testing by microfluidic mixing at high pressure.

Rapid prototyping of packaged glass devices: eliminating a process step in the manufacturing workflow from micromachining to die singularizing

Lucas A. Hof and Rolf Wüthrich

Department of Mechanical & Industrial Engineering, Concordia University, 1455 de Maisonneuve Blvd. West, Montreal, QC H3G 1M8, Canada

Abstract

Direct glass-to-glass bonding after micro-patterning in glass is often challenging, especially in the frame of rapid prototyping, as several special cleaning or other post-processing steps are needed before bonding is possible. In this study, we demonstrate that glass-to-glass bonding is possible directly after Spark Assisted Chemical Engraving (SACE) micromachining without any special post-treatments. This approach enables flexible prototyping of glass devices at relatively low cost, which is illustrated by fabrication of functional microfluidic devices. The machined and bonded glass device is evaluated both qualitatively and quantitatively on performance and shows good results.

Keywords: glass-to-glass bonding; microfabrication; rapid prototyping; Spark Assisted Chemical Engraving (SACE); microfluidics

5.1. Introduction

Lab-on-a-chip (LOC) and other microfluidic devices are widely used in various research fields including life science and diagnostics [72, 92, 101, 110]. While there is a clear trend to use low-

cost materials like PDMS for disposable devices, there is still a wide range of applications which demands glass as substrate material [75]. This is mainly because of its unique properties, like optical transparency, chemically inertness, well known surface chemistry, biocompatibility, thermal properties and mechanical strength.

There is as well a need for rapid prototyping of such devices. Key challenges for fabrication of glass devices, particularly in low batch sizes, are machining, due to the hardness and brittleness of glass [83, 138] and subsequent bonding [259, 260] to seal the device.

Bonding is the last and most critical step in microfluidic chip manufacturing, which can be one of the main factors resulting in failure of glass chip manufacturing [101, 259, 261]. Common methods for glass bonding include anodic [262], thermal fusion [262], and adhesion bonding [263], where each category represents a wide variety of techniques for specific applications. Successful glass bonding requires properly polished and clean surfaces (root mean square surface roughness < 0.6 nm [264]) without any irregularities [261, 265-267]. Intermediate steps are usually necessary after machining, jeopardizing the desired low-cost rapid prototyping approach.

Parallel batch processes, such as wet etching [94], for machining relatively low aspect-ratio structures in glass are well established and do not present excessive difficulties for glass-to-glass bonding. However, when using flexible technologies for low-cost rapid prototyping of glass devices the bonding step becomes a major challenge [268]. Thermal processes like LASER are fast and flexible but form bulges near the machining zone in glass, which leads to bonding difficulties, making post process steps necessary [138, 267, 269, 270]. Mechanical methods, such as diamond tool drilling or powder blasting, have to deal with the issue that small glass debris or abrasive particles can easily stick to the glass substrate leading to bonding defects [118, 271].

Hybrid technologies like spark assisted chemical engraving (SACE) [81, 186] are interesting as they attempt to combine the advantages of each process to satisfy most requirements for low-cost rapid prototyping of micro-structures in glass, which have to be subsequently bonded for device fabrication. In SACE technology, a voltage is applied between tool and counter electrode dipped in an alkaline solution. At high voltages (around 30V), the bubbles evolving around the tool electrode coalesce into a gas film. Discharges occur from the tool to the electrolyte through this gas film [186]. Glass machining happens by thermally promoted etching (breaking of Si-O-Si bonds) [221].

Bonding a glass cover on the top of a device micro-machined by SACE was not yet investigated and it is an open question if major intermediate steps are necessary before being able to successfully proceed to bonding.

In this study, the bonding of two glass wafers directly after micromachining by a low-cost prototyping micromachining method (SACE technology) is investigated and it is shown that no major intermediate steps are necessary for successful subsequent glass-to-glass bonding.

5.2. Materials and methods

5.2.1. Rapid prototyping on glass: micromachining & bonding

Four-inch square glass wafers Borofloat 33 from Schott® (thickness of 1.1 mm) with chemical composition 81% SiO_2 | 13% B_2O_3 | 4% Na_2O/K_2O | 2% Al_2O_3 [272], a common material in academia and industry as substrate for microfluidic glass devices, were used.

Micromachining of a simple microfluidic Y-mixer in glass is done by SACE technology [81] on a Microfor SACE from Posalux SA, Switzerland [224]. This versatile machine offers high precision glass micro-drilling, micro-milling, micro-cutting and micro 2.5D machining operations for rapid prototyping of glass devices (Figure 5.1.A). The implementation of a force-sensitive machining head allows the use of ultra-thin machining tools (diameters down to 30 μm), applying force-feedback algorithms (detecting forces down to 1 mN) and usage of the head as profilometer to measure machined features within the same setup.

SACE machining was done applying pulsed voltage (U_{high} = 35.00 V, U_{low} = 17.50 V, t_{high} : t_{low} = 2.5 : 0.1 ms) and 30 wt.% sodium hydroxide was deployed as electrolyte. The tungsten carbide tool-electrode (Ø = 100 μm) was rotated at 1000 rpm. A feed-rate of 30 mm/min is applied for machining of the channels in two steps (depth-of-cut = 50 μm, final channel depth = 100 μm). The input and output holes for the mixer are drilled by SACE process in force-feedback mode on the same machine avoiding alignment issues and long lead (calibration) time.

After machining, the wafers were rinsed with water to remove the electrolyte and then packaged and shipped to Micronit BV [273] for fusion bonding at high annealing temperature bonding. No additional steps (except water rinsing before bonding) were performed by Micronit BV.

A. Drilling Milling (2.5D) Cutting

B.

Flexible glass machining by established methods → Postprocessing: • polishing/flattening • particle removal → Glass-to-glass bonding → Die singularizing

Flexible glass machining by SACE → Glass-to-glass bonding → Die singularizing
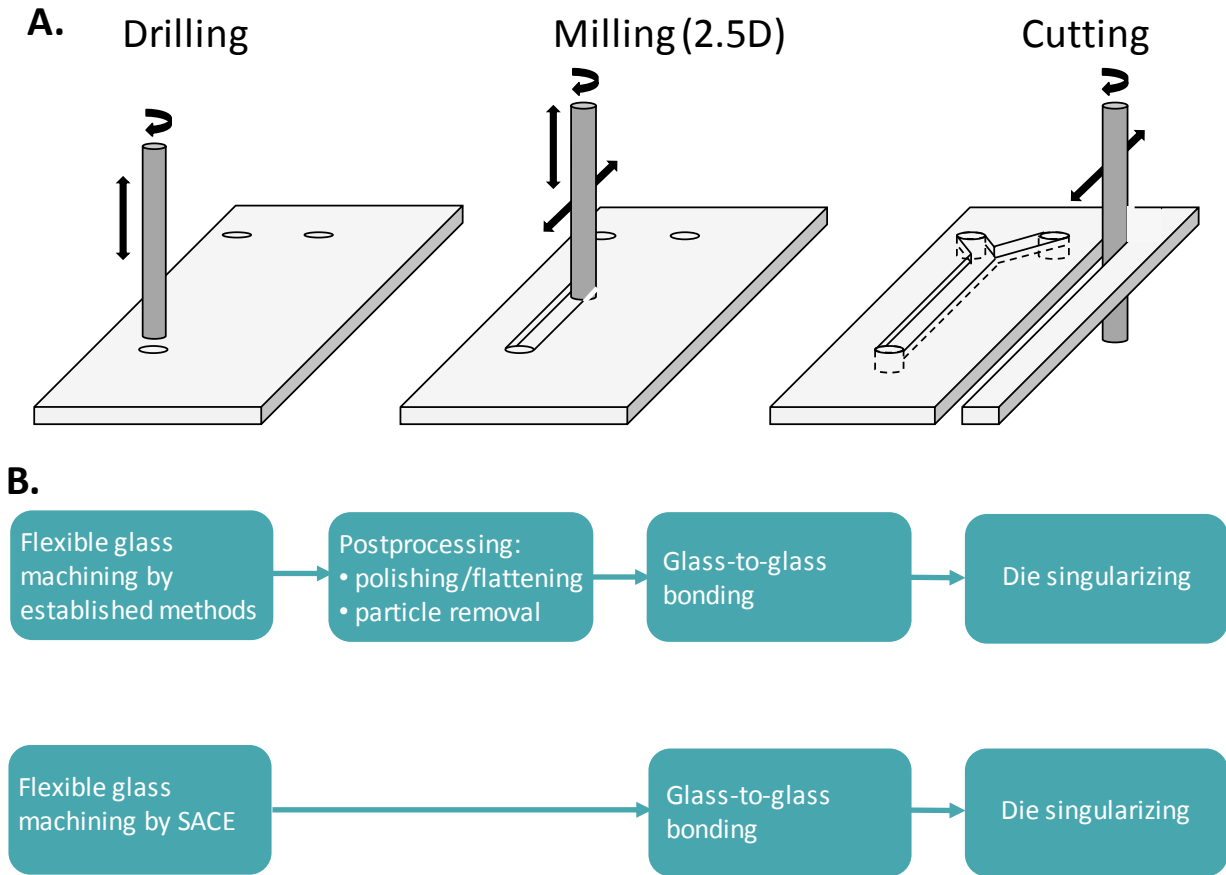
Figure 5.1. A. Versatile glass machining by SACE technology: drilling, milling and cutting by the same technology on the same setup. **B.** Comparison of process-flow (number of process steps) from glass micromachining to die singularizing for single device fabrication between established flexible glass machining approaches such as thermal (e.g. LASER) and mechanical methods (e.g. powder blasting) and SACE technology.

5.2.2. Bonding quality evaluation

To evaluate the quality of the direct glass-to-glass bonding after machining, the fabricated device is assessed both qualitatively and quantitatively. Characterization is done for mechanical properties and uniformity across the total bonded surface.

The bonding energy, as measure for the bonding strength of the bonded substrates, can be determined using a crack-opening method such as the razor blade insertion test [274, 275]. Therefore, a razor blade is inserted into the bonding interfaces and the crack propagation length is measured, which is used to calculate the bonding energy [275].

Presence of defects in the bonding such as delamination, voids and cracks are detected by Acoustic Microscopy [276] using Sonoscan® - Gen6™ C-Mode Scanning Acoustic Microscope

equipment. This non-destructive characterization method makes use of ultrasound to find hidden defects within materials. The high frequency (> 20 kHz) ultrasound signal propagates through solid and liquid materials, but will be fully reflected by air (i.e. pores) and largely deflected away by cracks or non-planar interfaces.

Cross-sections of the channel are prepared by diamond saw dicing (MTI corporation, model SYJ-40-LD) and successive mechanical polishing on a Buehler grinder-polisher (MetaServ 250) with fine grit polishing paper (BuehlerMet II abrasive paper, grit sizes 800 - 1200) and diamond particle polishing fluid (Buehler MetaDi Polycrystalline Diamond Suspension - 1 µm). Results are investigated by electronic microscopy (variable pressure S-3400N Hitachi SEM) to examine the bonding qualitatively.

Overall verification of proper functioning of the device without any leakage is performed by microscopic imaging (DLand 200x magnification USB microscope) of the device operating with DI water and coloured food dyes. Standard tube connectors are glued (2-component epoxy glue) on the inlets and outlet of the mixer, which are attached to two micropumps (NE-500 Syringe pump - New Era Pump Systems Inc.) for coloured solution supply.

5.3.   Results and discussion

Comparison of the process-flow, with respect to the number of major process steps, from glass micromachining to die singularizing for single device fabrication between established flexible glass machining approaches such as thermal (e.g. LASER) and mechanical methods (e.g. powder blasting) and SACE technology are presented in Figure 5.1.B. The proposed glass device fabrication process using SACE technology eliminates the cumbersome and time consuming postprocessing step which is needed for the alternative flexible machining approaches.

Assessment of the glass bonding strength was performed by the crack opening method. The bonded glass sheets (layer thickness = 1 mm) could not be separated by the razor blade (Wilkinson Sword Classic, thickness = 80 µm) insertion. Typical bonding energy values for weak hydrophilic SiO_2 - SiO_2 bonding are around 0.2 to 0.4 J/m2, while values around 1.2 J/m2 can be obtained upon subsequent annealing at T = 600 °C [264]. It can be concluded that the applied bonding exceeds both these bonding energy values as no separation was observed.

Acoustic microscopy imagining (Figure 5.2) confirms that no defects, such as voids, microcracks and delamination are present (they would appear as white structures on the image). Consequently, SACE process does not leave any particles or redeposited debris (forming bulges) on the substrate after machining, resulting in high quality direct (fusion) bonding without any required postprocessing (e.g. polishing) step after micromachining.
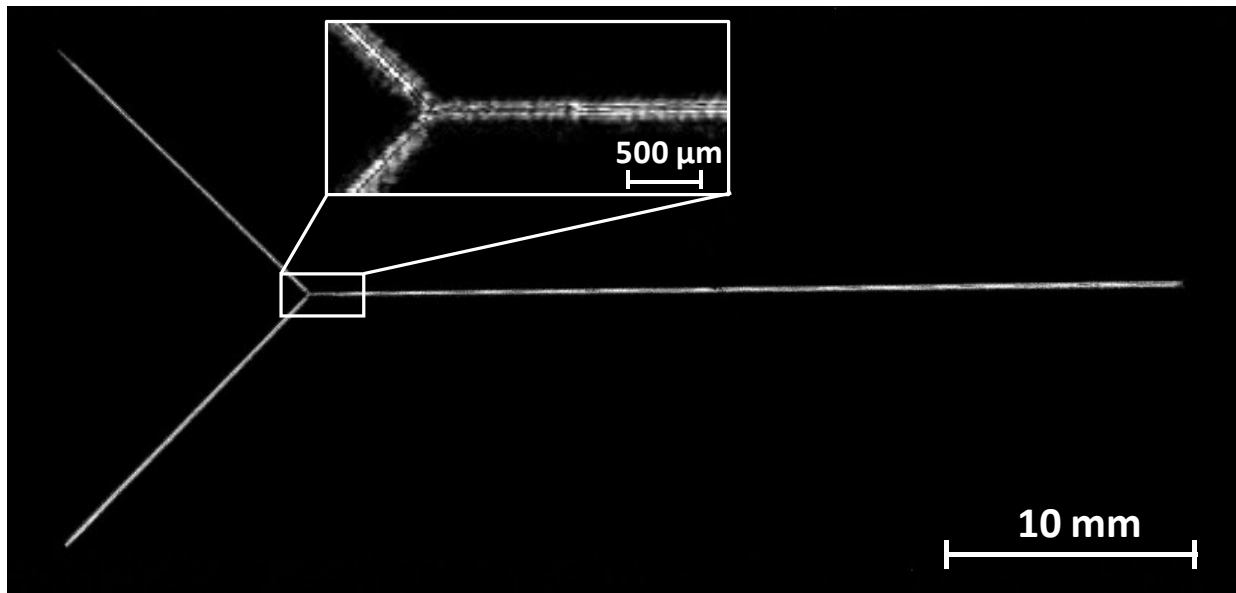
Figure 5.2. Acoustic image (Gen6™ C-Mode Scanning Acoustic Microscope, Sonoscan) of the bonded glass mixer. The inset presents a detail at higher magnification of the bonded channels.

Imagining of the cross section of the glass-to-glass bonded sample (Figure 5.3) by scanning electron microscope (SEM) reveals the good bonding quality of the cover glass onto the machined glass and confirms that no defects, such as bulges or debris near the entrances of the machined channel in glass, are present.
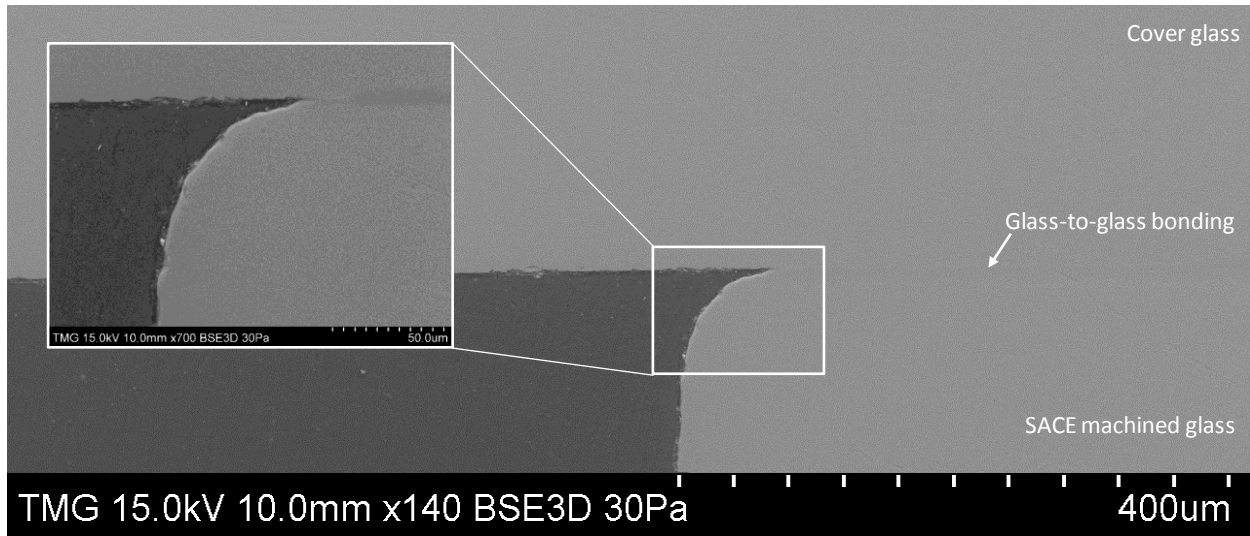
Figure 5.3. SEM micrograph (variable pressure S-3400N Hitachi SEM) of the cross-section of a direct glass-to-glass bonded SACE machined channel entrance. The inset shows one bonded channel entrance at higher magnification (scale bar = 50 µm).

Finally, practical operation and functioning of the micro-mixer is tested by supplying coloured dyes to the inlet ports by syringe pumps. Figure 5.4.A depicts the microscopic image of coloured dye mixing along the channel. No leakage was observed over the full range of syringe pump feedrates (0 – 2050 µL/s) corresponding to applied pressure drops of approximately 0 – 2.3kPa (based on channel dimensions - width = 320 µm - depth = 130 µm - and applying Navier-Stokes equation [73]).

A further example of a functional microdevice made out of glass by SACE technology is illustrated in Figure 5.4.B (design file) and Figure 5.4.C (fabricated glass device). This multilayered device consists of three glass layers (upper and lower layer thickness = 0.7 mm and middle layer thickness = 3.3 mm) with micromachined structures packaged together with fusion bonding by Micronit Microtechnologies BV [273]. All glass machining operations, including die singularizing (here: cutting) after bonding of the wafers, were performed by one single technology (SACE process) on an industrial Microfor SACE machine [224].
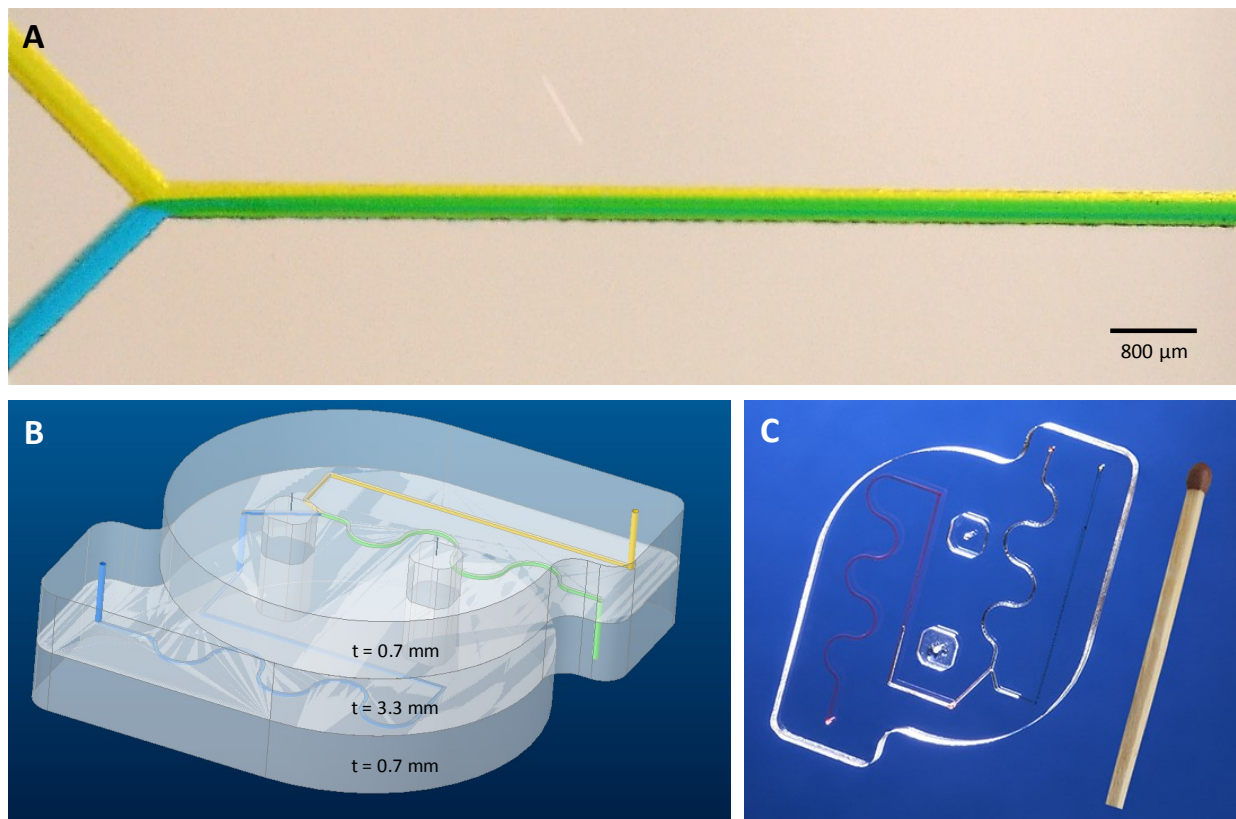
Figure 5.4. A. Microscopic image of leakage-free coloured dye mixing (supplied by syringe pumps NE-5000, New Era Pump Systems Inc.) in the bonded glass channel. **B.** Design file for a multilayered microdevice. **C.** Fabricated functional multilayer microdevice of glass machined by SACE technology.

5.4.   Conclusion

In this study, it is demonstrated that Spark Assisted Chemical Engraving (SACE) process is a promising method as rapid prototyping technology for glass device fabrication eliminating a process step in the manufacturing workflow from micromachining to die singularizing for single device fabrication out of a glass wafer. SACE process can do micromachining while leaving the glass surface intact such to allow subsequent direct glass-to-glass bonding. The glass surface remains defect-free after micromachining, leaving no bulges or redeposited material (debris) around the machined structure for successful subsequent direct glass bonding without any intermediate (post-processing) steps. This approach enables flexible prototyping of glass devices at relatively low cost, which is illustrated by fabrication of a functional microdevice. The machined and bonded glass device is evaluated both qualitatively and quantitatively on performance and shows good results for use in microfluidic applications.

Chapter 6

With the great technological advancement in the micro-technology field, micromachining of various materials has become a key task. New demands are being placed on microfabrication of complex architectures in robust materials. Iterative design optimization in a timely manner – *rapid prototyping* – places challenges on fabrication technologies. As mechanical components of microsystems *plastic* parts or *metallic* micro components are often used [277, 278]. The role of *glass* in Micro-Electro-Mechanical-Systems (MEMS) and Micro-Optical-Electro-Mechanical-Systems (MOEMS) has typically been limited to its integration into the final device-level product [110]. However, glass has several unique properties which can be exploited further for novel *indirect* applications in the micro-technology field, such as templates for hot embossing or tools (dies) for metal micro-forming techniques. Glass is interesting in these applications respectively mainly owing its low thermal expansion coefficient (3.25 µm·(m·k)$^{-1}$ for standard Borofloat 33, SCHOTT) and high hardness (433 HB for Borofloat 33 and 567 HB for Xensation, SCHOTT) and sufficiently high mechanical strength. These properties are important to limit deformations and meet the high precision (e.g. repeatability) demanded by these embossing and micro-forming processes. Sufficiently high fracture resistance of materials used in these applications is required. This depends largely on potential fracture sites [71], e.g. surface flaws, resulting in a demand of flaw-free, smooth surfaces of machined glass surfaces.

Nevertheless, glass remains a hard to machine material and especially flexible manufacturing methods are challenging to deploy on glass, which is the main reason that glass has not yet been considered a viable candidate for the discussed applications.

This chapter provides detailed examples of fabricated tooling of glass providing interesting novel solutions to reduce indirectly the manufacturing cost drivers related to part design – 1) reduction of tooling costs and rapid prototyping of tooling, 2) reduction of calibration procedures by high-precision machining, 3) ability to create complex parts (e.g. 2.5D or 3D features on tooling), 4) reduction of process steps in tooling fabrication.

SACE process is used as flexible manufacturing (i.e. rapid prototyping) technology for fabrication of consequently glass templates for microfabricated devices by hot embossing (section 6.1 - Glass imprint templates by spark assisted chemical engraving for microfabrication by hot embossing), and for manufacturing of glass tools (dies) for micro-forming of metal micro parts (section 6.2 - Towards high precision manufacturing of glass tools by Spark Assisted Chemical Engraving (SACE) for micro forming techniques).

In these sections, the use of SACE patterned glass templates for embossing of microstructures in thermoplastics and for micro deep drawing of metal sheets (thickness 25 μm) is demonstrated. This technique has the advantage of rapidly and accurately introducing features into glass substrates, with good control over all three dimensions. Optimization of the technique for generating the required smooth surfaces was demonstrated upon applying the developed SACP technology as detailed in chapter 3.

Section 6.1.

New rapid prototyping methods are needed for fast and error-free micropatterning in plastics [279], which are among the fastest growing materials for industrial and clinical MEMS components [280]. Established fabrication techniques such as milling, printing, ablation (sequential methods) and casting, injection moulding, hot embossing (template-based processes) have each their advantages and disadvantages defining its use for specific applications. Hot embossing has proven to be a market relevant technology (reduced energy consumption and residual thermal stress) for creating plastic micro-devices.

However, commercially available imprint templates are expensive and time-consuming to make, limiting its use for rapid prototyping applications. The fabrication of imprint templates in new materials can open the door for rapid prototyping by hot embossing and a seamless transition to production-level runs for developed designs. Glass is an interesting option as imprint template

material, due to its good thermomechanical properties, but it is lacking machining technologies to flexible fabricate such templates with the required smooth surface and high-precision. In section 6.2, the use of SACE machined glass templates for the embossing of microstructures in thermoplastics was demonstrated. This technique had the advantage of rapidly and accurately introducing features into glass substrates, with good control over all three dimensions.

The presented approach provides a solution for fabrication of low batch-size polymer based micro-systems as of today the mold fabrication process is very expensive (cleanroom processes using complex masking and etching processes) for small batch-sizes.

Glass imprint templates by spark assisted chemical engraving for microfabrication by hot embossing

Lucas A. Hof[1], Shane Guo[2], Minseok Seo[2], Rolf Wüthrich[1,3], Jesse Greener[2,4]

[1] *Department of Mechanical & Industrial Engineering, Concordia University, 1455 de Maisonneuve Blvd. West, Montreal, QC H3G 1M8, Canada*

[2] *FlowJEM Inc., 80 St. George Street, Toronto, ON M5S 3H6, Canada*

[3] *Posalux SA, 18, Fritz Oppliger, CH-2504 Biel/Bienne, Switzerland*

[4] *Département de Chimie, Université Laval, Québec, QC G1V 0A6, Canada*

Abstract

As the field of microelectromechanical systems (MEMS) matures, new demands are being placed on the microfabrication of complex architectures in robust materials, such as hard plastics. Iterative design optimization in a timely manner—rapid prototyping—places challenges on template

fabrication, for methods such as injection moulding and hot embossing. In this paper, we demonstrate the possibility of using spark assisted chemical engraving (SACE) to produce micro patterned glass templates. The direct, write-based approach enabled the facile fabrication of smooth microfeatures with variations in all three-dimensions, which could be replicated by hot embossing different thermoplastics. As a proof of principle, we demonstrated the technique for a high glass transition temperature polycarbonate. Good fidelity over more than 10 cycles provides evidence that the approach is viable for rapid prototyping and has the potential to satisfy commercial-grade production at medium-level output volumes. Glass imprint templates showed no degradation after use, but care must be taken due to brittleness. The technique has the potential to advance microfabrication needs in academia and could be used by MEMS product developers

Keywords: micro-fabrication; hot embossing; micro-machining; microfluidics; glass; thermoplastics; MEMS; spark assisted chemical engraving

6.1.1. Introduction

Micro electromechanical and micro optical electromechanical systems (MEMS and MOEMS) are poised to become a mainstream technology. One of the main developmental hurdles to overcome is devising new methods for fast and error-free micropatterning in plastics [279], which are among the fastest growing materials for industrial and clinical MEMS components [280]. Generally, fabrication techniques are either (i) sequential, such as milling, printing and ablation or (ii) template-based, such as casting, injection moulding and hot embossing, which create all features at the same time. Sequential methods can provide certain advantages, such as the straight-forward formation of three-dimensional features and a seamless design to prototyping workflow. However, they are not suitable for either high-volume requirements or even low-volume outputs, if the designs are too complex or high-density. On the other hand, moulding approaches that use a template, can be fast and accurate and are, therefore, more likely to be suitable for market-relevant volume demands. In hot embossing, a polymer is heated to its glass transition temperature (T_g) and then formed into shapes based on contact with a microstructured template surface. It is similar to injection moulding, but differs in that complete melting is not required, which reduces energy consumption and residual thermal stress [281-285]. The replication process is straight forward,

whereas the challenge lies in the fabrication of the imprint template. Typically, commercially available imprint templates are fabricated in metals such as nickel, using one or a combination of the following techniques: mechanical machining [286], laser ablation [287] and/or electroforming [286-288]. Such templates are advantageous in terms of their durability and thermal properties, but they are expensive and time-consuming to make. To date, the growth of hard plastics in final MEMS devices has only been possible due to the economies of scale that are realized in high-volume outputs, which can spread the cost of template development over many units. However, prototyping by hot embossing is still prohibitively expensive for complex designs requiring many iterations. Prototyping with lower cost techniques, such as casting polydimethylsiloxane (PDMS), is an option, but this will introduce new problems when switching fabrication modalities. Approaches for reducing the fabrication time and cost of the imprint templates by photolithography or by electroplating nickel through adhesive masks have been demonstrated, but both techniques have some limitations when considering the design aspect ratio and operating temperatures or feature resolution, respectively [282-289]. Furthermore, most of these approaches impose restrictions on the complexity of the design in the third dimension. So-called 2.5D templates can be achieved in multi-step fabrication processes, but this is time consuming, and requires specialized procedures. Recently, a new approach for producing 3D microfeatures in microfluidic channels has been shown, based on the control of embossing parameters to achieve controlled "partial" embossing, but the technique is still new and requires optimization [290]. The fabrication of imprint templates in new materials can open the door for rapid prototyping by hot embossing and a seamless transition to production-level runs for developed designs.

Literature reports on glass as an imprint template for polymer embossing are quite limited [291, 292]. One of the main reasons that glass has not been considered a viable candidate for microembossing is due to the difficultly in its microscale patterning. Thermal etching based on femto-second laser processing can create features with a sub-micron resolution, but the equipment required is expensive and involves extensive set-up optimization. The preferred method for micropatterning glass is wet or dry chemical etching techniques. However, etching rates are slow and realizing 3D structures is not straightforward [110]. Mechanical machining is complicated due to the hardness and brittleness of glass. It is also difficult to achieve high-aspect ratio structures and is slow, costly and results in poor surface quality [81]. Alternative machining approaches, such as glass moulding techniques (e.g., glass reflow), make use of a high temperature step to reflow

the glass into a micro-patterned silicon mould. However, multiple fabrication steps are needed (heating, lithography, patterning, vacuum cavities), processing times are very long and narrow patterns are complicated to achieve [82, 293, 294].

Recently, spark assisted chemical engraving (SACE) has been demonstrated as a promising approach for rapidly generating smooth, high aspect ratio 3D micro-structures in glass [81]. In this approach, a voltage is applied between a tool microelectrode and counter electrode, which are immersed in an electrolyte solution [81, 99]. The electrolysis of water under an electrical potential (DC or pulsed voltage), causes bubble formation around the tool electrode. An electrical discharge passes through the gas, and is largely localized to its tip, where the electric field is highest. Thus, the machining of nearby glass surfaces becomes possible due to thermally promoted hydroxide ions, which cause the localized breaking of Si–O–Si bonds [81, 221]:

$$2NaOH + SiO_2 \rightarrow Na_2SiO_3 + H_2O \tag{6.1}$$

More detailed information on the etching of silica glass in the presence of OH-containing electrolytes, can be found in the literature [70, 295, 296].

With the proper choice of processing parameters (temperature [221], voltage [192], electrolyte type, and its concentration [81, 99]), SACE can be optimized to rapidly produce smooth micro-structured glass features with shape control in three-dimensions. Relative to other techniques, it has high machining speeds (cm·s−1), a range of target materials (glasses [297], ceramics [298], and composite materials [299]) and is low-cost [81]. Thus, for the purpose of this work, SACE was selected as a method for producing imprint templates in glass for the testing and development of a new method for microfabrication applications requiring rapid prototyping in thermoplastics by hot embossing. The utility of glass templates was tested through the replication of micro features, including drill holes and channels with different depths and surface finishes.

6.1.2. Materials and Methods

Consumables included polycarbonate (PC) (Lexan 9034-112, Sabic Polymershapes, Brampton, ON, Canada), polypropylene (PP) (PolyPrime, Coquitlam, BC, Canada), cycloolifin polymer (COP) (Zeon, Zeonex, Louisville, KY, USA), polymethyl methacrylate (PMMA) (Plaskolite, Optix, Columbus, OH, USA), polystyrene (PS) (McMaster Carr, Elmhurst, IL, USA),

polydimethyl siloxane (PDMS) (Sylgard184, Dow Corning, Midland, MI, USA), glass (borosilicate, square 50.8 mm, thickness = 3.175 mm, Corning Inc., Corning, NY, USA), potassium hydroxide (KOH Cas 1310-58-3, Cayman Chemical Company, Ann Arbor, MI, USA), tool-electrodes (tungsten carbide cylinders, diameter=100 μm, Posalux SA, Biel/Bienne, Switzerland), and Trichloro (1H,1H,2H,2H-perfluorooctyl) silane (Sigma-Aldrich, Oakville, ON, Canada).

Milling designs were created using computer-aided design software (AutoCAD 2015, AutoDesk San Rafael, CA, USA). Glass machining was conducted using an industrial SACE system (Microfor SACE, Posalux SA, Biel/Bienne, Switzerland) and a home-build lab SACE set-up (SACE1, Electrochemical Green Engineering Group, Concordia University, Montreal, QC, Canada). A universal motion controller (XPS-C4, Newport, Irvine, CA, USA) was used to program the x,y,z axes. z-Direction control was achieved by a proportional–integral–derivative (PID) control loop using an optical sensor and voicecoil actuator on the machining head.

Embossing was accomplished using a converted hydraulic press (Model 3851-C Carver Inc., Wabash, IN, USA) with ±1 °C temperature control, compressed gas cooling was applied to the top and bottom platens, and ±0.05 MPa pressure control was applied between the platens. Embossing was conducted inside a custom compression chamber that was placed between the top and bottom platens, with leads for gas exchange and vacuum control. The temperatures inside the embossing chamber were determined to be 4–6 °C lower than the platen set values. No determination of the real pressures applied to the embossing tool and plastic substrate was made, but it was estimated to be between 0.2 and 0.4 MPa lower than the value determined by the external pressure gauge.

Evaluation of the microfeatures on the embossing template and embossed polymer substrate was conducted using optical profilometry (Veeco NT 1100, Veeco, Plainview, NY, USA) and optical microscopy (Olympus BX41, Olympus, Center Valley, PA, USA) was combined with the application of a charge-coupled device (CCD) camera (EvolutionTM VF, Media Cybernetics Inc., Silver Spring, MD, USA) using ImagePro software. Root mean square (RMS) roughness was conducted on optical profile images using the plugin "Analyse Stripes" in the open source software ImageJ (software developed by contributors worldwide).

6.1.3. Results and Discussion

6.1.3.1. Mould Fabrication Using SACE

6.1.3.1.1. System Operation

The electrochemical cell, containing the electrolyte (typical NaOH or KOH), counter electrode (stainless steel 316L, Advent Research Materials, Oxford, UK), and the target glass substrate, was mounted on an x,y stage (resolution, 1 μm), whereas the axial movement of the electrode tool (tungsten carbide) was performed on a high precision z-stage (resolution, 1 μm). High accuracy tool tips, with diameters of 100 μm, were used to enhance machining accuracy and resolution. In addition, tool rotation was implemented by a dc brushless motor, added to the z-axis stage to improve the uniformity of electrolyte flow around the tool, thus increasing the quality of the machined features. When high voltages (around 30 V) were applied between the counter electrode and the tool, the bubbles evolving around the tool electrode coalesced into a gas film, and electrical discharge was emitted from the tool and passed through the film to the electrolyte, as illustrated in Figure 6.. Usually, the voltage is pulsed between a high voltage (between 28 and 40 V) and a lower voltage (typically 17.5 V), with a period = 2.6 ms, and a duty cycle = 96.15%, in order to limit temperature buildup. The machining conditions for the SACE process of glass mould fabrication are denoted in Table 6.1.

C.

Machining head
(profilometer)
*mounted on
XYZ-stage*

Tool electrode
(rotating)

Glass sample

Cell
(electrolyte –
typical 30%wt. NaOH)
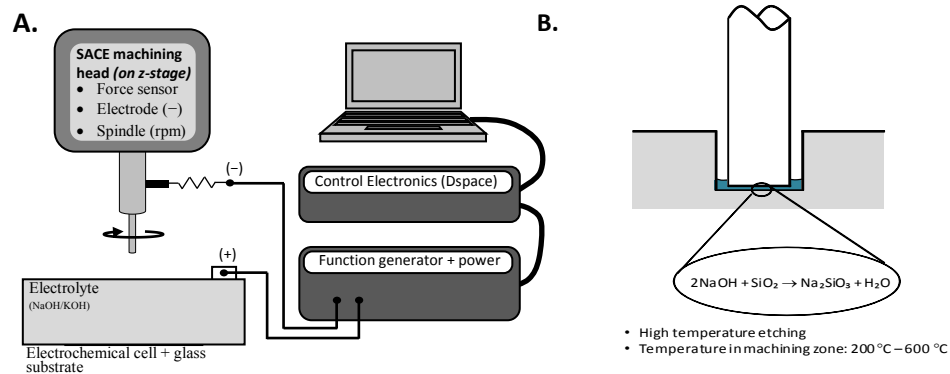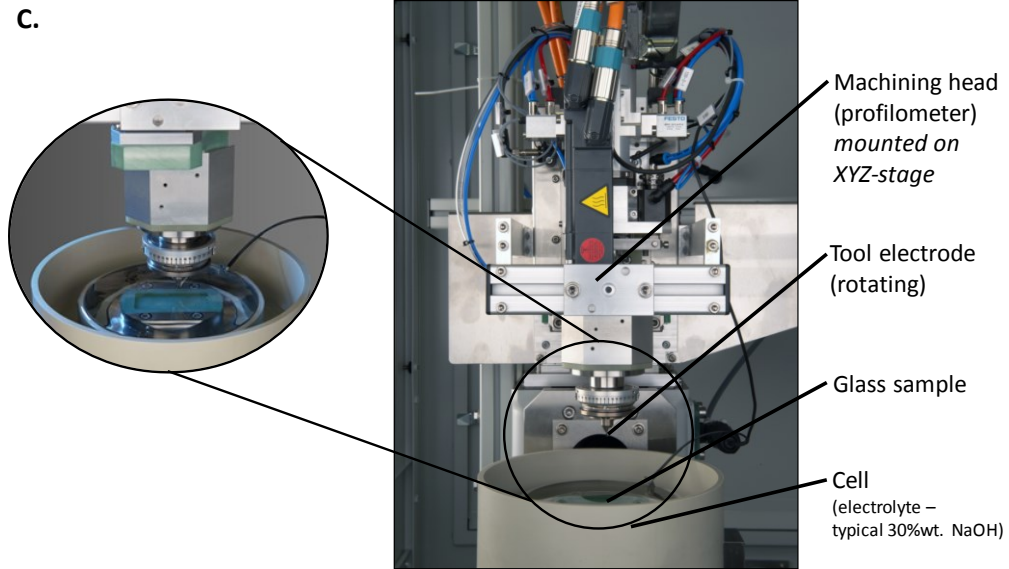
Figure 6.1. A. Laboratory spark assisted chemical engraving (SACE) versatile glass micromachining setup. **B.** Chemical mechanism responsible for the localized degradation of the SiO_2 network at the SACE tool tip (blue). **C.** Image of the industrial Microfor SACE machine (Posalux SA) used in this work with inset showing a close-up of the machining zone.

Table 6.1. SACE machining conditions.

Feature	Machining Mode	Electrolyte	Pulsed Voltage Input			
			High Level	Low Level	Period	Duty Cycle
Channels/lines	Constant depth-of-cut (50 μm) × *n*	20 wt % KOH	36 V	17.5 V	2.6 ms	96.15%
Holes	Gravity feed drilling	20 wt % KOH	36 V	17.5 V	2.6 ms	96.15%

6.1.3.1.2. Control over 3D Structure

The developed industrial SACE machine offered high precision glass micro-drilling, micro-milling, micro-cutting and micro 3D machining operations (Figure 6.2), while leaving the glass surface intact to allow subsequent glass-to-polymer templating. The implementation of a force-sensitive machining head with force-feedback algorithms could detect and maintain forces as low as 1 mN. This enabled the usage of narrow machining tools without bending or breaking, and secured its usage as an accurate profilometer for measuring machined features within the same set-up to an accuracy of 1 μm, enabling continuous three dimensional control.
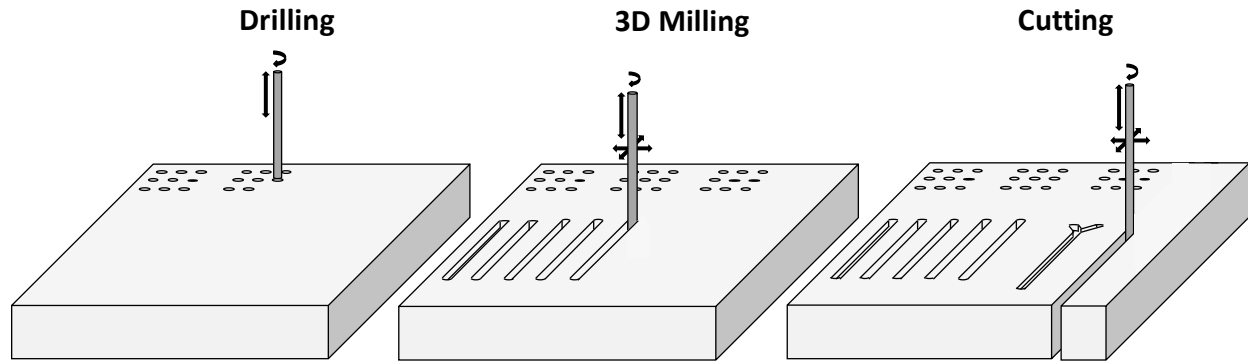
Figure 6.2. A graphic highlighting 3D drilling, milling, and cutting machining operations performed on the same glass substrate.

6.1.3.1.3. Surface Smoothness for Hot Embossing Applications

The SACE milling technique can be optimized to improve the surface uniformity of the etched features. This enhanced surface quality was achieved on the industrial Microfor SACE machine (Figure 6..C). It is proposed that a smoothed edge will have two positive effects for the present application of hot embossing. First, reduced surface area on the smoothed feature side walls, will reduce the friction between the template and plastic substrate during de-embossing, thereby lowering the force required to separate them. Second, there will be a reduction in the number of potential fracture sites on a smooth glass surface, in comparison to a rough one. Together, these factors should strongly improve the quality of the embossed features and the longevity of the imprint template, by reducing the chance of damage during de-embossing.

For the purpose of this study, SACE process parameters were chosen in order to reduce the surface roughness of the cut side walls. It should be noted that surface smoothness optimization experiments are ongoing, and the results presented in this paper are based on preliminary results produced when using the Microfor SACE machine (Posalux SA). To evaluate the smoothness of the machined side wall, a measurement was made for the surface distance index (SDI), which is defined as:

$$\text{SDI} = d_s/d_{sl} \tag{6.2}$$

where d_s is the total path length, including wall roughness, between two points along the machined edge and d_{sl} is the distance of the straight line between the end points.

SACE optimization reveals a SDI improvement of 0.089 (i.e., about 9%), based on a measured SDI of 1.098 for the fast rough cut (Figure 6.3.A.), and an SDI of 1.009 for the optimized cut (Figure 6.3.B.). These correspond to a RMS surface roughness of 3.77 and 1.13 µm, respectively.
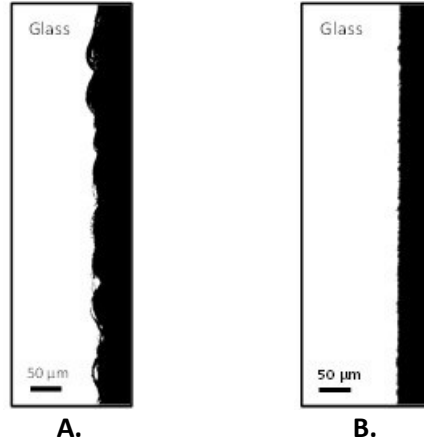
Figure 6.3. Top-view microscope images of example surfaces after SACE milling: a cut made with the lab set-up (**A.**). and a cut made on the industrial Microfor SACE machine (Posalux SA) (**B.**). Scale bars are in 50 µm.

6.1.3.1.4. Fabrication and Evaluation of a Glass Imprint Template

To demonstrate the approach for hot embossing, glass imprint template moulds were fabricated, containing features for analysis, including drilled holes and channels (Figure 6.4). Additionally, other features were added to subsequent glass templates, including spiral patterns, rings, and crosses. Due to the flexibility in prototyping, the features had a range of depths, ranging from 50 to 750 µm on the same glass substrate, leading to aspect ratios of between 0.2 and 3.0. While the technique has been used to create aspect ratios of 10 or higher [81], we chose to work with smaller values in order to demonstrate the technique without complications related to de-embossing high aspect ratio features. For a comparison of the feature quality after a polishing step, a series of channels were fabricated using the same protocol as above.

Features were analysed using a combination of optical profilometry and cross-sections in replicates of the glass mould, which were easier to cut and examine. To achieve the latter, a double replication process was undertaken, resulting in a positive PDMS part which could be cross-sectioned with a blade and viewed with a regular transmission light microscope. The replication process started by casting PDMS against the glass mould. This formed a negative of the glass

mould. Then, a second replica was formed by casting PDMS against the first, to create a positive replica. In each replication stage, the casting surface was silonized to enable separation of the parts.
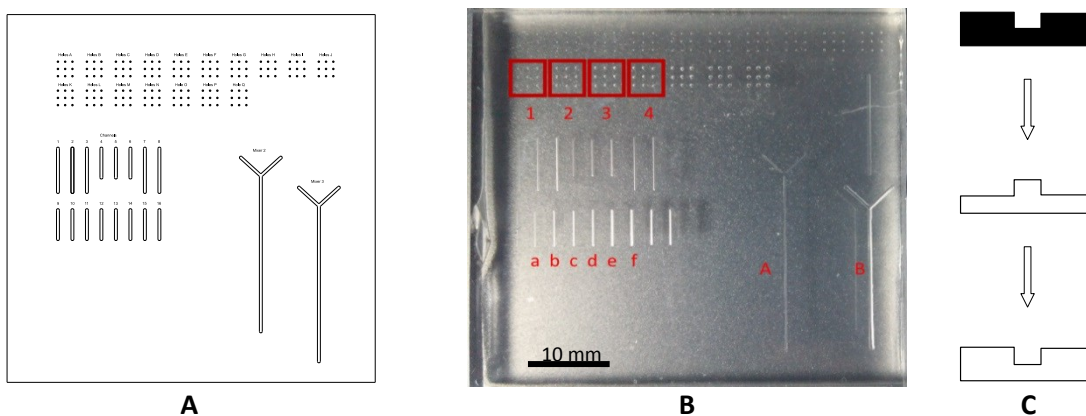
Figure 6.4. A schematic from the CAD file (**A.**). that was used to produce the glass template by SACE milling for this work (**B.**). Highlighted regions include drill arrays (red box 1–4) and trenches ("a"– "f", "A", "B"). A schematic showing a double replication procedure of the original template (black) for producing positive replicates in PDMS (white) (**C.**).

6.1.3.1.5. Time to Create a Stamp

The time required to create a channel feature on the glass substrate was not a key optimization parameter in this study. Instead, focus was placed on achieving features with low surface roughness (< several microns). Nevertheless, it is instructive to evaluate this parameter as a benchmark for future optimization. As an example, the features a, d, and f, shown in Figure 6.4.B., required 21 min, 23 min, and 25 min, respectively, based on their length (L = 5 mm), number of passes (depth-of-cut per pass = 50 µm) required (P_a = 2, P_d = 8, P_f = 12) and additional optimization steps. Therefore, it is reasonable to conclude that a complete new master, with significantly higher complexity, could be fabricated in under a day. This is nearly an order of magnitude faster than current methods, before having considered the arbitrary SACE ability to make 3D features at the same time. Chemical methods, such as deep reactive ion etching (DRIE) etching and wet etching, have very low etching rates, with average rates of 0.01 and 0.1 µm·s^{-1}, respectively. Moreover, they need cleanroom facilities and require additional sophisticated masking steps. In addition, wet etching (standard masking procedures) limits the achievable aspect ratio to one. Mechanical methods, such as drilling and milling (feed rates around 100 µm·s^{-1}), and powder blasting (feed rates around 1 µm·s^{-1}), have feed rates which are similar to, or faster than, SACE technology. However, machined surfaces suffer from high surface roughness and

microcracks. It is uncertain whether such glass surfaces could work for repetitive cycling through hot embossing steps. Thermal processes, such as ultra-short laser technologies (e.g., Femto-second laser), have increased feed rates (around 10–10,000 $\mu m \cdot s^{-1}$), however, these technologies need extensive set-up optimization and are expensive. The use of a hybrid technology such as SACE seems to be an appropriate choice for the rapid prototyping of glass moulds.

6.1.3.2. Use of Glass Moulds as Imprint Templates for Microfabrication

6.1.3.2.1. Glass Properties

Table 6.2 compares relevant glass properties with other materials used for hot embossing templates. The most widely used material is Ni, which has a low thermal expansion, high thermal conductivity, and good mechanical properties. However, the cost and time required to produce Ni imprint templates is substantial, rendering it ineffective for prototyping. In searching for alternative materials for embossing templates, researchers have looked to polymeric materials, such as PDMS, photoresists and epoxy resins. The major drawback of these materials includes poor thermal conductivity and high linear expansion coefficients. Their hardness is also generally much lower than that of Ni, even with process optimizations [300]. Low hardness can lead to blemishes in the template from microscopic dust and debris, thereby limiting their practical life-times. In addition, fabricating 3D structures is challenging.

Glass is an interesting option, due to its good thermomechanical properties. First, glass is superior to all other options in terms of its low thermal expansion. Hardness prevents degradation of the template [301]. Glass and polymer-based template materials all suffer from low thermal conductivity. This means that overall embossing times can be longer than those of metal stamps. However, the difference is in terms of minutes, which is not significant for low and medium production levels. Fracture toughness is related to material brittleness and is a measure of a material's ability to resist cracking. It is one of the most relevant mechanical properties for hot embossing. In glass, this is affected by ion type and concentration [302, 303]. The low fracture toughness of glass is its greatest drawback for hot embossing applications. However, as discussed later, this problem can be overcome by following certain fabrication protocol.

Table 6.2. Comparison of relevant properties for different hot embossing template materials.

Material	Linear Temp. Expansion Coefficient (μm·(m·k)$^{-1}$)	Thermal Conductivity (W·(m·k)$^{-1}$)	Hardness (GPa)	Fracture Toughness (MPa·m$^{1/2}$)	Tensile Strength (MPa)	Compressive Strength (MPa)
Glass borosilicate (toughened) [304]	4.0	1.05	6.2 [305], [306]	0.7 [307] / 2 [308]	30/200	1000
PDMS (Stylgard 184) [309]	310	0.15 [310]	N/A [1]	-	7 [311]	2–50
Photoresist (SU-8 series) [312]	52	0.2	0.3 [313]	-	73	-
Epoxy resins [314]	-	-	N/A[2] [314], [315]	400	70 [316]	-
Ni	13.0	91	6.3–11.8	100–150	-	-

[1] The elastomer PDMS has a measured hardness of 50 in the Shore A scale, a scale ranging from 1 to 100 for the softest polymer materials; [2] the resin elastomer Conapoxy has a measured hardness of 90 in the Shore D scale, a scale ranging from 1 to 100 for the hardest polymer-based materials.

6.1.3.2.2. Embossing Protocol

Due to the non-zero water absorption by most thermoplastics used here, films (0.5 mm) were first dehydrated before embossing, by pre-heating in an oven at roughly 80 °C for t_d = 40–80 min. The glass imprint template was then loaded with its features facing up, onto the bottom side of the custom embossing chamber, which was itself on the bottom platen of the hot press. The thermoplastic material was placed on top of the glass template (Figure 6.5.A). Following this, the chamber was closed and a vacuum was applied, while the system heated to an embossing temperature T_e. An embossing pressure (p_e) was then applied, which forced the heated polymer into the machined cavities in the glass template (Figure 6.5.B). After two minutes, the system temperature was reduced to the de-embossing temperature (T_d), followed by the breaking of the vacuum and the separation of the moulded plastic from the template (Figure 6.5.C). Relevant thermal properties, as well as the embossing parameters for different thermoplastic materials, are given in Table 6.3.

Table 6.3. Material properties and embossing conditions for materials used in this study.

Material	Material Properties		Embossing Conditions			
	T_g [1] (°C)	T_m [1] (°C)	t_d [2] (min)	T_e/T_d [3] (°C)	P_e [4] (PSI)	t_e [5] (min)
COP	138	210	50–100	150/130	70	5
PMMA	113	160	75–90	145/80	130	5
PC	149	155	40–80	175/145	150	5
PS	101	240	70–80	115–125/100	120–130	5
PP	−6	164	N/A	145/100	150	5

To demonstrate the robustness of the technique, we carried out replication on PC, which had the highest T_g of the test materials used in this study. Figure 6.5.D,E. show the images of certain features on the glass template and the results from the embossed PC. The glass template features included (i) drill holes, (ii) channels and (iii) curved shapes (Figure 6.5.D.). All template features (i) and (iii) were fabricated with a home-build instrument, whereas (ii) was produced on the commercial SACE instrument to achieve low surface roughness.
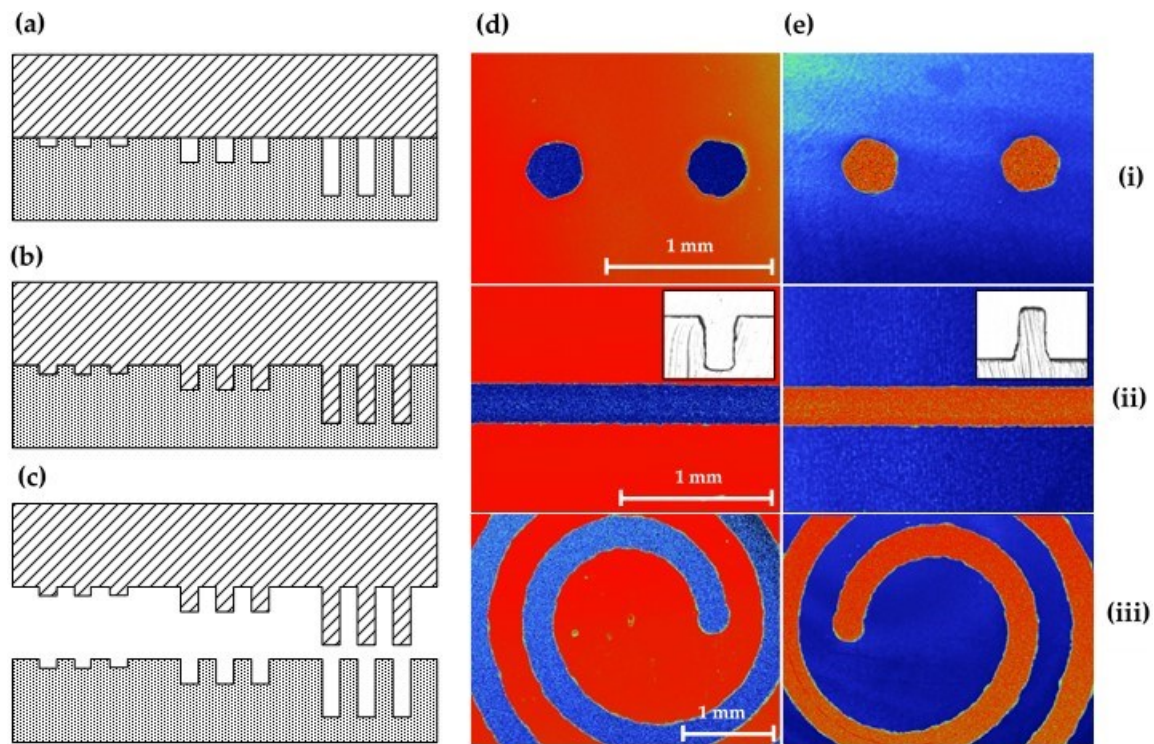
Figure 6.5. The process of embossing includes (**A**) putting a polymer sheet in light contact with the glass template while the system temperature is elevated to T_e. (**B**) After stabilization of temperature, embossing pressure is applied and the heated polymer conforms to the template bas-relief features. (**C**) After cooling to T_d, the master is separated from the patterned polymer. Optical profilometry of (**D**) features on the glass template and (**E**) the embossed PC substrate for vertical drill holes (**i**), straight trenches (**ii**), and spiral pattern (**iii**). Red and blue colours show raised and recessed surfaces, respectively. Inset figures for straight trenches in glass and the corresponding embossed PC were acquired from microscopy of cross-sections. Scale bars for template images (**D**) are each 1 mm and common for the corresponding image in (**E**).

6.1.3.3. Repetitive Embossing Using a SACE Imprint Template

Lastly, we determined the fidelity of the technique under repeated use. Generally, the number of fabrication cycles during prototyping is three [317]. In order to demonstrate that glass moulds can exceed the durability required for prototyping purposes, 11 embossing cycles were undertaken on PC, for three designs (from Figure 6.4), each with different dimensions. After each embossing cycle, the feature height (h), width (w) and root mean surface roughness (Rq), were measured, from optical profilometry results. Table 6.4 shows the summarized results for the embossed substrates after cycles one, five and eleven. These are compared to the same parameters in the glass imprint template. Reproducibility was good for smaller features but became less certain for larger structures. While optimization is required, we note that lower tolerances may be acceptable for larger features.

6.1.3.4. Discussion

The role of glass in MEMS and MOEMS has typically been limited to its integration into the final device-level product [110]. Until now, the idea of using glass as a template surface for high energy fabrication processes like hot embossing, has been presented as little more than a curiosity. Of the two major challenges in accomplishing this, brittleness and difficultly in surface patterning, it is our opinion that it is the latter which was the true road block. With new glass microfabrication methods like SACE, this can be overcome. The question then turns to proper utilization of the glass template, to ensure suitable longevity for MEMS prototyping output levels, at least. Here, we discuss some guidelines that were developed for achieving this goal, followed by suggested avenues for further development.

First, the concern of brittle glass templates that can crack during use, is both justified and avoidable. Contrary to our initial direction, however, thick glass templates can actually cause more problems than they solve. Apart from the practical problems of incorporating a thicker-than-usual template into embossing apparatus, the low thermal conductivity of thick glass samples necessitates longer warm-up times. Failure to do so can result in improper embossing, due to lower-than-expected temperatures. Worse, the application of pressure before the temperature has been stabilized can result in template failure due to temperature gradients. Furthermore, the common application of a flexible pad, used to redistribute pressure gradients from misaligned
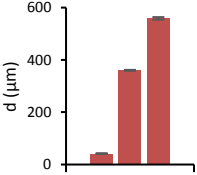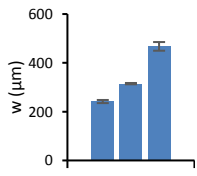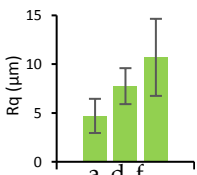
platens, should be avoided with glass templates. In fact, pressure gradients are acceptable as long as the template is held fast and supported at all points. Thus, placing the template against a solid, smooth surface, such as the embossing chamber floor, is ideal. In this case, dust and other small particles must be carefully removed.

In order to complete a rapid transition to the volume-level production after prototyping, the two phases should mirror each other as much as possible. Using hot embossing during prototyping is an asset in this case, but the imprint templates should also be similar. For example, taking advantage of the 3D writing capabilities of SACE for prototypes, will not translate well to volume production phases, if a more robust template material is required, necessitating its redevelopment of the fabrication protocol with new methods. Here, we look forward to new opportunities for using a SACE-produced glass template as a master from which to directly produce more robust templates, such as the casting of epoxies. Lastly, the technique demonstrated here is well-suited for the accurate removal of small amounts of glass material. As the replication process produces inverse geometries, protrusions are easily fabricated by embossing, whereas depressions are more difficult. Identifying and overcoming these and other limitations should be contemplated in order for glass imprint templates to find their place amongst the new wave of emerging microfabrication techniques.

6.1.4. Conclusions

In this work, the use of SACE milled glass templates for the embossing of microstructures in thermoplastics was demonstrated. This technique had the advantage of rapidly and accurately introducing features into glass substrates, with good control over all three dimensions. Optimization of the technique for generating smooth surfaces was demonstrated using a new commercially available SACE machine. With proper care during embossing, the use of glass templates provides a viable alternative to expensive and time-consuming template fabrication methods. Here, it is demonstrated that repeated embossing cycles ($n > 10$) generate samples with minimal variation in their features from run-to-run, especially for small features. This preliminary work opens the door to further developments that can significantly reduce the time and cost required for the production of microfabricated plastic parts.

Table 6.4. Embossing results for substrates after embossing process cycles one, five and eleven.

Feature	Glass Template				1st Embossing			5th Embossing			11th Embossing			Feature Statistics Line a, d, f
Name *d*	Image	*d*	*w*	*Rq*	*d*	*w*	*Rq*	*d*	*w*	*Rq*	*d*	*w*	*Rq*	Average *d*, *w*, *Rq*
Line a 50		42	251	6.9	42	237	5.3	42	239	3.5	41	239	3.1	
Line d 350		361	318	8.8	362	316	8.8	358	313	5.0	359	312	8.4	
Line f 550		565	457	11.6	556	471	18.5	560	491	9.4	554	451	6.2	

All dimensions (*d*, *w*, *Rq*) are in micrometers. Image resolution in the *z*-direction was ±4 µm.

Section 6.2.

Metal forming processes are often used for producing metal parts especially for large volume production runs. Micro-forming techniques are used in the case of high-precision submillimeter-sized parts. Challenges in metal-forming processes are development of robust, adaptable and intelligent forming processes, which are able to react to unforeseen disturbances and as such could be added to the list of flexible high-precision manufacturing processes for mass-personalization. Research studies aiming to address this challenge by development of self-correcting forming processes are reported by [86]. Another challenge to address is the fabrication of molds in hardened metals as limited technologies are currently available. Mostly because of the strict requirements on uniformly machined feature entrances required for high quality forming process performance. The presented work aims to add possibilities of real-time measurement of the micro forming process for enhanced process control by fabricating optical transparent molds of (hardened) glass, offering in-situ monitoring of the metal micro-forming process, which provides more insights in this deep-drawing process for its further understanding and optimization. In addition, this study contributes to address the issue of fabricating uniform and smooth feature (here submillimeter holes) entrances on hard materials (here glass) for forming dies.

The presented study shows the feasibility of this approach of using glass dies, machined by SACE technology, for metal micro-forming and further research is ongoing to conduct experiments on optical visualization of metal micro forming behaviour using the fabricated transparent glass molds.

Towards high precision manufacturing of glass tools by Spark Assisted Chemical Engraving (SACE) for micro forming techniques

Lucas A. Hof[1], Lukas Heinrich[2], Rolf Wüthrich[1,3]

[1] *Department of Mechanical & Industrial Engineering, Concordia University, 1455 de Maisonneuve Blvd. West, Montreal, QC H3G 1M8, Canada*

[2] *BIAS - Bremer Institut für angewandte Strahltechnik GmbH, Klagenfurter Straße 5, D - 28359 Bremen, Germany*

[3] *Posalux S.A., 18, F. Oppliger, PO Box 6075, CH-2500 Biel/Bienne 6, Switzerland*

Abstract

Micro deep drawing is well suited for the production of small metal parts in high quantities. Due to size effects the down scaling of the process leads to higher geometry deviations of the forming tools and a change in tribology resulting in a smaller process window compared to the macro scale. Spark assisted chemical engraving (SACE) of silicate glass provides an efficient way for rapid prototyping glass tools with smooth surfaces ($R_z < 1\mu m$), high aspect ratio (<10) and high accuracy (~1μm). In SACE technology, an electrochemical process heats a tool-electrode which promotes local etching of the glass substrate.

In this study the potential of such tools for micro deep drawing is investigated. Dies with a diameter of 1 mm are produced by SACE technology and characterized by microscopy and micro deep drawing experiments. It is shown that these tools can be used for deep drawing of blanks made of steel 1.4301 with an initial thickness of 25 μm. Due to the optical transparency of the material these glass tools provide great potential for an in-process observation during the forming step and

a better understanding of the micro deep drawing process. In addition, high precision dies can be achieved with high process flexibility and with uniform, smooth hole entrances increasing the deep micro deep drawing process performance. This results in repeatable metal part manufacturing by micro forming.

Keywords: Micro deep drawing, advanced manufacturing, micro forming, spark assisted chemical engraving (SACE), glass micro-machining, in-process characterization

6.2.1. Introduction

With the great technological advancement in the micro-technology field, micromachining of various materials has become a key task. As mechanical components of microsystems plastic parts are often used and their manufacturing in the micro range is already well studied [277]. Metallic micro components offer an interesting alternative due to considerably different material properties. These components can be produced in high quantities at relatively low cost per part by forming processes such as micro deep drawing. However, the downscaling of conventional forming processes to the micro scale leads to new challenges [278]. Therefore, improvement and research of the micro deep drawing process is needed [318-320]. In conventional deep drawing a change of tooling geometry in micrometer range normally does not influence the drawability because of a sufficient formability of the work piece material. But due to changed tribology [321] and material behaviour [322] in micro range only smaller process windows can be achieved [323]. Furthermore, the relative deviation from the nominal tooling geometry, caused in its manufacturing process, is increasing with decreasing size in the micro range because the accuracy of manufacturing reaches its limits [318, 319, 324]. For repeatable and successful micro deep drawing process, uniform die radius is key [318, 319] and still challenging to achieve.

Besides plastic and metal as material for microsystems, glass is essential for the fabrication of micro-devices including micro electro mechanical systems (MEMS), optical MEMS (MOEMS), miniaturized total analysis systems (µTAS) and microfluidic devices [75, 92]. This is mainly because of its unique properties, such as mechanical strength, thermal properties, transparency, chemical inertness and bio-compatibility. Moreover, glass is RF transparent, making it an excellent material for sensor and energy transmission devices.

Using glass dies for micro deep drawing processes is still a largely unexploited area of research and application. This optical transparent material for the tooling (dies) has great potential for in-process observation during the forming step leading to a better understanding of the micro deep drawing process.

However, the hardness and brittleness of glass complicates its micro-fabrication. In particular machining crack and burr-free high-aspect ratio structures is still challenging due to long machining times, high machining costs and poor surface quality [81, 83, 113].

Table 6.5. Features of the four main groups drilling technologies for glass.

Process		Aspect ratio	Machining speed (serial)	Surface roughness (R$_a$)	Minimum dimensions	Rapid prototyping (serial mode)	Mass fabrication (parallel mode)	Tooling complexity / costs	Applicable to wide range of glass types	Equipment costs / complexity
		low -- high ++	low -- high ++	high -- low ++	[μm]	non-applicable -- applicable ++	non-applicable -- applicable ++	complex -- simple ++	non-applicable -- applicable ++	expensive -- cheap ++
Mechanical	Mechanical drilling	-	+	-	150	++	--	--	++	++
	Powder blasting	--	-	--	50	--	++	--	++	+
	ASJ	--	--		300	+	-	-	++	+/-
	USM	-	--	-	200 (10)	+	-	-	++	-
Thermal	Laser drilling	++	++	-	5	++	-	++	+	-
	FEDM	-	+	+	20	-	+	+	--	-
Chemical	Wet etching	--	--	+	1	--	++	--	-	-
	DRIE	++	--	++	0.5	--	++	--	--	--
Hybrid	SACE	+	+	+	100	++	--	++	++	+

Methods to micro-machine glass can be divided into four groups (see Table 6.5) [83]: thermal, chemical, mechanical and hybrid. Thermal processes, e.g. laser, are fast and flexible but usually form bulges around the rims of the micro-hole entrances complicating the micro deep drawing process when using the machined glass part as die. Chemical processes produce smooth surfaces but require expensive masks while mechanical methods are relatively slow and exhibit poor surface roughness. Hybrid technologies, like Spark Assisted Chemical Engraving (SACE), are favourable as they attempt to combine the good outcomes of each process to satisfy most requirements for the desired micro-structures in glass [81, 83, 185, 221]. In SACE technology an electrochemical process heats a tool-electrode which promotes local etching of the glass substrate [81, 185, 221].

In this study the potential of SACE machined glass tools for micro deep drawing is investigated. SACE process is optimized for the micro forming process and a deep drawing feasibility study is conducted. Research is ongoing to characterize the deep drawing in-process to develop a better understanding of its mechanisms.

6.2.2. Glass micromachining

Main requirements to achieve high surface quality glass dies in a flexible way (rapid prototyping) are surface roughness, feed-rate and minimum possible dimensions. Table 6.5 summarizes the qualitative comparison of the different glass micromachining technologies based on the achievable aspect ratios, machining speed and surface roughness. Low aspect ratios are defined to be below 10, low machining speeds refer to speeds below 100 µm/s and low surface roughness (high quality) refers to roughness lower than 100 nm (R_a < 100 nm).

Hybrid methods such as SACE perform well in drilling high aspect ratio and smooth surface micro-holes. These assets of SACE technology combined with its relative high machining speeds compared to chemical methods and low-cost compared to femto-laser technologies make SACE perfectly suitable for rapid prototyping of micro-scale glass devices.

6.2.3. Principles & experimental setup

6.2.3.1. Glass tooling manufacturing equipment

In SACE technology, a voltage is applied between tool and counter electrode dipped in an alkaline solution, typically NaOH or KOH (see Figure 6.6). At high voltages (around 30 V), the bubbles evolving around the tool electrode coalesce into a gas film and discharges occur from the tool to the electrolyte. Glass machining becomes possible due to thermally promoted etching (breaking of the Si-O-Si bond) [81].
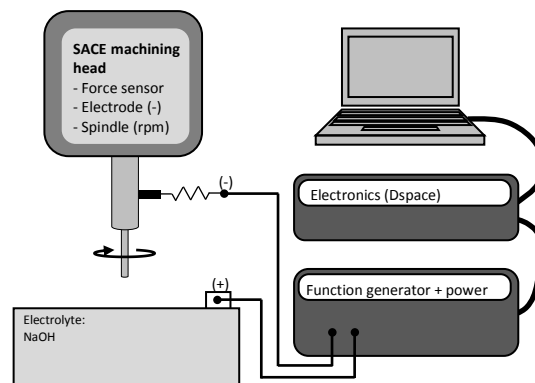
Figure 6.6. Developed laboratory setup for SACE machining. The machining head is mounted on a high precision z-stage, and the electrochemical cell is mounted on high precision x,y stages (x,y,z stages: positioning accuracy = 1 µm).

The glass dies were fabricated on a versatile industrial SACE-machine (see Figure 6.7) as developed together by EGE Group, Concordia University and Posalux SA [224] which offers high precision glass micro-drilling, micro-milling, micro-cutting and micro 2.5D machining operations (see Figure 6.8) while leaving the glass surface micro-crack, debris and bulge free. Implementation of a force-sensitive machining head allows the use of ultra-thin machining tools (diameter down to 30 μm), applying force-feedback algorithms (detecting forces down to 1 mN) and usage of the head as profilometer to measure machined features within the same setup.

Figure 6.7. Industrial machine Microfor SACE developed by Posalux SA and EGE Group, Concordia University, consisting of a versatile force-sensitive head for SACE machining and use as profilometer [224].
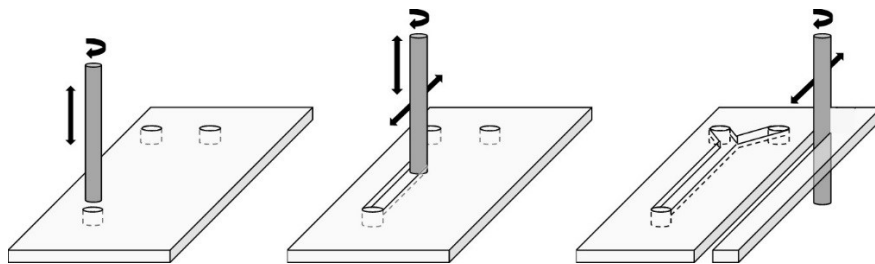
Figure 6.8. Versatile glass machining by SACE: drilling, milling and cutting by the same technology on the same setup.

Typically, drilling of through and blind holes of diameters from 100 μm to several millimetres can be achieved with low circularity error (typically < 1 μm) and depths as deep as 3 mm. Drilling is relatively fast (a 700 μm deep hole is drilled in typically 2 seconds).

6.2.3.2. Micro deep drawing setup and principles

In micro deep drawing a circular blank is clamped between a blank holder and die and then deep-drawn into the die with a cylindrical punch until a cup is formed (see Figure 6.9). A key parameter to characterize the drawing process is the drawing ratio β. It is defined as the ratio between the initial blank diameter D_0 and the punch diameter D_p (equation 6.3).

$$\beta = D_o/D_p \tag{6.3}$$
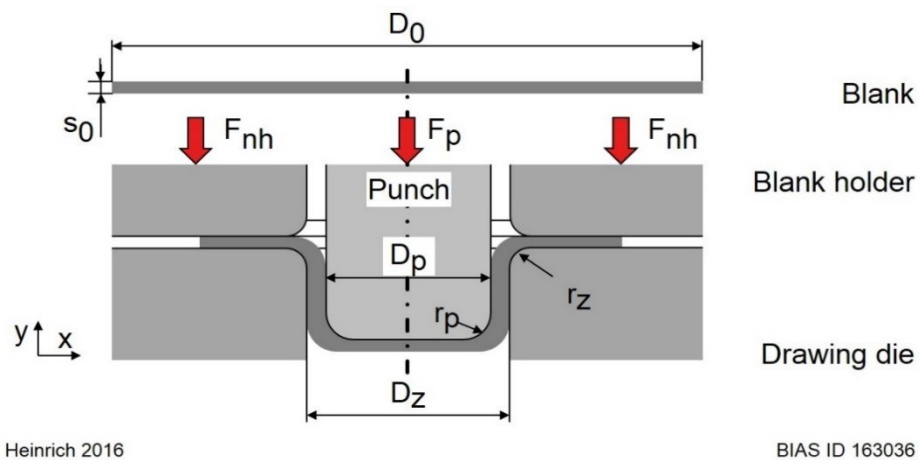
Figure 6.9. Micro deep drawing process

The blanks are made of stainless austenitic nickel-chromium steel 1.4301 (X5CrNi18-10). In order to cut out the blanks an ultra-short pulsed laser with a wave length of 1030 nm was used to prevent burr formation at the edge of the blank. Punch and blank holder are made of ledeburitic powder-metallurgical steel 1.2379 (X153CrMoV12). For the drawing die, the glass tool insert is used, which is positioned in a tool holder (see Figure 6.10). The relevant geometrical parameters used in the experiment can be found in Table 6.6. The drawing process is carried out on a home-built single axis micro forming press developed by [318] with a maximum punch force of 540 N. The punch is driven and controlled by a NI 9514 servo drive interface. The punch velocity was set to 10 mm/s and HBO 947/11 was used as lubricant. The initial blank holder pressure is p_{nh} = 5

MPa. The blank holder acts passively and is supported by two springs with adjustable spring tension in order to set the desired blank holder pressure.

Table 6.6. Process parameters for deep drawing experiments

Punch diameter D_p (mm)	1.000
Punch radius r_p (mm)	0.100
Die diameter D_z (mm)	1.160
Die radius r_z (mm)	0.100
Blank diameter D_0 (mm)	1.700
Sheet thickness s_0 (mm)	0.025
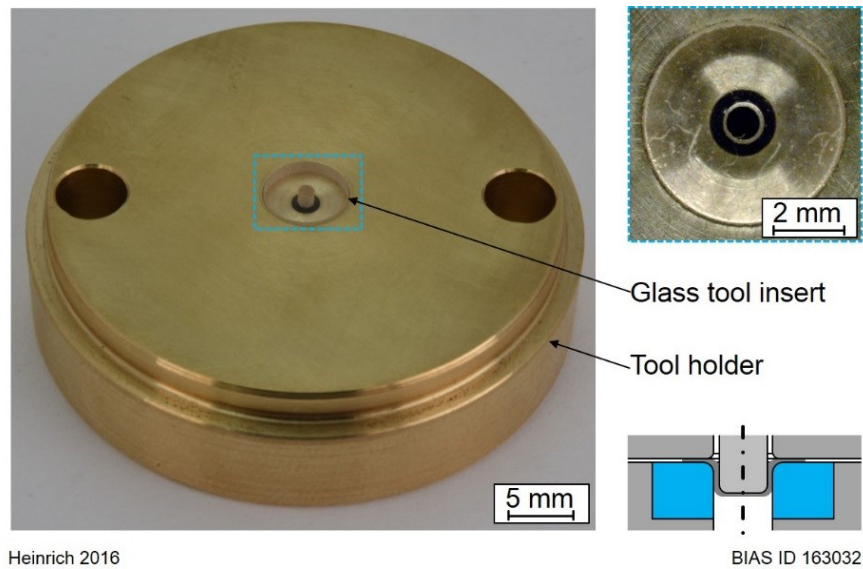
Figure 6.10. Designed tooling (die) for this deep drawing process

6.2.4. Results and discussion

Tooling with constant die radius is preferred for good deep drawing results (radius r_z in Figure 6.9 and for tooling see Figure 6.10). Preliminary tests were conducted by SACE machining for the glass dies. These results are presented in Figure 6.11.

The glass die was machined by SACE process in cutting mode in 10 steps with depth-of-cut = 200 µm. The pulsed voltage was programmed at: $U_{HighLevel}$ = 38 V, $U_{LowLevel}$ = 17.5 V, period (T) = 2.6 ms, duty cycle (defined as: pulse width/T) = 96.15 %. A tungsten carbide tool-electrode (diameter = 100 µm) was deployed as tool and 20 wt.% potassium hydroxide (KOH) was used as electrolyte in the machining cell.
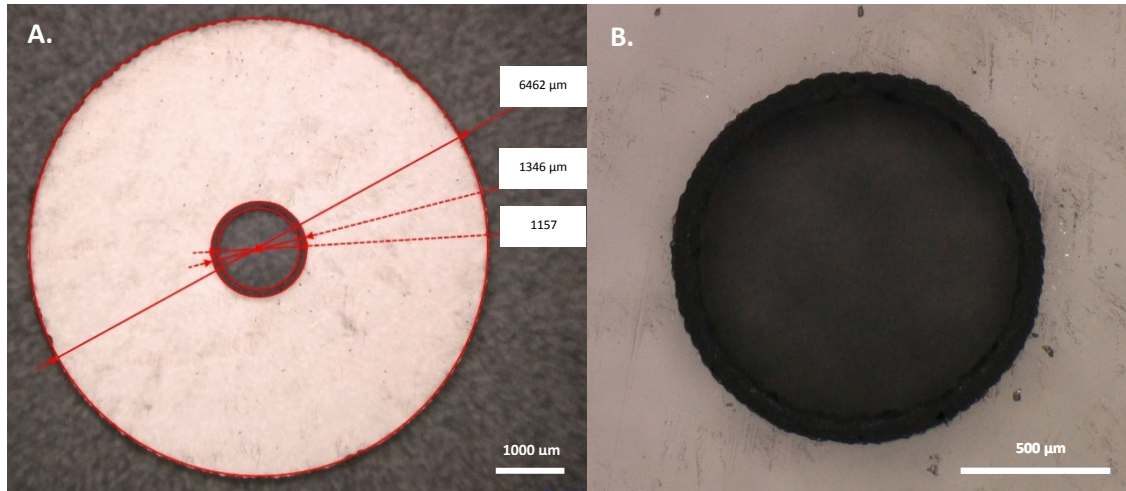
Figure 6.11. A. Glass tooling manufactured by SACE technology. **B.** Detail of the machined glass tool (die).

Ten cups with a drawing ratio of β = 1.7 were formed using the glass drawing die and the conventional metal punch and blank holder. All the produced cups are without cracks. However, wrinkles can be found at the sides of the cup (see Figure 6.12). This indicates that the process parameters such as blank holder pressure were not chosen ideally. Figure 6.13 shows the glass drawing die before and after one and ten cups were deep-drawn. No cracks are observed at the radius or the surface of the tool.
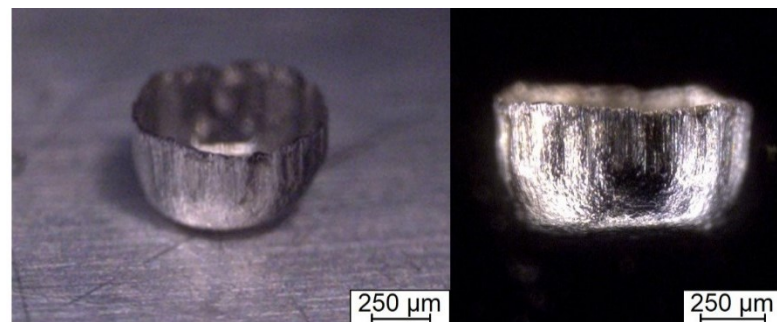
Material	1.4301	Punch diameter	1 mm
Thickness	25 µm	Drawing ratio	1.7
Blank diameter	1.7 mm	Holder preasure	5 MPa

Heinrich 2016 · BIAS ID 163035

Figure 6.12. Micro cup deep-drawn with glass tool.

No. of Parts: 0   1   10

Heinrich 2016   BIAS ID 160334
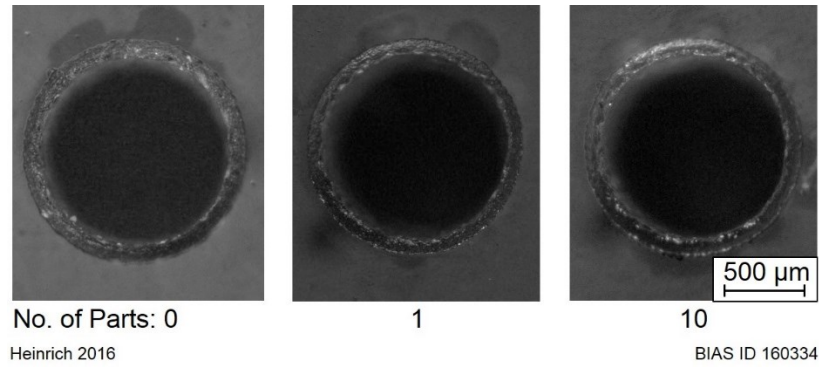
Figure 6.13. Top view of glass tool before forming and after one and ten cups were drawn.

6.2.5. Conclusion

In this study, the potential of glass tools for micro deep drawing was investigated. Dies with a diameter of 1 mm were produced on a Microfor SACE machine and characterized by microscopy and micro deep drawing experiments. It was shown that these tools can be used for deep drawing of blanks made of steel 1.4301 with an initial thickness of 25 μm. However, the process parameters of the drawing process have to be further investigated in order to achieve a better drawing result.

In a next step, due to the optical transparency of the used material, these glass tools provide great potential for an in-process observation during the forming step and a better understanding of the micro deep drawing process. In addition, high precision dies can be achieved with high process flexibility and with uniform, smooth hole entrances increasing the deep micro deep drawing process performance. This will lead to better repeatability for metal part manufacturing by micro forming.

Chapter 7

7.1. Conclusions

Throughout the presented research study, an electrochemical discharge machining process, spark assisted chemical engraving (SACE), was developed to an industrial level machine tool together with industrial partner Posalux SA [60] and more importantly, a methodology was developed and validated to adapt SACE from mass-fabrication process to a flexible manufacturing technology for high-precision glass mass-personalization. Solutions were proposed to address the research question:

How can we mass-manufacture batch-size-1, i.e. mass-personalized, high-precision products made of hard-to-machine materials such as glass economically on-demand?

New manufacturing process criteria were proposed and proven to be necessary for evaluating manufacturing processes on suitability for mass-personalization. They must have the capability to 1) address the issues of tooling costs (avoid any part specific tooling), 2) handle complex parts and 3) reduce production steps (as in each new step parts will have to be transferred from one manufacturing system to another resulting in new overhead and error introduction due for example to alignment or tooling) and 4) must abandon long calibration runs (in-process automated calibration strategies are needed). Throughout this thesis, SACE technology was progressively developed from mass-fabrication technology towards a process for mass-personalization of high-

precision glass parts by addressing the challenges of these four drivers of part related manufacturing costs (Figure 7.1).
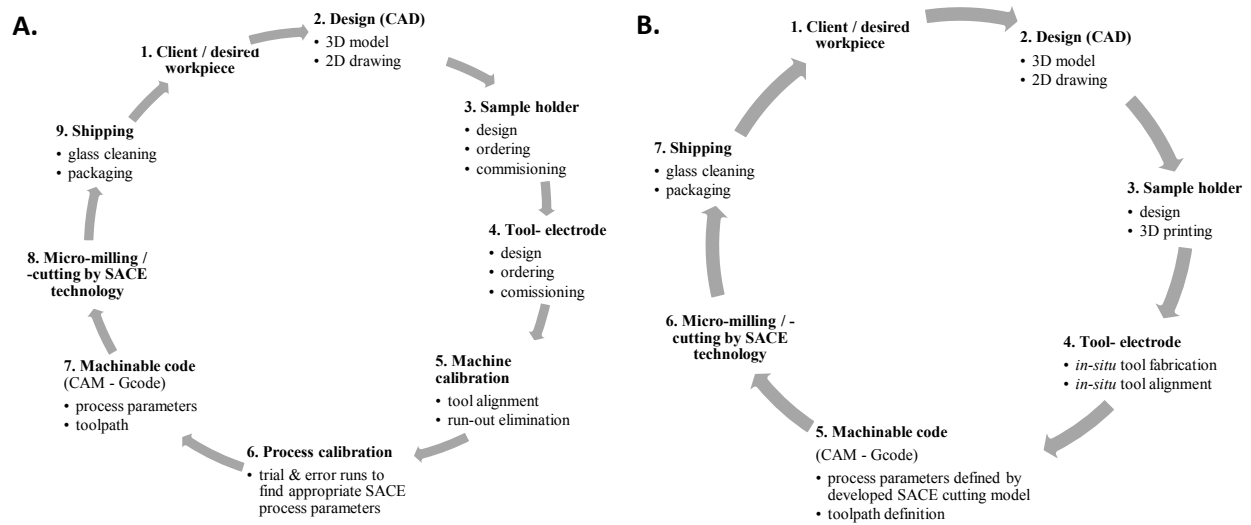
Figure 7.1 A. Manufacturing process flow in SACE machining from client design to finalized product in current SACE technology situation (mass-fabrication). **B.** Manufacturing process flow in SACE machining from client design to finalized product in the developed SACE approach for *mass-personalization*.

More detailed and specific conclusions of each part of the research study are outlined in the different chapters 1 to 6. The most significant conclusions are briefly summarized below:

- A comprehensive review of micro-hole drilling technologies in glass with high precision is presented, grouped in mechanical, chemical, thermal and hybrid technologies, and assessed to the four proposed manufacturing design criteria for mass-personalization:

    1. Abandon lengthy calibration runs;
    2. Avoid any part specific tooling (reduce tooling costs and complexity);
    3. Be able to handle complex parts;
    4. Reduce production steps (each step increases overhead and introduces machining errors);

- Hybrid technologies, for example SACE process, show potential for use as high-precision mass-personalization manufacturing technology, however SACE technology can currently only be used effectively for mass-fabrication as machining overhead of this process is still very high jeopardizing its use for this batch size-1 production. Three main issues are identified:

- Contrary to micro-hole drilling on glass substrates, no models are available for glass cutting and milling to define process parameters without the need of time-consuming trial and error runs;

- Extensive calibration is needed for tool-workpiece alignment and tool run-out elimination to achieve the desired high-precision (~ 1 μm);

- Part specific tooling is required for proper clamping of the glass workpiece (almost each production cycle demands changing dimensions in the case of mass-personalization) to attain high precision.

- A model for SACE cutting and milling process operations was developed and empirically validated allowing direct relation of the machining input parameters (e.g. voltage, feed-rate) to the desired machining outcome (e.g. feature depth), enabling a drastical increase of automation across the manufacturing process workflow from desired design to establishing of machinable code containing all necessary manufacturing execution information (e.g. toolpath definition, machining voltage settings, feed-rate, depth of cut, machining time, achievable quality), which is key for suitable manufacturing processes for mass-personalization;

- It is empirically found and confirmed by a numerical transient heat model, that tools of 100 μm diameter are optimal for glass micro-cutting by SACE technology in terms of machining time:

  - Using larger tool diameters will rapidly decrease the heat source efficiency and subsequently reduce dramatically the machining speed (by factor 5 using a 200 μm diameter tool);

  - Deploying smaller tools (< 100 μm) will not contribute to increased efficiency as for 100 μm (and smaller) diameter tools cutting time becomes independent of the tool diameter;

- It is shown that the usage of a force sensitive machining head is essential to prevent bending and/or breaking of such small (100 μm diameter) tools. Therefore, an industrial grade force-sensitive SACE machining head (sensitivity ~ 1 mN) was developed with our industrial partner (resulting in patent WO 2017 / 064583 A1 (2017) [60].

- The significance of heat propagation through the glass workpiece as main limiting factor to determine the maximal machining speed was confirmed;

- A strategy was developed to reduce the surface roughness of cut (down to $R_z \sim 1$ µm) by introducing Spark Assisted Chemical Polishing (SACP);
- Possible routes for increasing MRR for SACE micro-cutting and -milling were proposed:
  - Using small tool diameters are most efficient. This is the case for 100 µm diameter tool-electrodes;
  - Increase the normalized heat power κ. However, this result in poor machining quality ($R_z > 50$ µm), applying the developed SACP technology can partially solve this roughness issue;
  - For small and medium batch sizes (lots > 1) a multi-tool head can be deployed as effective strategy;
- An in-situ fabrication method for the needed tool-electrodes is developed, eliminating the need of cumbersome and lengthy calibration procedures, reducing costs and lead times compared to conventional SACE machining approaches;
- Low-cost rapid prototyping technology is deployed for part specific tooling fabrication for precise clamping of the workpiece to obtain the required high precision and allowing a consistent, smooth electrolyte flow across the glass workpiece;
- It was demonstrated that SACE process is promising as rapid prototyping technology for glass device fabrication eliminating a process step in the manufacturing workflow from micromachining to die singularizing for single device fabrication out of a glass wafer. This approach enables flexible prototyping of glass devices at relatively low cost, which was illustrated by fabrication of a functional microdevice;
- Novel applications were proposed and fabricated using glass as substrate material and SACE technology for rapid prototyping of templates to process polymers and metals with high-precision in the microtechnology field:
  - Fabrication of glass templates for microfabricating devices by hot embossing. This technique had the advantage of rapidly and accurately introducing features into glass substrates, with good control over all three dimensions.
  - Manufacturing of glass tools (dies) for micro-forming of metal micro parts. Micro deep drawing of thin metal sheets (thickness 25 µm) was successfully performed without showing significant tool wear of the fabricated glass dies.

7.2. Contributions

Current manufacturing technologies are very well optimized for mass production; however, they face many issues to produce mass-personalized products. Guidelines were proposed and evaluated, in the presented research study, as requirement for manufacturing processes allowing mass-personalization. It was shown throughout this thesis work, by a case study for high-precision glass parts, how the micro-machining process *SACE* can be developed towards a manufacturing process for high-precision glass mass-personalization, respecting these guidelines *i.e.,* reducing manufacturing overhead introduced by the four key drivers of manufacturing costs related to a specific part design (calibration, tooling, processing steps, complexity).

Thus far SACE process was never deployed for high-precision glass mass-personalization by industry and academia. Three main issues of current SACE technology are preventing its use for this highly flexible manufacturing approach:

1. No models are available for glass cutting and milling, relating SACE process input parameters to a desired output such as MRR (feed-rate together with depth-of-cut per machining pass). Such a model is a key requirement for setting up efficiently (i.e. low setup time) manufacturing systems with a high degree of automation. Currently, it takes a significant number of trial and error runs before the process parameters (machining voltage, feed-rate, depth-of-cut) for appropriate cutting and milling operation settings are found;

2. Extensive calibration is needed for tool-workpiece alignment and tool run-out elimination to achieve the desired high-precision (~ 1 µm);

3. Part specific tooling is required for proper clamping of the glass workpiece (almost each production cycle demands changing dimensions in the case of mass-personalization) to attain high precision.

These issues are progressively addressed throughout the outlined research study, resulting in the main contributions of this work:

- **Glass mass-personalization by SACE technology**
  SACE technology was progressively developed from mass-fabrication technology towards a process for mass-personalization of high-precision glass parts by addressing the challenges of

the four key drivers of part related manufacturing costs (calibration, tooling, complexity, processing steps);

In order to achieve this transition of SACE technique towards an *Industry 4.0* manufacturing process, the following milestones were accomplished;

- **Development of a process model for SACE cutting and milling**

  A model for SACE cutting and milling process operations was developed and empirically validated allowing direct relation of the machining input parameters (e.g. voltage, feed-rate) to the desired machining outcome (e.g. feature depth), enabling a considerable increase of automation across the manufacturing process workflow from desired design to establishing of machinable code containing all necessary manufacturing execution information (e.g. toolpath definition, machining voltage settings, feed-rate, depth of cut, machining time, achievable quality), which is key for suitable manufacturing processes for mass-personalization. Application of this established normalized model could be extended to other heat-driven processes as well;

- ***In-situ* fabrication methods and low-cost rapid prototyping for tooling were developed**

  An in-process fabrication method for the needed tool-electrodes is developed, eliminating the need of cumbersome and lengthy calibration procedures, reducing costs and lead times compared to conventional SACE machining approaches.

  Low-cost rapid prototyping technology is deployed for part specific tooling fabrication for precise clamping of the workpiece to obtain the required high precision and allowing a consistent, smooth electrolyte flow across the glass workpiece;

- **Spark Assisted Chemical Polishing (SACP) was introduced**

  A strategy was developed to reduce the surface roughness of cut (down to $R_z \sim 1$ μm) by introducing Spark Assisted Chemical Polishing (SACP), which is carried out on the same setup as machining, avoiding alignment and tool calibration issues;

To show the viability of the developed mass-personalization approach some case-studies towards industrial applications were performed using glass in a non-traditional, indirect way. Novel applications were proposed and fabricated using glass as substrate material and SACE

technology for rapid prototyping of templates to process polymers and metals with high-precision in the microtechnology field:

- **Fabrication of glass imprint templates** for microfabricating devices by *hot embossing*. This technique had the advantage of rapidly and accurately introducing features into glass substrates, with good control over all three dimensions.

- **Manufacturing of glass tools (dies)** for *micro-forming* of metal micro parts. Micro deep drawing of thin metal sheets (thickness 25 µm) was successfully performed without showing significant tool wear of the fabricated glass dies.

The proposed manufacturing process criteria as presented throughout this research work can be used as a first step to assess a given technology on suitability for mass-personalization. It was shown that addressing the proposed four part related manufacturing cost drivers 1) calibration, 2) tooling, 3) complexity, 4) multiple process steps is essential:

1. Calibration runs increase dramatically the setup times for each different workpiece jeopardizing effective manufacturing process work flow as needed for mass-personalization;

2. Part specific tooling add significantly to machining overhead increasing drastically the cost per product;

3. As mass-personalization demands manufacturing of a wide variety of geometries, compatible processes need to be able to handle complex shapes;

4. Each new manufacturing step demands transfer of parts from one manufacturing system to another resulting in new overhead and error introduction due for example to alignment or tooling.

7.3. Outlook

- Guidelines were proposed as requirement for manufacturing processes allowing mass-personalization. It was shown throughout the presented thesis work how the micro-machining process *SACE* can be developed towards a manufacturing process for high-precision glass mass-personalization, respecting these guidelines. Although the presented work serves as good case-study for high-precision *glass* micro-machining, more work has to be done to establish practically proven design guidelines for more general use (e.g. to find additional criteria). In order to address the more universal research question - *how can we mass-manufacture batch-size-1, i.e. mass-personalized, high-precision products economically on-demand?* - further studies need to be carried out for different materials and applications.

- Hybrid manufacturing technologies seem to be good candidates to fulfill the criteria for mass-personalization manufacturing processes. Continuing research in the field of electrochemical manufacturing technologies seem promising. For example, post-processing of additively manufactured complex metal parts could be performed by electrochemical polishing and personalized thin-walled metallic structures could be realized using electroforming and low-cost 3D printing. Industry starts to adopt hybrid processes for mass-personalized metal part fabrication, for example by laser machining followed by an automated bending step (adaptable fixtures), which in fact is similar as the process of 4D printing.

References

[1]   "Oxford English Dictionary." [Online]. Available: http://www.oed.com/. [Accessed: 19-Apr-2018].

[2]   D. Dornfeld and D.-E. Lee, "Future of precision manufacturing," in *Precision Manufacturing*, Boston, MA: Springer US, 2008, pp. 665–703.

[3]   D. M. Upton, "What really makes factories flexible," *Harv. Bus. Rev.*, pp. 74–84, 1995.

[4]   G. Pourabdollahian and G. Copani, "Market Analysis, Technological Foresight, and Business Models for Micro-manufacturing," in *Micro-Manufacturing Technologies and Their Applications: A Theoretical and Practical Guide*, I. Fassi and D. Shipley, Eds. Cham: Springer International Publishing, 2017, pp. 261–291.

[5]   H. Kagermann, J. Helbig, A. Hellinger, and W. Wahlster, "Umsetzungsempfehlungen für das Zukunftsprojekt Industrie 4.0: Deutschlands Zukunft als Produktionsstandort sichern; Abschlussbericht des Arbeitskreises Industrie 4.0," Berlin, Frankfurt/Main, 2013.

[6]   L. Ghezzi and H. G. Bock, *Math for the Digital Factory*. .

[7]   I. Csiszár and M. Jaikumar, "From Filing and Fitting to Flexible Manufacturing: A Study in the Evolution of Process Control," *Found. Trends® Technol. Inf. Oper. Manag.*, vol. 1, 2005.

[8]   R. DeVor and et al., "EM-SIM, End Milling Simulation Software," *ARPA/NSF Machine Tool - Agile Manufacturing Institute, University of iIinois, Champaign-Urbana*, 1996.

[9]   D. Dornfeld and D.-E. Lee, "Introduction to precision manufacturing," in *Precision Manufacturing*, Boston, MA: Springer US, 2008, pp. 1–35.

[10]   S. Kalpakjian, *Manufacturing processes for engineering materials*. Reading, MA:

Addison-Wesley, 1984.

[11] G. Boothroyd, *Fundamentals of Metal Machining and Machine Tools*. New York: McGraw-Hill, 1975.

[12] H. W. Dickinson and R. Jenkins, *James Watt and the History of the Steam Engine*. Clarendon, 1927.

[13] M. Berg, *The Age of Manufactures, 1700-1820: Industry, Innovation and Work in Britain*, 2nd ed. Routledge, 1994.

[14] P. Mantoux, *The Industrial Revolution in the Eighteenth Century: An outline of the beginnings of the modern factory system in England*. Taylor & Francis Ltd, 1928.

[15] J. Burke, *Connections*, 1st ed. Boston, MA: Little, Brown & Company, 1978.

[16] R. Schonberger, *Japanese manufacturing techniques: Nine hidden lessons in simplicity*. New York: The Free Press, 1982.

[17] T. Ohno, *Toyota Production System: Beyond Large-Scale Production*. Productivity Press, 1988.

[18] C. F. Oduoza, "Lean Thinking Constraints in Traditional Batch," *Adv. Prod. Eng. Manag.*, vol. 3, no. 4, pp. 181–192, 2008.

[19] P. A. McKeown, "High Precision Manufacturing and the British Economy," *Proc. Inst. Mech. Eng. Part B Manag. Eng. Manuf.*, vol. 200, no. 3, pp. 147–165, Aug. 1986.

[20] P. Shore and P. Morantz, "Ultra-precision: enabling our future," *Philos. Trans. R. Soc. A Math. Phys. Eng. Sci.*, vol. 370, no. 1973, p. 3993 LP-4014, Aug. 2012.

[21] N. Taniguchi, "On the Basic Concept of Nano-Technology," *Proc. Intl. Conf. Prod. London, 1974*, 1974.

[22] W. Thomson, "Electrical units of measurement," *Pop. Lect. Addresses*, vol. 1, no. a lecture delivered at the Institution of Civil Engineers, London (3rd May 1883), p. 73, 1889.

[23] G. V. Shirley and R. Jaikumar, "Turing machines and Gutenberg technologies: the postindustrial marriage," vol. 1, pp. 36–43, 1988.

[24] T. Moriwaki, "Intelligent machine tool: perspective and themes for future development," *ASME/PED, Manuf. Sci. Eng.*, vol. 68, no. 2, pp. 841–849, 1994.

[25] T. Moriwaki and K. Shirase, "Intelligent machine tools: current status and evolutional architecture," *Int. J. Manuf. Technol. Manag.*, vol. 9, no. 3/4, pp. 204–218, 2006.

[26] D. Dornfeld and D.-E. Lee, "Precision manufacturing applications and challenges," in *Precision Manufacturing*, Boston, MA: Springer US, 2008, pp. 555–663.

[27] K. Schwab, *The Fourth Industrial Revolution*, First edit. New York: Crown Business, 2017.

[28] M. Brettel, M. Klein, and N. Friederichsen, "The Relevance of Manufacturing Flexibility in the Context of Industrie 4.0," *Procedia CIRP*, vol. 41, pp. 105–110, 2016.

[29] P. R. Spena, P. Holzner, E. Rauch, R. Vidoni, and D. T. Matt, "Requirements for the Design of Flexible and Changeable Manufacturing and Assembly Systems: A SME-survey," *Procedia CIRP*, vol. 41, pp. 207–212, 2016.

[30] M. Lafou, L. Mathieu, S. Pois, and M. Alochet, "Manufacturing System Flexibility: Product Flexibility Assessment," *Procedia CIRP*, vol. 41, pp. 99–104, 2016.

[31] M. Cantamessa and C. Capello, "Flexibility in Manufacturing -- An Empirical Case-Study Research," in *Design of Flexible Production Systems: Methodologies and Tools*, T. Tolio, Ed. Berlin, Heidelberg: Springer Berlin Heidelberg, 2009, pp. 19–40.

[32] B. J. Pine II, *Mass Customization: The New Frontier in Business Competition*. Boston, MA: Harvard Business School Press, 1993.

[33] G. Da Silveira, D. Borenstein, and H. S. Fogliatto, "Mass customization : Literature review and research directions," vol. 72, no. 49, 2001.

[34] N. E. Bingham, "Toffler, Alvin. Future shock. New York: Bantam Books, Inc., 1971 (540 pages)," *Sci. Educ.*, vol. 56, no. 3, pp. 438–440, Jul. 1972.

[35] D. Gerwin, "Manufacturing Flexibility: A Strategic Perspective," *Manage. Sci.*, vol. 39, no. 4, pp. 395–410, 1993.

[36] K. Mahmood, T. Karaulova, T. Otto, and E. Shevtshenko, "Performance Analysis of a Flexible Manufacturing System (FMS)," *Procedia CIRP*, vol. 63, pp. 424–429, 2017.

[37] A. Oke, "A framework for analysing manufacturing flexibility," *Int. J. Oper. Prod. Manag.*, vol. 25, no. 10, pp. 973–996, 2005.

[38] Y. Koren, S. J. Hu, P. Gu, and M. Shpitalni, "Open-architecture products," *CIRP Ann. - Manuf. Technol.*, vol. 62, no. 2, pp. 719–729, 2013.

[39] D. Mourtzis and M. Doukas, "Design and planning of manufacturing networks for mass customisation and personalisation: Challenges and outlook," *Procedia CIRP*, vol. 19, no. C, pp. 1–13, 2014.

[40] Deloitte, "Industry 4.0. Challenges and solutions for the digital transformation and use of exponential technologies," *Deloitte*, pp. 1–30, 2015.

[41] World Economic Forum, "Manufacturing Our Future - Cases on the Future of Manufacturing," *White Pap.*, no. May, 2016.

[42] M. Hankel and B. Rexroth, "The Reference Architectural Model Industrie 4.0 (RAMI 4.0)," *ZWEI Die Elektroind.*, vol. 1, no. April, pp. 1–2, 2015.

[43] K.-D. Thoben, S. Wiesner, and T. Wuest, "'Industrie 4.0' and Smart Manufacturing – A Review of Research Issues and Application Examples," *Int. J. Autom. Technol.*, vol. 11, no. 1, pp. 4–16, 2017.

[44] P. Sykes, "Advanced versus Smart Manufacturing in Aerospace and Defense," *Aerospace & Defense Manufacturing 2016, Supplement to Advanced Manufacturing, Society of Manufacturing Engineers (SME)*, pp. 134–135, 2016.

[45] Siemens AG, "Digitalization in machine building - Twins with potential," *The Magazine*, Oct-2017.

[46] E. Wallace and F. Riddick, "Panel on Enabling Smart Manufacturing," 2013.

[47] M. Peshkin and J. E. Colgate, "Cobots," *Ind. Robot Int. J. Robot. Res. Appl.*, vol. 26, no. 5, pp. 335–341, 1999.

[48] D. Thomas and S. Gilbert, "Costs and Cost Effectiveness of Additive Manufacturing - A Literature Review and Discussion," *NIST Spec. Publ.*, vol. 1176, pp. 1–77, 2014.

[49] S. J. Hu, "Evolving paradigms of manufacturing: From mass production to mass customization and personalization," *Procedia CIRP*, vol. 7, pp. 3–8, 2013.

[50] D. Brander, A. Bærentzen, A. Evgrafov, J. Gravesen, S. Markvorsen, T. B. Nørbjerg, P. Nørtoft, and K. Steenstrup, "Hot Blade Cuttings for the Building Industries," in *Math for the Digital Factory*, L. Ghezzi, D. Hömberg, and C. Landry, Eds. Cham: Springer International Publishing, 2017, pp. 253–272.

[51] T. Kellner, "The FAA Cleared the First 3D Printed Part to Fly in a Commercial Jet Engine from GE," 2015.

[52] R. Hudson, "Hybrid Manufacturing Opens Door to New Manufacturing Future," *Aerospace & Defense Manufacturing, Supplement to Advanced Manufacturing, Society of Manufacturing Engineers (SME)*, p. 47, 2016.

[53] M. Lusic, M. Wimmer, C. Maurer, and R. Hornfeck, "Engineering framework for

enabling mass customisation of curvilinear panels with large surfaces by using pin-type tooling," *Procedia CIRP*, vol. 37, pp. 265–270, 2015.

[54] H. Gaub, "Customization of mass-produced parts by combining injection molding and additive manufacturing with Industry 4.0 technologies," *Reinf. Plast.*, vol. 60, no. 6, pp. 401–404, 2016.

[55] C. Kaiser, T. V. Fischer, T. Schmeltzpfenning, M. Stöhr, and A. Artschwager, "Case study: Mass customisation of individualized orthotics - The FASHION-ABLE virtual development and production framework," *Procedia CIRP*, vol. 21, pp. 105–110, 2014.

[56] N. Jun and J. Lee, "Emerging and Disruptive Technologies for the Future of Manufacturing," *Case study no. 7, World Econ. Forum, Glob. Agenda Counc. Futur. Manuf.*, pp. 0–3, 2015.

[57] J. Lorincz, "Hybrid machines make parts using the brand new and tried-and-true," *Manufacturing Engineering, Publication of SME*, pp. 66–70, Apr-2018.

[58] "Metalfab1 - Additive Industries." [Online]. Available: https://additiveindustries.com/systems/metalfab1. [Accessed: 25-Apr-2018].

[59] B. Brune, "Seven key benefits emanating from tech in Trumpf's just-built smart factory," *Smart Manufacturing, Publication of SME*, pp. 8–13, Mar-2018.

[60] R. Wuthrich, L. A. Hof, J. D. Abou Ziki, G. Cusanelli, and P. Thibaut, "Spark Assisted Chemical Engraving Machine, A workpiece machined by the machine, and a process related thereof," WO 2017/064583 A1, 2017.

[61] N. Kawahara, T. Suto, T. Hirano, Y. Ishikawa, T. Kitahara, N. Ooyama, and T. Ataka, "Microfactories; new applications of micromachine technology to the manufacture of small products," *Microsyst. Technol.*, vol. 3, no. 2, pp. 37–41, Feb. 1997.

[62] Y. Okazaki, N. Mishima, and K. Ashida, "Microfactory—Concept, History, and Developments," *J. Manuf. Sci. Eng.*, vol. 126, no. 4, pp. 837–844, Feb. 2005.

[63] T. Kitahara, "Microfactory and microlathe," in *International Workshop on Microfactories*, 1998, pp. 1–8.

[64] D. Huo, K. Cheng, and F. Wardle, "Design of Precision Machines," in *Machining Dynamics: Fundamentals, Applications and Practices*, K. Cheng, Ed. London: Springer London, 2009, pp. 283–321.

[65] D. Dornfeld and D.-E. Lee, "Process planning for precision manufacturing," in *Precision*

Manufacturing, Boston, MA: Springer US, 2008, pp. 425–453.

[66]   J. M. Stein and D. A. Dornfeld, "Integrated Design and Manufacturing for Precision Mechanical Components," in *Integrated Design and Manufacturing in Mechanical Engineering*, 1997, pp. 367–376.

[67]   H. Nakazawa, *Principles of precision engineering; translated by Ryu Takeguchi*. New York: Oxford University Press Oxford, 1994.

[68]   D. Dornfeld and D.-E. Lee, "Machine design for precision manufacturing," in *Precision Manufacturing*, Boston, MA: Springer US, 2008, pp. 37–48.

[69]   R. E. DeVor, T.-H. Chang, and J. W. Sutherland, *Statistical Quality Design and Control*. New York: Mcmillan, 1992.

[70]   E. Le Bourhis, *Glass, Mechanics and Technology*. Wiley-VCH, 2014.

[71]   D. Hèulsenberg, A. Harnisch, and A. Bismarck, *Microstructuring of Glasses*. Berlin, Heidelberg: Springer Berlin Heidelberg, 2008.

[72]   G. M. Whitesides, "The origins and the future of microfluidics.," *Nature*, vol. 442, no. 7101, pp. 368–373, 2006.

[73]   N.-T. Nguyen and S. T. Wereley, *Fundamentals and applications of microfluidics*, Second edi. Boston, London: Artech House integrated microsystems series, 2006.

[74]   H. A. Stone and S. Kim, "Microfluidics : Basic Issues , Applications , and Challenges," *AIChE J.*, vol. 47, no. 6, pp. 1250–1254, 2001.

[75]   D. Sinton, "Energy: the microfluidic frontier.," *Lab Chip*, vol. 14, no. 17, 2014.

[76]   "SCP Science." [Online]. Available: http://www.scpscience.com/. [Accessed: 24-Apr-2018].

[77]   I. P. Prikhodko, S. A. Zotov, A. A. Trusov, and A. M. Shkel, "Microscale glass-blown three-dimensional spherical shell resonators," *J. Microelectromechanical Syst.*, vol. 20, no. 3, pp. 691–701, 2011.

[78]   D. T. Nguyen, C. Meyers, T. D. Yee, N. A. Dudukovic, J. F. Destino, C. Zhu, E. B. Duoss, T. F. Baumann, T. Suratwala, J. E. Smay, and R. Dylla-Spears, "3D-Printed Transparent Glass," *Adv. Mater.*, vol. 29, no. 26, pp. 1–5, 2017.

[79]   F. Kotz, K. Arnold, W. Bauer, D. Schild, N. Keller, K. Sachsenheimer, T. M. Nargang, C. Richter, D. Helmer, and B. E. Rapp, "Three-dimensional printing of transparent fused silica glass," *Nature*, vol. 544, no. 7650, pp. 337–339, 2017.

[80] D. J. Guckenberger, T. E. de Groot, A. M. D. Wan, D. J. Beebe, and E. W. K. Young, "Micromilling: a method for ultra-rapid prototyping of plastic microfluidic devices," *Lab Chip*, vol. 15, no. 11, pp. 2364–2378, 2015.

[81] R. Wüthrich and J. D. Abou Ziki, *Micromachining Using Electrochemical Discharge Phenomenon*. Elsevier, 2015.

[82] N. Van Toan, M. Toda, and T. Ono, "An investigation of processes for glass micromachining," *Micromachines*, vol. 7, no. 3, pp. 19–22, 2016.

[83] L. A. Hof and J. A. Ziki, "Micro-hole drilling on glass substrates-A review," *Micromachines*, vol. 8, no. 2, pp. 1–23, 2017.

[84] K. Kolari, V. Saarela, and S. Franssila, "Deep plasma etching of glass for fluidic devices with different mask materials," *J. Micromechanics Microengineering*, vol. 18, no. 6, p. 064010, 2008.

[85] C. Iliescu, B. Chen, and J. Miao, "On the wet etching of Pyrex glass," *Sensors Actuators, A Phys.*, vol. 143, no. 1, pp. 154–161, 2008.

[86] C. Liu and X. Xu, "Cyber-physical Machine Tool - The Era of Machine Tool 4.0," *Procedia CIRP*, vol. 63, pp. 70–75, 2017.

[87] N. P. Bansal and R. H. Doremus, "Handbook of Glass Properties," in *Handbook of Glass Properties*, 1st Editio., San Diego: Academic Press, 2013, p. 680.

[88] Apple Inc., "iPhone 8 introduces an all‑new glass design." [Online]. Available: https://www.apple.com/ca/iphone-8/. [Accessed: 18-May-2018].

[89] M. Töpper, I. Ndip, R. Erxleben, L. Brusberg, N. Nissen, H. Schröder, H. Yamamoto, G. Todt, and H. Reichl, "3-D Thin film interposer based on TGV (Through Glass Vias): An alternative to Si-interposer," in *2010 Proceedings 60th Electronic Components and Technology Conference (ECTC)*, 2010, pp. 66–73.

[90] B. Sawyer, B. C. Chou, J. Tong, W. Vis, K. Panayappan, S. Deng, H. Tournier, V. Sundaram, and R. Tummala, "Design and Demonstration of 2.5D Glass Interposers as a Superior Alternative to Silicon Interposers for 28 Gbps Signal Transmission," in *2016 IEEE 66th Electronic Components and Technology Conference (ECTC)*, 2016, pp. 972–977.

[91] Swift Glass Company, "Industry-Compliant Glass Drilling." [Online]. Available: https://www.swiftglass.com/glass-drilling. [Accessed: 18-May-2018].

[92] J. Voldman, M. L. Gray, and M. A. Schmidt, "Microfabrication in biology and medicine.," *Annu. Rev. Biomed. Eng.*, vol. 1, pp. 401–425, 1999.

[93] D. Sarvela, "Overview of glass micro machining processes for MEMS applications," *MEMS Journal*, 2010. [Online]. Available: http://www.memsjournal.com/2010/11/overview-of-glass-micro-machining-processes-for-mems-applications.html.

[94] C. Iliescu, F. E. H. Tay, and J. Miao, "Strategies in deep wet etching of Pyrex glass," *Sensors Actuators, A Phys.*, vol. 133, no. 2 SPEC. ISS., pp. 395–400, 2007.

[95] S. Takahashi, K. Horiuchi, K. Tatsukoshi, M. Ono, N. Imajo, and T. Mobely, "Development of Through Glass Via (TGV) formation technology using electrical discharging for 2.5/3D integrated packaging," *Proc. - Electron. Components Technol. Conf.*, pp. 348–352, 2013.

[96] S. Yoshida, "AGC Succeeds in Developing Micro Hole Drilling Processing Technology for Ultra-thin Glass with a Thickness in the Order of Microns — Toward Application for Laminated Semiconductor Components —," *Asahi Glas. Co., Ltd.*, pp. 2–4, 2012.

[97] A. Tseng, Y. T. Chen, C. L. Chao, K. J. Ma, and T. P. Chen, "Recent developments on microablation of glass materials using excimer lasers," *Opt. Lasers Eng.*, vol. 45, no. 10, pp. 975–992, 2007.

[98] A. Ghobeity, H. Getu, M. Papini, and J. K. Spelt, "Surface evolution models for abrasive jet micromachining of holes in glass and polymethylmethacrylate (PMMA)," *J. Micromechanics Microengineering*, vol. 17, no. 11, pp. 2175–2185, 2007.

[99] R. Wüthrich and V. Fascio, "Machining of non-conducting materials using electrochemical discharge phenomenon - An overview," *Int. J. Mach. Tools Manuf.*, vol. 45, no. 9, pp. 1095–1108, 2005.

[100] C. K. Fredrickson and Z. H. Fan, "Macro-to-micro interfaces for microfluidic devices," *Lab Chip*, vol. 4, no. 6, pp. 526–533, 2004.

[101] Y. Temiz, R. D. Lovchik, G. V. Kaigala, and E. Delamarche, "Lab-on-a-chip devices: How to close and plug the lab?," *Microelectron. Eng.*, vol. 132, pp. 156–175, 2015.

[102] L. Brusberg, M. Queisser, C. Gentsch, H. Schröder, and K.-D. Lang, "Advances in CO2-Laser Drilling of Glass Substrates," *Phys. Procedia*, vol. 39, no. Ic, pp. 548–555, 2012.

[103] R. Delmdahl and R. Paetzel, "Laser Drilling of High-Density Through Glass Vias (TGVs)

for 2.5D and 3D Packaging," *J. Microelectron. Packag. Soc.*, vol. 21, no. 2, pp. 53–57, 2014.

[104]   S. Karimelahi, L. Abolghasemi, and P. R. Herman, "Rapid micromachining of high aspect ratio holes in fused silica glass by high repetition rate picosecond laser," *Appl. Phys. A Mater. Sci. Process.*, vol. 114, no. 1, pp. 91–111, 2014.

[105]   S. Z. Chavoshi and X. Luo, "Hybrid micro-machining processes: A review," *Precis. Eng.*, vol. 41, pp. 1–23, 2015.

[106]   P. Cardoso and J. P. Davim, "a Brief Review on Micromachining of Materials," vol. 30, pp. 98–102, 2012.

[107]   D. E. Brehl and T. A. Dow, "Review of vibration-assisted machining," *Precis. Eng.*, vol. 32, no. 3, pp. 153–172, 2008.

[108]   B. Lauwers, F. Klocke, A. Klink, A. E. Tekkaya, R. Neugebauer, and D. Mcintosh, "Hybrid processes in manufacturing," *CIRP Ann. - Manuf. Technol.*, vol. 63, no. 2, pp. 561–583, 2014.

[109]   S. P. Leo Kumar, J. Jerald, S. Kumanan, and R. Prabakaran, "A Review on Current Research Aspects in Tool-Based Micromachining Processes," *Mater. Manuf. Process.*, vol. 29, no. 11–12, pp. 1291–1337, 2014.

[110]   C. Iliescu, H. Taylor, M. Avram, J. Miao, and S. Franssila, "A practical guide for the fabrication of microfluidic devices using glass and silicon," *Biomicrofluidics*, vol. 6, no. 1, pp. 16505–1650516, 2012.

[111]   A. K. Jain and P. M. Pandey, "Study of Peck drilling of borosilicate glass with µRUM process for MEMS," *J. Manuf. Process.*, vol. 22, pp. 134–150, 2016.

[112]   H.-H. Kim, S. Chung, S.-C. Kim, W.-H. Jee, and S.-C. Chung, "Condition Monitoring of Micro-Drilling Processes on Glass by using Machine Vision," in *Proceedings of the ASPE*, 2006, vol. 21, pp. 535–538.

[113]   S. T. Chen, Z. H. Jiang, Y. Y. Wu, and H. Y. Yang, "Development of a grinding-drilling technique for holing optical grade glass," *Int. J. Mach. Tools Manuf.*, vol. 51, no. 2, pp. 95–103, 2011.

[114]   B. J. Park, Y. J. Choi, and C. N. Chu, "Prevention of Exit Crack in Micro Drilling of Soda-Lime Glass," *CIRP Ann. - Manuf. Technol.*, vol. 51, no. 1, pp. 347–350, 2002.

[115]   D. Solignac, a. Sayah, S. Constantin, R. Freitag, and M. a M. Gijs, "Powder blasting for

the realisation of microchips for bio-analytic applications," *Sensors Actuators, A Phys.*, vol. 92, no. 1–3, pp. 388–393, 2001.

[116] E. Belloy, a. Sayah, and M. a M. Gijs, "Oblique powder blasting for three-dimensional micromachining of brittle materials," *Sensors Actuators, A Phys.*, vol. 92, no. 1–3, pp. 358–363, 2001.

[117] H. Wensink, J. W. Berenschot, H. V. Jansen, and M. C. Elwenspoek, "High resolution powder blast micromachining," *Proc. IEEE Thirteen. Annu. Int. Conf. Micro Electro Mech. Syst. (Cat. No.00CH36308)*, pp. 769–774, 2000.

[118] H. Wensink, "Fabrication of microstructures by Powder Blasting," University of Twente, The Netherlands, 2002.

[119] S. Schlautmann, H. Wensink, R. Schasfoort, M. Elwenspoek, and A. Van Den Berg, "Powder-blasting technology as an alternative tool for microfabrication of capillary electrophoresis chips with integrated conductivity sensors," *J. Micromechanics Microengineering*, vol. 11, no. 4, pp. 386–389, 2001.

[120] L. Zhang, T. Kuriyagawa, Y. Yasutomi, and J. Zhao, "Investigation into micro abrasive intermittent jet machining," *Int. J. Mach. Tools Manuf.*, vol. 45, no. 7–8, pp. 873–879, Jun. 2005.

[121] H. Nouraei, K. Kowsari, J. K. Spelt, and M. Papini, "Surface evolution models for abrasive slurry jet micro-machining of channels and holes in glass," *Wear*, vol. 309, no. 1–2, pp. 65–73, 2014.

[122] K. Kowsari, H. Nouraei, D. F. James, J. K. Spelt, and M. Papini, "Abrasive slurry jet micro-machining of holes in brittle and ductile materials," *J. Mater. Process. Technol.*, vol. 214, no. 9, pp. 1909–1920, 2014.

[123] A. Schorderet, E. Deghilage, and K. Agbeviade, "Tool type and hole diameter influence in deep ultrasonic drilling of micro-holes in glass," *Procedia CIRP*, vol. 6, pp. 565–570, 2013.

[124] C. Zhang, R. Rentsch, and E. Brinksmeier, "Advances in micro ultrasonic assisted lapping of microstructures in hard–brittle materials: a brief review and outlook," *Int. J. Mach. Tools Manuf.*, vol. 45, no. 7–8, pp. 881–890, Jun. 2005.

[125] B. H. Yan, a. C. Wang, C. Y. Huang, and F. Y. Huang, "Study of precision micro-holes in borosilicate glass using micro EDM combined with micro ultrasonic vibration

machining," *Int. J. Mach. Tools Manuf.*, vol. 42, no. 10, pp. 1105–1112, 2002.

[126] K. I. Ishikawa, H. Suwabe, T. Nishide, and M. Uneda, "Study on combined vibration drilling by ultrasonic and low-frequency vibrations for hard and brittle materials," *Precis. Eng.*, vol. 22, no. 4, pp. 196–205, 1998.

[127] K. Egashira and T. Masuzawa, "Microultrasonic Machining by the Application of Workpiece Vibration," *CIRP Ann. - Manuf. Technol.*, vol. 48, no. 1, pp. 131–134, Jan. 1999.

[128] A. A. Guzzo, P.L., Shinohara, A.H., Raslan, "A Comparative Study on Ultrasonic Machining of Hard and Brittle Materials," in *COBEF 2003 – II Brazilian Manufacturing Congress*, 2003.

[129] K. Egashira, K. Mizutani, and T. Nagao, "Ultrasonic Vibration Drilling of Microholes in Glass," *CIRP Ann. - Manuf. Technol.*, vol. 51, no. 1, pp. 339–342, Jan. 2002.

[130] K. Egashira, R. Kumagai, R. Okina, K. Yamaguchi, and M. Ota, "Drilling of microholes down to 10 μm in diameter using ultrasonic grinding," *Precis. Eng.*, vol. 38, no. 3, pp. 605–610, 2014.

[131] C. Khan Malek, L. Robert, J. J. Boy, and P. Blind, "Deep microstructuring in glass for microfluidic applications," *Microsyst. Technol.*, vol. 13, no. 5–6, pp. 447–453, 2007.

[132] K. Okazaki, S. Torii, T. Makimura, H. Niino, K. Murakami, D. Nakamura, a. Takahashi, and T. Okada, "Sub-wavelength micromachining of silica glass by irradiation of CO_2 laser with Fresnel diffraction," *Appl. Phys. A Mater. Sci. Process.*, vol. 104, no. 2, pp. 593–599, 2011.

[133] A. K. Dubey and V. Yadava, "Laser beam machining—a review," *Int. J. Mach. Tools Manuf.*, vol. 48, no. 6, pp. 609–628, 2008.

[134] J. Bovatsek and R. S. Patel, "DPSS Lasers Overcome Glass Process Challenges," *Photonics Spectra*, 2012. [Online]. Available: http://www.photonics.com.

[135] Femtoprint SA, "3D printing for glass microdevices." [Online]. Available: www.femtoprint.ch.

[136] Fraunhofer ILT, "Selective Laser Etching of Glass and Sapphire." [Online]. Available: http://www.ilt.fraunhofer.de/en/publication-and-press/brochures/brochure_Selective_Laser_ Etching_of_Glass_and_Sapphire.html.

[137] D. J. Hwang, T. Y. Choi, and C. P. Grigoropoulos, "Liquid-assisted femtosecond laser

drilling of straight and three-dimensional microchannels in glass," *Appl. Phys. A Mater. Sci. Process.*, vol. 79, no. 3, pp. 605–612, 2004.

[138] C. K. Chung, S. L. Lin, H. Y. Wang, T. K. Tan, K. Z. Tu, and H. F. Lung, "Fabrication and simulation of glass micromachining using CO2 laser processing with PDMS protection," *Appl. Phys. A*, vol. 113, no. 2, pp. 501–507, 2013.

[139] S. Nikumb, Q. Chen, C. Li, H. Reshef, H. Y. Zheng, H. Qiu, and D. Low, "Precision glass machining, drilling and profile cutting by short pulse lasers," *Thin Solid Films*, vol. 477, no. 1–2, pp. 216–221, 2005.

[140] A. Ran, L. Yan, D. Yan-Ping, F. Ying, Y. Hong, and G. Qi-Huang, "Laser Micro-Hole Drilling of Soda-Lime Glass with Femtosecond Pulses," *Chinese Phys. Lett.*, vol. 21, no. 12, pp. 2465–2468, 2004.

[141] M. Castillejo, P. M. Ossi, and L. Zhigilei, *Lasers in Materials Science*. Springer, 2014.

[142] L. Brusberg, H. Schroder, M. Topper, and H. Reichl, "Photonic System-in-Package technologies using thin glass substrates," *Electron. Packag. Technol. Conf. 2009. EPTC '09. 11th*, 2009.

[143] P. R. Herman, A. Oettl, K. P. Chen, and R. S. Marjoribanks, "Laser micromachining of 'transparent' fused silica with 1-ps pulses and pulse trains," *Proc. SPIE*, vol. 3616, no. January, pp. 148–155, 1999.

[144] Y. Wu, W. Jia, C. Y. Wang, M. Hu, X. Ni, and L. Chai, "Micro-hole fabricated inside FOTURAN glass using femtosecond laser writing and chemical etching," *Opt. Quantum Electron.*, vol. 39, no. 14, pp. 1223–1229, 2007.

[145] Y. Zhou, M. H. Hong, J. Y. H. Fuh, L. Lu, B. S. Lukyanchuk, and Z. B. Wang, "Near-field enhanced femtosecond laser nano-drilling of glass substrate," *J. Alloys Compd.*, vol. 449, no. 1–2, pp. 246–249, 2008.

[146] H. Huang, L. Yang, and J. Liu, "Micro-hole drilling and cutting using femtosecond fiber laser," *Opt. Eng.*, vol. 53, no. 5, p. 051513, 2014.

[147] I. Kono, A. Nakanishi, S. Warisawa, and M. Mitsuishi, "Study on Non-Crack Laser Machining of Glass by using Absorbent Powder," in *American Society Precision Engineering Proceedings*, 2005, pp. 1793–1997.

[148] D. Basting and G. Marowsky, *Excimer laser technology*. 2005.

[149] N. Rivzi, "Micro Manufacturing with lasers," *Med-Tech Innovation*, pp. 16–21, 2012.

[150] Corning, "Corning Gorilla Glass." [Online]. Available: https://www.corning.com/gorillaglass/worldwide/en.html.

[151] C. K. Chung and S. L. Lin, "CO2 laser micromachined crackless through holes of Pyrex 7740 glass," *Int. J. Mach. Tools Manuf.*, vol. 50, no. 11, pp. 961–968, 2010.

[152] Fraunhofer Institute For Reliability And Microintegration IZM, "CO2 -Laser-Drilling of Through- Glass Vias (TGVs)."

[153] Mitsubishi Electric Corporation, "Mitsubishi Electric Develops Micro Glass-processing Technology Incorporating Pulsed CO 2 Laser," 2014.

[154] B. Keiper, H. Exner, U. Löschner, and T. Kuntze, "Drilling of glass by excimer laser mask projection technique," *J. Laser Appl.*, vol. 12, no. 5, p. 189, 2000.

[155] C. Iliescu, B. Chen, and J. Miao, "Deep wet etching-through 1mm pyrex glass wafer for microfluidic applications," in *Micro Electro Mechanical Systems, 2007. MEMS. IEEE 20th International Conference on*, 2007, pp. 393–396.

[156] N. Fertig, C. Meyer, R. H. Blick, C. Trautmann, and J. C. Behrends, "Microstructured glass chip for ion-channel electrophysiology.," *Phys. Rev. E. Stat. Nonlin. Soft Matter Phys.*, vol. 64, no. 4 Pt 1, p. 040901, 2001.

[157] C. Iliescu, J. Jing, F. E. H. Tay, J. Miao, and T. Sun, "Characterization of masking layers for deep wet etching of glass in an improved HF/HCl solution," *Surf. Coatings Technol.*, vol. 198, no. 1–3, pp. 314–318, 2005.

[158] T. Sugita, K. Tsujino, and M. Matsumura, "Making Microholes in Glass by Electrochemical Local Acidification of Fluoride-Containing Solution," *ECS J. Solid State Sci. Technol.*, vol. 1, no. 1, pp. P1–P4, 2012.

[159] X. Li, T. Abe, Y. Liu, and M. Esashi, "Fabrication of high-density electrical feed-throughs by deep-reactive-ion etching of Pyrex glass," *J. Microelectromechanical Syst.*, vol. 11, no. 6, pp. 625–630, 2002.

[160] J. H. Park, N.-E. Lee, J. Lee, J. S. Park, and H. D. Park, "Deep dry etching of borosilicate glass using SF6 and SF6/Ar inductively coupled plasmas," *Microelectron. Eng.*, vol. 82, no. 2, pp. 119–128, Oct. 2005.

[161] T. Akashi and Y. Yoshimura, "Deep reactive ion etching of borosilicate glass using an anodically bonded silicon wafer as an etching mask," *J. Micromechanics Microengineering*, vol. 16, no. 5, p. 1051, 2006.

[162] P. W. Leech, "Reactive ion etching of quartz and silica-based glasses in CF4/CHF3 plasmas," *Vacuum*, vol. 55, no. 3–4, pp. 191–196, Dec. 1999.

[163] K. Kolari, "Deep plasma etching of glass with a silicon shadow mask," *Sensors Actuators, A Phys.*, vol. 141, no. 2, pp. 677–684, 2008.

[164] X. Li, T. Abe, and M. Esashi, "Deep reactive ion etching of Pyrex glass using SF6 plasma," *Sensors Actuators, A Phys.*, vol. 87, no. 3, pp. 139–145, 2001.

[165] S. Queste, R. Salut, S. Clatot, J. Y. Rauch, and C. G. Khan Malek, "Manufacture of microfluidic glass chips by deep plasma etching, femtosecond laser ablation, and anodic bonding," *Microsyst. Technol.*, vol. 16, no. 8–9, pp. 1485–1493, 2010.

[166] B. Lauwers, "Surface integrity in hybrid machining processes," *Procedia Eng.*, vol. 19, pp. 241–251, 2011.

[167] U. Heisel, R. Eisseler, R. Eber, J. Wallaschek, J. Twiefel, and M. Huang, "Ultrasonic-assisted machining of stone," *Prod. Eng.*, vol. 5, no. 6, pp. 587–594, 2011.

[168] J. Gan, X. Wang, M. Zhou, B. Ngoi, and Z. Zhong, "Ultraprecision Diamond Turning of Glass with Ultrasonic Vibration," *Int. J. Adv. Manuf. Technol.*, vol. 21, no. 12, pp. 952–955, 2003.

[169] F. Klocke and O. Rubenach, "Ultrasonic-assisted diamond turning of glass and steel," *Ind. Diam. Rev.*, pp. 229–239, 2000.

[170] T. Moriwaki, E. Shamoto, and K. Inoue, "Ultraprecision ductile cutting of glass by applying ultrasonic vibration," *CIRP Ann. - Manuf. Technol.*, vol. 41, 1992.

[171] R. Malhotra, I. Saxena, K. Ehmann, and J. Cao, "Laser-induced plasma micro-machining (LIPMM) for enhanced productivity and flexibility in laser-based micro-machining processes," *CIRP Ann. - Manuf. Technol.*, vol. 62, no. 1, pp. 211–214, 2013.

[172] K. L. Choo, Y. Ogawa, G. Kanbargi, V. Otra, L. M. Raff, and R. Komanduri, "Micromachining of silicon by short-pulse laser ablation in air and under water," *Mater. Sci. Eng. A*, vol. 372, no. 1–2, pp. 145–162, 2004.

[173] J. Choi, B. Jeon, and B. Kim, "Chemical-assisted ultrasonic machining of glass," *J. Mater. Process. Technol.*, vol. 191, pp. 153–156, 2007.

[174] T. Tateishi, N. Yoshihara, J. Yan, and T. Kuriyagawa, "Study on electrorheological fluid-assisted microultrasonic machining," *Int. J. Abras. Technol.*, vol. 2, no. 1, pp. 70–82, 2009.

[175] T. Tateishi, N. Yoshihara, J. W. Yan, and T. Kuriyagawa, "Fabrication of High-Aspect Ratio Micro Holes on Hard Brittle Materials -Study on Electrorheological Fluid-Assisted Micro Ultrasonic Machining-," in *Key Engineering Materials*, 2009, vol. 389–390, pp. 264–270.

[176] T. Tateishi, K. Shimada, N. Yoshihara, J. W. Yan, and T. Kuriyagawa, "Effect of Electrorheological Fluid Assistance on Micro Ultrasonic Machining," *Adv. Mater. Res.*, vol. 69–70, pp. 148–152, 2009.

[177] A. Schubert, H. Zeidler, M. H. Oschätzchen, J. Schneider, and M. Hahn, "Enhancing Micro-EDM using Ultrasonic Vibration and Approaches for Machining of Nonconducting Ceramics," *Strojniški Vestn. - J. Mech. Eng.*, vol. 59, no. 3, pp. 156–164, 2013.

[178] N. Mohri, Y. Fukuzawa, T. Tani, N. Saito, and K. Furutani, "Assisting Electrode Method for Machining Insulating Ceramics," *{CIRP} Ann. - Manuf. Technol.*, vol. 45, no. 1, pp. 201–204, 1996.

[179] J. Edelmann, C. Worsch, A. Schubert, and C. Rüssel, "Micro structuring of inorganic glass by hot embossing of coated glass wafers," *Microsyst. Technol.*, vol. 16, no. 4, pp. 553–560, 2010.

[180] B.-H. Yan, C.-T. Yang, F.-Y. Huang, and Z.-H. Lu, "Electrophoretic deposition grinding (EPDG) for improving the precision of microholes drilled via ECDM," *J. Micromechanics Microengineering*, vol. 17, no. 2, pp. 376–383, 2007.

[181] B. R. Sarkar, B. Doloi, and B. Bhattacharyya, "Parametric analysis on electrochemical discharge machining of silicon nitride ceramics," *Int. J. Adv. Manuf. Technol.*, vol. 28, no. 9, pp. 873–881, 2006.

[182] M. R. Razfar, J. Ni, A. Behroozfar, and S. Lan, "An investigation on Electrochemical Discharge micro-drilling of glass," in *ASME 2013 International Manufacturing Science and Engineering Conference Collocated with the 41st North American Manufacturing Research Conference, MSEC 2013*, vol. 2, 2013.

[183] D. J. Kim, Y. Ahn, S. H. Lee, and Y. K. Kim, "Voltage pulse frequency and duty ratio effects in an electrochemical discharge microdrilling process of Pyrex glass," *Int. J. Mach. Tools Manuf.*, vol. 46, no. 10, pp. 1064–1067, 2006.

[184] E. S. Lee, D. Howard, E. Liang, S. D. Collins, and R. L. Smith, "Removable tubing interconnects for glass-based micro-fluidic systems made using ECDM," *J.*

Micromechanics Microengineering, vol. 14, no. 4, pp. 535–541, 2004.

[185] S. K. Jui, A. B. Kamaraj, and M. M. Sundaram, "High aspect ratio micromachining of glass by electrochemical discharge machining (ECDM)," *J. Manuf. Process.*, vol. 15, no. 4, pp. 460–466, 2013.

[186] R. Wüthrich and L. A. Hof, "The gas film in spark assisted chemical engraving (SACE) - A key element for micro-machining applications," *Int. J. Mach. Tools Manuf.*, vol. 46, no. 7–8, pp. 828–835, 2006.

[187] L. A. Hof, "3D Microstructuring of glass," Delft University of Technology, The Netherlands, 2004.

[188] Z.-P. Zheng, J.-K. Lin, F.-Y. Huang, and B.-H. Yan, "Improving the machining efficiency in electrochemical discharge machining (ECDM) microhole drilling by offset pulse voltage," *J. Micromechanics Microengineering*, vol. 18, no. 2, p. 025014, 2008.

[189] Z.-P. Zheng, W.-H. Cheng, F.-Y. Huang, and B.-H. Yan, "3D microstructuring of Pyrex glass using the electrochemical discharge machining process," *J. Micromechanics Microengineering*, vol. 17, no. 5, pp. 960–966, 2007.

[190] M.-S. Han, B.-K. Min, and S. J. Lee, "Modeling gas film formation in electrochemical discharge machining processes using a side-insulated electrode," *J. Micromechanics Microengineering*, vol. 18, no. 4, p. 045019, 2008.

[191] C.-P. Cheng, K.-L. Wu, C.-C. Mai, C.-K. Yang, Y.-S. Hsu, and B.-H. Yan, "Study of gas film quality in electrochemical discharge machining," *Int. J. Mach. Tools Manuf.*, vol. 50, no. 8, pp. 689–697, Aug. 2010.

[192] Z.-P. Zheng, H.-C. Su, F.-Y. Huang, and B.-H. Yan, "The tool geometrical shape and pulse-off time of pulse voltage effects in a Pyrex glass electrochemical discharge microdrilling process," *J. Micromechanics Microengineering*, vol. 17, no. 2, p. 265, 2007.

[193] C. Wei, J. Ni, and D. Hu, "Electrochemical discharge machining using micro-drilling tools," *Trans. North Am. Manuf. Res. Inst. SME*, vol. 38, pp. 105–111, 2010.

[194] C. K. Yang, K. L. Wu, J. C. Hung, S. M. Lee, J. C. Lin, and B. H. Yan, "Enhancement of ECDM efficiency and accuracy by spherical tool electrode," *Int. J. Mach. Tools Manuf.*, vol. 51, no. 6, pp. 528–535, 2011.

[195] R. Wüthrich, B. Despont, P. Maillard, and H. Bleuler, "Improving the material removal rate in spark-assisted chemical engraving (SACE) gravity-feed micro-hole drilling by tool

vibration," *J. Micromechanics Microengineering*, vol. 16, no. 11, p. N28, 2006.

[196] M. Rusli and K. Furutani, "Performance of micro-hole drilling by ultrasonic-assisted electro-chemical discharge machining," *Adv. Mater. Res.*, vol. 445, pp. 865–870, 2012.

[197] M. R. Razfar, A. Behroozfar, and J. Ni, "Study of the effects of tool longitudinal oscillation on the machining speed of electrochemical discharge drilling of glass," *Precis. Eng.*, vol. 38, no. 4, pp. 885–892, 2014.

[198] M.-S. Han, B.-K. Min, and S. J. Lee, "Geometric improvement of electrochemical discharge micro-drilling using an ultrasonic-vibrated electrolyte," *J. Micromechanics Microengineering*, vol. 19, no. 6, p. 65004, 2009.

[199] X. D. Cao, B. H. Kim, and C. N. Chu, "Micro-structuring of glass with features less than 100 μm by electrochemical discharge machining," *Precis. Eng.*, vol. 33, no. 4, pp. 459–465, 2009.

[200] C.-P. Cheng, K.-L. Wu, C.-C. Mai, Y.-S. Hsu, and B.-H. Yan, "Magnetic field-assisted electrochemical discharge machining," *J. Micromechanics Microengineering*, vol. 20, no. 7, p. 75019, 2010.

[201] J. D. Abou Ziki and R. Wüthrich, "Forces exerted on the tool-electrode during constant-feed glass micro-drilling by spark assisted chemical engraving," *Int. J. Mach. Tools Manuf.*, vol. 73, pp. 47–54, 2013.

[202] J. D. Abou Ziki and R. Wüthrich, "Nature of drilling forces during spark assisted chemical engraving," *Manuf. Lett.*, vol. 4, pp. 10–13, 2015.

[203] J. D. Abou Ziki, "Spark Assisted Chemical Engraving: A Novel Approach for Quantifying the Machining Zone Parameters Using Drilling Forces," Concordia University Montreal, Quebec, Canada, 2014.

[204] UKAM, "UKAM Industrial Superhard Tools, Micro Diamond Drills product catalogue." [Online]. Available: www.ukam.com /micro_core_drills.htm.

[205] A. Sayah, P.-A. Thivolle, V. K. Parashar, and M. a M. Gijs, "Fabrication of microfluidic mixers with varying topography in glass using the powder-blasting process," *J. Micromechanics Microengineering*, vol. 19, no. 8, p. 085024, 2009.

[206] S. H. Yeo and L. K. Tan, "Effects of ultrasonic vibrations in micro electro-discharge machining of microholes," *J. Micromechanics Microengineering*, vol. 9, no. 4, p. 345, 1999.

[207] M. Bu, T. Melvin, G. J. Ensell, J. S. Wilkinson, and A. G. R. Evans, "A new masking technology for deep glass etching and its microfluidic application," *Sensors Actuators, A Phys.*, vol. 115, no. 2–3 SPEC. ISS., pp. 476–482, 2004.

[208] J. Chae, J. M. Giachino, and K. Najafi, "Fabrication and characterization of a wafer-level MEMS vacuum package with vertical feedthroughs," *J. Microelectromechanical Syst.*, vol. 17, no. 1, pp. 193–200, 2008.

[209] J. M. Nagarah and D. A. Wagenaar, "Ultradeep fused silica glass etching with an HF-resistant photosensitive resist for optical imaging applications," *J. Micromechanics Microengineering*, vol. 22, no. 3, p. 35011, 2012.

[210] A. Goyal, V. Hood, and S. Tadigadapa, "High speed anisotropic etching of Pyrex® for microsystems applications," *J. Non. Cryst. Solids*, vol. 352, no. 6–7, pp. 657–663, May 2006.

[211] T. Ichiki, Y. Sugiyama, R. Taura, T. Koidesawa, and Y. Horiike, "Plasma applications for biochip technology," *Thin Solid Films*, vol. 435, no. 1–2, pp. 62–68, Jul. 2003.

[212] K. Kolari, "Plasma etching of high aspect ratio structures on glass," in *Proceedings of 19th micromechanics Europe workshop*, 2008, pp. 81–84.

[213] S. Queste, G. Ulliac, J.C. Jeannot, C.K. Malek, "DRIE of nonconventional materials: first results," in *Proceedings of the 4th international conference on multimaterial micro manufacture*, 2008, pp. 171–174.

[214] A. Salleo, F. Y. Génin, M. D. Feit, A. M. Rubenchik, T. Sands, S. S. Mao, and R. E. Russo, "Energy deposition at front and rear surfaces during picosecond laser interaction with fused silica," *Appl. Phys. Lett.*, vol. 78, no. 19, pp. 2840–2842, 2001.

[215] M. Pavius, C. Hibert, P. Fluckiger, P. Renaud, L. Rolland, and M. Puech, "Profile angle control in SiO2 deep anisotropic dry etching for MEMS fabrication," in *Micro Electro Mechanical Systems, 2004. 17th IEEE International Conference on. (MEMS)*, 2004, pp. 669–672.

[216] Schott, "Foturan Glass." [Online]. Available: http://www.design.caltech.edu/micropropulsion/ foturane.html.

[217] P. Maillard, B. Despont, H. Bleuler, and R. Wüthrich, "Geometrical characterization of micro-holes drilled in glass by gravity-feed with spark assisted chemical engraving (SACE)," *J. Micromechanics Microengineering*, vol. 17, no. 7, p. 1343, 2007.

[218] J. P. Desbiens and P. Masson, "ArF excimer laser micromachining of Pyrex, SiC and PZT for rapid prototyping of MEMS components," *Sensors Actuators, A Phys.*, vol. 136, no. 2, pp. 554–563, 2007.

[219] R. Wüthrich, U. Spaelter, Y. Wu, and H. Bleuler, "A systematic characterization method for gravity-feed micro-hole drilling in glass with spark assisted chemical engraving (SACE)," *J. Micromechanics Microengineering*, vol. 16, no. 9, p. 1891, 2006.

[220] R. Wüthrich, V. Fascio, D. Viquerat, and H. Langen, "Study of Spark assisted Electrochemical Etching - Force Measurements," in *International Workshop on Microfactories (IWMF 2000)*, 2000, pp. 201–204.

[221] J. D. Abou Ziki, L. A. Hof, and R. Wüthrich, "The machining temperature during Spark Assisted Chemical Engraving of glass," *Manuf. Lett.*, vol. 3, pp. 9–13, 2015.

[222] T. Tutui, "Electrical-discharge Machining of Glass," *J. Japan Soc. Precis. Eng.*, vol. 26, no. 309, pp. 596–600, 1960.

[223] H. Kurafuji and K. Suda, "Electrical discharge drilling of glass," *Ann. CIRP*, vol. 16, pp. 415–419, 1968.

[224] Posalux S.A., "Microfor SACE." [Online]. Available: https://www.posalux.ch/site/en/products/microfor_sace/sace. [Accessed: 11-Jan-2018].

[225] D. J. Kim, Y. Ahn, S. H. Lee, and Y. K. Kim, "Voltage pulse frequency and duty ratio effects in an electrochemical discharge microdrilling process of Pyrex glass," *Int. J. Mach. Tools Manuf.*, vol. 46, no. 10, pp. 1064–1067, 2006.

[226] ISO 6983-1:2009, "Automation systems and integration - Numerical control of machines - Program format and definitions of address words." 2009.

[227] S. Xú, N. Anwer, and S. Lavernhe, "Conversion of G-code programs for milling into STEP-NC," 2014.

[228] S. Stemmler, D. Abel, O. Adams, and F. Klocke, "Model Predictive Feed Rate Control for a Milling Machine," *IFAC-PapersOnLine*, vol. 49, no. 12, pp. 11–16, 2016.

[229] V. Dhokia, S. Kumar, P. Vichare, S. Newman, and R. D Allen, "Surface roughness prediction model for CNC machining of polypropylene," *Proc. Inst. Mech. Eng. Part B J. Eng. Manuf.*, vol. 222, pp. 137–157, 2008.

[230] A. Naylor, P. Hackney, N. Perera, and E. Clahr, "a Predictive Model for the Cutting Force in Wood Machining Developed Using Mechanical Properties," *Bioresources*, vol. 7, no. 3,

pp. 2883–2894, 2012.

[231] M. H. Ali, B. A. Khidhir, M. N. M. Ansari, and B. Mohamed, "FEM to predict the effect of feed rate on surface roughness with cutting force during face milling of titanium alloy," *HBRC J.*, vol. 9, no. 3, pp. 263–269, 2013.

[232] G. Kant and K. S. Sangwan, "Predictive modelling and optimization of machining parameters to minimize surface roughness using artificial neural network coupled with genetic algorithm," *Procedia CIRP*, vol. 31, pp. 453–458, 2015.

[233] A. T. Abbas, M. Alata, A. E. Ragab, M. M. El Rayes, and E. A. El Danaf, "Prediction Model of Cutting Parameters for Turning High Strength Steel Grade-H: Comparative Study of Regression Model versus ANFIS," *Adv. Mater. Sci. Eng.*, vol. 2017, 2017.

[234] M. Abd Rahman, M. Yeakub Ali, A. Saddam Khairuddin -, D. Sonowal, D. Sarma, and P. Bakul Barua, "Comparison with Experimental Results of Models and Modelling with Fuzzy Logic of the Effect on Surface Roughness of Cutting Parameters in Machining of Co28Cr6Mo wrought Steels Effects on Vibration and Surface Roughness in High Speed Micro End- Milling of I," *IOP Conf. Ser. Mater. Sci. Eng.*, 2017.

[235] S. Tangjitsitcharoen and H. Lohasiriwat, "Intelligent monitoring and prediction of tool wear in CNC turning by utilizing wavelet transform," *Int. J. Adv. Manuf. Technol.*, Dec. 2017.

[236] S. Lavernhe, C. Tournier, and C. Lartigue, "Model for performance prediction in multi-axis machining," no. 1, pp. 5–6, 2009.

[237] S. Dinesh, K. Rajaguru, V. Vijayan, and A. G. Antony, "Investigation and Prediction of Material Removal Rate and Surface Roughness in CNC Turning of EN24 Alloy Steel," *Mech. Mech. Eng.*, vol. 20, no. 4, pp. 451–466, 2016.

[238] E. B. Brousseau, S. S. Dimov, and D. T. Pham, "Some recent advances in multi-material micro- and nano-manufacturing," *Int. J. Adv. Manuf. Technol.*, vol. 47, no. 1–4, pp. 161–180, 2010.

[239] S. S. Dimov, E. B. J. P. Brousseau, R. Minev, and S. Bigot, "Micro- and nano-manufacturing: Challenges and opportunities," 2011, vol. 226, pp. 3–15.

[240] F. Feucht, J. Ketelaer, A. Wolff, M. Mori, and M. Fujishima, "Latest machining technologies of hard-to-cut materials by ultrasonic machine tool," *Procedia CIRP*, vol. 14, pp. 148–152, 2014.

[241] M. Necati Ozisik, *Heat Conduction*, Second Edi. New York: John Wiley & Sons Inc., 1993.

[242] J. Wall, *Transient Heat Conduction : Analytical Methods*. 2009.

[243] G. Yang, A. D. Migone, and K. W. Johnson, "Heat capacity and thermal diffusivity of a glass sample," *Phys. Rev. B*, vol. 45, no. 1, pp. 157–160, 1992.

[244] Mathworks, *Partial Differential Equation Toolbox User's Guide R2016a*. 2016.

[245] National Instruments, "LabVIEW User Manual," vol. 134113, no. 320999. Austin, TX, 2008.

[246] Siemens AG, "SIMATIC IPC477D." pp. 1–5, 2014.

[247] F. Charbonneau, "Improving the sparks assisted chemical engraving (SACE) for industrial application," Concordia University, 2016.

[248] Newport - ILS, "High-Performance Mid-Range Travel Linear Stages." pp. 1–4, 2014.

[249] S. Awtar, "Synthesis and Analysis of Parallel Kinematic XY Flexure Mechanisms," Massachusetts Institute of Technology, 2004.

[250] Newport Corporation, "XPS-Q8 Universal High-Performance Motion Controller / Driver." Irvine, CA, p. 232, 2015.

[251] Tcl Developer Xchange site, "Tool Command Language (Tcl)." [Online]. Available: https://www.tcl.tk/. [Accessed: 24-Apr-2018].

[252] Occidental Chemical Corporation (OxyChem), "Caustic Potash Handbook," Dallas, 2013.

[253] L. A. Hof and R. Wüthrich, "Micromachining glass with in-situ fabricated micro-tools," in *Conference Proceedings of the 16th EUSPEN International Conference & Exhibition*, 2016.

[254] A. Bildstein and J. Seidelmann, *Industrie 4.0-Readiness: Migration zur Industrie 4.0-Fertigung, in: Bauernhansl, T; ten Hompel, M; Vogel-Heuer, B.(Eds.): Industrie 4.0 in Produktion, Automatisierung und Logistik*. Wiesbaden: Springer Vieweg, 2014.

[255] H. (National A. of S. and E. Kagermann, W. (German R. C. for A. I. Wahlster, and J. (Deutsche P. A. Helbig, "Recommendations for implementing the strategic initiative INDUSTRIE 4.0," *Final Rep. Ind. 4.0 WG*, no. April, p. 82, 2013.

[256] C. Scheuermann, S. Verclas, and B. Bruegge, "Agile Factory - An Example of an Industry 4.0 Manufacturing Process," *3rd IEEE Int. Conf. Cyber-Physical Syst. Networks Publ.*, vol. 2008, p. 5, 2015.

[257] J. Hiemenz and Stratasys Inc., "3D Printing Jigs , Fixtures and Other Manufacturing Tools," *Stratasys*, pp. 1–9, 2015.

[258] C. K. Yang, C. P. Cheng, C. C. Mai, a. Cheng Wang, J. C. Hung, and B. H. Yan, "Effect of surface roughness of tool electrode materials in ECDM performance," *Int. J. Mach. Tools Manuf.*, vol. 50, no. 12, pp. 1088–1096, 2010.

[259] Y. Xu, C. Wang, L. Li, N. Matsumoto, K. Jang, Y. Dong, K. Mawatari, T. Suga, and T. Kitamori, "Bonding of glass nanofluidic chips at room temperature by a one-step surface activation using an O2/CF4 plasma treatment," *Lab Chip*, vol. 13, no. 6, pp. 1048, 2013.

[260] Y. Xu, C. Wang, Y. Dong, and L. Li, "Low-temperature direct bonding of glass nanofluidic chips using a two-step plasma surface activation process," pp. 1011–1018, 2012.

[261] N. Chiem, L. Lockyear-shultz, P. Andersson, C. Skinner, and J. Harrison, "Room temperature bonding of micromachined glass devices for capillary electrophoresis," *Science (80-.).*, vol. 4005, no. MAY 2000, pp. 147–152, 2000.

[262] C. Duan, W. Wang, and Q. Xie, *Review article: Fabrication of nanofluidic devices*, vol. 7, no. 2. 2013.

[263] A. Iles, A. Oki, and N. Pamme, "Bonding of soda-lime glass microchips at low temperature," *Proc. 2006 Int. Conf. Microtechnologies Med. Biol.*, pp. 109–111, 2006.

[264] H. Moriceau, F. Rieutord, F. Fournel, Y. Le Tiec, L. Di Cioccio, C. Morales, A. M. Charvet, and C. Deguet, "Overview of recent direct wafer bonding advances and applications," *Adv. Nat. Sci. Nanosci. Nanotechnol.*, vol. 1, no. 4, p. 043004, 2011.

[265] U. Gösele, Y. Bluhm, G. Kästner, P. Kopperschmidt, G. Kräuter, R. Scholz, a. Schumacher, S. Senz, Q.-Y. Tong, L.-J. Huang, Y.-L. Chao, and T. H. Lee, "Fundamental issues in wafer bonding," *J. Vac. Sci. Technol. A Vacuum, Surfaces, Film.*, vol. 17, no. 4, p. 1145, 1999.

[266] M. Stjernström and J. Roeraade, "Method for fabrication of microfluidic systems in glass," *J. Micromechanics Microengineering*, vol. 8, no. 1, pp. 33–38, 1999.

[267] C. K. Chung, H. C. Chang, T. R. Shih, S. L. Lin, E. J. Hsiao, Y. S. Chen, E. C. Chang, C. C. Chen, and C. C. Lin, "Water-assisted CO2laser ablated glass and modified thermal bonding for capillary-driven bio-fluidic application," *Biomed. Microdevices*, vol. 12, pp. 107–114, 2010.

[268] Different industrial key players in the glass microfabrication field, "Private communications." 2017.

[269] A. Ben-Yakar, A. Harkin, J. Ashmore, R. L. Byer, and H. a Stone, "Thermal and fluid processes of a thin melt zone during femtosecond laser ablation of glass: the formation of rims by single laser pulses," *J. Phys. D. Appl. Phys.*, vol. 40, no. 5, pp. 1447–1459, 2007.

[270] C. K. Chung and S. L. Lin, "Laser Micromachining," *J. Micromechanics Microengineering*, vol. 21, no. 6, p. 65023, 2011.

[271] H. Wensink, H. V Jansen, J. W. Berenschot, and M. C. Elwenspoek, "Mask materials for powder blasting," *J. Micromechanics Microengineering*, vol. 10, no. 2, p. 175, 2000.

[272] SCHOTT North America Inc., "Borofloat 33 - General Information." [Online]. Available: www.us.schott.com/borofloat. [Accessed: 11-Jan-2018].

[273] "Micronit Microtechnologies BV." [Online]. Available: https://www.micronit.com/. [Accessed: 11-Jan-2018].

[274] H. Noh, K. Moon, A. Cannon, P. J. Hesketh, and C. P. Wong, "Wafer bonding using microwave heating of parylene intermediate layers," *J. Micromechanics Microengineering*, vol. 14, no. 4, pp. 625–631, 2004.

[275] N. Cocheteau, a M. Pantel, F. Lebon, I. Rosu, S. A. Zaid, and I. Savin, "Mechanical characterisation of direct bonding," *Evolution (N. Y).*, pp. 1–6, 2013.

[276] "Sonoscan, sound technology with vision." [Online]. Available: http://www.sonoscan.com. [Accessed: 11-Jan-2018].

[277] U. Mescheder, *Mikrosystemtechnik : Konzepte und Anwendungen*, no. 2., überarb. und erg. Auflage. Stuttgart: Vieweg + Teubner, 2004.

[278] H. Justinger and G. Hirt, "Analysis of Size-Effects in the Miniaturized Deep Drawing Process," in *Sheet Metal 2007*, 2007, vol. 344, pp. 791–798.

[279] E. Berthier, E. W. K. Young, and D. Beebe, "Engineers are from PDMS-land, Biologists are from Polystyrenia," *Lab Chip*, vol. 12, no. 7, p. 1224, 2012.

[280] Yole Development, "Market and Technology Trends for Microfluidic Applications - September 21," 2011.

[281] N. S. Cameron, H. Roberge, T. Veres, S. C. Jakeway, and H. John Crabtree, "High fidelity, high yield production of microfluidic devices by hot embossing lithography: rheology and stiction.," *Lab Chip*, vol. 6, no. 7, pp. 936–41, 2006.

[282] J. Greener, W. Li, J. Ren, D. Voicu, V. Pakharenko, T. Tang, and E. Kumacheva, "ESI: Rapid, cost-efficient fabrication of microfluidic reactors in thermoplastic polymers by combining photolithography and hot embossing.," *Lab Chip*, vol. 10, no. 4, pp. 522–4, 2010.

[283] P. W. Leech, "Hot Embossing Of Microchannels in Cyclic Olefin Copolymer," *Cambridge Journals Online*, vol. 1191, no. 5, pp. 1–12, 2009.

[284] B. D. Gates, Q. Xu, J. C. Love, D. B. Wolfe, and G. M. Whitesides, "Unconventional Nanofabrication," *Annu. Rev. Mater. Res.*, vol. 34, no. 1, pp. 339–372, 2004.

[285] D. Yao, P. Nagarajan, L. Li, and A. Y. Yi, "A two-station embossing process for rapid fabrication of surface microstructures on thermoplastic polymers," *Polym. Eng. Sci.*, vol. 47, no. 4, pp. 530–539, 2007.

[286] T. Schaller, L. Bohn, J. Mayer, and K. Schubert, "Microstructure grooves with a width of less than 50 ??m cut with ground hard metal micro end mills," *Precis. Eng.*, vol. 23, no. 4, pp. 229–235, 1999.

[287] P. P. Shiu, G. K. Knopf, M. Ostojic, and S. Nikumb, "Rapid fabrication of tooling for microfluidic devices via laser micromachining and hot embossing," *J. Micromechanics Microengineering*, vol. 18, no. 2, p. 025012, 2008.

[288] T. Shibata, Y. Takahashi, T. Kawashima, T. Kubota, M. Mita, T. Mineta, and E. Makino, "Micromachining of electroformed nickel mold using thick photoresist microstructure for imprint technology," *Microsyst. Technol.*, vol. 14, no. 9–11, pp. 1359–1365, 2008.

[289] R. Novak, N. Ranu, and R. a Mathies, "Rapid fabrication of nickel molds for prototyping embossed plastic microfluidic devices.," *Lab Chip*, vol. 13, no. 8, pp. 1468–71, 2013.

[290] M. Debono, D. Voicu, M. Pousti, M. Safdar, R. Young, E. Kumacheva, and J. Greener, "One-Step Fabrication of Microchannels with Integrated Three Dimensional Features by Hot Intrusion Embossing," *Sensors*, vol. 16, no. 12, p. 2023, 2016.

[291] L. Zhang, F. Gu, L. Tong, and X. Yin, "Simple and cost-effective fabrication of two-dimensional plastic nanochannels from silica nanowire templates," *Microfluid. Nanofluidics*, vol. 5, no. 6, pp. 727–732, 2008.

[292] H. Niino, X. Ding, R. Kurosaki, a. Narazaki, T. Sato, and Y. Kawaguchi, "Imprinting by hot embossing in polymer substrates using a template of silica glass surface-structured by the ablation of LIBWE method," *Appl. Phys. A*, vol. 79, no. 4–6, pp. 827–828, 2004.

[293] J. W. Liu, Q. a Huang, J. T. Shang, and J. Y. Tang, "Micromachining of Pyrex7740 Glass for Micro-Fluidic Devices," in *14th International Conference on Miniaturized Systems for Chemistry and Life Sciences*, 2010, no. October, pp. 1907–1909.

[294] R. U. M. Haque and K. D. Wise, "A glass-in-silicon reflow process for three-dimensional microsystems," *J. Microelectromechanical Syst.*, vol. 22, no. 6, pp. 1470–1477, 2013.

[295] S. S. Zumdahl and D. J. DeCoste, *Introductory Chemistry*, Seventh ed. Brooks/Cole, Cengage Learning, 2010.

[296] D. C. Boyd, P. S. Danielson, D. A. Thompson, M. Velez, S. T. Reis, and R. Brow, "Glass," in *Kirk-Othmer Encyclopedia of Chemical Technology*, 2004.

[297] X. D. Cao, B. H. Kim, and C. N. Chu, "Micro-structuring of glass with features less than 100 μm by electrochemical discharge machining," *Precis. Eng.*, vol. 33, no. 4, pp. 459–465, 2009.

[298] S. K. Chak and P. Venkateswara Rao, "The drilling of Al2O3 using a pulsed DC supply with a rotary abrasive electrode by the electrochemical discharge process," *Int. J. Adv. Manuf. Technol.*, vol. 39, no. 7–8, pp. 633–641, 2008.

[299] J. W. Liu, T. M. Yue, and Z. N. Guo, "An analysis of the discharge mechanism in electrochemical discharge machining of particulate reinforced metal matrix composites," *Int. J. Mach. Tools Manuf.*, vol. 50, no. 1, pp. 86–96, 2010.

[300] M. Kim, B.-U. Moon, and C. H. Hidrovo, "Enhancement of the thermo-mechanical properties of PDMS molds for the hot embossing of PMMA microfluidic devices," *J. Micromechanics Microengineering*, vol. 23, no. 9, p. 095024, 2013.

[301] R. W. Jaszewski, H. Schift, J. Gobrecht, and P. Smith, "Hot embossing in polymers as a direct way to pattern resist," *Microelectron. Eng.*, vol. 41, pp. 575–578, 1998.

[302] N. Soga, "Elastic moduli and fracture toughness of glass," *J. Non. Cryst. Solids*, vol. 73, no. 1–3, pp. 305–313, 1985.

[303] M. Yamane and J. D. Mackenzie, "Vicker's Hardness of glass," *J. Non. Cryst. Solids*, vol. 15, no. 2, pp. 153–164, 1974.

[304] Saint Gobain Glass, "Glass physical properties." [Online]. Available: http://uk.saint-gobain-glass.com/trade-customers/physical-properties.

[305] T. E. Wilantewicz and J. R. Varner, "Vickers indentation behavior of several commercial glasses at high temperatures," *J. Mater. Sci.*, vol. 43, no. 1, pp. 281–298, 2008.

[306] I. L. Denry and J. A. Holloway, "Elastic constants, Vickers hardness, and fracture toughness of fluorrichterite-based glass-ceramics," *Dent. Mater.*, vol. 20, no. 3, pp. 213–219, 2004.

[307] H. Matzke, E. Toscano, J. Routbort, and K. Reimann, "Temperature Dependence and Fracture Toughness and Elastic Moduli of a Waste Glass," *J. Am. Ceram. Soc.*, vol. 69, no. 7, p. C-138-C-139, 1986.

[308] F. Petit, A. C. Sartieaux, M. Gonon, and F. Cambier, "Fracture toughness and residual stress measurements in tempered glass by Hertzian indentation," *Acta Mater.*, vol. 55, no. 8, pp. 2765–2774, 2007.

[309] I. D. Johnston, D. K. McCluskey, C. K. L. Tan, and M. C. Tracey, "Mechanical characterization of bulk Sylgard 184 for microfluidics and microengineering," *J. Micromechanics Microengineering*, vol. 24, p. 035017, 2014.

[310] MIT, "Material Properties PDMS." [Online]. Available: http://www.mit.edu/~6.777/matprops/pdms.htm.

[311] A. I. M. Greer, I. Vasiev, B. Della-Rosa, and N. Gadegaard, "Fluorinated ethylene–propylene: a complementary alternative to PDMS for nanoimprint stamps," *Nanotechnology*, vol. 27, no. 15, p. 155301, 2015.

[312] Microchem, "Material properties." [Online]. Available: http://www.microchem.com/pdf/SU-8 3000 Data Sheet.pdf.

[313] J. Hammacher, A. Fuelle, J. Flaemig, J. Saupe, B. Loechel, and J. Grimm, "Stress engineering and mechanical properties of SU-8-layers for mechanical applications," *Microsyst. Technol.*, vol. 14, no. 9–11, pp. 1515–1523, 2008.

[314] R. K. Jena, C. Y. Yue, and K. X. Yun, "Effect of a CNT based composite micromold on the replication fidelity during the microfabrication of polymeric microfluidic devices," *Rsc Adv.*, vol. 4, no. 24, pp. 12448–12456, 2014.

[315] Cytec Idustries Inc., "Conapoxy FR-1080." [Online]. Available: http://www.needfill.co.kr/cd/FR-1080.html.

[316] Ellsworthadhesives, "Epoxy Resins Material properties." [Online]. Available: http://www.ellsworthadhesives.co.uk/media/wysiwyg/files/cytec/CytecElectronicsBrochure-EU.pdf.

[317] "Statistics based on 2011–2016 order statistics from FlowJEM Inc. Unpublished work." .

[318] G. Behrens, M. Ruhe, H. Tetzel, and F. Vollertsen, "Effect of tool geometry variations on the punch force in micro deep drawing of rectangular components," *Prod. Eng.*, vol. 9, no. 2, pp. 195–201, Apr. 2015.

[319] G. Behrens, F. O. Trier, H. Tetzel, and F. Vollertsen, "Influence of tool geometry variations on the limiting drawing ratio in micro deep drawing," *Int. J. Mater. Form.*, vol. 9, no. 2, pp. 253–258, Apr. 2016.

[320] M. Geiger, M. Kleiner, R. Eckstein, N. Tiesler, and U. Engel, "Microforming," *CIRP Ann.*, vol. 50, no. 2, pp. 445–462, 2001.

[321] F. Vollertsen and Z. Hu, "Tribological Size Effects in Sheet Metal Forming Measured by a Strip Drawing Test," *CIRP Ann.*, vol. 55, no. 1, pp. 291–294, 2006.

[322] J. T. Gau, C. Principe, and J. Wang, "An experimental study on size effects on flow stress and formability of aluminm and brass for microforming," *J. Mater. Process. Technol.*, vol. 184, no. 1–3, pp. 42–46, 2007.

[323] F. Vollertsen, D. Biermann, H. N. Hansen, I. S. Jawahir, and K. Kuzman, "Size effects in manufacturing of metallic components," *CIRP Ann.*, vol. 58, no. 2, pp. 566–587, 2009.

[324] Z. Hu et al., "Forming tools for micro deep drawing—influence of geometrical tolerance of forming tools on the punch force in micro deep drawing," *wt Werkstattstech. online*, vol. H 11 (12), pp. 814–819, 2009.

Appendix

This appendix contains a list of different drilling techniques with their main feature characteristics for drilling micro-holes in glass. It provides supporting values on the technologies for micro-hole drilling on glass as presented and discussed in chapter twoannex.

Table A.1. List of different drilling techniques with their main feature characteristics for drilling micro-holes in glass.

Mechanical Methods	Material	Diameter (μm)	Aspect Ratio	Taper Angle * (°)	Speed (μm/s)	Depth (μm)	Surface Roughness (nm)	References
Grinding-drilling	optical grade glass and quartz	1011–1323	3.96–3.02	-	5	4000	-	[113]
Micro-drilling	soda-lime glass	100–400	1.3–0.33	-	125	130	-	[114]
Mechanical drilling	glass	>150	4–14	-	slow	-	-	[204]
Powder blasting (30 μm particles)	glass	150–1000	0.07–0.24	-	0.083–0.133	10–240	-	[205]
Powder blasting	glass	<50	2.5	-	0.4	-	2500	[117]
AJM (abrasive jet micromachining)	borosilicate glass	800	<0.06	-	32	50	high	[98]
ASJ (Abrasive slurry jet)	-	390	0.9	-	4.38	350	-	[121]
ASJM (Abrasive slurry jet—Al₂O₃ 10 μm particle slurry flowrate:1.67 mL/s)	Borosilicate glass	800	1.13	-	1.88	900	frosting	[122]
	-	2000	1.5	34	0.56	3000	-	[122]
Micro-ultra-sonic (abrasive grains)	pyrex 7740	420	>10	0.6	-	5000	1000	[131]
Ultrasonic (combined with EDM)	glass	150	3–4	-	0.13–0.15	-	-	[206]

Method	Material	Diameter (μm)	Aspect Ratio	Taper Angle * (°)	Speed (μm/s)	Depth (μm)	Surface Roughness (nm)	References
Ultrasonic vibration drilling	-	10	2	-	0.05	20	no cracks	[40]
Ultrasonic vibration drilling (combining ultrasonic and low-frequency/diamond core drill)	glass	964	-	-	16.67	-	-	[126]
Ultrasonic grinding (cemented tungsten carbide micro pins)	crown glass	10–30	-	-	0.25–0.27	-	-	[130]

Chemical Methods	Material	Diameter (μm)	Aspect Ratio	Taper Angle * (°)	Speed (μm/s)	Depth (μm)	Surface Roughness (nm)	References
wet etching (HF + mask Cr/Au/Cr/Au + SPR220-7)	glass	-	0.78	-	0.24–0.07	300	-	[207]
wet etching (HF 49% + mask Si/Si-carbide/photo-resist)	glass	3000	0.33	-	0.13	1000	-	[85]
HF etching (mask Cr/Au (50 nm/1 μm) + photoresist AZ7220)	Pyrex 7740	±1600	±0.3	44	0.238	500	-	[94]
HF etching (49% HF)	Pyrex 7740	240	0.58	-	0.14	140	-	[208]
HF etching (HFPR-mask)	fused silica	-	0.70	-	0.01	600	10	[209]
DRIE etching (Ni/a-Si/SU-8 masks deep plasma etching)	glass	200	1.25	-	>0.035	250	-	[84]
DRIE (SF_6 plasma)	Pyrex glass	40–80	>10	10	0.01	200	-	[164]
DRIE (C_4F_8/O_2—Ni mask 8 μm)	glass	3	40	4–14	0.017	120	2–10	[165]
DRIE (SF_6/Ar—Ni 5 μm)	glass	-	-	-	0.0089	20	1.97	[210]
DRIE (SF_6—Cr)	glass	-	-	4	0.02	<20	very high	[211]
DRIE ($C_4F_8/He/O_2$—Si wafer 400 μm)	glass	83.33	3	8–20	0.0083	250	-	[212]
DRIE ($C_4F_8/He/O_2$—Si wafer 400 μm)	glass	100	3	-	0.0058	300	-	[212]
DRIE (C_4F_8/O_2—Ni mask 5 μm)	glass	22.86	3.5	8–20	0.012	80	-	[84]
DRIE (SF_6—Ni mask)	glass	20	10	4	0.01	200	4	[164]
DRIE (SF_6—Ni mask)	glass	-	-	>4	0.0125	40	-	[160]
DRIE (SF_6/Ar—Ni mask)	glass	-	-	4	0.009	27	-	[160]
DRIE (C_4F_8/O_2—Ni mask 6 μm)	glass	20	6	4–14	0.013	120	2	[213]
DRIE	glass	>1	30	-	0.0055	-	-	[214]
Deep anisotropic dry etching	-	50	-	0.4	0.0001	-	-	[215]

Thermal Methods	Material	Diameter (μm)	Aspect Ratio	Taper Angle * (°)	Speed (μm/s)	Depth (μm)	Surface Roughness (nm)	References
Femtosecond laser (liquid assisted)	-	5–70	40–50	-	30	-	-	[137]
Laser drilling (femtosecond pulses)	fused silica	7–10	3	-	-	30	<HAZ, no cracks, smooth	[141]

Laser drilling (femtosecond pulses)	Foturan glass	56	7.05	-	100–1000	395	-	[144]
Laser drilling femtosecond fiber laser	soda-lime glass	400	2.5	10	-	1000	no cracks, HAZ, rough	[146]
TiSa laser (fs pulse width)	D263T glass foil	208 99	2.4 5.1	15 10	-	500 505	<HAZ, no debris	[142]
Laser (absorbent powder)	glass	200	>12	-	100	2500	-	[147]
Laser drilling (short pulse solid state laser)	Nippon sheet glass	15	0,017	-	-	0.25	no cracks, smooth	[139]
CO_2 laser	D263T glass foil	<100	>5	3	2000	500	smooth	[102]
CO_2 laser	glass	71	7,04	3	<2000	500	-	[152]
CO_2 laser	glass	122	4,10	10	<2000	500	-	[152]
CO_2 laser (pulsed)	alkali free glass	25	4	-	20,000	100	-	[153]
Laser (CO_2 infrared laser/Ni grid mask)	-	9.2	0.00043	-	-	0.004	irregular	[132]
LALP (CO_2 laser, 6W—workpiece immersed in water)	Pyrex 7740	280	1.79	24	11,400	500	no cracks	[151]
Laser (selective etching)	glass	25	40	-	10	-	-	[216]
Focused EDM	Alkali-free EN-A1	20	5	-	500–200	100	-	[95]
	-	65.5	7.6	2	-	500	smooth	[95]

Hybrid Methods	Material	Diameter (µm)	Aspect Ratio	Taper Angle * (°)	Speed (µm/s)	Depth (µm)	Surface Roughness (nm)	References
ECDM	glass	180–40	11	-	1	1200	250–350	[185]
ECDM (pulsed voltage + offset)	glass	455	0.99	-	7.5	450	-	[188]
ECDM (EPDG polishing)	-	210	2.38	0.4°	-	500	5	[180]
SACE (gravity feed)	glass	540	0.37	-	-	200	smooth	[217]
SACE (gravity feed)	glass	600	0.55	-	-	330	HAZ	[217]